LABORATORY STUDY OF INFLUENCE OF NOSE ANGLE ON SEDIMENT DISTRIBUTION AT CHANNEL BIFURCATION

G.M. Tarekul Islam

A thesis submitted to the Department of Water Resources Engineering in partial fulfilment of the requirements for the Degree of Master of Science in Water Resources Engineering.

Department of Water Resources Engineering
Bangladesh University of Engineering & Technology
Dhaka

October, 1996

CERTIFICATE OF RESEARCH

This is to certify that except where specific reference to other investigators is made, the work described in this thesis is the result of the investigation of the candidate. Neither this thesis nor any part thereof has been submitted elsewhere for the award of any degree or diploma.

(Prof. Ainun Nishat)
Countersigned by the supervisor

(G.M. Tarekul Islam)
Signature of the Candidate

Bangladesh University of Engineering & Technology
Department of Water Resources Engineering

Recommendation of the Board of Examiners

We hereby recommend that the project thesis prepared by G.M. Tarekul Islam entitled **"Laboratory Study of Influence of Nose Angle on Sediment Distribution at Channel Bifurcation"** be accepted as fulfilling this part of the requirements for the degree of Master of Science in Water Resources Engineering.

Dr. Ainun Nishat
(Chairman)

Dr. M. Fazlul Bari
(Member)

Dr. M.R. Kabir
(Member)

A.K.M. Shamsul Hoque
(External Member)

Dr. M. Monowar Hossain
(Head of the Department)

October 20, 1996

TABLE OF CONTENTS

Page

ACKNOWLEDGEMENT

I express my deepest sense of gratitude and profound respect to my thesis supervisor Dr. Ainun Nishat, Professor, Department of Water Resources Engineering, BUET for his continuous encouragement, constant guidance and keen interest throughout the progress of the work. I consider it a great opportunity to have a share of some of his knowledge and expertise and find myself proud to work with him.

My gratitude is due to Prof. M.F. Bari, Project Director and Mr. M.C.L.M. van Mierlo, Coordinating Resident Engineer of BUET-DUT University Linkage Project for managing financial support to carry out the laboratory work. Besides this, Mr. van Mierlo gave me valuable suggestions and inspiration for the study and Prof. Bari offered guidance in statistical analyses. I am also grateful to Mr. J.J. Veldman who succeeded Mr. van Mierlo as Coordinating Resident Engineer for his interest in my work.

Dr. M. Monowar Hossain, Professor and Head, Department of Water Resources Engineering provided every facility to work in the laboratory (even in holidays). I express my sincere thanks to him.

Dr. M.R. Kabir, Associate Professor, Department of Water Resources Engineering contributed me in many ways by providing valuable suggestions and nice comments. He tolerated a lot of questions and quarries from me. I express my gratitude to him.

Acknowledgements are also due to Mr. A.K.M. Shamsul Hoque, Chief Engineer planning, Bangladesh Water Development Board for his valuable comments and suggestions.

I offer my sincere thanks to Prof. Dr. Ir. M. de Vries of the Department of Civil Engineering, Delft University of Technology, the Netherlands for his comments on the draft of my thesis. During this study I was an awardee of Lamminga Foundation Scholarship, administered by Prof. de Vries. This enabled me to support myself during my laboratory work. I am grateful to the Foundation.

I am specially indebted to Dr. S.M. Nazrul Islam, Professor, Department of Mechanical Engineering for his advice and inspiration to complete the thesis work.

I am also grateful to Mr. Lutfor Rahman, graduate student in the Department of Water Resources Engineering for cooperation.

Thanks are due to Mr. Firoj Alam Mia, Administrative Officer of BUET-DUT University Linkage Project for his assistance and cooperation, Mr. M.A. Mannan Khan for his typing of the thesis and Mr. Md. Abul Kalam Azad for draughting of some of the figures.

Finally I would like to thank Mr. Md. Nazimuddin, Mr. Golam Mostafa and Mr. Md. Bedar Hossain of Hydraulics and River Engineering Laboratory and Mr. Md. Shaiful for providing assistance in my laboratory work.

G.M. Tarekul Islam
October, 1996

ABSTRACT

Bifurcations are typical features in alluvial rivers as well as in estuaries. The morphological behaviour of bifurcation is not as yet a properly understood phenomenon. This is why river engineers are confronted with this problem. The complexity of the bifurcation lies in the determination of the sediment distribution ratio of the downstream branches. The distribution ratio is determined by the local three dimensional flow pattern. The determination of the distribution ratio is a difficult task. In order to get some idea about how the sediments distribute over the downstream branches, a study has been carried out using a physical model at the Hydraulics and River Engineering Laboratory of Bangladesh University of Engineering and Technology.

This study describes the influence of nose angle (the angle between the tip of the nose and the symmetrical line of a bifurcation) on sediment distribution at channel bifurcation. A total of four different noses have been used to investigate the influence. For each nose, three upstream discharges (e.g. 20 l/s, 30 l/s and 40 l/s) have been used. From the experiments, a set of data on q_1/q_2 and s_1/s_2 (where q_1, q_2 and s_1, s_2 are the discharges and sediment transports per unit width through branch 1 and 2 respectively) have been collected. These data have been set to the following nodal point relation (the relation between the ratio of downstream discharges and the ratio of the downstream sediment transport rates):

$$\frac{s_1}{s_2} = M\left(\frac{q_1}{q_2}\right)^k$$

where M is a coefficient and k is an exponent. It has been found that the nose angle has a great influence on sediment distribution to the downstream branches. As the nose angle changes, the power and the coefficient of the nodal point relation change to a great extent. The value of coefficient, M in the nodal point relation increases as the discharge increases for nose angles of 6.97^0, 0^0 and -3.50^0. For nose angle of -10.38^0, the coefficient decreases with increase of discharge. For a particular upstream discharge the coefficient M increases as the nose angle changes from negative to positive ($-10.38^0 \leq \theta \leq 6.97^0$). The value of the exponent, k in the nodal point relation increases as the discharge increases when the nose angle is held constant. When the discharge is held constant at 30 l/s, it is found that the maximum value of the coefficient, k occurs for symmetric nose ($\theta = 0^0$). Similar is the case for the upstream discharge of 40 l/s. But when the upstream discharge is 20 l/s, the maximum value of k is found for $\theta = -10.38^0$. It is concluded from this study that the distribution of sediment to the downstream branches is independent of upstream discharge. The nose angle is the major variable for the distribution of sediment.

LIST OF MAIN SYMBOLS

Symbol n	Description	Dimensio
a	water depth	[L]
B	width	[L]
C	Chezy's roughness coefficient	$[L^{1/2}T^{-1}]$
D_{50}	sediment size	[L]
g	acceleration due to gravity	$[LT^{-2}]$
h	water level	[L]
i	slope of bed level	[-]
L	length of branch	[L]
M	coefficient in nodal point relation	[-]
n	power in sediment transport formula	[-]
Q_i	total discharge in branch i	$[L^3T^{-1}]$
Q_0	total upstream discharge	$[L^3T^{-1}]$
q_i	discharge per unit width in branch i	$[L^2T^{-1}]$
S_i	sediment transport rate in branch i	$[L^3T^{-1}]$
S_{ie}	sediment transport capacity in branch i	$[L^3T^{-1}]$
s_i	sediment transport per unit width in branch i	$[L^2T^{-1}]$
T	adaptation time	[T]
u	flow velocity	$[LT^{-1}]$
v	volume of sand	$[L^3]$
ρ	density of water	$[ML^{-3}]$
ρ_s	density of sediment	$[ML^{-3}]$
ϵ	porosity of sediment	[-]
J	Jacobian	[-]
k	power in nodal point relation	[-]
α	constant	[-]
β	constant	[-]
Δ	relative density of sediment	[-]

LIST OF TABLES

Page

LIST OF FIGURES

Page

CHAPTER 1

INTRODUCTION

1.1 General

Bifurcations are typical features in alluvial rivers as well as in estuaries. In braided rivers confluences and bifurcations occur regularly. In estuaries, when the direction of tidal flow turns around an island or a char, confluence becomes bifurcation and vice versa. Fig. 1.1 and 1.2 show the definition sketches of bifurcation and confluence.

At a confluence two rivers (or river branches) meet and join into one single river. The conditions governing the confluence are simple. There will be mass balancing of water and sediment as shown in Fig. 1.1, where Q_i is the discharge and S_i is the sediment transport in branch *i*. In this case Q_1, Q_2, S_1 and S_2 are known; the values of Q_0 and S_0 simply follow from the two mass balance equations.

A bifurcation occurs when a river separates into two (or more) branches. The mass balances of water and sediment are the same as for a confluence (Fig. 1.2). The conditions governing the bifurcation however are different from those for a confluence,

In this case Q_0 and S_0 are known and Q_1, Q_2, S_1 and S_2 are unknown. As a result the two mass balance equations are not sufficient to determine the distribution of flow and sediment into the branches.

With this simple description of a bifurcation the problem arising can clearly be seen: two extra equations have to be found in order to obtain four equations necessary to determine the values of the four unknown quantities: Q_1, Q_2, S_1 and S_2.

In order to find the values of Q_1, Q_2, S_1 and S_2, one has to know how water and sediment distribute over the downstream branches. In other words, one has to know the ratio between the downstream Q_i and the ratio between the downstream S_i. In these ways two extra equations may be obtained. The distribution of the discharge Q_0 into Q_1 and Q_2 is completely determined by the geometry and friction coefficients of the downstream branches. It is such that given the geometry of the downstream branches, only one water level occurs at the bifurcation. This computation is not a major problem.

The problem is the determination of the distribution of the sediment. The distribution ratio of the sediment of the two downstream branches is determined by the local three dimensional flow pattern (Vries, 1992). The determination of the ratio S_1/S_2 is a difficult task; this has resulted a multitude of proposed nodal point relations. The relation between the ratio of downstream discharges and the ratio of the downstream sediment transport rates is called nodal point relation.

The nodal point relation determines the distribution of sediment to the downstream branches, which differs from bifurcation to bifurcation (Akkerman, 1993, after Wang and Kaaij, 1994). The nose angle (the angle between the tip of the nose and the symmetrical line of a bifurcation) may be an important parameter which affects nodal point relation. There is no field or prototype data on nodal point relationship. Laboratory studies in this respect are also of recent origin and importance of studies to find the influence of nose angle on sediment distribution at channel bifurcation is being recognised (Hannan, 1996).

In recent years software packages have been developed for simulation of river engineering problems. One such package is WENDY (Delft Hydraulics, 1991). It consists of a comprehensive set of application software for the simulation of water flow, sediment transport, morphology and water quality in open channel networks. However the software uses coefficient and exponents based on theoretical assumption and have not been evaluated against experimental data.

The morphological behaviour of a river at bifurcation is not as yet a properly understood phenomenon. Because the combined transport of water and sediment in rivers is a complex process. It is difficult to study the morphological behaviour of the bifurcation in rivers both in the laboratory and in the field. Recently Dekker and van Voorthuizen (1994), Roosjen and Zwanenberg (1995) and Hannan (1996) have studied the morphology of river bifurcation on the physical model of river bifurcation built in the Hydraulics and River Engineering Laboratory of Bangladesh University of Engineering and Technology. This study uses the facilities developed earlier but concentrates on the distribution of sediment over the downstream branches with nose angle as a major variable.

1.2 Examples of river bifurcation

As mentioned earlier that bifurcations are a common feature in alluvial rivers as well as in estuaries. In a braided river channel bifurcation occurs around every middle bar. Fig. 1.3 shows a stretch of the Jamuna.

Another example of bifurcation is the distribution of flows of the Barak river at Zokigonj into the Surma and the Kushiyara (Fig. 1.4).

Offtakes of distribution are important examples of bifurcation. As for example flow of the Ganges bifurcates into the Gorai forming the Ganges-Gorai bifurcation (Fig. 1.5), Similarly the Brahmaputra near Jamalpur forms the Brahmaputra - old Brahmaputra bifurcation.

The Rhine river bifurcates into the Waal and Pannerdens channel just downstream of the German-Dutch border. Another bifurcation is situated near Westervoort, a distance 11 km downstream of Pennerdens (Fig. 1.6)

1.3. Importance of laboratory studies on channel bifurcation

Bifurcations are mostly found in deltas, but also in braided sections of a river. The braided river in the upstream end of the middle course has more than one channel, with a sequence of confluences and bifurcations forming a multitude of islands in the river. The course of a braided river is very unstable and unpredictable, leading to serious problems for an engineer trying to tame the river with hydraulic structures. The morphological behaviour and the effect of the bifurcations on the stability of the downstream branches strongly influence the stability of the braided river system as a whole. A better understanding of the morphological processes at a bifurcation would clearly contribute to the understanding of the behaviour of the islands in the braided river. This could help improve the prediction of the course of such a river, facilitating the task of the engineer trying to regulate the river.

Where the river forms a delta, the flow patterns are dominated by bifurcations. Because of the unknown behaviour of bifurcation, it has proved to be difficult to implement the layout of a delta into a one-dimensional morphodynamic model. The result of the behaviour of bifurcations in river is therefore relevant for the development of these models (Dekker and van Voorthuizen, 1993).

Bangladesh is a land of rivers. Several of her rivers are braided in nature. The river network in estuary experiences many bifurcations and confluences. In braided rivers confluences and bifurcations occur regularly. So a good insight is necessary about river bifurcation so that it can be known how the river will respond due to the construction of river training works.

As an example of a current river engineering problem involving the construction of the bridge over the Jamuna river (braided) in Bangladesh which is characterised by a repetition of bifurcations and confluences. The main channel of this river is known to shift upto several kilometers a year, in a rather unpredictable way. Major flow guiding constructions are being built to try to stabilise the course of the river to keep the river flowing under the bridge. In order to minimise costs and to align the flow guiding structures in an effective way, a prediction of the possible changes in the course of the river had to be made. This prediction was based on a probability method using statistical data. A better physical understanding of the morphological behaviour of the bifurcations in braided river could have contributed to a more accurate prediction.

Moreover, the design of the hydraulic structures could be improved as the effectiveness of the applied hydraulic structures would be better understood. The results obtained by the model on river bifurcation can also be used to access the future situation of the river and suggestions can be made with regards to design.

1.4 Objectives of the Study

The following are the objectives of the research work:

- to find the influence of nose angle on sediment distribution at the bifurcation of channel and
- determination of variation of discharge at the bifurcation of channel depending on nose angle.

1.5 Assumptions and limitations of the study

The study is based on the physical model of river bifurcation and some assumptions have been made. In order to simulate the results of the experiments of the physical model of river bifurcation some additional assumptions were made when designing the model. Apart from these the model itself implies some limitations. The following are the assumptions and limitations of the model.

Assumptions:

- the river bifurcates only into two downstream branches;
- there is no bank erosion;
- the upstream discharge is constant in time;
- the sediment load consists of bed load only, i.e. no suspended load or wash load occurs;
- the downstream water levels are constant as in the natural rivers which discharge into a sea;
- possible influences of tides and salt water are neglected;
- no transport of sediment occurs over the crest of Rehbock weirs;
- the supply of sediment is constant during the run of the experiment; and
- the Chezy's roughness coefficient, C is assumed to be 30 $m^{1/2}/s$.

Limitations

- the widths of the branches are fixed;
- small deviations of the upstream discharge, water levels at the end of the branches and the amount of sand feeded upstream, which are unavoidable are neglected;
- all the sediment transport is assumed to be bed load; this creates limitations for the upstream discharge and the ratio of the discharges in the downstream branches;
- for a proper working of the sand traps the sediment transport needs to be bed load only;
- the height of the model wall is fixed; this restricts the maximum water level; together with the assumption of bed load, this also restricts the upstream discharge; and
- the sand is not uniformly feeded over the width of the model; it is assumed that the water movements distribute the sediment equally over the width before the sediment reaching the bifurcation.
- there is no mathematical model available in the department of WRE with which the results of the experiments can be simulated.

CHAPTER 2

MATHEMATICAL INVESTIGATION OF RIVER BIFURCATION

2.1 Introduction

This chapter presents the theoretical investigations of river bifurcation. The distribution of sediment over the downstream branches is governed by the local geometry. So it is difficult to give a general algorithm. A mathematical analysis was given by Wang et al. (1993) which has been the main basis of this chapter.

Basic variables:

The definition of the basic variables is shown in Fig. 2.1. The dependent variables are the flow velocity(u), sediment transport(S), water depth(a), and the bed level(z). The independent variables are the longitudinal distance(x) and time(t). The water level, h is equal to z+a. The longitudinal slope is *i*.

Assumptions:

The following assumptions are made in order to investigate river bifurcation theoretically

- the height of the wave is relatively small compared with the water depth and the propagating time through the whole branch of the wave is relatively short compared to the morphological time scale.
- the lengths of the two downstream branches are relatively short, so that the time needed for a wave caused by disturbances at the bed to travel through a downstream branch is much smaller than the morphological time scale (the time necessary for closing one of the branches) of the system.
- the water level at the downstream boundary does not change.
- the morphological changes in the upstream river due to disturbances in the downstream branches can be neglected.
- the flow is steady.
- the downstream branches discharge into the same lake or sea.

Basic equations:

The basis of the analysis is formed by the following four equations:

- the momentum equation for the water movement:

$$\frac{\partial u}{\partial t}+u\frac{\partial u}{\partial x}+g\frac{\partial a}{\partial x}+g\frac{\partial z}{\partial x}=-g\frac{u|u|}{C^2 a} \qquad (2.1)$$

- the mass balance for the water movement

$$\frac{\partial a}{\partial t}+u\frac{\partial a}{\partial x}+a\frac{\partial u}{\partial x}=0 \qquad (2.2)$$

- the momentum equation for the sediment movement

$$s = f(u, \Delta, D_{50}, C, \text{etc.}) \qquad (2.3)$$

where u = flow velocity
Δ = bulk relative density of sediment
= $(\rho_s - \rho)/\rho$
D_{50} = sediment size
C = Chezy's roughness coefficient

The momentum equation can be substituted by the power law as

$$S = Bmu^n \tag{2.4}$$

in which, m = sediment transport coefficient
n = a positive exponent
B = width

- the mass balance for the sediment movement

$$\frac{\partial z}{\partial t} + \frac{\partial s}{\partial x} = 0 \tag{2.5}$$

The mass-balance for sediment movement in each branch yields

$$\frac{\partial a_i}{\partial t} = -\frac{S_i - S_{ie}}{B_i L_i} \tag{2.6}$$

with: B_i = width of branch *i*
L_i = length of branch *i*
S_i = sediment transport inflow into the branch as supplied by the main channel according to the nodal point relation
S_{ie} = sediment transport outflow from the branch according to the transport capacity, determined by equation (2.3)

The quantities S_i and S_{ie} depend on the variables a_1 and a_2. The sediment transport is assumed to be related to the velocity by eq. (2.4), in which the power n has the value 5 (Engelund-Hansen sediment transport formula).

The sediment inflow S_1 and S_2 in the respective downstream branches is determined by the nodal point relation. Different types of nodal point relations have been proposed in the literature. First the following nodal point relation is considered:

$$\frac{S_1}{S_2} = \frac{Q_1}{Q_2} \tag{2.7}$$

which describes that sediment is distributed according to discharge.

2.2 Distribution of sediment influenced by discharge

The nodal point relation in between branch 0 and 1 is

$$\frac{S_1}{S_0}=\frac{Q_1}{Q_0} \tag{2.8}$$

Mass-balance for water can be written as

$$Q_1+Q_2=Q_0 \tag{2.9}$$

From eq. (3.8) and (3.9)

$$S_1=\frac{Q_1}{Q_1+Q_2}S_0 \tag{2.10}$$

Sediment transport by Engelund-Hansen formula (Vries, 1993) is

$$S_0=B_0 m u_0^5=B_0 m\left(\frac{Q_0}{B_0 a_0}\right)^5=\frac{mQ_0^5}{B_0^4 a_0^5} \tag{2.11}$$

Water motion described by the Chezy formula (Vries, 1993)

$$Q_j=B_j C_j a_j^{\frac{3}{2}} i_j^{\frac{1}{2}}=B_j C_j a_j^{\frac{3}{2}}\left(\frac{\Delta h_j}{L_j}\right)^{\frac{1}{2}} \tag{2.12}$$

Thus

$$Q_1=B_1 C_1 a_1^{\frac{3}{2}}\left(\frac{\Delta h_1}{L_1}\right)^{\frac{1}{2}} \tag{2.13}$$

and

$$Q_2=B_2 C_2 a_2^{\frac{3}{2}}\left(\frac{\Delta h_2}{L_2}\right)^{\frac{1}{2}} \tag{2.14}$$

Geometric relation (Vries, 1993)

$$i_1 L_1=i_2 L_2 \tag{2.15}$$

$$\text{or}\quad \frac{\Delta h_1}{L_1}L_1=\frac{\Delta h_2}{L_2}L_2$$

$$\text{or}\quad \Delta h_1=\Delta h_2$$

Assuming $C_1 = C_2$, using geometric relation and substituting the value of S_0, Q_1 and Q_2 from eq. (2.11), (2.13) and (2.14) respectively in eq. (2.10)

$$S_1 = \frac{\dfrac{B_1}{L_1^{1/2}} a_1^{3/2}}{\dfrac{B_1}{L_1^{1/2}} a_1^{3/2} + \dfrac{B_2}{L_2^{1/2}} a_2^{3/2}} \frac{mQ_0^5}{B_0^4 a_0^5} \tag{2.16}$$

Let $\dfrac{B_1}{L_1^{1/2}} = \beta_1$ and $\dfrac{B_2}{L_2^{1/2}} = \beta_2$

$$\therefore \quad S_1 = \frac{\beta_1 a_1^{3/2}}{\beta_1 a_1^{3/2} + \beta_2 a_2^{3/2}} \frac{mQ_0^5}{B_0^4 a_0^5} \tag{2.17}$$

Similarly,

$$S_2 = \frac{\beta_2 a_2^{3/2}}{\beta_1 a_1^{3/2} + \beta_2 a_2^{3/2}} \frac{mQ_0^5}{B_0^4 a_0^5} \tag{2.18}$$

Now,

$$S_{1e} = \frac{mQ_1^5}{B_1^4 a_1^5} = \frac{mQ_0^5}{B_1^4 a_1^5}\left(\frac{Q_1}{Q_0}\right)^5 = \frac{mQ_0^5}{B_1^4 a_1^5}\left(\frac{\beta_1 a_1^{3/2}}{\beta_1 a_1^{3/2} + \beta_2 a_2^{3/2}}\right)^5 \tag{2.19}$$

Similarly,

$$S_{2e} = \frac{mQ_0^5}{B_2^4 a_2^5}\left(\frac{\beta_2 a_2^{3/2}}{\beta_1 a_1^{3/2} + \beta_2 a_2^{3/2}}\right)^5 \tag{2.20}$$

Substituting the value of S_1 from eq. (2.17) and S_{1e} from eq. (2.19) in eq. (2.6)

$$\frac{\partial a_1}{\partial t} = \frac{mQ_0^5}{B_0^5 L_1}\left[-\left(\frac{B_0}{B_1}\right)\frac{1}{a_0^5}\frac{\beta_1 a_1^{3/2}}{\beta_1 a_1^{3/2} + \beta_2 a_2^{3/2}} + \left(\frac{B_0}{B_1}\right)^5 \frac{1}{a_1^5}\left(\frac{\beta_1 a_1^{3/2}}{\beta_1 a_1^{3/2} + \beta_2 a_2^{3/2}}\right)^5\right] \tag{2.21}$$

Similarly by substituting the value of S_2 from eq. (2.18) and S_{2e} from eq. (2.20) in eq. (2.6).

$$\frac{\partial a_2}{\partial t} = \frac{mQ_0^5}{B_0^5 L_2}\left[-\left(\frac{B_0}{B_2}\right)\frac{1}{a_0^5}\frac{\beta_2 a_2^{3/2}}{\beta_1 a_1^{3/2} + \beta_2 a_2^{3/2}} + \left(\frac{B_0}{B_2}\right)^5 \frac{1}{a_2^5}\left(\frac{\beta_2 a_2^{3/2}}{\beta_1 a_1^{3/2} + \beta_2 a_2^{3/2}}\right)^5\right] \tag{2.22}$$

This system of differential equations describes the morphological behaviour of a river at a bifurcation. Although the system is too complicated to solve analytically, it is possible to gain qualitative insight in the behaviour of these equations by means of studying the nature of the singular points. A point (a_1,a_2) is called singular point if both derivatives vanish. This physically means that the singular points (a_1,a_2) represent the equilibria of the river system. They can be either stable, neutrally stable or unstable. The singular points are found by setting the derivatives equal to zero:

$$\frac{mQ_0^5}{B_0^5 L_1}\left[-\left(\frac{B_0}{B_1}\right)\frac{1}{a_0^5}\frac{\beta_1 a_1^{3/2}}{\beta_1 a_1^{3/2}+\beta_2 a_2^{3/2}}+\left(\frac{B_0}{B_1}\right)^5\frac{1}{a_1^5}\left(\frac{\beta_1 a_1^{3/2}}{\beta_1 a_1^{3/2}+\beta_2 a_2^{3/2}}\right)^5\right]=0 \qquad (2.23)$$

$$\frac{mQ_0^5}{B_0^5 L_2}\left[-\left(\frac{B_0}{B_2}\right)\frac{1}{a_0^5}\frac{\beta_2 a_2^{3/2}}{\beta_1 a_1^{3/2}+\beta_2 a_2^{3/2}}+\left(\frac{B_0}{B_2}\right)^5\frac{1}{a_2^5}\left(\frac{\beta_2 a_2^{3/2}}{\beta_1 a_1^{3/2}+\beta_2 a_2^{3/2}}\right)^5\right]=0 \qquad (2.24)$$

There are three singular points to these differential equations. One represents an equilibrium in which both branches of the river remain open; the other two represent the equilibrium in which one of the branches closes.

There is one singular point (a_1,a_2) for which both branches are open, i.e. both coordinates are positive numbers. So equations (2.23) and (2.24) have to be solved in order to find a_1 and a_2.

Divide eq. (2.23) by eq. (2.24)

$$\left(\frac{B_2}{B_2}\right)\left(\frac{\beta_1}{\beta_2}\right)\left(\frac{a_1}{a_2}\right)^{3/2}=\left(\frac{B_2}{B_1}\right)^5\left(\frac{\beta_1}{\beta_2}\right)^5\left(\frac{a_1}{a_2}\right)^{5/2}$$

$$\Rightarrow \quad \frac{a_1}{a_2}=\left(\frac{B_1}{B_2}\right)^4\left(\frac{\beta_2}{\beta_1}\right)^4=\left(\frac{B_1}{B_2}\right)^4\left(\frac{B_2}{B_1}\right)^4\left(\frac{L_1^{1/2}}{L_2^{1/2}}\right)^4=\left(\frac{L_1}{L_2}\right)^2$$

$$\therefore \quad a_2=a_1\left(\frac{L_2}{L_1}\right)^2 \qquad (2.25)$$

Substitute the value a_2 in eq. (2.23)

$$\left(\frac{B_1 a_1^{3/2}}{L_1^{1/2}}+\frac{B_2}{L_2^{1/2}}a_1^{3/2}\left(\frac{L_2}{L_1}\right)^3\right)^4=a_0^5\left(\frac{B_o}{B_1}\right)^4\left(\frac{B_1}{L_1^{1/2}}\right)^4 a_1$$

$$\Rightarrow a_1^6\left(\frac{B_1}{L_1^{1/2}}+\frac{B_2 L_2^{5/2}}{L_1^3}\right)^4=a_o^5\frac{B_o^4}{L_1^2}a_1$$

$$\Rightarrow a_1^5\left[\frac{B_1}{B_o}+\frac{B_2}{B_o}\left(\frac{L_2}{L_1}\right)^{5/2}\right]^4=a_o^5$$

$$\therefore \quad a_1 = a_o\left[\frac{B_1}{B_o} + \frac{B_2}{B_o}\left(\frac{L_2}{L_1}\right)^{5/2}\right]^{-4/5} \tag{2.26}$$

Similarly by substituting the value of a_1 from eq. (2.25) in eq. (2.24)

$$a_2 = a_o\left[\frac{B_2}{B_o} + \frac{B_1}{B_o}\left(\frac{L_1}{L_2}\right)^{5/2}\right]^{-4/5} \tag{2.27}$$

There are two singular points (a_1, o) and (o, a_2) for which one of the branches is closed. the value of a_1 and a_2 can be found by setting $a_2 = 0$ in eq. (2.23) and $a_1 = 0$ in eq. (2.24) respectively. Thus the open branches have height respectively.

$$a_1 = a_o\left(\frac{B_o}{B_1}\right)^{4/5} \tag{2.28}$$

and

$$a_2 = a_o\left(\frac{B_o}{B_2}\right)^{4/5} \tag{2.29}$$

In the simple case for which $B_1 = B_2 = B_{0/2}$ and $L_1 = L_2$, the first singular point is found from eq. (2.26) and (2.27) which is (a_o,a_o). The second and third singular points are found from eq. (2.28) and (2.29) which are ($2^{4/5}a_0$,0) and (0,$2^{4/5}a_0$).

Now, in order to investigate whether the singular points are stable or not, the following approach is followed.

A system of differential equations of the form:

$$\begin{bmatrix} \frac{dx}{dt} \\ \frac{dy}{dt} \end{bmatrix} = \begin{bmatrix} f(x,y) \\ g(x,y) \end{bmatrix} \tag{2.30}$$

with singular point (x_o,y_o) can be linearized locally by taking the Jacobian.

$$\begin{bmatrix} \frac{\partial x}{\partial t} \\ \frac{\partial y}{\partial t} \end{bmatrix} = \begin{bmatrix} \frac{\partial f}{\partial x}(x_0, y_0) & \frac{\partial f}{\partial y}(x_0, y_0) \\ \frac{\partial g}{\partial x}(x_0, y_0) & \frac{\partial g}{\partial y}(x_0, y_0) \end{bmatrix} = J(x_0, y_0)\begin{bmatrix} x - x_0 \\ y - y_0 \end{bmatrix} \tag{2.31}$$

Its eigenvalues are $\frac{\partial f}{\partial x}(x_o, y_o) - \frac{\partial g}{\partial x}(x_o, y_o)$ and $\frac{\partial f}{\partial x}(x_o, y_o) + \frac{\partial g}{\partial x}(x_o, y_o)$

A singular point is stable if both the eigenvalues of the Jacobian $J(x_o,y_o)$ have a negative real part.

First the equilibrium state with both branches open is looked at. This equilibrium is represented by the singular point (a_o,a_o) as mentioned earlier. The Jacobian at point (a_o,a_o) is determined by the following way:

The functions f and g are

$$f=\frac{mQ_0^5}{B_0^5L_1}\left[-\left(\frac{B_0}{B_1}\right)\frac{1}{a_0^5}\frac{\beta_1 a_1^{3/2}}{\beta_1 a_1^{3/2}+\beta_2 a_2^{3/2}}+\left(\frac{B_0}{B_1}\right)^5\frac{1}{a_1^5}\left(\frac{\beta_1 a_1^{3/2}}{\beta_1 a_1^{3/2}+\beta_2 a_2^{3/2}}\right)^5\right] \tag{2.32}$$

$$g=\frac{mQ_0^5}{B_0^5L_2}\left[-\left(\frac{B_0}{B_2}\right)\frac{1}{a_0^5}\frac{\beta_2 a_2^{3/2}}{\beta_1 a_1^{3/2}+\beta_2 a_2^{3/2}}+\left(\frac{B_0}{B_2}\right)^5\frac{1}{a_2^5}\left(\frac{\beta_2 a_2^{3/2}}{\beta_1 a_1^{3/2}+\beta_2 a_2^{3/2}}\right)^5\right] \tag{2.33}$$

The functions f and g can be written with the assumptions $B_1 = B_2 = B_0/2$ and $L_1 = L_2$ as

$$f=\frac{mQ_0^5}{32B_1^5L_1}\left[\frac{-2}{a_0^5}\frac{a_1^{3/2}}{a_1^{3/2}+a_2^{3/2}}+32\frac{a_1^{5/2}}{(a_1^{3/2}+a_2^{3/2})^5}\right] \tag{2.34}$$

$$g=\frac{mQ_0^5}{32B_1^5L_1}\left[\frac{-2}{a_0^5}\frac{a_2^{3/2}}{a_2^{3/2}+a_2^{3/2}}+32\frac{a_2^{5/2}}{(a_1^{3/2}+a_2^{3/2})^5}\right] \tag{2.35}$$

$$\frac{\partial f}{\partial a_1}=\frac{mQ_0^5}{32B_1^5L_1}\left[\frac{-2}{a_0^5}\frac{3/2a_1^{1/2}}{a_1^{3/2}+a_2^{3/2}}-\frac{2}{a_0^5}(-1)(3/2)\frac{a_1^{1/2}}{(a_1^{3/2}+a_2^{3/2})^2}\right.,$$

$$\left.+32.\frac{5}{2}.\frac{a_1^{3/2}}{(a_1^{3/2}+a_2^{3/2})^5}+32\frac{a_1^{5/2}(-5)}{(a_1^{3/2}+a_2^{3/2})^6}.3/2a_1^{1/2}\right]_{(a_0,a_0)}$$

$$=\frac{mQ_0^5}{32B_1^5L_1}\left[\frac{-3}{2a_0^6}+\frac{3}{4a_0^6}+\frac{5}{2a_0^6}-\frac{15}{4a_0^6}\right]$$

$$\therefore\quad \frac{\partial f}{\partial a_1}=\frac{mQ_0^5}{32a_0^5B_1^5L_1}(-2) \tag{2.36}$$

$$\frac{\partial g}{\partial a_1}=\frac{mQ_0^5}{32B_1^5L_1}\left[\frac{-2}{a_0^5}a_2^{3/2}\frac{(-1)3/2a_1^{1/2}}{(a_1^{3/2}+a_2^{3/2})^2}+32a_2^{5/2}(-5)\frac{3/2a_1^{1/2}}{(a_1^{3/2}+a_2^{3/2})^6}\right]_{(a_0,a_0)}$$

$$=\frac{mQ_0^5}{32B_1^5L_1}\left[\frac{3}{4a_0^6}-\frac{15}{4a_0^6}\right]$$

$$\therefore \quad \frac{\partial g}{\partial a_1}=\frac{mQ_0^5}{32a_0^6B_1^5L_1}(-3) \tag{2.37}$$

Thus the Jacobian at (a_0,a_0) is equal to

$$\frac{mQ_0^5}{32a_0^6B_1^5L_1}\begin{bmatrix}-2 & -3\\ -3 & -2\end{bmatrix} \tag{2.38}$$

The above matrix has eigen values - 5 and +1. This means that the singular point at (a_o,a_o) is a saddle point. It follows that the equilibrium at (a_o,a_o) is unstable. The rate between attraction and repulsion is 5:1, which means that the evolution of the river tends to the unstable equilibrium rapidly at first, but eventually it moves slowly.

At $(2^{4/5}\ a_o,\ o)$, the Jacobin is equal to

$$\frac{mQ_0^5}{32a_0^6B_1^5L_1}\begin{bmatrix}-5 & 0\\ 0 & 0\end{bmatrix} \tag{2.39}$$

and at $(o,\ 2^{4/5}\ a_o)$, the Jacobian is

$$\frac{mQ_0^5}{32a_0^6B_1^5L_1}\begin{bmatrix}0 & 0\\ 0 & -5\end{bmatrix} \tag{2.40}$$

So, at both points the eigen values are -5 and o. This case is a little hard to analyze because if one of the eigen values is zero, the equilibrium can be either stable or unstable. It will be shown in the following that they are stable.

In the plane, the points (a_1,a_2) for which the derivative $\frac{da_1}{dt}$ is zero lie on two curves: one curve is given by (Wang et al., 1993)

$$a_1=\frac{(a_1^{3/2}+a_2^{3/2})^4}{16a_o^5} \tag{2.41}$$

The other is the positive y-axis. Similarly, the points for which $\frac{da_2}{dt}$ is zero lie on two curves, one of which is the positive x-axis. The singular points are the points of intersection of one pair of curves with the other pair. The curves divide the plane into four regions: one for which $\frac{da_1}{dt}$ and $\frac{da_2}{dt}$ are positive, one for which both derivatives are negative and two regions for which the derivatives are of opposite sign. This is depicted in Fig. (2.2) In all four regions the direction of the vector ($\frac{da_1}{dt}$, $\frac{da_2}{dt}$) is known. So, the direction in which the branches develop can be determined.

From Fig. (2.2) the phase diagram of the differential equation, Fig. (2.3) can be found. The equilibria on the x-axis and y-axis are stable, the singular point (a_0,a_0) is unstable.

2.3 Distribution of sediment influenced by channel width

Wang et al. (1993) also described the nodal point relation which describes the distribution of sediment according to width as follows:

$$\frac{S_1}{S_2}=\frac{B_1}{B_2} \tag{2.42}$$

As the ratio B_1/B_2 is constant, the river always settles down in an unrealistic equilibrium in which a closed channel still transports a part of the sediment. However, physically sediment distributed according to width at nodal point is quite sensible in case of bed load transport. Therefore, the nodal point relation has to be considered under different assumptions. In particular it is assumed that the width B linearly depends on the depth.

$$B_1 = \alpha_1\, a_1,\ B_2 = \alpha_2\, a_2 \tag{2.43}$$

in which: α_1 and α_2 are constants.

The differential equation which describes the evolution of the river is given in eq. (2.6). The equation of equilibrium transports in the channel is given in eq. (2.19) and (2.20).

For the nodal point relation $S_1/S_2 = \alpha_1 a_1/\alpha_2 a_2$, sediment transports in the channel is

$$S_1=\frac{\alpha_1 a_1}{\alpha_1 a_1+\alpha_2 a_2}S_0 \tag{2.44}$$

and

$$S_2=\frac{\alpha_2 a_2}{\alpha_1 a_1+\alpha_2 a_2}S_0 \tag{2.45}$$

So the differential equation becomes

$$\frac{\partial a_1}{\partial t}=\frac{S_o}{2\alpha_1 a_1 L_1}\left[\frac{\beta_1^5 a_1^{5/2}}{(\beta_1 a_1^{3/2}+\beta_2 a_2^{3/2})^5}\left(\frac{B_o}{B_1}\right)^4 a_o^5-\frac{\alpha_1 a_1}{\alpha_1 a_1+\alpha_2 a_2}\right] \quad (2.46)$$

$$\frac{\partial a_2}{\partial t}=\frac{S_o}{2\alpha_2 a_2 L_2}\left[\frac{\beta_2^5 a_2^{5/2}}{(\beta_1 a_1^{3/2}+\beta_2 a_2^{3/2})^5}\left(\frac{B_o}{B_2}\right)^4 a_o^5-\frac{\alpha_2 a_2}{\alpha_1 a_1+\alpha_2 a_2}\right] \quad (2.47)$$

These equations are treated the same way as in the previous section. First the singular point in the symmetric case is looked at.

2.3.1 Symmetric case:

If $\alpha_1 = \alpha_2$ and $L_1 = L_2$, then the differential equations simplify considerably and it is straight forward to compute the singular points:

$$\frac{\beta_1 a_1^{5/2}}{(\beta_1 a_1^{3/2}+\beta_2 a_2^{3/2})^5}\left(\frac{B_o}{B_1}\right)^4 a_o^5-\frac{a_1}{a_1+a_2}=0 \quad (2.48)$$

$$\frac{\beta_2 a_2^{5/2}}{(\beta_1 a_1^{3/2}+\beta_2 a_2^{3/2})^5}\left(\frac{B_o}{B_2}\right)^4 a_o^5-\frac{a_2}{a_1+a_2}=0 \quad (2.49)$$

The quotient of these equations renders

$$\frac{a_1}{a_2}=\left(\frac{\beta_1}{\beta_2}\right)^5\left(\frac{a_1}{a_2}\right)^{5/2}\left(\frac{B_2}{B_1}\right)^4=\left(\frac{a_1}{a_2}\right)^5\left(\frac{a_1}{a_2}\right)^{5/2}\left(\frac{a_2}{a_1}\right)^4=\left(\frac{a_1}{a_2}\right)^{7/2} \quad (2.50)$$

The three singular points are (a_1,a_2), (a_1,o) and (o,a_2)

First the stability of the first singular point is considered. If the singular point is denoted by (a,a), then it follows from eq. (2.48).

$$\frac{a^{5/2}}{(2a^{3/2})^5}\frac{B_o^4 a_o^5}{\alpha^4 a^4}-\frac{1}{2}=0 \quad (2.51)$$

which can be reduced to

$$a^9=\frac{1}{16}\frac{B_o^4 a_o^5}{\alpha^4} \quad (2.52)$$

The stability of the singular point (a,a) depends on the eigenvalues of the Jacobian of the differential equation. Symbolically the differential equation can be represented as

$$\frac{\partial a_1}{\partial t}=f(a_1,a_2),\ \frac{\partial a_2}{\partial t}=f(a_1,a_2) \quad (2.53)$$

The Jacobian is equal to

$$J = \begin{bmatrix} \dfrac{\partial f}{\partial a_1} & \dfrac{\partial f}{\partial a_2} \\ \dfrac{\partial f}{\partial a_2} & \dfrac{\partial f}{\partial a_1} \end{bmatrix} \tag{2.54}$$

Its eigen values are $\dfrac{\partial f}{\partial a_1} - \dfrac{\partial f}{\partial a_2}, \ \dfrac{\partial f}{\partial a_1} + \dfrac{\partial f}{\partial a_2}$

If both eigenvalues are negative, the singular point is stable, but if one of the eigenvalues is positive it is not.

The function f is equal to

$$f(a_1, a_2) = \frac{S_o}{2\alpha a_1 L_1}\left[\frac{\beta_1^5 a_1^{5/2}}{(\beta_1 a_1^{3/2} + \beta_2 a_2^{3/2})^5}\left(\frac{B_o}{B_1}\right)^4 a_o^5 - \frac{a_1}{a_1 + a_2}\right] \tag{2.55}$$

The function $S_0/2\alpha a_1 L_1$ is positive and of no importance. So the following derivative is determined

$$\frac{\partial}{\partial a_1}\left[\frac{\beta_1^5 a_1^{5/2}}{(\beta_1 a_1^{3/2} + \beta_2 a_2^{3/2})^5}\left(\frac{B_o}{B_1}\right)^4 a_o^5 - \frac{a_1}{a_1 + a_2}\right]_{(a,a)}$$

$$= \frac{\partial}{\partial a_1}\left[\frac{a_1^{7/2}}{(a_1^{5/2} + a_2^{5/2})^5}\frac{B_o^4 a_o^5}{\alpha^4} - \frac{a_1}{a_1 + a_2}\right]_{(a,a)}$$

$$= \frac{B_o^4 a_o^4}{\alpha^4}\left[\frac{7}{2}\frac{a_1^{5/2}}{(a_1^{5/2} + a_2^{5/2})^5} - 5\left(\frac{5}{2}\right)a_1^{3/2}\frac{a_1^{7/2}}{(a_1^{5/2} + a_2^{5/2})^6}\right]_{(a,a)} - \left[\frac{1}{a_1 + a_2} - \frac{a_1}{(a_1 + a_2)^2}\right]_{(a,a)} \tag{2.56}$$

$$= 16a^9\left[\frac{7}{64a^{10}} - \frac{25}{128a^{10}}\right] - \frac{1}{2a} + \frac{1}{4a} = -\frac{13}{8a}$$

The other partial derivative can be derived the same way:

$$\frac{\partial}{\partial a_2}\left[\frac{a_1^{7/2}}{(a_1^{5/2} + a_2^{5/2})^5}\frac{B_o^4 a_o^5}{\alpha^4} - \frac{a_2}{a_1 + a_2}\right]_{(a,a)}$$

$$= \frac{B_o^4 a_o^4}{\alpha^4}\left[-5\left(\frac{5}{2}\right)a_2^{3/2}\frac{a_1^{7/2}}{(a_1^{5/2} + a_2^{5/2})^6}\right]_{(a,a)} + \left[\frac{1}{a_1 + a_2}\right]_{(a,a)} \tag{2.57}$$

$$=16a^{9}\left[-\frac{25}{128\,a^{10}}\right]-\frac{1}{2a}=-\frac{23}{8a}$$

It follows that the sum of the derivatives is negative, where as their difference is positive. Thus the singular point (a,a) is unstable.

In the same way, the Jacobian at the singular points (a_1, o) and (o,a_2) can be calculated. These singular points are stable. So, in the symmetric case, the stable equilibria have one of the channels closed. This is similar to the nodal point relation $S_1 : S_2 = Q_1 : Q_2$.

2.3.2 The general case:

In the previous section, it has been considered the special case in which the widths and the lengths of the two channels are exactly the same. In general, these quantities are differing. The general case may be thought of as a deformation of the symmetric case: for a given channel network, start with a symmetric situation and slowly deform the channels until the situation as given is reached.

The deformation idea can be made precise mathematically.

$$\frac{\alpha_1 a_1}{\alpha_2 a_2}=\left(\frac{\beta_1}{\beta_2}\right)^5\left(\frac{a_1}{a_2}\right)^{5/2}\left(\frac{B_2}{B_1}\right)^4=\left(\frac{B_1}{B_2}\right)^5\left(\frac{L_2}{L_1}\right)^{5/2}\left(\frac{a_1}{a_2}\right)^{5/2}\left(\frac{B_2}{B_1}\right)^4$$

$$=\left(\frac{B_1}{B_2}\right)^5\left(\frac{L_1}{L_2}\right)^{5/2}\left(\frac{a_1}{a_2}\right)^{5/2}=\left(\frac{\alpha_1}{\alpha_2}\right)\left(\frac{a_1}{a_2}\right)^{7/2}\left(\frac{L_2}{L_1}\right)^{5/2} \quad (2.58)$$

The differential equation has three singular points regardless the choice of the parameters B, L, α. This means that there are no abrupt changes when the geometry of the channel is deformed, i.e. when the parameters B, L, α change. Stable equilibria remain stable, unstable equilibria remain unstable. So, the general case is qualitatively the same as the symmetric case.

The analysis shows that the sediment distribution according to width leads to the same kind of behaviour as distribution according to discharge, provided the channel width depends on the channel depth. It is, therefore, best to keep all option open in an one dimensional model leading to the general nodal point relation:

$$\frac{S_1}{S_2}=\left(\frac{Q_1}{Q_2}\right)^k\left(\frac{B_1}{B_2}\right)^{1-k} \quad (2.59)$$

2.4 Distribution of sediment influenced by nodal point relation

The general nodal point relation is given in eq. (2.59). Thus the nodal point relation between branch 1 and 0 is

$$\frac{S_1}{S_0}=\left(\frac{Q_1}{Q_0}\right)^k\left(\frac{B_1}{B_0}\right)^{1-k} \qquad (2.60)$$

$$or \quad S_1=\left(\frac{Q_1}{Q_0}\right)^k\left(\frac{B_1}{B_0}\right)^{1-k}S_0=\left(\frac{Q_1}{Q_1+Q_2}\right)^k\left(\frac{B_1}{B_0}\right)^{1-k}\frac{mQ_0^5}{B_0^4a_0^5}$$

$$\therefore \quad S_1=\left(\frac{\beta_1a_1^{3/2}}{\beta_1a_1^{3/2}+\beta_2a_2^{3/2}}\right)^k\left(\frac{B_1}{B_0}\right)^{1-k}\frac{mQ_0^5}{B_0^4a_0^5}$$

Similarly,

$$S_2=\left(\frac{\beta_2a_2^{3/2}}{\beta_1a_1^{3/2}+\beta_2a_2^{3/2}}\right)^k\left(\frac{B_2}{B_0}\right)^{1-k}\frac{mQ_0^5}{B_0^4a_0^5}$$

Using eq. (2.6), (2.19), (2.20), (2.61) and (2.62), the following set of differential equations can be found.

$$\frac{\partial a_1}{\partial t}=\frac{mQ_0^5}{B_0^5L_1}\left[-\left(\frac{B_0}{B_1}\right)^k\frac{1}{a_0^5}\left(\frac{\beta_1a_1^{3/2}}{\beta_1a_1^{3/2}+\beta_2a_2^{3/2}}\right)^k+\left(\frac{B_0}{B_1}\right)^5\frac{1}{a_1^5}\left(\frac{\beta_1a_1^{3/2}}{\beta_1a_1^{3/2}+\beta_2a_2^{3/2}}\right)^5\right] \qquad (2.63)$$

$$\frac{\partial a_2}{\partial t}=\frac{mQ_0^5}{B_0^5L_1}\left[-\left(\frac{B_0}{B_2}\right)^k\frac{1}{a_0^5}\left(\frac{\beta_2a_2^{3/2}}{\beta_1a_1^{3/2}+\beta_2a_2^{3/2}}\right)^k+\left(\frac{B_0}{B_2}\right)^5\frac{1}{a_2^5}\left(\frac{\beta_2a_2^{3/2}}{\beta_1a_1^{3/2}+\beta_2a_2^{3/2}}\right)^5\right] \qquad (2.64)$$

These two equations describe the morphological behaviour of a river at bifurcation. As in the previous case, the behaviour of the equations can be obtained by studying the singular points. The singular points can be found by setting the derivatives equal to zero:

$$\frac{mQ_0^5}{B_0^5L_1}\left[-\left(\frac{B_0}{B_1}\right)^k\frac{1}{a_0^5}\left(\frac{\beta_1a_1^{3/2}}{\beta_1a_1^{3/2}+\beta_2a_2^{3/2}}\right)^k+\left(\frac{B_0}{B_1}\right)^5\frac{1}{a_1^5}\left(\frac{\beta_1a_1^{3/2}}{\beta_1a_1^{3/2}+\beta_2a_2^{3/2}}\right)^5\right]=0 \qquad (2.65)$$

$$\frac{mQ_0^5}{B_0^5L_1}\left[-\left(\frac{B_0}{B_2}\right)^k\frac{1}{a_0^5}\left(\frac{\beta_2a_2^{3/2}}{\beta_1a_1^{3/2}+\beta_2a_2^{3/2}}\right)^k+\left(\frac{B_0}{B_2}\right)^5\frac{1}{a_2^5}\left(\frac{\beta_2a_2^{3/2}}{\beta_1a_1^{3/2}+\beta_2a_2^{3/2}}\right)^5\right]=0 \qquad (2.66)$$

From the system of differential equations three singular points can be derived. There is one singular point (a_1,a_2) for which both branches are open, i.e. both a_1 and a_2 are positive. So eq. (2.65) and (2.66) have to be solved in order to find a_1 and a_2.

Divide eq. (2.65) by eq. (2.65)

$$\left(\frac{B_2}{B_1}\right)^k\left(\frac{\beta_1}{\beta_2}\right)^k\left(\frac{a_1}{a_2}\right)^{3k/2} = \left(\frac{B_2}{B_1}\right)^5\left(\frac{\beta_1}{\beta_2}\right)^5\left(\frac{a_1}{a_2}\right)^{5/2}$$

$$\Rightarrow \left(\frac{a_1}{a_2}\right)^{\frac{5-3k}{2}} = \left(\frac{B_1}{B_2}\right)^{5-k}\left(\frac{\beta_2}{\beta_1}\right)^{5-k} = \left(\frac{B_1}{B_2}\right)^{5-k}\left(\frac{B_2}{B_1}\right)^{5-k}\left(\frac{L_1^{1/2}}{L_2^{1/2}}\right)^{5-k} = \left(\frac{L_1}{L_2}\right)^{\frac{5-k}{2}}$$

$$\therefore \quad a_2 = a_1\left(\frac{L_2}{L_1}\right)^{\frac{5-k}{5-3k}} \qquad (2.67)$$

Eq. (2.65) can be written as

$$\left(\beta_1 a_1^{3/2} + \beta_2 a_2^{3/2}\right)^{5-k} = a_0^5\left(\frac{B_0}{B_1}\right)^{5-k}\beta_1^{5-k} a_1^{\frac{5-3k}{2}} \qquad (2.68)$$

Now, substitute the value of a_2 from eq. (3.67) in eq. (3.68)

$$\left[\frac{B_1 a_1^{3/2}}{L_1^{1/2}} + \frac{B_2}{L_2^{1/2}} a_1^{3/2}\left(\frac{L_2}{L_1}\right)^{\frac{15-3k}{10-6k}}\right]^{5-k} = a_0^5\left(\frac{B_0}{B_1}\right)^{5-k}\left(\frac{B_1}{L_1^{1/2}}\right)^{5-k} a_1^{\frac{5-3k}{2}}$$

$$\Rightarrow \quad a_1^{\frac{15-3k}{2}}\left[\frac{B_1}{L_1^{1/2}} + \frac{B_2}{L_2^{1/2}}\left(\frac{L_2}{L_1}\right)^{\frac{15-3k}{10-6k}}\right]^{5-k} = a_0^5\left(\frac{B_0}{L_1^{1/2}}\right)^{5-k} a_1^{\frac{5-3k}{2}}$$

$$\Rightarrow \quad a_1^5\left[\frac{B_1}{B_0} + \frac{B_2}{B_0}\left(\frac{L_2}{L_1}\right)^{\frac{10}{10-6k}}\right]^{5-k} = a_0^5$$

$$\therefore \quad a_1 = a_0\left[\frac{B_1}{B_0} + \frac{B_2}{B_0}\left(\frac{L_2}{L_1}\right)^{\frac{10}{10-6k}}\right]^{-\frac{5-k}{5}} \qquad (2.69)$$

Similarly by substituting the value of a_1 from eq. (2.67) in eq. (2.66),

$$a_2 = a_0\left[\frac{B_2}{B_0} + \frac{B_1}{B_0}\left(\frac{L_1}{L_2}\right)^{\frac{10}{10-6k}}\right]^{-\frac{5-k}{5}} \qquad (2.70)$$

There are also another two singular points $(a_1,0)$ and $(0,a_2)$ for which one of the branches is closed. Thus the value of a_1 and a_2 can be found by setting $a_2 = 0$ in eq. (2.65) and $a_1 = 0$ in eq. (2.66). The open branches have height respectively:

$$a_1 = a_o\left(\frac{B_o}{B_1}\right)^{4/5} \qquad (2.71)$$

$$\text{and} \quad a_2 = a_o \left(\frac{B_o}{B_2} \right)^{4/5} \tag{2.72}$$

In the simple case for which $B_1 = B_2 = B_0/2$ and $L_1 = L_2$, the singular points are (a_0,a_0), $(2^{4/5}a_0,0)$ and $(0,2^{4/5}a_0)$.

In order to find whether the singular points are stable or not, the eigenvalues of the following Jacobian have to be determined.

$$J = \begin{bmatrix} \frac{\partial f}{\partial a_1} & \frac{\partial f}{\partial a_2} \\ \frac{\partial g}{\partial a_1} & \frac{\partial g}{\partial a_2} \end{bmatrix} \tag{2.73}$$

where :

$$f = \frac{\partial a_1}{\partial t} = \frac{-mQ_0^5}{B_0^5 L_1} \left[-\left(\frac{B_0}{B_1}\right)^k \frac{1}{a_0^5} \left(\frac{\beta_1 a_1^{3/2}}{\beta_1 a_1^{3/2} + \beta_2 a_2^{3/2}} \right)^k - \left(\frac{B_0}{B_1}\right)^5 \frac{1}{a_1^5} \left(\frac{\beta_1 a_1^{3/2}}{\beta_1 a_1^{3/2} + \beta_2 a_2^{3/2}} \right)^5 \right] \tag{2.74}$$

$$g = \frac{\partial a_2}{\partial t} = \frac{-mQ_0^5}{B_0^5 L_1} \left[-\left(\frac{B_0}{B_2}\right)^k \frac{1}{a_0^5} \left(\frac{\beta_2 a_2^{3/2}}{\beta_1 a_1^{3/2} + \beta_2 a_2^{3/2}} \right)^k - \left(\frac{B_0}{B_2}\right)^5 \frac{1}{a_2^5} \left(\frac{\beta_2 a_2^{3/2}}{\beta_1 a_1^{3/2} + \beta_2 a_2^{3/2}} \right)^5 \right] \tag{2.75}$$

The eigenvalues are $\frac{\partial f}{\partial a_1} - \frac{\partial g}{\partial a_1}$ *and* $\frac{\partial f}{\partial a_1} + \frac{\partial g}{\partial a_1}$

A singular point is stable if both the eigenvalues of the Jacobian have a negative real part. First the singular point (a_0,a_0) is looked at.

For $B_1 = B_2 = B_0/2$ and $L_1 = L_2$, the functions f and g can be written as

$$f = \frac{mQ_0^5}{32 B_1^5 L_1} \left[-\frac{2}{a_0^5} \left(\frac{a_1^{3/2}}{a_1^{3/2} + a_2^{3/2}} \right)^k + 32 \frac{a_1^{5/2}}{\left(a_1^{3/2} + a_2^{3/2}\right)^5} \right] \tag{2.76}$$

$$g = \frac{mQ_0^5}{32 B_1^5 L_1} \left[-\frac{2}{a_0^5} \left(\frac{a_2^{3/2}}{a_1^{3/2} + a_2^{3/2}} \right)^k + 32 \frac{a_2^{5/2}}{\left(a_1^{3/2} + a_2^{3/2}\right)^5} \right] \tag{2.77}$$

$$\frac{\partial f}{\partial a_1}=\frac{mQ_0^5}{32B_1^5L_1}\left[-\frac{2^k}{a_0^5}k\left(\frac{a_1^{3/2}}{a_1^{3/2}+a_2^{3/2}}\right)^{k-1}\left\{\frac{\frac{3}{2}a_1^{1/2}}{a_1^{3/2}+a_2^{3/2}}+\frac{a_1^{3/1}(-1)(3/2)a_1^{1/2}}{\left(a_1^{3/2}+a_2^{3/2}\right)^2}\right\}\right.$$

$$\left.+\;32\left(\frac{5}{2}\right)\frac{a_1^{3/2}}{\left(a_1^{3/2}+a_2^{3/2}\right)^5}+32\,\frac{a_1^{5/2}(-5)\frac{3}{3}a_1^{1/2}}{\left(a_1^{3/2}a_2^{3/2}\right)^6}\right]_{(a_0,\,a_0)}$$

$$=\frac{mQ_0^5}{32B_1^5L_1}\left[-\frac{3k}{2a_0^6}+\frac{3k}{4a_0^6}+\frac{5}{2a_0^6}-\frac{15}{4a_0^6}\right]$$

$$\therefore\quad \frac{\partial f}{\partial a_1}=\frac{mQ_0^5}{32B_1^5L_1a_0^6}\left(-\frac{3k+5}{4}\right) \tag{2.78}$$

$$\frac{\partial g}{\partial a_1}=\frac{mQ_0^5}{32B_1^5L_1}\left[-\frac{2^k}{a_0^5}k\left(\frac{a_2^{3/2}}{a_1^{3/2}+a_2^{3/2}}\right)^{k-1}\frac{a_2^{3/2}(-1)\left(\frac{3}{2}\right)a_1^{1/2}}{\left(a_1^{3/2}+a_2^{3/2}\right)^2}+32\,a_2^{5/2}(-5)\frac{\frac{3}{2}a_1^{1/2}}{\left(a_1^{3/2}+a_2^{3/2}\right)^6}\right]_{(a_0,\,a_0)}$$

$$=\frac{mQ_0^5}{32B_1^5L_1}\left[-\frac{3k}{2a_0^6}+\frac{3k}{4a_0^6}+\frac{5}{2a_0^6}-\frac{15}{4a_0^6}\right]$$

$$=\frac{mQ_0^5}{32B_1^5L_1}\left[\frac{3k}{4a_0^6}-\frac{15}{4a_0^6}\right]$$

$$\therefore\quad \frac{\partial g}{\partial a_1}=\frac{mQ_0^5}{32B_1^5L_1a_0^6}\left(-\frac{15-3k}{4}\right) \tag{2.79}$$

Thus the Jacobian is

$$J=\frac{mQ_0^5}{32B_1^5L_1a_0^6}\begin{bmatrix}-\frac{3k+5}{4} & -\frac{15-3k}{4}\\ -\frac{15-3k}{5} & -\frac{3k+5}{4}\end{bmatrix} \tag{2.80}$$

For the above matrix, the eigenvalues are -5, - (3k-5)/2. The first eigenvalue is negative. The sign of the second eigenvalue depends on the value of k. For the situation in which k<5/3, the second eigenvalue is positive. The singular point at (a_0,a_0) becomes a saddle point resulting in an unstable equilibrium (Fig. 2.4). In the case k > 5/3, both eigenvalues are negative. The singular point at (a_0,a_0) becomes a sink (Fig. 2.5). This equilibrium represents a stable situation.

The two equilibria which represent the situation one branch open and one branch closed are represented by their respective singular points $(2^{4/5}a_0,0)$ and $(0,^{4/5}a_0)$. The same analysis holds for these equilibria. Taking the Jacobian and studying the eigenvalues for these singular points, shows that both equilibria are unstable for $k<5/3$ and stable for $k>5/3$, a can be seen from Fig. 2.4 and 2.5.

The previous analysis is made under the assumptions: $B_1 = B_2 = B_0/2$ and $L_1 = L_2$. This leads to the fact that the line $a_1 = a_2$ represents a line of saddle point and sink.

In the analysis so far, the sediment transport formula of Engelund-Hansen is used. Other transport formulae use threshold values for the flow velocity to carry sediment. An example of these kinds of transport formulae is the transport formula of Meyer - Peter - Muller. Using this kind of formula in the previous analysis gives more singular points. A more detailed description can be found in Wang and Kaaij (1994).

For the general analysis using arbitrary values of B_1, B_2, L_1 and L_2, the analysis and figures become more complicated, but they do not change qualitatively.

CHAPTER 3

REVIEW OF PREVIOUS STUDIES

3.1 Introduction

Bifurcation is one of the complex and unsolved problems in river engineering. Very little literature is available on the subject of bifurcations. This scarcity in available literature must, however, not be seen as an indication of the unimportance of the subject, but rather shows the difficulty of the problem with which many river engineers are confronted. The literature so far found through an extensive survey, however, are described in the following sections.

3.2 Morphological aspects of river bifurcation

3.2.1 Morphological equilibrium of river bifurcation

The morphological equilibrium condition of river bifurcating into two branches was analyzed by Vries (1992, after Wang et al., 1993). In that analysis, it was shown that there are three equilibrium states. One equilibrium state describes the situation where both the downstream branches are open. The other two equilibrium states describe the situation where one of the downstream branches is closed.

3.2.2 Morphological behaviour of river bifurcation

Dekker and van Voorthuizen (1994) studied the morphological behaviour of river bifurcation. They concluded that the stability of the network is determined by the value of k in the nodal point relation (eq. 2.59), and not by the configuration of the downstream branches. For large values of k (>5/3), the bifurcation is stable (with both branches open), and for small values of k (<5/3) it is unstable (with one of the branches closing). They also concluded that the configuration of the downstream branches (i.e. the respective widths of the branches or the presence of a groyne etc.) does influence the equilibrium depths attained in each branch; this is due to a difference in conveyance of the respective branches.

The influence of the value of k on the morphological time-scale was also analyzed in the theoretical model, and resulting predictions were once again confirmed by the numerical computations. It was concluded that, although the value of k does not influence the value of the equilibrium depths in the respective branches, it determines the resulting morphological time-scale. The larger, the value of k, the faster equilibrium is reached.

They also constructed an experimental test rig in the Hydraulics and River Engg. Laboratory, BUET, Dhaka to conduct experiment on river bifurcation. The test rig was built within the frame work of the BUET-DUT University Linkage Project. The construction was based on a design made in the Netherlands (Dekker and van Voorthuizen, 1993, after Dekker and van Voorthuizen, 1994).

In order to investigate the influence of the shape of bifurcation on the sediment distribution, they recommended three different tips or noses.

3.2.3 Secondary currents and morphological evolution in a bifurcated channel

Flow and sediment distributions at bifurcations in braided channel systems are important for short and long term morphological development. Richardson and Thorne (1995) studied the secondary currents and morphological evolution in a bifurcated channel. They tried to understand the factors which are important in determining the sediment transport distribution at bifurcation. They defined secondary currents as currents which occur in the plane normal to the axis of the primary flow. Sediment transport is strongly influenced by the secondary flow pattern.

Their hypothesis for the pattern of secondary circulation in a bifurcated channel is shown Fig. (3.1). This hypothesis of secondary flow pattern is consistent with the main morphological features of bifurcating channels. After the study they concluded that the pattern of secondary currents in a bifurcating channel is more complex than the hypothesis shown in Fig. (3.1).

It was suggested that curvature of the flow at the point of hydraulic division of the two streams of water induces vertical flow that is clockwise in the left channel and counter clockwise in the right channel. Along the middle third of the divided reach, strong vertical flow exists with a counter clockwise rotation in the left channel and clockwise rotation in the right channel. Flow patterns, bed topography and morphological changes in this middle reach correspond to the hypothesised system shown in Fig. (3.1).

3.3 Determination of nodal point relations using measured data

A literature survey on the sediment distribution at bifurcation points in natural rivers and artificial channel was carried out by Akkerman (1993, after Wang and kaaij, 1994). It was found that the curvature effect at the bifurcation and immediately upstream of the bifurcation is very important for the sediment distribution. This indicates that the sediment distribution relation or the nodal point relation is different from bifurcation to bifurcation.

3.3.1 Determination of nodal point relation using laboratory data

Wang and Kaaij (1994) fitted three data sets collected by Akkerman (1993, after Wang and Kaaij, 1994) to the power relation (eq. 2.59) and linear relation (eq. 3.10) in order to investigate the validity of the relation and in order to find an indication of the value of the power k in the relation. The fitting was done by a regression analysis using least-square. The nodal point relations found for different channels are described below.
For the Pannerdens Channel:

$$\frac{S_1}{S_2} = 2.436 \left(\frac{Q_1}{Q_2}\right)^{2.326} \tag{3.3}$$

As Fig. (3.2) shows, the agreement between the data and this relation is good and it is certainly better than that between the data and the linear relation (eq. 3.10). The width ratio of the two branches leads to $B_1/B_2 = 0.52$, which agrees well with the map.

Bifurcation Westervoort:

For the bifurcation at Westervoort, the data does not fit the relation at al. The data suggests the tendency that the larger the ratio Q_1/Q_2, the smaller the ratio S_1/S_2 which is of course strange. It was noted by Akkerman (1993, after Wang and Kaaij, 1994) that the sediment distribution at this bifurcation was disturbed by various human measures.

For the Jonglei Channel:

$$\frac{S_1}{S_2} = 2.977\left(\frac{Q_1}{Q_2}\right)^{2.938} \tag{3.4}$$

The agreement between the relation and the data seems to be good but it is noted that in this case the data only cover three values of Q_1/Q_2. The relation leads to $B_1/B_2 = 0.57$, which also agrees well with the map. Also for this case the power relation is clearly better than the linear relation.

3.3.2 Determination of the nodal point relation using prototype data

A prototype data set from the Pannerdens channel was analyzed by Fokkink (1994, after Wang and Kaaij, 1994), who found the following relation

$$\frac{s_1}{s_2} = 50\left(\frac{Q_1}{Q_2}\right)^{5.99} \tag{3.5}$$

The coefficients are clearly different from those from the scale model data set. However, it must be mentioned that measurements in nature is much more difficult than in a scale model, which means that the quality of the prototype data is usually much lower. This relation leads to $B_1/B_2 = 0.47$, which is still not far from what the map indicates.

Based on the developed nodal point relations by the data, they concluded that the sediment distribution ratio S_1/S_2 clearly depends on the discharge ratio and they suggested that the power relation (eq. 2.59) works well for most situations but the coefficients vary from case to case.

3.3.3 Research on river bifurcation carried out at BUET

A physical model on river bifurcation was built in the Hydraulics and River Engineering Laboratory, BUET, Dhaka. Roosjen and Zwanenburg (1995) and Hannan (1996) conducted experiments on this model using two different types of noses. The first nose was symmetrical and the second nose was asymmetrical (the tip is directed towards branch 1 reducing the inflow area of this branch by 50 percent with respect to the symmetrical tip. They conducted the experiments with 20 l/s, 30 l/s and 40 l/s discharges for each nose type. They used the same sediment size. The experiments on nose 1 had been completed and that on nose 2 had been completed partly. They fitted the data on the general nodal point relation (eq. 2.59) which can also be written as

$$\frac{s_1}{s_2} = M\left(\frac{q_1}{q_2}\right)^k \tag{3.6}$$

In which:

s_i = sediment transport per unit width at bifurcation in branch i
q_i = discharge per unit width at bifurcation in branch i
M = constant with value 'one'

For the first nose different values of k were found for different upstream discharges. For the second nose, however, only one value of k was found. When the upstream discharge is held constant at 40 l/s, a different value of k was found for the two different nose types. When constant upstream discharge of 30 l/s was applied only one value of k was found for two nose types.

They also simulated the data of the experiments using a computer program WENDY. The results found in the computer simulation agree well with the experimental results.

Hannan (1995) fitted the data of the experiments to the following nodal point relation

$$\frac{s_2}{s_3} = k\left(\frac{q_2}{q_3}\right)^m \tag{3.7}$$

where q_2, q_3 and s_2, s_3 are discharges and sediment transports per unit width respectively and k and m are constants. The subscripts 2 and 3 represent branch 2 and branch 3 respectively.

He concluded that the value of k and m are not the same for the same nose for different discharges. For each nose he found that the value of m increases with increase in discharge. He also found that the value of m is greater than 5/3 for all the three discharges (20 l/s, 30 l/s and 40 l/s) and concluded that it fits well with the theoretical analysis.

3.4 1D Network morphodynamic models

3.4.1 1D Mathematical computer models

Delft Hydraulics developed an one-dimensional model WENDY (Delft Hydraulics, 1991). Another model SOBEK was developed jointly by Rijswaterstaat/RIZA and Delft Hydraulics (Delft Hydraulics and Rijkwaterstaat/RIZA, 1992).

The WENDY software package consists of a comprehensive set of application software for the simulation of water flow, sediment transport, morphology and water quality in open channel networks. In particular, WENDY is applicable in river and estuary studies and river and estuary engineering.

For distribution of sediment over the two bifurcating branches, WENDY has two default options.
One options is

$$\frac{S_1}{S_2} = \frac{Q_1}{Q_2} \tag{3.8}$$

Where S_1 and S_2 represent the sediment transport rates and Q_1 and Q_2 represent the discharges over the two downstream branches. In the SOBEK model, this option will probably be the default option for all bifurcations with two downstream branches and the only option for bifurcations with three or more downstream branches.

The second default option is

$$\frac{S_1}{S_2} = \frac{B_1}{B_2} \tag{3.9}$$

where B_1 and B_2 represent the widths of the two downstream branches.

This relation may give serious problems. The widths are constant during a one dimensional computation. As a consequence, the ratio B_1/B_2 is constant resulting in a constant ratio S_1/S_2. This means that even when for example one of the branches is almost closed, the same amount of sediment is transported into the branch. This is physically not realistic.

In the WENDY manual (Delft Hydraulics, 1991), a warning is given for using these options:

"In many cases these two possibilities will not lead to satisfactory results. When a model is calibrated, it will appear that the calibration results are strongly influenced by the sediment distribution at bifurcation".

Another option which is available in both WENDY and SOBEK model is

$$\frac{S_1}{S_2} = \alpha \left(\frac{Q_1}{Q_2}\right) + \beta \tag{3.10}$$

where α and β are constants to be given by the user. It is a linear equation. But sediment transport rate hardly varies linearly with discharge. Besides, when the number of the branches changes, it becomes a non-linear equation. when α=1 and β=1, it is similar to the first default option.

The application of WENDY program has an important restriction : as WENDY is a one dimensional model, problem areas strongly governed by two or three dimensional effects are not represented well. However, practice has shown that in many cases basically two dimensional (horizontal) flow can be properly simulated with WENDY provided that the flow system has a typical gully character (Delft Hydraulics, 1991). Moreover, WENDY can account for non-uniform flow distribution in the flow channels.

3.4.2 Nodal point relations in 1D network morphodynamic models

Wang et.al (1993) analyzed the nodal point relations in 1D network morphodynamic models. They first performed computation on a numerical example using the nodal point relation $S_1/S_2 = Q_1/Q_2$. They considered the equilibrium state with the two branches open (symmetrical). To examine whether the equilibrium state is stable, they allowed a small disturbance in depth ($a_1 < a_2$). They found that the disturbance causes over loading in branch 1 and under loading in branch 2. This means that branch 1, which is shallower, will become even shallower and the deeper branch 2 will become even deeper. This indicates that the equilibrium state ($a_1 = a_2$) is unstable and the computation converges to the situation that branch 1 is closed. Similarly, if the initially disturbed state is such that $a_1 > a_2$, then the computation will converge to the situation that branch 2 is closed.

After numerical computation, they made a theoretical analysis. Using the nodal point relation $S_1/S_2 = Q_1/Q_2$, they found that there are three equilibrium states. The first equilibrium state describes the situation in which both branches of the river remain open; the other two states describe the situation in which one of the branches closes. They also found that the first equilibrium state is unstable and the latter pair is stable. On the basis of their analysis, they proposed the nodal point relation $S_1/S_2 = (Q_1/Q_2)^m$ instead of $S_1/S_2 = Q_1/Q_2$, where m is a constant. With this new nodal point relation, they found that there are three equilibria. The equilibrium at (a,a) is unstable if $m < 5/3$ and stable if $m > 5/3$ provided Engelund-Hansen transport formula is used. They also used the nodal point relation $S_1/S_2 = B_1/B_2$ where the sediment distribution is constant and found that there is no stable equilibrium. So they recommended to exclude this nodal point relation.

3.4.3 Fundamental aspect of 1D morphodynamic models

Fokkink and Wang (1993) extended the analysis carried out by Wang et. al (1993). The analysis was extended in two ways, first by taking the hydraulic radius into account and second by considering a width-depth relation of bed.

They proposed the following general nodal point relation:

$$\frac{S_1}{S_2} = \left(\frac{Q_1}{Q_2}\right)^k \left(\frac{B_1}{B_2}\right)^l \tag{3.11}$$

In which:

S denotes sediment transport, Q denotes discharge and B denotes channel width. The indices denote the different channels and k is a positive exponent and l is equal to 1-k.

If B_1 is equal to B_2, the new nodal point relation is the same as the old one proposed by Wang et. al (1993). The width have been incorporated in this relation because the widths of channels 1 and 2 have a strong influence on the equilibrium position. With this new nodal point relation, they concluded that if k is smaller than 5/3, the nodal point relation unstable and if k is larger than 5/3, the nodal point relation is stable. If hydraulic radius is taken into account then the nodal point relation is stable if k is larger than 5; it can be stable or unstable if k is in between 5/3 and 5, depending on the geometry of the network; it is unstable if k is smaller than 5/3.

A number of WENDY simulation have been carried out for bifurcations in non-tidal rivers. The general nodal point relation (eq. 2.59) was applied in the simulations. Different values of l (with k=1-l) were used. Further different geometries of the bifurcation were considered in the simulations. In agreement with the theoretical analysis, the bifurcation appears to be stable (both branches remain open) for large values of l and unstable (one of the branches closes) for small values of l. It was also concluded from the computational results that the critical value is larger than the theoretical value. Because hydraulic radius was approximated by depth in the theoretical analysis.

For the simulations for the case of bifurcation at the downstream side of a tidal river the same conclusion was drawn. The bifurcation is stable when the value of k is large and unstable when the value of k is small. This agrees fully with the conclusions from the theoretical analysis.

3.4.4 Morphodynamic development of secondary channel

Wang and Kaaij (1994) analyzed the possible equilibrium states after the construction of the secondary channel, the stability of the equilibrium states and the time scale of the morphological development when the system is not in equilibrium. They extended the analysis of Wang et. al (1993) by using Meyer-Peter-Muller (MPM) sediment transport formula. The following observations were found.

For small value of k (smaller than about 1.3), there are three equilibrium states. The equilibrium state with both branches open is unstable. The other two equilibrium states with only one of the branches open are stable. This is the same as the conclusion drawn from the analysis of Wang et. al (1993). However, the critical value of k is no more a constant. It depends on the sediment transport parameter.

For a large value of k (larger than 1.3), there are in total five equilibrium states. Three with both branches open are stable and the two equilibrium states of which the positions depend on the value of k, are unstable.

According to their analysis on morphological time scale, there are basically two morphological time scales with different order of magnitude. As a consequence the system will first react with the smaller time scale and then develop with the larger time scale. The closer of the secondary channel is related to the larger time scale. This means that for the first period the minor change of the secondary channel may be neglected. Therefore rapid siltation in the main channel is expected in this period. Corresponding to the slow closer of the secondary channel the main channel starts to erode after the first period, tending to restore the original bed level.

They also performed numerical simulations with SOBEK. Most of the simulations show a similar behaviour of the system. Only the case with time varying discharge and the case with finer sediment in the secondary channel show significant difference in the behaviour of the system. This means that the final morphological evolution on the design of the secondary channel should be based on the time-varying discharge and that special attention should be paid to the grain size in the secondary channel.

3.4.5 Stability of river bifurcation in 1D morphodynamic models

The stability of river bifurcation in 1D morphodynamic model was analyzed by Wang et. al (1995). They considered the nodal point relation that the ratio between the sediment transports into the downstream branches is proportional to a power of the discharge ratio. The influence of the nodal point relation appears to be crucial for the stability of the bifurcation in the model. For large values of the exponent, the bifurcation is stable, i.e. the downstream branches remain open. For small values of the exponent, the bifurcation is unstable: only one of the branches tends to remain open. The exponent also has a strong influence on the morphological time-scale of the network.They also verified the conclusions by numerical simulations using a package for one dimensional network modelling.

3.4.6 Sensitivity analysis of 1D morphodynamic network models

The morphodynamic behaviour of 1D network model is extremely sensitive to certain parameters in the sediment transport formula and nodal-point relation. Fokkink et. al (1995) analyzed the sensitivity of three parameters (k,n,c) in 1D network morphodynamic model. One parameter (k) is from the nodal point relation (eq. 3.11) and the other two parameters (n,c) are from the sediment transport formula. The sediment transport formula is

$$s = M(u - c)^n \tag{3.12}$$

In this equation, M is a constant and n is a positive exponent. The constant c is a threshold value which signifies the initiation of sediment transport. The optional choice of the parameters depends on the sediment transport formula. For instance the threshold value c is zero if the Engelund-Hansen formula is used, whereas it is positive for the Meyer-Peter-Muller formula.

There are obvious three equilibrium states independent of c: branch 1 and branch 2 have depth equal to the main channel (state A); branch 2 is closed (state B); branch 1 is closed (state C). For large values of k, A turns into a stable case and B, C are unstable. There are two extra unstable states D and E in the case that c is greater than zero. The states B and C remain stable for large values of k. For small values of c, the states D and E are close to B and C. For large values of C, they are close to A. For c equal to zero, i.e. a power-law transport formula, B coincides with D and C coincides with E.

In summary, the exponent k and n mainly influence the state A, whereas the threshold value c influences the states B,C,D,E.

CHAPTER 4

EXPERIMENTAL SET-UP AND METHODOLOGY

4.1 Introduction

A basic set-up of the physical model to study the river bifurcation phenomenon was constructed in 1993 at the laboratory of Water Resources Engineering Department by previous investigators (Roosjen and Zwanenberg, 1995 and Hannan, 1996). This set-up was such constructed so that experiments can be conducted as per requirement of the objective to know the insight of the behaviour of river bifurcation. The set-up also had the flexibility needed to carry out further studies in future. Thus the available facilities were adopted and modified for the purpose of this study.

4.2 The experimental set-up

The construction of the experimental set-up was based on a design made by Dekker and van Voorthuizen (1993). The layout of the model is shown in Fig. 4.1. The model consists of two parts: permanent part and temporary part (Fig.4.2).

4.2.1 The permanent part

The permanent part is the experimental facility necessary for storage and regulation of water circulation through the model and guidance of this water to and from the temporary part. The permanent part can be divided into three elements: the water supply system, the sediment supply system and the regulating and measuring system of the model.

4.2.1.1 The water supply system

The circulation of the water within the model is a closed system. From the downstream reservoir the water is transported by means of the pipeline to the upstream reservoir. Consequently it flows through the experimental model and returns to the downstream reservoir. The water supply system consists of the downstream reservoir, the pipe line system and the upstream reservoir.

The downstream reservoir

The downstream reservoir serves many functions. It provides required suction head necessary for the pump, it serves as an independent water supply system. There is a spillway and a valve at the end of the downstream reservoir. The spillway is used to remove excess water. The valve attached to the reservoir is used to empty the reservoir for cleaning or repairing purpose.

The pipeline system

The transport of water is taken care of by the pipeline system. The pump sucks the water from the downstream reservoir into the pipeline. The T-joint on top of the pump divides the water over the excess pipe and the delivery or supply pipe. Both the pipes contain valves. As the pump delivers a constant discharge, the required discharge through the model must be supplied by operating these valves. The excess pipe dumps the water back into the downstream reservoir. The delivery pipe transports the water to the upstream reservoir.

The upstream reservoir

The upstream reservoir consists of two basins. The water from the pipeline enters the upstream reservoir in the stilling reservoir. The function of this small rectangular reservoir is to dampen the turbulence in the water caused by all the bends in the pipeline. The stilling reservoir is separated by a wall from the larger basin of the upstream reservoir.

For maintenance purposes the upstream reservoir can be emptied through a small pipe with a valve, incorporated in one of the walls. By opening the valve the water flows away into an existing drain in the laboratory.

4.2.1.2 The sediment supply system

Just as the water, the sediment also circulates during an experiment. Starting the model introduces a sediment transport as a result of the flow velocity. Sand is transported downstream and has to be refilled from upstream. Therefore, two sand feeders placed at the beginning of branch 0 provide for the supply of sand. The amount of sediment supply depends on the equilibrium state in branch 0. A motor is used to run the sandfeeder. The sand first falls on a sand distributor via a tube which is connected to the sandfeeder. The sand distributor distributes the sand over the inflow section of branch 0.

4.2.1.3 The regulating and measuring system

The regulating and measuring system consist of tail gates, stilling basins and transition flumes, guiding vanes and tubes, approach channels, Rehbock weirs, stilling basins connected with Rehbock weirs.

The tail gates

The regulating function of the downstream end is provided by two tail gates. The tailgates rotate around a horizontal axis. They are used to fix the downstream water level constant.

Another function of tail gates is to close the model during non-running periods. The tail gates prevent the water from flowing away, which would cause an unacceptable dry bed.

The stilling basins and transition flumes

Behind the tail gates the water falls into a stilling basin. In case of the water from branch 1 this is a larger basin than in case of branch 2. Just after stilling basins there are two transition flumes.

The guiding vanes and tubes

To ensure a more smooth flow towards the approach channels, guiding vanes are placed between the transition flumes and the approach channels. These vanes guide the water around the corner. In order to prevent creation of extra unwanted turbulence in the approach channels, on both the upstream and downstream side of the guiding vanes PVC-tubes are fixed.

The approach channel

Two approach channels are provided after the guiding vanes. The function of both the approach channels is to reduce the turbulence in the water.

The Rehbock weirs

The Rehbock weirs form the measuring facility of the model. The discharge distribution over branch 1 and branch 2 is measured with the Rehbock weirs. The weirs are placed at the downstream end of the approach channels.

The stilling basins connected with Rehbock weirs

For the measurement of the water height above the Rehbock weirs two stilling basins are built along the downstream reservoir. A hole is implemented in the floor of the approach channel through which a pipeline is fixed. The pipeline (dia = 1.5 cm) connects the approach channel with the stilling basin. The water level in the stilling basin is representative for the water level at the Rehbock weir. In the stilling basin the water level is measured with a point gauge.

4.2.2 The temporary part

The temporary part consists of the actual experimental model of river bifurcation. It is a mobile bed model with fixed banks. The layout of the model comprises of three branches: a main branch (denoted by branch 0) which bifurcates into two separate branches: branch 1 and branch 2. To avoid accidental equilibrium during experimentation, branch 1 and branch 2 have different widths. The different elements of the temporary part (Fig. 4.3) are described in the following sections.

4.2.2.1 Inflow section

An inflow section and inflow branch of considerable length are needed to ensure an equal distribution of sediment transport and stable flow conditions before the water reaches the bifurcation. Water flows from the upstream reservoir via the inflow section. PVC tubes (dia = 2.7 am; length = 30 m) are placed over the width of entrance gate in order to reduce larger eddies present in the upstream reservoir and thus stabilize the flow. A sandfeeder situated on the side of the tubes distributes sand over the width of the channel into the flow. The distribution of sand over the width of the channel is done by a wooden structure which is called sand distributor.

4.2.2.2 The characteristics of branch 0

This is the main branch of the river which splits up at the bifurcation. The width and length of branch 0 is 1.00 m and 4.55 m.

4.2.2.3 The characteristics of branch 1 and branch 2

At the bifurcation, the flow is split into branch 1 and branch 2. The width, length and radius of branch 1 and branch 2 are given below.

Branch 1 : Width(B_1) = 0.40 m; Length(L_1) = 8.60 m; Radius(R_1) = 23.5 m.
Branch 2 : Width(B_2) = 0.60 m; Length(L_2) = 8.40 m; Radius(R_2) = 25.5 m.

4.2.2.4 Configuration of the bifurcation

The distribution of sediment transport rate to the downstream branches is governed by the local flow pattern at the bifurcation. Thus the shape of bifurcation plays an important role in this distribution. Therefore, the nose of the bifurcation is implemented as a flexible component of the model : whereas the entire model is made of brick work. Different shapes of noses can be constructed to conduct the experiment.

4.2.2.5 Sandtraps

There are two sandtraps in the model. One is located at the end of branch 1 and another is located at the end of branch 2. The main function of sandtrap is to intercept the sediment transported through the branch so that the average sediment transport rate can be determined for the branch. Another function of sandtrap is to prevent the sand from coming into the permanent part of the model which includes the reservoir and the pump system.

The length, width and capacity of each sandtrap is given below:
Sandtrap 1: Length = 2.0 m; Width = 0.4 m; Capacity = 0.63 m^3.
Sandtrap 2: Length = 2.0 m; Width = 0.6 m; Capacity = 0.72 m^3.

4.2.2.6 Outflow section

At the downstream end of the model, the water in each branch flows over a tail gate into the permanent part of the model where the discharge is measured before spilling into the downstream reservoir. The tail gates regulate the water level in each branch and prevent the sand bed from running dry.

4.3 Fixation of reference level

The water level and bed level measurements have to be taken with respect to a specific reference level. The method of fixing the reference level is as follows.

Fill the model with water to a certain arbitrary level (z) above the laboratory floor. In order to prevent movement of water, take care that the ceiling fans are not working. This should provide a perfectly horizontal water level. Now measure this water level with the equipment to be used for measuring water levels and bed levels during the experiments. There is no need to adjust the zero's of the measuring instruments of this arbitrary reference level. The zero's of the measuring instruments should be such that one can later on measure the bed levels and water levels, which he anticipates to occur in the model during the experiments. For each measuring instrument it is now obtained a reading (x), corresponding to a water level or bed level, having an elevation of z above the laboratory floor. For any other reading (y), the elevation (elev.) of the water level or bed level above the laboratory floor can be computed by using eq. (4.1)

$$\text{elev.} = z - x + y \tag{4.1}$$

For illustration, eq. (4.1) is depicted in Fig. 4.1

It is not important to know the exact elevation of the still standing water level in the model above the laboratory floor. Important is that all bed levels and water levels refer to the same reference level.

There are two measuring beams: one is wooden made and another is made of iron. There are two separate pins. One is called long pin and the other is called short pin. The iron measuring beam is used for branches 1 and 2 and the wooden measuring beam is used for branch 0. No corrections for thickness of the wooden measuring beam etc. are required. They are incorporated into the reference level. In addition, no correction for long pin or short pin is required. However, a record is kept whether the reference level refers to a short pin or a long pin. For accuracy, 5 points are measured in a cross-section located in branch 1 and 2 and 10 points in a cross-section located in branch 0. These distances are marked on the measuring beams. The reference levels are measured at these locations. In these way the bending of the measuring beam is corrected.

The position of the measuring beam is located on the side walls in such a way that it can exactly be placed in the same way on the side walls everytime. The cross-sections 9,10,11 and 12 are relocated in such a way that they are perpendicular to the flow direction. All the measuring devices are checked whether they are standing exactly vertical.

Before the start of the experiment, it is checked whether the zero or some else of one of the gauges might have changed. This can be done in the following way:

There is a still-standing water level in the model before starting an experiment. Now a new temporarily set of reference levels is measured for each individual measuring device. The old fixed reference levels are subtracted from each temporarily reference level for each measuring device. For each measuring device, the same constant value should be obtained. In case one particular measuring device gives an other value, something is wrong.

4.4 Calibration of the instruments

Calibration of Rehbock's weirs, sandfeeder and sand buckets needs to be done to ease the work for conducting experiments. The procedures of their calibration are described in the following sections.

4.4.1 Calibration of Rehbock weirs

The discharge distribution over the two downstream branches of the bifurcation is measured by the use of Rehbock weirs. The discharge equation of a Rehbock weir is (ISO, 1975, after Dekker and van Voorthuizen, 1994)

$$Q_R = C_c \frac{2}{3}\sqrt{2g}\; b\; h_c^{3/2} \tag{4.2}$$

with

$$h_c = h+h_k = H+0.0072 \tag{4.3}$$

$$C_c = 0.602 + 0.083\ h/p \tag{4.4}$$

where:

Q_R is the discharge measured over the Rehbock weir;
C_c is the coefficient of discharge;
b is the measured width of the weir;
h_c is the effective piezometric head with respect to the level of the crest;
h is the measured head;
K_h is an experimentally determined quantity which compensates for the influence of surface tension and viscosity;
P is the apex height in meters.

The width and the apex height of both Rehbock weirs were measured by Dekker and van Voorthuizen (1994).

Rehbock weir 1: p = 0.1719 m; b = 0.4969 m.
Rehbock weir 2: p = 0.1753 m; b = 0.4978 m.

Using the above constant values and the equation, calibration tables of the Rehbock weirs were made by Hannan (1995). These tables are used to find the discharge just knowing the measured head h.

4.4.2 Calibration of sandfeeder

Calibration of sandfeeder is required to supply the sediment corresponding to a particular discharge. The sandfeader belongs to the speeds ranging from 0 to 250 rpm. At each speed the amount of sand per hour is measured three times. Then it is averaged. Thus a calibration table is prepared showing the amount of sand that outflows per hour for a particular speed. The calibration table is given bellow:

Table 4.1 Calibration chart of sandfeeder

Speed in rpm	0	25	50	75	100	125	150	175	200	225	250
Amount of sand in kg/hr	0	4.70	18.68	29.05	34.75	38.10	41.85	44.97	47.97	48.33	51.83

4.4.3 Calibration of sand buckets

Sand buckets are required to carry the sand from the sandtrap for measurement. These sand buckets need to be calibrated so that the amount of sand from sandtrap can be found just knowing the point gauge reading of water level in the sand bucket and the weight of bucket, sand and water in the balance. First the empty weight of the bucket is measured. Then the bucket is filled up with water to a certain level. Then the weight of bucket and water is measured. At the same time the point gauge reading of the water level is taken. The difference of the two weights gives the weight of water corresponding to a particular point gauge reading. Thus for different levels the weight of water is measured. And a calibration chart is prepared showing the weight of water corresponding to a particular point gauge reading for a particular bucket.

4.5 Preparation of initial bed

For preparation of initial bed, the normal depths in the three branches have to be known because for the run one needs to put the bed level in the model in such a away that a uniform flow is obtained. If the flow is not uniform, the results of the experiments could be influenced by non-uniform flow conditions. Besides, if the normal depths are not known, then it is not known whether there will be any sediment transport in both the two downstream branches or not.

The normal depths are calculated in the following way:

First the upstream discharge, Q_0 and the ratio of the downstream discharges, Q_1/Q_2 are chosen. From the values of Q_0 and Q_1/Q_2, the values of Q_1 and Q_2 are found as

$$Q_1 = \frac{Q_0}{1 + \frac{1}{Q_1/Q_2}} \tag{4.5}$$

$$Q_2 = \frac{Q_0}{1 + Q_1/Q_2} \tag{4.6}$$

Now, Chezy's formula for uniform flow is

$$u_0 = C\sqrt{h_o i} \tag{4.7}$$

Now,
$$Q_0 = A_o u = B_0 h_0 C\sqrt{h_0 i} \tag{4.8}$$

$$\therefore \quad h_0 = \frac{\left[\frac{Q_0}{B_0 C}\right]^{2/3}}{i^{1/3}} \tag{4.9}$$

Similarly

$$h_1 = \frac{\left[\frac{Q_1}{B_1 C}\right]^{2/3}}{i^{1/3}} \tag{4.10}$$

and
$$h_2 = \frac{\left[\frac{Q_2}{B_2 C}\right]^{2/3}}{i^{1/3}} \tag{4.11}$$

where:

h_o, h_1, h_2	=	normal depths of water in branch 0, branch 1 and branch 2 respectively
Q_0	=	upstream discharge
Q_1, Q_2	=	downstream discharge in branch 1 and branch 2 respectively
C	=	Chezy's roughness coefficient
i	=	longitudinal bed slope
B_0, B_1, B_2	=	widths of branch 0, branch 1 and branch 2 respectively.

Using these normal depths and the reference level, the initial bed is prepared. In order to save time, a spreadsheet programme has been developed to compute initial bed level reading.

4.6 Determination of upstream sediment load

Determination of upstream sediment load to be supplied during an experiment for a particular discharge is needed so that equilibrium condition (i.e. no siltation, no erosion) is achieved. To determine the upstream sediment load Engelund-Hansen sediment load transport formula is used which is as follows:

$$\frac{s}{\sqrt{g\,\Delta D^3}} = \frac{0.05}{(1-\epsilon)}\,\frac{C^2}{g}\,\theta^{5/2} \tag{4.12}$$

in which:

s = sediment transport in situ, including pores in m^2/s
g = acceleration due to gravity ($g = 9.814\ m/s^2$)

$$\Delta = \frac{\rho_s - \rho}{\rho}$$

ρ_s = density of sediment = 2650 kg/m^3
ρ = density of water = 1000 kg/m^3
D = D_{50} = sediment size in m
ϵ = porosity (content of pores)
C = chezy coefficient $m^{1/2}/s$

$$\theta = \frac{hi}{\Delta D}$$

i = slope of water level
h = depth of water in m

The Engelund-Hansen sediment transport formula is used because it has been observed that this formula is more accurate for the physical model of river bifurcation than the other formulae (e.g. van Rejn, Einstein etc.).

The sand which is used in the experiment has D_{50} equal to 270 μm and the value of chezy's roughness coefficient is assumed to be 30 $m^{1/2}/s$. For a particular discharge the normal depth is known. Thus the amount of sediment to be supplied from the sandfeeder can be found to maintain equilibrium condition.

4.7 Measurement of parameters describing bifurcation

The main objective of this study is to find the influence of nose angle on sediment distribution at channel bifurcation. The measurements which are needed are described in the following sections.

4.7.1 Measurement of discharge

The individual discharges of branch 1 and branch 2 are measured with the respective Rehbock weirs. The water level at the crest of the weirs is measured in stilling basins with point gauges, with an accuracy of 0.05 mm. The zeros of the point gauges were set by filling the two approach channels with water upto the crest level of the weirs; the point gauges were then adjusted and the zeros fixed. The water levels in the stilling basins are measured at every 15 minutes. Using the calibration chart, the discharges are found.

4.7.2 Measurement of water level

The water level is measured at four places in the model: in stilling basins placed at the beginning and end of each branch and at bifurcation.

The stilling basins I, III and IV are fixed stilling basins. They render the water level present in a fixed place of the adjacent branch, namely the water level immediately in front of it. The water seeps through a hole in a wooden plate fixed in the wall of the branch. This wooden plate can be moved up and down to ensure that the seepage hole is always located between the water level and the bed level. Stilling basin II, which is located near the bifurcation, is a flexible stilling basin. This stilling basin is completely closed (i.e. there is no connecting hole from basin to the branch). The water is syphoned into the stilling basin via a Pitot tube mounted on a frame laid across the width of the channel. The Pitot tube can be moved to different spots in the channel so that it is possible to measure the water level at different places, near the bifurcation. This is necessary because different shapes of noses are used which each includes different local flow patterns. It must be noted that the Pitot tube is merely used as a syphon, and not as a measuring device: the readings are done with a point gauge in the stilling basin.

Stilling basins III and IV are placed directly upstream of the sandtraps. They are used together with the tail gates to regulate the downstream water level. This water level is checked at regular intervals during experimentation to ensure that the correct downstream boundary condition is being induced.

The water level in a stilling basin is measured with a point gauge. The zeros of the point gauges were set by filling the branches of the model with water, which made a horizontal reference level to which all four gauges were related.

4.7.3 Measurement of bed levels

Measurement of bed levels is done both at the start and at the end of the experiment. The bed level is measured with a point gauge in which a special pin is used. A square plate of 2x2 cm^2 is fixed to the point of the pin to prevent it from sinking too deep into the sand bed.

In branch 0, the bed level is measured in 10 points of each cross-section. In branch 1 and 2, the bed level is measured in 5 points of each cross-section.

4.8 Sediment transport measurement

The sediment transport rates in branches 1 and 2 are determined with the help of the sandtraps located at the end of each branch. These sandtraps intercept all sediment transported through the branches. In the following sections, the detailed procedure of determining sediment transport rate is given.

4.8.1 Measuring the sand in the sandtrap

For measuring the amount of sand in the sandtraps, the following procedure is followed. Buckets filled with sand and water are compared with buckets filled with only water. The weight that is found is the submerged weight of sand. This can be proved by the following calculation:

If : W = weight of bucket
V_1 = total volume
V_2 = volume of sand in situ
ϵ = porosity of sand
ρ = density of water
ρ_s = density of sand

Then:

weight of bucket and water is

$$W_1 = W + (V_1 \times \rho)$$

weight of bucket, water and sand:

$$W_2 = W+(V_1-V_2)\ \rho+V_2\ (1-\epsilon)\ \rho_s+V_2\ \epsilon\rho$$

Subtracting from each other gives:

$$\begin{aligned} W_2-W_1 &= \{W+(V_1-V_2)\ \rho+V_2\ (1-\epsilon)\ \rho_s+V_2\ \epsilon\rho\} - \{W + (V_1 \times \rho)\} \\ &= V_2\rho+V_2(1-\epsilon)\rho_s+V_2\epsilon\rho \\ &= V_2(1-\epsilon)\rho_s-V_2(1-\epsilon)\rho \\ &= V_2(1-\epsilon)(\rho_s-\rho) \end{aligned}$$

From above, it is seen that this is the law of Archimedes. The first part of the equation represents the weight of dry sand and the second part the lift force caused by the water. So comparing the two buckets leads to the submerged weight of sand.

In practice, measuring the sand is as follows. After an experiment has been done, the stop locks will be placed. Then the water in the sand trap can be syphoned out. Next buckets can be filled with sand and brought to the scale. On the laboratory floor, a scale is placed. Above the scale a point gauge is hinged to the wall. So the weight and water level can be measured in one time.

The buckets have been standardized, so for every bucket tables of weight and water levels have been made. When a certain water level is found, the weight of water and bucket can be found in the table. Subtracting this weight from the weight found, gives the submerged weight of the sand.

To compare the amount of sand, found in the sandtrap with the change in bed level, the volume of the sand has to be known. This can be done by dividing the weight by the submerged density of the sand (1650 kg/m^3). Now the volume of sand with the pores is found. Here the pore volume is about 40%. So to correct the volume for the pore volume it is multiplied by 100/60.

4.8.2 Determination of volume of sand deposited or eroded in the branches

As mentioned earlier that the bed level measurements are taken both at the start and at the end of the experiment. The difference of these two bed level measurements gives the depth of deposition or erosion. Now the volume of sand deposited or eroded in between two cross-sections can be determined by the following formula.

$$V_{1\text{-}2}=\frac{1}{2}(B_1h_1+B_2h_2)L_{1\text{-}2} \qquad (4.13)$$

in which:

$V_{1\text{-}2}$ = volume of sand deposited or eroded in between cross-sections 1 and 2
B_1, B_2 = width of cross-sections 1 and 2 respectively.
h_1, h_2 = difference between initial and final bed level readings
$L_{1\text{-}2}$ = distance between cross-sections 1 and 2.

In the similar way, the volume of sediment deposited or eroded in other cross-sections is determined. Thus if V_o, V_1 and V_2 are the volumes of sediment deposited or eroded in branch 0, 1 and 2 respectively, then

$$V_0 = V_{1\text{-}2} + V_{2\text{-}3} + \ldots + V_{8\text{-}9} \qquad (4.14)$$
$$V_1 = V_{9\text{-}10}(R) + V_{10\text{-}11}(R) + \ldots + V_{41\text{-}39} \qquad (4.15)$$
$$V_2 = V_{9\text{-}10}(L) + V_{10\text{-}11}(L) + \ldots + V_{40\text{-}26} \qquad (4.16)$$

If the volume is positive it means deposition and if negative it means erosion.

Here, it is noted that branch 0 belongs to cross-sections 1 through 9, branch 1 belongs to cross-sections 9(R) through 40 and branch 2 belongs to cross-sections 9(L) through 26. Cross-sections 41 and 40 have been introduced in between cross-sections 38 & 39 and 25 & 26 respectively. The letters R and L refer to right and left respectively.

4.8.3 Sediment balance

Let,

ST_1, ST_2 = volume of sediment traped in sandtrap 1 and 2 respectively
V_{sf} = volume of sediment supplied by the sandfeeder
S_o, S_1, S_2 = volumes of sediment flowing through branch 0, 1 and 2 respectively.

Now,

$$S_0 = f\,(V_{sf}, V_0, V_1, V_2, ST_1, ST_2) \tag{4.17}$$
$$S_1 = f\,(V_{sf}, V_0, V_1, V_2, ST_1, ST_2) \tag{4.18}$$
$$S_2 = f\,(V_{sf}, V_0, V_1, V_2, ST_1, ST_2) \tag{4.19}$$

Sediment balance in branch 0 (Fig. 4.6):

In - out = storage
$$\Rightarrow V_{sf} - S_0 = V_0$$
$$\Rightarrow S_0 = V_{sf} - V_0 \tag{4.20}$$

Sediment balance in branch 1 (Fig. 4.7):

In - out = storage
$$\Rightarrow S_1 - ST_1 = V_1$$
$$\Rightarrow S_1 = V_1 + ST_1 \tag{4.21}$$

Sediment balance in branch 2 (Fig. 4.8):

In - out = storage
$$\Rightarrow S_2 - ST_2 = V_2$$
$$\Rightarrow S_2 = V_2 + ST_2 \tag{4.22}$$

4.8.4 Sediment transport rate

Sediment transport rate is determined by dividing the amount of sediment by the time elapsed. Thus the sediment transport rates in branch 0, 1 and 2 respectively are

$$s_0 = \frac{S_0}{T} \tag{4.23}$$

$$s_1 = \frac{S_1}{T} \tag{4.24}$$

$$s_2 = \frac{S_2}{T} \tag{4.25}$$

In which:

s_0, s_1, s_2= sediment transport rates in branch 0, 1 and 2 respectively
T = total experimentation time

4.9 Checklist to conduct the experiments

Running the experiment and collecting data requires not only a great deal of physical work but also a careful observation. In order to facilitate work, the following checklist has been developed (after Dekker and van voorthiuzen, 1994).

Before running:

- choose the upstream discharge, Q_0
- estimate the rate of sand to be supplied
- prepare the initial bed using Q_0, Q_1, Q_2 and reference level established ago.
- fill up the model with water
- take initial bed level readings
- be sure that the sand feeder is filled.
- be sure that the sandtraps are empty
- be sure that the valves are positioned so that the right discharge can be obtained.
- install the Pitot tube
- check the zero levels of the four stilling basins and two measuring frames.
- check the zero levels of the two Rehbock weirs to the stilling basins.

During running:

- put the date and experiment number on every form
- fill in the head form
- measure at the start and at the end the sandfeeder capacity
- check whether the Pitot tube is still running
- check whether the holes to the stilling basins are still open
- measure the discharge at every 15 minutes
- make a graph showing the discharge against time.
- measure the water level at every 30 minutes.
- when the levels in the downstream branches are changing adjust them by tail gates
- check the sandfeeder at every hour.

After running:

- put the stop locks in and make them water tight with the help of tube
- syhpon the water out from the sandtraps
- when the water is out of the sandtraps, let someone make them empty and measure the weight of sand coming out.
- during syphoning and emptying measure the final bed level readings of the run.
- input the data obtained to the computer in order to get the desired results.

4.10 Description of the noses used in the experiment

There are four noses. The first three noses were designed by Dekker and van Voorthuizen (1994). The last nose is designed by the author.

Nose 1 is a symmetrical nose (Fig. 4.9). The experiments using this nose were completed through an on going research project.

Nose 2 is a asymmetrical nose (Fig. 4.10) from which the tip is directed towards branch 1 reducing the inflow area of this branch by 50% with respect to the symmetrical tip.

Nose 3 is also a asymmetrical nose (Fig. 4.11) from which the tip is directed towards branch 2 reducing the inflow of this branch by 50% with respect to the symmetrical tip.

Nose 4 Fig. (4.12) is designed in such a way that it's tip divides the inflow area of the main branch equally.

4.11 Nose angle

The main objective of this study is to find the influence of nose angle on sediment distribution at channel bifurcation. The nose angle is defined in the following way:

The nose angle, θ may be defined as the angle between the tip of the nose and the symmetrical line of a bifurcation.

It is positive when the tip rotates in the counter clockwise direction and negative in the clockwise direction from the symmetrical line. Thus symmetrical nose corresponds to nose angle of 0°. Fig. 4.13 shows the definition sketch of nose angle. According to this definition, the different nose angles are shown in Fig. 4.14.

4.12 Experiment numbering

In order to prevent mixing of the results of the runs, the experiments are coded. The procedure of experiment numbering is described below.

The experimental numbering is chosen in such a way that all the variables can be recognized. For the experiments, several influences are studied - the upstream discharge, the nose type (i.e. nose angle), the discharge ratio.

The first number of the experiment code represents the upstream discharge. In the former section, it is described that three different upstream discharges are used. There is a discharge of 20 l/s, represented by a one in the code, a discharge of 30 l/s represented by a two in the code and a discharge of 40 l/s represented by three in the code.

The second number in the code represents the nose type. The symmetrical nose is represented by number one. The other nose members has been described in chapter 4.

In order to get different points of Q_1/Q_2 and S_1/S_2, the discharge ratio Q_1/Q_2 is changed. The third number in the code represents the discharge ratio. For each change the third number in the code is increased by one.

For a particular discharge ratio, the run is continued until equilibrium is reached. This may take several days. The forth number of the code represents the day of the run.

According to this numbering system, the experiment number 2341 contains the following features: the upstream discharge of 20 l/s, the third nose type is used, the fourth change of the discharge ratio and the first day of the run.

As the experiments of nose no. 1 were performed by Roosjen and Zwanenberg (1995) and Hannan (1996), so their numbering system is to some extent different from the system described above.

CHAPTER 5

ANALYSIS OF DATA, RESULTS AND DISCUSSIONS

5.1 Data collection

For collection of data four different nose angles, viz: 0^0, 6.97^0, -3.50^0 and -10.38^0 were choosen. Discharge in the main branch was choosen according to the carrying capacity of the channel. And sediment load in the main branch was selected for equilibrium condition, i.e. non-scouring, non-silting condition, using Engelund-Hansen sediment transport formula. For each nose angle three discharge values viz: 20 l/s, 30 l/s and 40 l/s were used. Corresponding average sediment loads were 18 kg/hr, 28 kg/hr and 44 kg/hr respectively. Data for nose angle of 0^0 were collected by previous investigator (Roosjen and Zwanenburg, 1995 and Hannan, 1996). And data for other three nose angles were collected during the present study. Measurements on the downstream branches include water level, bed level, discharges, sediment transport. The data on discharges and sediment transports in the downstream branches are presented in table 5.1 through 5.12.

Table 5.1 Data on Q_1/Q_2 and S_1/S_2 for $\theta = 0^0$ and $Q_0 = 20$ l/s
(Source: Roosjen and Zwanenburg, 1995 and Hannan, 1996)

Run No.	Q_1(l/s)	Q_2(l/s)	$S_1(m^3)$	$S_2(m^3)$	Q_1/Q_2	S_1/S_2
1311a	5.09	13.64	0.0222	0.1491	0.38	0.149
1321a	8.83	9.72	0.1045	0.0639	0.91	1.635
1321b	10.88	7.38	0.1571	0.0259	1.47	6.074
1331a	7.39	11.03	0.0855	0.0767	0.67	1.114
1331b	6.61	11.77	0.0626	0.109	0.56	0.574
1331c	6.11	12.19	0.0397	0.132	0.50	0.30
1341a	4.90	13.74	0.0322	0.137	0.36	0.235

Table 5.2 Data on Q_1/Q_2 and S_1/S_2 for $\theta = 0^0$ and $Q_0 = 30$ l/s
(Source: Roosjen and Zwanenburg, 1995 and Hannan, 1996)

Run No.	Q_1(l/s)	Q_2(l/s)	$S_1(m^3)$	$S_2(m^3)$	Q_1/Q_2	S_1/S_2
1111	9.53	18.78	0.0515	0.1375	0.51	0.374
1121	18.45	9.46	0.2427	-0.045	1.95	-5.32
1131a	9.32	22.21	0.0256	0.1769	0.42	0.145
1131b	9.95	20.42	0.0111	0.1029	0.49	0.108
1131c	11.96	18.26	0.0877	0.0878	0.65	0.999
1141a	12.94	18.94	0.0762	0.0762	0.68	1.00
1141b	12.41	19.20	0.0796	0.095	0.65	0.841
1141c	12.72	18.99	0.0784	0.0878	0.67	0.894

Table 5.3 Data on Q_1/Q_2 and S_1/S_2 for $\theta = 0^0$ and $Q_0 = 40$ l/s
(Source: Roosjen and Zwanenburg, 1995 and Hannan, 1996)

Run No.	Q_1(l/s)	Q_2(l/s)	$S_1(m^3)$	$S_2(m^3)$	Q_1/Q_2	S_1/S_2
1211a	12.56	26.04	0.0251	0.1806	0.48	0.139
1211b	13.66	24.99	0.067	0.1257	0.56	0.534
1211c	13.10	25.21	0.073	0.1299	0.52	0.562
1221a	15.57	22.85	0.1187	0.0923	0.68	1.286
1221b	14.44	24.00	0.0992	0.131	0.60	0.758
1221c	14.38	24.18	0.0764	0.1113	0.59	0.687

Table 5.4 Data on Q_1/Q_2 and S_1/S_2 for $\theta = 6.97^0$ and $Q_0 = 20$ l/s

Run No.	Q_1(l/s)	Q_2(l/s)	$S_1(m^3)$	$S_2(m^3)$	Q_1/Q_2	S_1/S_2
1211	3.916	16.349	0.0183	0.0418	0.239	0.437
1212	3.599	16.856	0.0176	0.0845	0.213	0.208
1213	3.427	16.994	0.0264	0.121986	0.201	0.216
1221	3.782	16.582	0.0217	0.0743	0.228	0.292
1231	6.830	12.585	0.0619	0.0780	0.542	3.438
1232	4.162	15.329	0.0245	0.0444	0.271	0.551
1233	3.449	16.061	0.0173	0.0617	0.214	0.280
1241	5.374	13.973	0.0408	0.0318	0.384	1.280
1242	4.033	15.465	0.0179	0.0577	0.260	0.310
1251	6.922	13.475	0.0546	0.0068	0.513	7.898
1261	6.559	13.934	0.0638	0.0084	0.470	3.623
1271	6.935	13.518	0.0580	0.0212	0.513	2.727
1281	6.480	13.905	0.0543	0.0192	0.466	2.819

Table 5.5 Data on Q_1/Q_2 and S_1/S_2 for $\theta = 6.97^0$ and $Q_0 = 30$ l/s

Run No.	Q_1(l/s)	Q_2(l/s)	$S_1(m^3)$	$S_2(m^3)$	Q_1/Q_2	S_1/S_2
2211	9.838	20.812	0.1235	0.032	0.472	3.860
2221	8.149	24.271	0.0985	0.0935	0.335	1.053
2222	5.201	26.891	0.020	0.126	0.193	0.159
2231	12.174	20.334	0.174	-0.0039	0.598	-43.601
2232	6.540	26.126	0.0409	0.1063	0.250	0.383
2241	8.681	23.721	0.1086	0.0669	0.365	1.621
2242	5.479	27.066	0.0240	0.1271	0.202	0.189
2251	9.074	21.127	0.1154	0.0606	0.429	1.902

Table 5.6 Data on Q_1/Q_2 and S_1/S_2 for $\theta = 6.97^0$ and $Q_0 = 40$ l/s

Run No.	Q_1(l/s)	Q_2(l/s)	$S_1(m^3)$	$S_2(m^3)$	Q_1/Q_2	S_1/S_2
3211	11.733	29.121	0.0963	0.0221	0.402	4.351
3212	7.624	33.404	0.0422	0.119	0.228	0.377
3213	6.727	34.351	0.0184	0.0825	0.195	0.224
3221	14.818	26.119	0.0887	-0.0182	0.567	-4.867
3222	9.773	30.877	0.0796	0.0674	0.316	1.18
3223	6.774	33.942	0.0264	0.0972	0.199	0.271
3231	11.164	30.167	0.0813	0.0467	0.370	1.737
3241	11.218	28.762	0.0986	0.0343	0.3900	2.871

Table 5.7 Data on Q_1/Q_2 and S_1/S_2 for $\theta = -10.38^0$ and $Q_0 = 20$ l/s

Run No.	Q_1(l/s)	Q_2(l/s)	$S_1(m^3)$	$S_2(m^3)$	Q_1/Q_2	S_1/S_2
1311	10.896	10.310	0.0070	0.0648	1.056	0.108
1312	13.404	7.901	0.0478	0.0414	1.696	1.155
1313	14.922	6.350	0.0565	0.0239	2.349	2.361
1321	8.183	13.140	-0.0182	0.1016	0.622	-0.179
1322	10.316	11.134	0.0047	0.0411	0.926	0.116
1323	12.732	8.768	0.0190	0.0398	1.452	0.479
1324	14.388	7.086	0.0446	0.0192	2.030	2.316
1325	15.509	5.964	0.0236	0.0119	2.606	2.106

Table 5.8 Data on Q_1/Q_2 and S_1/S_2 for θ = -10.38^0 and Q_0 = 30 l/s

Run No.	Q_1(l/s)	Q_2(l/s)	S_1(m^3)	S_2(m^3)	Q_1/Q_2	S_1/S_2
2311	14.813	14.866	0.0032	0.0872	0.996	0.037
2312	17.820	11.733	0.0416	0.0473	1.518	0.878
2313	20.002	9.562	0.051	0.0157	2.091	3.231
2321	15.833	13.793	0.0161	0.1022	1.147	0.157
2322	19.212	10.348	0.0738	0.0483	1.856	1.527
2323	20.841	8.788	0.0600	0.0151	2.371	3.968
2324	21.562	8.007	0.0616	0.0222	2.692	2.768

Table 5.9 Data on Q_1/Q_2 and S_1/S_2 for θ = -10.38^0 and Q_0 = 40 l/s

Run No.	Q_1(l/s)	Q_2(l/s)	S_1(m^3)	S_2(m^3)	Q_1/Q_2	S_1/S_2
3311	20.678	20.106	0.0071	0.1239	1.028	0.057
3312	24.719	16.198	0.0544	0.0819	1.526	0.663
3313	28.084	12.914	0.078	0.0433	2.174	1.799
3314	28.353	12.598	0.1009	0.0366	2.250	2.750
3315	28.910	12.245	0.0913	0.0197	2.360	4.638
3316	29.098	12.244	0.0901	0.0342	2.376	2.630
3321	22.316	18.625	0.0182	0.1191	1.198	0.153
3322	26.185	14.774	0.0893	0.0674	1.772	1.325
3323	28.274	12.639	0.0986	0.0232	2.236	7.238

Table 5.10 Data on Q_1/Q_2 and S_1/S_2 for θ = -3.50^0 and Q_0 = 20 l/s

Run No.	Q_1(l/s)	Q_2(l/s)	S_1(m^3)	S_2(m^3)	Q_1/Q_2	S_1/S_2
1411	7.398	12.824	0.0122	0.0593	0.576	0.205
1412	8.574	11.781	0.0239	0.0574	0.727	0.417
1421	12.639	7.789	0.0361	0.0210	1.622	1.718

Table 5.11 Data on Q_1/Q_2 and S_1/S_2 for θ = -3.50^0 and Q_0 = 30 l/s

Run No.	Q_1(l/s)	Q_2(l/s)	S_1(m^3)	S_2(m^3)	Q_1/Q_2	S_1/S_2
2411	10.468	18.599	0.0148	0.0753	0.562	0.197
2412	12.888	16.984	0.0365	0.0705	0.758	0.517
2413	13.374	15.446	0.0326	0.0460	0.865	0.708
2421	18.145	11.906	0.0639	0.0076	1.524	8.345
2422	15.578	13.616	0.0654	0.0155	1.144	4.213

Table 5.12 Data on Q_1/Q_2 and S_1/S_2 for θ = -3.50^0 and Q_0 = 40 l/s

Run No.	Q_1(l/s)	Q_2(l/s)	S_1(m^3)	S_2(m^3)	Q_1/Q_2	S_1/S_2
3411	20.080	20.995	0.0806	0.0523	0.956	1.539
3412	19.195	21.932	0.0666	0.0740	0.872	0.889
3421	12.269	28.796	-0.0301	0.1524	0.426	-.0197
3422	15.320	25.992	0.0266	0.1108	0.589	0.240
3431	23.359	17.886	0.0985	0.0006	1.305	9.000
3432	19.931	20.985	0.0746	0.0415	0.949	1.795

5.2 Development of nodal point relation

The general nodal point relation is

$$\frac{s_1}{s_2}=\left(\frac{q_1}{q_2}\right)^k \tag{3.6}$$

$$\text{or} \quad \frac{S_1/B_1}{S_2/B_2}=\left(\frac{Q_1/B_1}{Q_2/B_2}\right)^k$$

$$\text{or} \quad \frac{S_1}{S_2}=\left(\frac{Q_1}{Q_2}\right)^k\left(\frac{B_1}{B_2}\right)^{1-k} \tag{2.59}$$

This general nodal point relation includes the influence of widths only.

Thus in a more general form, the nodal point relation can be written as

$$\frac{s_1}{s_2}=M\left(\frac{q_1}{q_2}\right)^k \tag{5.1}$$

in which M represents the influence of widths and all other possible influence.

Eq. (5.1) can be linearised by taking logarithms.

$$\log\left(\frac{s_1}{s_2}\right)=\log M+k\log\left(\frac{q_1}{q_2}\right) \tag{5.2}$$

$$\text{or } y = \beta_0 + \beta_1 x \tag{5.3}$$

where, $y = \log (s_1/s_2)$, $x = \log (q_1/q_2)$, $\beta_0 = \log M$ and $\beta_1 = k$

Now, we can write the linear, first order model

$$y = \beta_0 + \beta_1 x + \xi \tag{5.4}$$

where ξ is the increament by which an individual y may fall off the regresstion line.

Now β_0, β_1 and ξ are unknown in Eq. (5.4), and in fact ξ would be difficult to discover since it changes for each observation y. However, β_0 and β_1 remain fixed and although we cannot find them exactly without examining all possible occurrences of y and x, we can use the information provided by the data in table 5.1 through 5.12 to give us estimates b_0 and b_1 of β_0 and β_1; thus we can write

$$\hat{y} = b_0 + b_1 x \tag{5.5}$$

where $\hat{y}$ denotes the predicted value of y for a given x, when b_0 and b_1 are determined.

$$b_1 = \frac{\sum x_i y_i - (\sum x_i)(\sum y_i)/n}{\sum x_i^2 - (\sum x_i)^2/n} \tag{5.6}$$

$$b_0 = \bar{y} - b_1 \bar{x} \tag{5.7}$$

100 (1 - α)% confidence limit

for β_1 is : $$b_1 \pm \frac{t\,(n-2,\, 1-\frac{1}{2}\alpha)\, s}{\{\sum (x_i - \bar{x})^2\}^{\frac{1}{2}}} \tag{5.8}$$

for β_0 is : $$b_0 \pm t\,(n-2,\, 1-\frac{1}{2}\alpha) \left\{ \frac{\sum x_i^2}{n \sum (x_i - \bar{x})^2} \right\}^{\frac{1}{2}} s \tag{5.9}$$

where $$s = \left\{ \frac{\sum (y_i - \hat{y}_i)}{n-2} \right\}^{\frac{1}{2}} \tag{5.10}$$

The goodness-of-fit can be expressed by R^2

where $$R^2 = \frac{\sum (\hat{y}_i - \bar{y})^2}{\sum (y_i - \bar{y})^2} \tag{5.11}$$

Now, the nodal point relations for different upstream discharges and different nose angles and the value R^2 are given in the following table

Table 5.13 Nodal point relations and the value of R^2

θ	Q	Nodal point relation $s_1/s_2 = M\ (q_1/q_2)^k$	R^2
-10.38^0	20 l/s 30 l/s 40 l/s	$s_1/s_2 = 0.052\ (q_1/q_2)^{3.367}$ $s_1/s_2 = 0.018\ (q_1/q_2)^{4.499}$ $s_1/s_2 = 0.014\ (q_1/q_2)^{4.762}$	0.933 0.903 0.934
-3.50^0	20 l/s 30 l/s 40 l/s	$s_1/s_2 = 0.458\ (q_1/q_2)^{1.978}$ $s_1/s_2 = 0.509\ (q_1/q_2)^{3.989}$ $s_1/s_2 = 0.523\ (q_1/q_2)^{4.529}$	0.986 0.973 0.964
6.97^0	20 l/s 30 l/s 40 l/s	$s_1/s_2 = 9.601\ (q_1/q_2)^{2.854}$ $s_1/s_2 = 16.405\ (q_1/q_2)^{3.401}$ $s_1/s_2 = 30.158\ (q_1/q_2)^{3.659}$	0.976 0.989 0.974
0^0 [1]	20 l/s 30 l/s 40 l/s	$s_1/s_2 = 1.237\ (q_1/q_2)^{2.537}$ $s_1/s_2 = 1.397\ (q_1/q_2)^{4.632}$ $s_1/s_2 = 2.035\ (q_1/q_2)^{5.531}$	0.970 0.870 0.800

[1] Results obtained by previous investigators (Roosjen and Zwanenburg, 1995, Hannan, 1996)

The value of R^2 (the ratio of the sum of squares due to regression and sum of squares about mean indicates the accuracy of curve fitting. If R^2 equals to one, the curve fits perfectly. The 'lack of fit' can be checked from the plots of residuals (deviation of the ith observation from its predicted or fitted value) versus log (q_1/q_2). Two different cases can be occurred. Firstly, the nodal point relation completely describes the relation between the sediment transport ratio and the discharge ratio. For this situation the residuals consist of the measuring errors only. Plots of the residuals versus the discharge ratio show a random pattern. Secondly, the equation does not completely describes the relation between the sediment transport ratio and the discharge ratio. The residuals consist of the measurement errors and an extra factor. In this case, plots of residuals versus the discharge ratio indicate a relation between the two and an extra term should be added to the equation described earlier.

Now, from the plots (Figure 5.1 through 5.9) of the residuals versus the discharge ratio, it is seen that a clear pattern cannot be found. Thus no relation exists between the residuals and the discharge ratio, so an extra term does not need to be added to the nodal point relation.

5.2.1 Confidence interval of linear regression coefficients

The coefficient, M and the exponent, k of the general nodal point relation (Eq. 2.60) for diffeent nose angles were estimated by linear regression analysis as discussed in section 5.2.

In this section, the confidence interval for M and k has been determined. The following tables show the 95% confidence interval for M and k.

Table 5.14 95% confidence interval for M

θ, Q	Lower bound M	M	Upper bound M
θ = - 10.38^0, Q = 20 l/s	0.020	0.052	0.141
θ = - 10.38^0, Q = 30 l/s	0.003	0.018	0.098
θ = - 10.38^0, Q = 40 l/s	0.004	0.013	0.043
θ = - 3.50^0, Q = 20 l/s	0.096	0.458	2.181
θ = - 3.50^0, Q = 30 l/s	0.289	0.510	0.905
θ = - 3.50^0, Q = 40 l/s	0.419	0.524	0.655
θ = 6.97^0, Q = 20 l/s	7.153	9.606	12.901
θ = 6.97^0, Q = 30 l/s	7.485	16.506	36.400
θ = 6.97^0, Q = 40 l/s	16.359	30.027	55.114

Table 5.15 95% confidence interval for k

θ, Q	Lower bound k	k	Upper bound k
θ = - 10.38^0, Q = 20 l/s	2.332	3.368	4.404
θ = - 10.38^0, Q = 30 l/s	2.807	4.506	6.205
θ = - 10.38^0, Q = 40 l/s	3.743	4.910	6.078
θ = - 3.50^0, Q = 20 l/s	-1.008	1.979	4.965
θ = - 3.50^0, Q = 30 l/s	2.762	3.989	5.216
θ = - 3.50^0, Q = 40 l/s	3.653	4.529	5.406
θ = 6.97^0, Q = 20 l/s	2.518	2.854	3.190
θ = 6.97^0, Q = 30 l/s	2.481	3.410	4.339
θ = 6.97^0, Q = 40 l/s	2.972	3.653	4.334

5.3 Analysis of data

A total of 67 runs have been performed for three different nose types and for three upstream discharges (i.e. 20 l/s, 30 l/s, 40 l/s). For each discharge, the results of 2 runs are analysed and the changes in bed level across cross section and variation of discharge with run time are shown. The criterion for selecting two runs per discharge is that the first run represents the first day of running and the second run represents the last day of running when the equilibrium is more or less achieved.

5.3.1 Analysis of data for runs with nose no. 1 ($\theta = 0^0$)

Data for nose no. 1 was analysed earlier by Roosjen and Zwanenburg (1995) and Hannan (1996) and has been summarised in section 3.3.3.

5.3.2 Runs with nose no. 2 ($\theta = 6.97^0$)

With the second nose, a total of 29 runs have been performed. For the upstream discharge of 20 l/s, 30 l/s and 40 l/s; 13, 8 and 8 runs have been done respectively.

For run no. 1231, the initial bed has been prepared by taking a discharge ratio of 1.0 i.e. a discharge of 10 l/s in branch 1 and a discharge of 10 l/s in branch 2. During the run it is found that the discharge in branch 1 decreases and the discharge in branch 2 increases (Fig. B.1). This changing occurs in order to achieve equilibrium condition. It is also found that there is deposition in branch 1 and erosion in branch 2 (Fig. A.1). The reason is that the width of branch 1 at bifurcation is 0.20 m whereas the actual width of branch 1 is 0.40 m. Thus for a constant discharge the velocity is more at the point of bifurcation than that of the actual width. So its sediment transport capacity is also large. When this discharge with sediment load enters the actual branch whose width (0.40 m) is more, dissipates energy resulting in a deposition in branch 1. Similarly the width of branch 2 at bifurcation is 0.80 m whereas the actual width is 0.60 m. So for a constant discharge the velocity is less at the point of bifurcation than that of the actual width. When the water comes to the actual width, its velocity increases. So its sediment transport capacity becomes higher than that of the bifurcation. This causes erosion in branch 2.

For run no. 1233 which is the continuation of run no. 1231, the discharges through the two downstream branches do not change remarkably (Fig. B.2). It means that equilibrium is more or less achieved. This can be seen from bed level change of this run. The bed levels are more or less constant (Fig. A.2).

For run no. 2241, it is seen that branch 1 has been deposited and branch 2 has been eroded (Fig. A.3). And the discharge in branch 1 decreases and that of branch 2 increases (Fig. B.3). Run no. 2242 is the continuation of run no. 2241. Here the bed level is more or less same before and after the run (Fig. A.4) and the discharge in branch 1 and branch 2 do not vary to a large extent (Fig. B.4). This means that the equilibrium condition is achieved.

For run no. 3211, it is seen that branch 1 goes under deposition and branch 2 under erosion (Fig. A.5). And the discharge in branch 1 decreases and that of branch 2 increases (Fig. B.5). This is because the initial disturbed condition was such that the discharge in branch 1 is larger and in branch 2 is smaller than the equilibrium discharge in the two branches. The equilibrium situation is achieved in run no. 3213 (continuation of run no. 3211). The bed level evolution and variation of discharge with run time of run no. 3213 are shown in Fig. A.6 and B.6 respectively.

For nose no. 2, it is seen that the maximum scour depth occurs on the outer face (i.e. on the face where the width is larger) of the nose. Because the flow gets obstructed at the tip of the nose. This causes vortex (i.e. secondary flow). The secondary flow is greater on the outer edge of the nose than the inner edge. Thus the maximum scour hole occurs on the outer face of the nose.

5.3.3 Runs with nose no. 3 ($\theta = -10.38^0$)

With nose no. 3, a total of 24 runs have been performed. For upstream discharge of 20 l/s, 30 l/s and 40 l/s, the number of runs performed are 8, 7 and 9 respectively.

For run no. 1311, the initial bed has been prepared with a discharge ratio of 0.67 i.e. a discharge of 8 l/s in branch 1 and a discharge of 12 l/s in branch 2. For nose no. 3, this discharge (8 l/s) in branch 1 is the less than the equilibrium discharge and the discharge (12 l/s) in branch 2 is more than the equilibrium discharge. The geometry of nose no. 3 is such that the width of branch 1 at bifurcation is 0.70 m and that of branch 2 at bifurcation is 0.30 m. From this run it is seen that discharge in branch 1 increases and that of branch 2 decreases (Fig. A.7). And the branch 1 erodes and branch 2 silts (Fig. B.7). The reason behind this is explained below.

The width of branch 1 at the point of tip (0.7 m) is more than the actual width (0.4 m). As a result for a constant discharge, the velocity is less at the point of tip and sediment transport is also less. But the width gradually decreases upto the end of the nose. So velocity will be more, causing energy rise to transport sediment. Now the sediment coming through water is less than the transport capacity, so there occurs erosion. On the other hand, the width of branch 2 at the point of tip (0.3 m) is less than the actual width (0.6 m). As a result, for a constant discharge velocity is more at the point of tip which causes more sediment transport. But the width gradually increases upto the end of the nose. So velocity becomes less and energy dissipates. This causes sediment transport capacity to be low. Thus the extra sediment is deposited to that branch.

For run no. 1313 which the continuation of run no. 1311, it is seen that the discharge in the two branches do not change remarkably (Fig. A.8) and the bed levels are more or less constant (Fig. B.8). This means that equilibrium is achieved.

The same conclusions can be drawn for run no. 2321 and 2224 of upstream discharge 30 l/s and 3311 and 3316 of upstream discharge 40 l/s. The bed level evolutions of run no. 2221, 2224, 3311 and 3316 are shown in Fig. A.9, A.10, A.11 and A.12 respectively. The variations of discharge with run time of the above runs are shown in Fig. B.9, B.10, B.11 and B.12 respectively.

For nose no. 3, it is seen that the maximum scour depth occurs on the outer face of the nose. The reason is same as of nose 2.

5.3.4 Runs with nose no. 4 (θ = -3.50^0)

With nose no. 4, a total of 14 runs have been performed. For the upstream discharge of 20 l/s, 30 l/s and 40 l/s, the total numbers of runs are 3, 5 and 6 respectively.

The deposition or erosion in a branch or increasing or decreasing of discharge in a branch depends on the initial disturbed condition i.e. how much discharges are allowed to the branches. This disturbance is done by the discharge ratio.

For run no. 1411, the initial bed has been prepared by using a discharge ratio of 0.5 i.e. a discharge of 6.67 l/s in branch 1 and a discharge of 13.33 l/s in branch 2. After the run it is found that these is a erosion in branch 1 and a deposition in branch 2 (Fig. A.13) and discharge in branch 1 increases and that of branch 2 decreases (Fig. B.13).

For run no. 1412, which is the continuation of run no. 1411, it is seen that the discharge in branch 1 is still increasing and that of branch 2 is decreasing (Fig. B.14). There is also erosion in branch 1 and siltation in branch 2 (Fig. A.14). This means that equilibrium condition is not achieved.

The reasons for deposition or erosion and increasing or decreasing of discharge that have been explained in the previous articles for nose no. 2 and nose no. 3 are the same for nose no. 4. The bed level evolutions of run no. 2411, 2413, 3411 and 3412 are shown in Fig. A.15, A.16, A.17 and A.18 respectively. The variations of discharge with run time of the above runs are shown in Fig. B.15, B.16, B.17 and B.18 respectively.

5.4 Influence of nose angle on M and k

The nodal point relation determines the distribution of sediment to the downstream branches. The value of the coefficient, M and the power, k in the nodal point relation for different nose angles and upstream discharges are given in table 5.16 and 5.17 respectively.

Table 5.16 Variation of M with θ

θ	Values of M for		
	Q_0=20 l/s	Q_0=30 l/s	Q_0=40 l/s
6.97	9.601	16.405	30.158
0^0	1.237	1.397	2.035
-3.50^0	0.458	0.509	0.523
-10.38^0	0.052	0.018	0.014

Table 5.17 Variation of k with θ

θ	Values of k for		
	Q_0=20 l/s	Q_0=30 l/s	Q_0=40 l/s
6.97^0	2.854	3.401	3.659
0^0	2.537	4.632	5.510
-3.50^0	1.978	3.989	4.529
-10.38^0	3.367	4.499	4.765

From table 5.16, it is seen that for $\theta = 0$, the value of the coefficient M increases as the discharge increases. Similar is the case for other nose angles except for nose angle $\theta = -10.38^0$ where the coefficient decreases as the discharge increases. For a particular upstream discharge the coefficient M increases as the nose angle changes from negative to positive ($-10.38^0 \leq \theta \leq 6.97^0$).

From table 5.17, it is seen that for a particular nose angle, the value of the exponent k increases as the discharge increases. When the discharge is held constant at 30 l/s, it is found that the maximum value of the coefficient, k occurs for symmetric nose ($\theta = 0^0$). Similar is the case for the upstream discharge of 40 l/s. But when the upstream discharge is 20 l/s, the maximum value of k is found for $\theta = -10.38^0$.

5.5 Variation of s_1/s_2 and q_1/q_2 with discharge

The variations of s_1/s_2 and q_1/q_2 with discharge for differents nose angles are shown in Fig. 5.10, 5.11, 5.12 and 5.13. From these figures, it is seen that for a particular discharge ratio, the sediment transport ratio increases as the discharge increases for nose angle of 6.97^0, 0^0 and -3.50^0. But when the nose angle is -10.38^0, the variation of s_1/s_2 with q_1/q_2 is almost same for the discharges of 30 l/s and 40 l/s. So it is concluded that more points on s_1/s_2 and q_1/q_2 should be obtained to get a better evidence.

5.6 Variation of s_1/s_2 and q_1/q_2 with nose angle

Fig. 5.14, 5.15 and 5.16 show the variation of s_1/s_2 and q_1/q_2 with nose angles for the upstream discharge of 20 l/s, 30 l/s and 40 l/s respectively. From the figures, it is seen that for a particular sediment tpansport ratio, the discharge ratio increases as the nose angle changes from positive to negative. It is also seen that the upstream discharges do not influence too much the sediment transport ratio with discharge ratio. Thus s_1/s_2 vs. q_1/q_2 has been plotted independent of the upstream discharge in Fig. 5.17. From this figure, it is seen that the data shows good correlation between s_1/s_2 and q_1/q_2. It can therefore be concluded that sediment distribution to the downstream branches is independent of upstream discharge. The nose angle is the major variable for sediment distribution.

CHAPTER 6

CONCLUSIONS AND RECOMMENDATIONS FOR FURTHER STUDIES

6.1 Introduction

The study is based on the experimental results from the physical model of river bifurcation built in the Hydraulics and River Engineering Laboratory of BUET. The conclusions so far obtained from the study and the recommendations for further study are given below.

6.2 Conclusions

The following conclusions have been derived from the study.

1. The value of the coefficient M in the nodal point relation increases as the discharge increases for nose angles of 6.97^0,0^0 and -3.5^0. For nose angle -10.38^0, the coefficient decreases with increase of discharge.

2. For a particular upstream discharge the coefficient, M increases as the nose angle changes from negative to positive ($-10.38^0 \leq \theta \leq 6.97^0$).

3. The value of the exponent, k in the nodal point relation increases as the discharge increases when the nose angle is held constant. That means for a particular nose angle sediment transport in branch 1 increases as the exponent increases.

4. The distribution of sediment to the downstream branches is independent of upstream discharge. The nose angle is the major variable for the distribution of sediment.

6.3 Recommendations

The following are the recommendations for further studies.

1. The study has been performed based on a limited number of experiments. In order to find better evidence more experiments should be performed.

2. The experiments so far performed are valid only for a particular sediment size. In order to get an idea about how the sediment size influences the distribution of sediment to the downstream branches, it is recommended to use at least another two sediment sizes.

3. The results so far obtained from the study are valid only for bed load sediment. But in nature, this rarely happens. So in order to compare the results with natural bifurcation, experiments should be done using suspended sediment. This will obviously require some modifications of the model.

4. The seasonal effect of discharge is not considered in the study. As in nature the discharge varies seasonally, the experiments can be done with a varying upstream discharge. It may be gradually increasing or decreasing.

5. The results of the experiments should be simulated with a mathematical computer model (e.g. WENDY, SOBEK etc.).

6. The results of the study should be compared with the prototype data i.e. with actual situation in the field.

REFERENCES

Akkerman,G.J. (1993), *"Zandverdeling bij splitsingspunten, Literatuurinventarisatie voor inlaten van nevengelen,"* Delft Hydraulics, Report Q 1573. (After Wang et.al, 1994).

Best, J.L. and C.S. Bristow (1993), *"Braided Rivers",* The Geotechnical Society, London.

Dekker, P.D. and J.M. van Voorthuizen (1994), *"Research on the Morphological Behaviour of Bifurcations in Rivers",* Delft University of Technology, The Netherlands.

Dekker, P.D. and J.M. van Voorthuizen (1993), *"Detailed design for an experimental research on bifurcations"*, Preliminary studies for M.Sc. thesis work, unpublished manuscript (after Dekker and van voorthuizen, 1994).

Delft Hydraulics (1991), *"WENDY",* Volume 2, Reference Guide.

Delft Hydraulics and Rijkswaterstaat/RIZA (1992), *"SOBEK"*, Functional design - sediment transport and morphology (draft), (after Wang et.al, 1993).

Draper, N.R. and H. Smith (1981), "*Applied Regression Analysis*", Second Edition, John Wiley & Sons, Inc.

Fokkink, R.J. and Z.B. Wang (1993), *"Study of fundamental aspects of ID-network morphodynamic models",* DYNASTER project, Delft Hydraulics, The Netherlands.

Fokkink, R.J., Z.B. Wang and M.H.I. Schropp (1995), *"On 1D morphodynamic network work models"*, Proceedings of the XXVI th Congress of International Association for Hydraulic Research, London.

Hannan, A. (1995)," *Detailed Design of an Experimental Setup on Bifurcation",* 39th Annual Convention, IEB, Chittagong.

Hannan, A. (1996), "*A Laboratory Study of Sediment Distribution at Channel Bifurcation*", M.Sc. Engineering Thesis, Dept. of Water Resources Engineering, BUET, Dhaka.

Hossain, M.M. (1993), *"Lecture Notes on River Engineering (Structural Aspects of River Training Works)"*, Department of Water Resources Engineering, BUET, Dhaka.

Hossain, M.M. and M.R. Kabir (1995), "*Lecture Notes on Sediment Transport*", Dept. of Water Resources Engineering, Faculty of Civil Engineering, BUET, Dhaka.

ISO (1975), *Liquid flow measurement in open channels using thin-plate weirs and venturi flumes*, ISO, Geneva, (after Dekker and van Voorthuizen, 1994).

Jansen, P.Ph, L.van Bendegom, J.J.van den Berg, M.de Vries and A. Zanen (1979), *"Principles of River Engineering"*, Pitman, London.

Matin, M.A. (1993), *"Morphological Computation (Lecturer Notes)"*, Department of Water Resources Engineering, Bangladesh University of Engineering & Technology, Dhaka.

Przedwojski, B., R.Blazejewski and K.W. Pilarezyk (1995), *"River Training Techniques - Fundamentals, Design and Applications"*, A.A. Balkema, Rotherdam, Netherlands.

Richardson, W.R.R. and C.R. Thorne (1995), *"Study of Secondary Currents and Morphological Evolution in a Bifurcated Channel"*, FAP 24 and University of Nottingham Joint Study.

Roosjen, R. and C. Zwanenburg (1995), *"Research on bifurcation in rivers"*, M.Sc. Thesis, Faculty of Civil Engineering, Delft University of Technology, The Netherlands.

Vries, M.de (1992), *"River Engineering Lecture Notes f10"*, Delft University of Technology, Faculty of Civil Engineering, The Netherlands.

Vries, M.de (1993), " *Note on River Engineering for Braided Rivers"*, Workshop on River Engineering, Dhaka, Bangladesh.

Vries, M.de and Z.B.Wang (1995), *"Applied Mathematics for the Aquatic Environment"*, Workshop for Applied Mathematics in Water Resources Engineering, Dhaka, Bangladesh.

Wang, Z.B., R.J. Fokkink and B. Karssen (1993), *"Theoretical Analysis on Node Point Relations in ID Network Morphodynamic Models"*, DYNASTAR project, Report, Part III, Delft Hydraulics, The Netherlands.

Wang, Z.B., R.J. Fokkink, M. de Vries and A. Langerak (1995), *"Stability of river bifurcations in 1D morphodynamic models"*, Journal of Hydraulic Research, Vol. 33, No.6.

Wang, Z.B. and Th.van der Kaaij (1994), *"Morphodynamic Development of Secondary Channel Systems Along Rhine Branches in the Netherlands"*, Delft Hydraulics, The Netherlands.

FIGURES

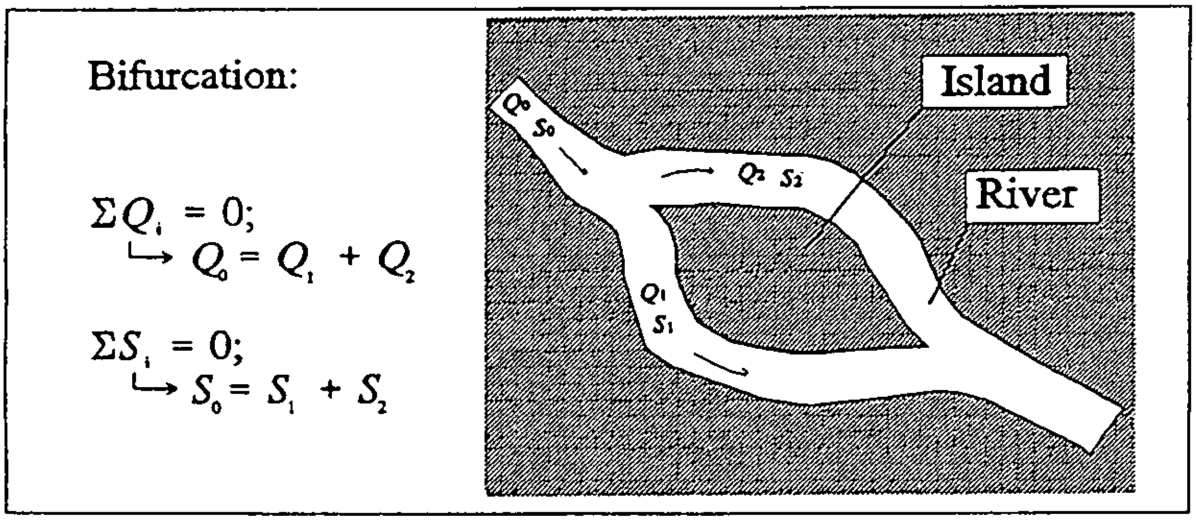

Fig. 1.1 Confluence in a river

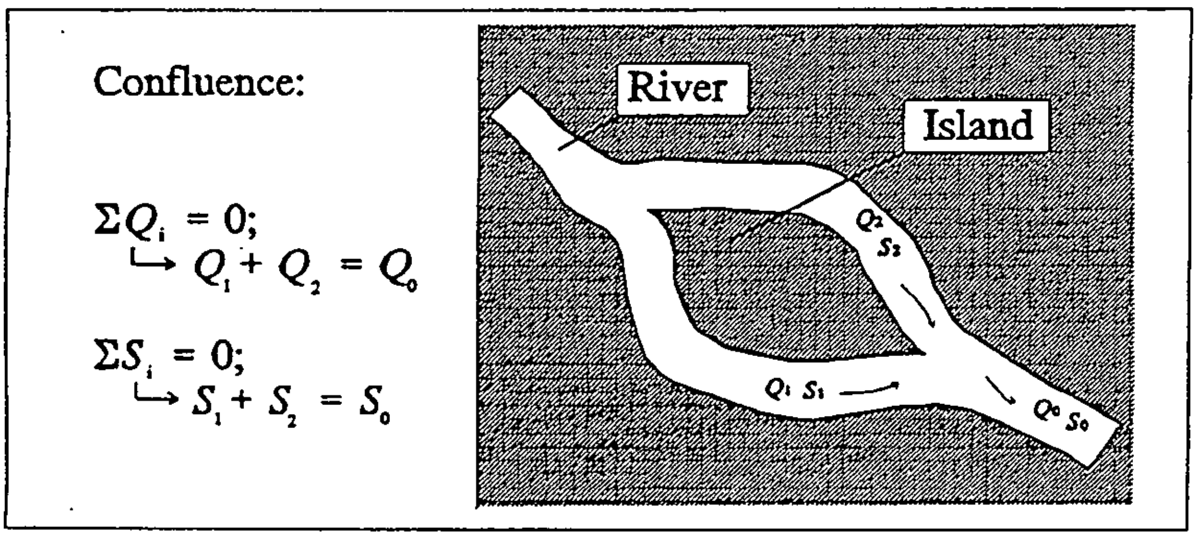

Fig. 1.2 Bifurcation in a river

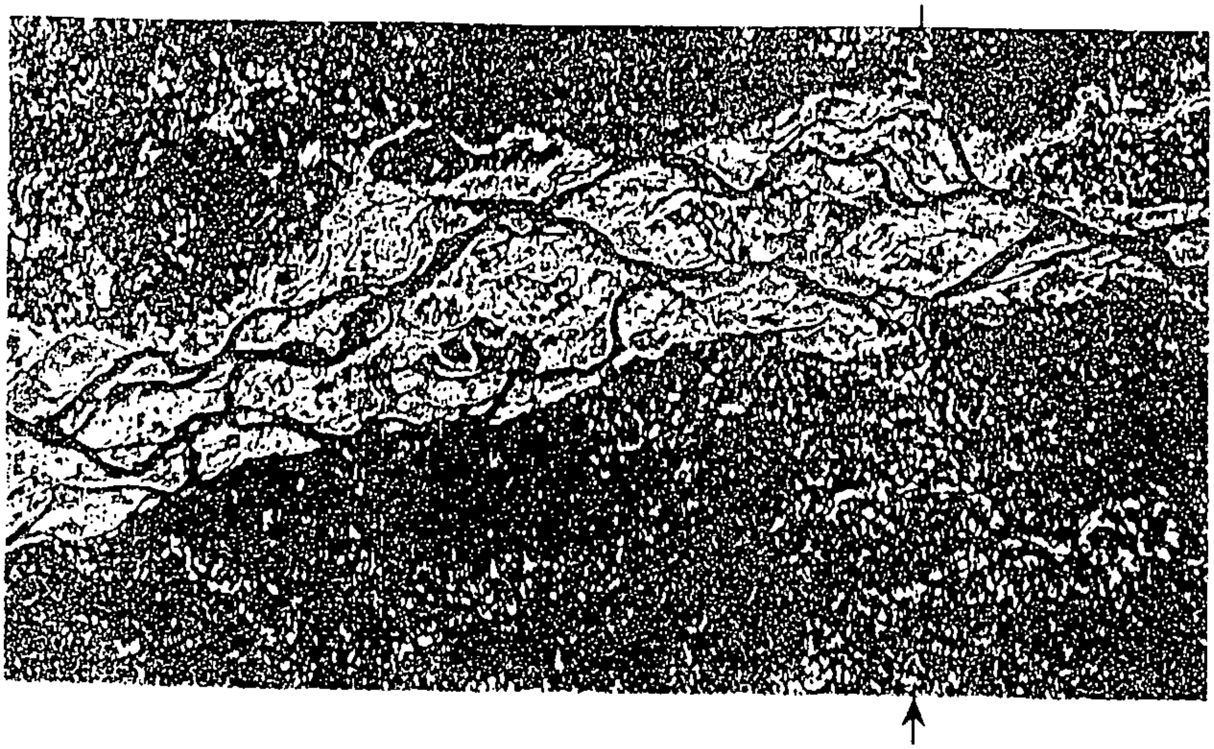

Fig. 1.3 Plan form of the Jamuna

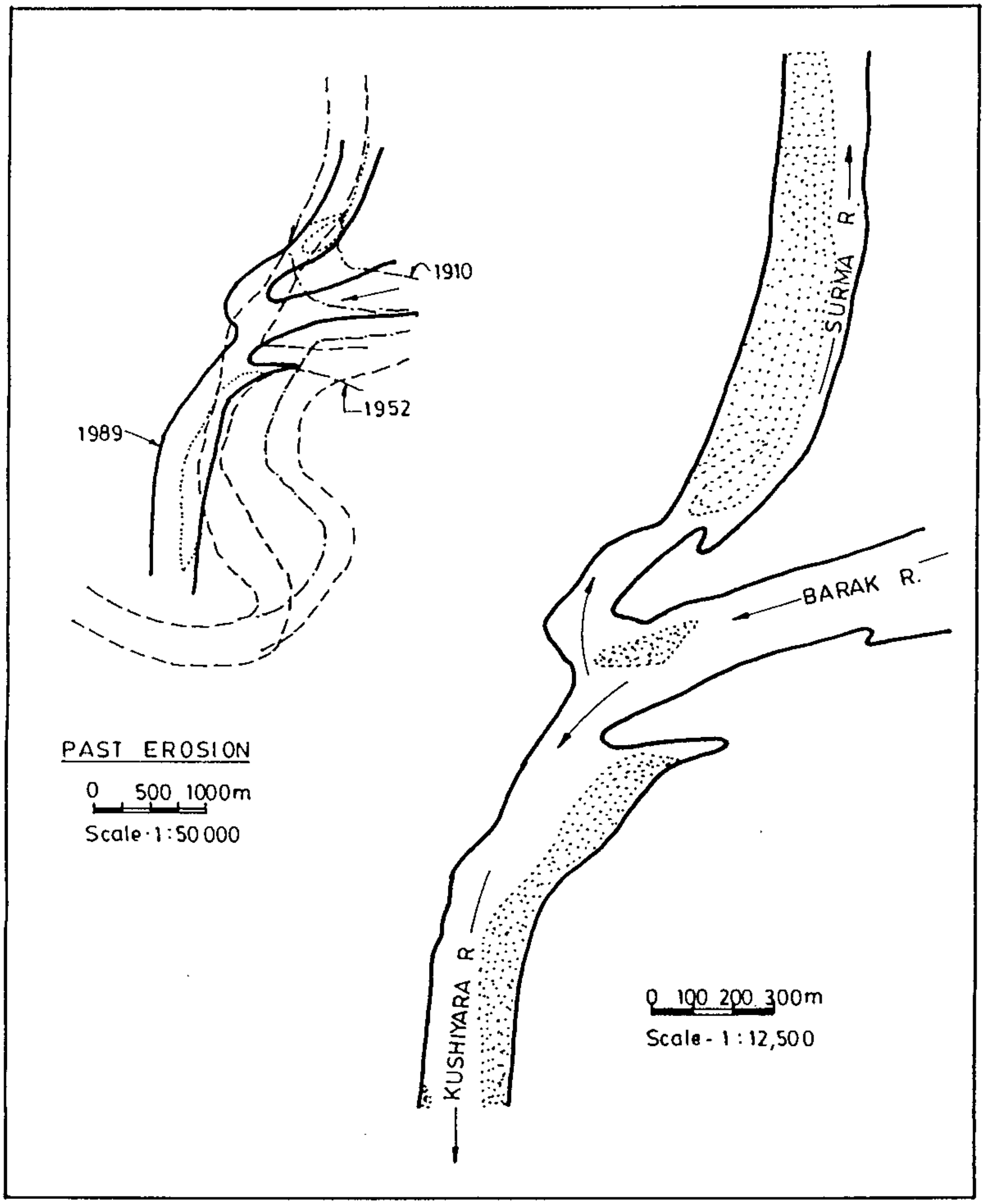

Fig. 1.4 Bifurcation of the Barak river

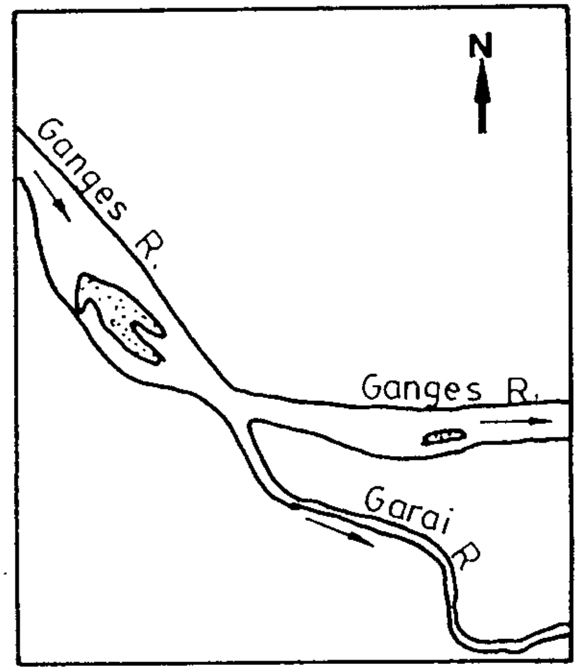

Fig. 1.5 Bifurcation of the Ganges near Kushtia

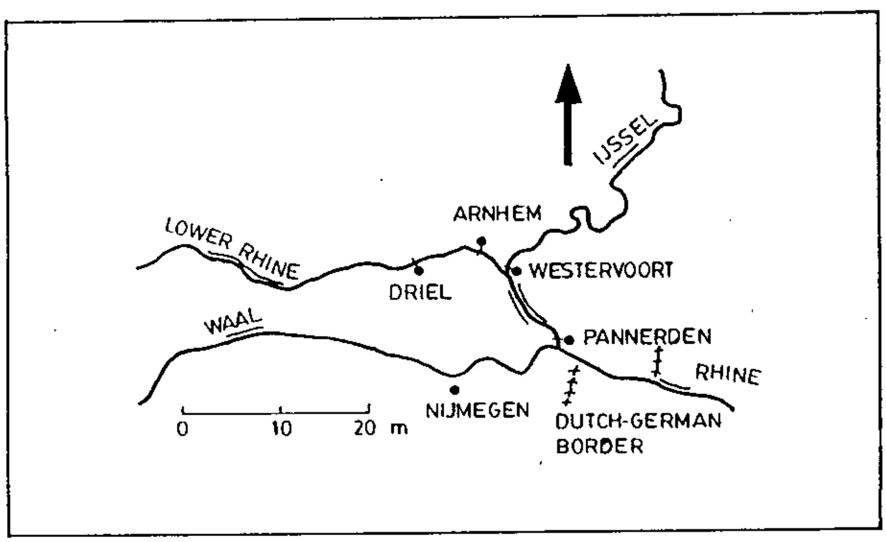

Fig. 1.6 Bifurcation of the Rhine river

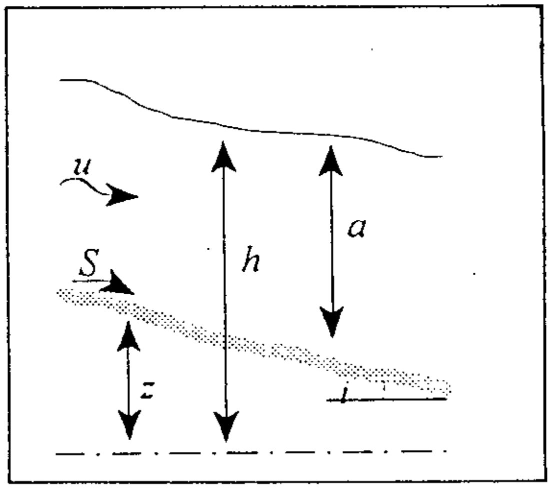

Fig. 2.1 Definition sketch of the basic variables

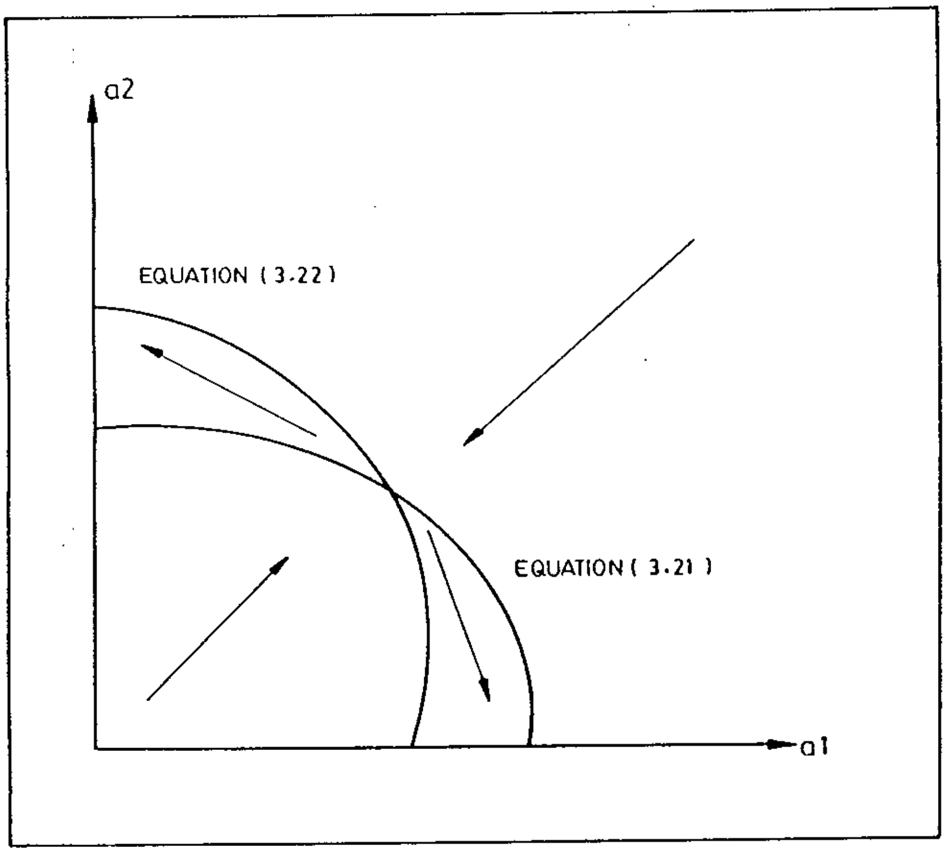

Fig. 2.2 Graphical representation of eq. 2.21 and 2.22

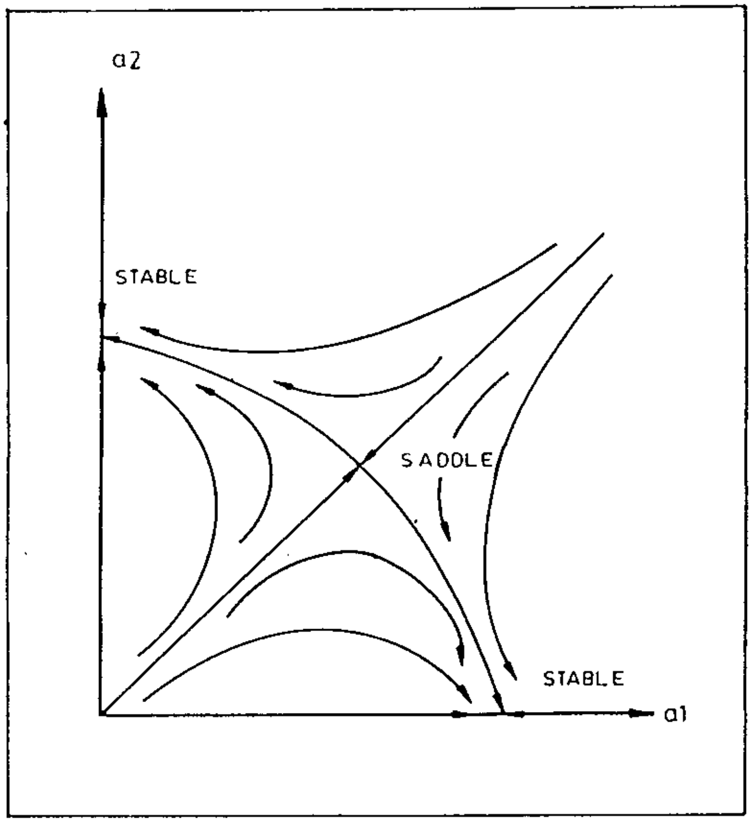

Fig. 2.3 Phase diagram

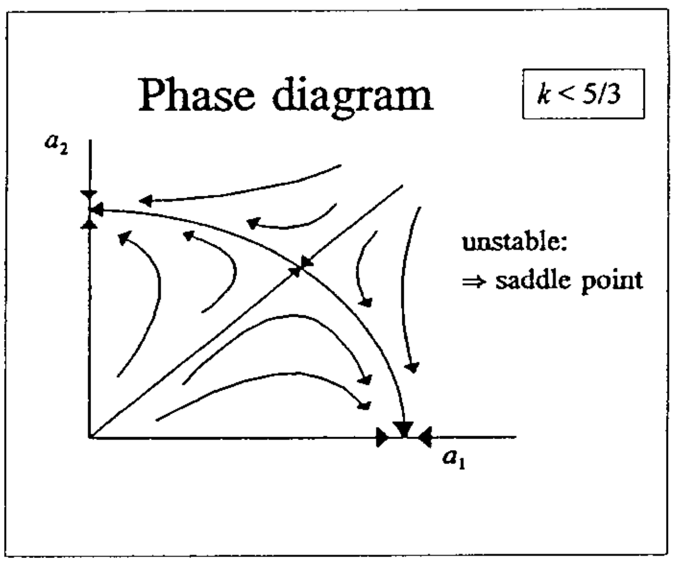

Fig. 2.4 Phase diagram for k<5/3

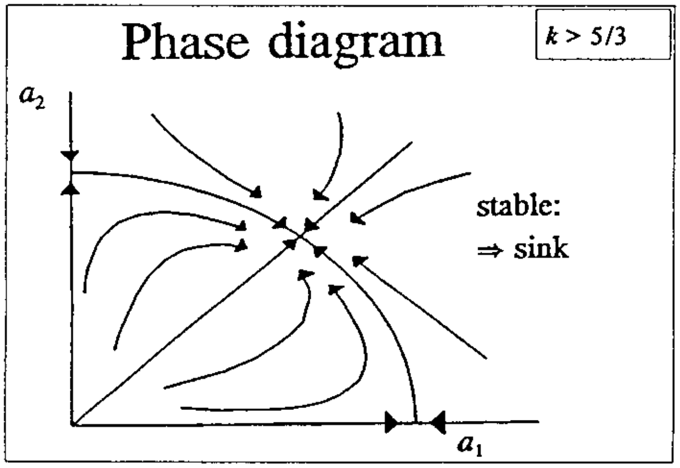

Fig. 2.5 Phase diagram for k>5/3

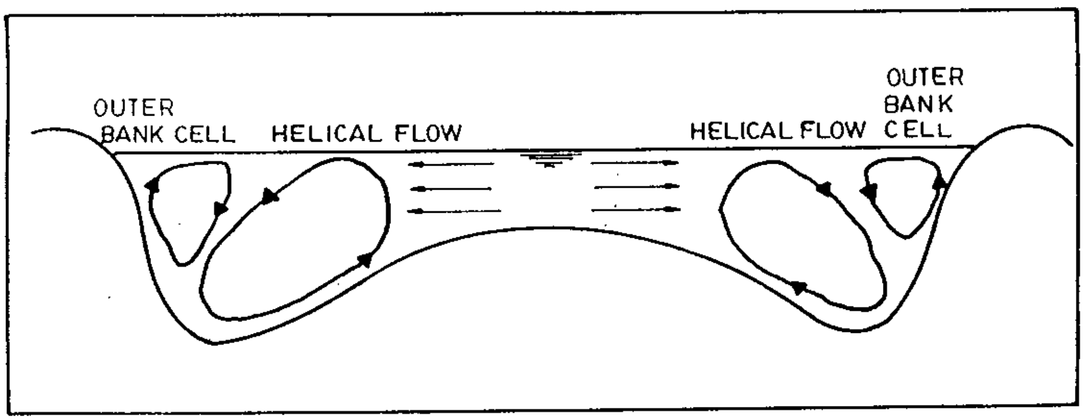

Fig. 3.1 Conceptual hypothesis for the pattern of secondary circulation
in a bifurcated channel

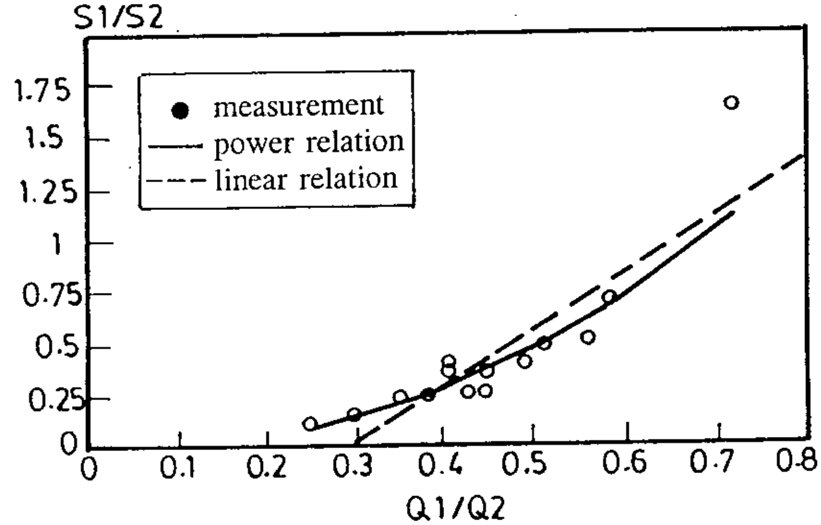

Fig. 3.2 Nodal point relation of Pannerdens channel

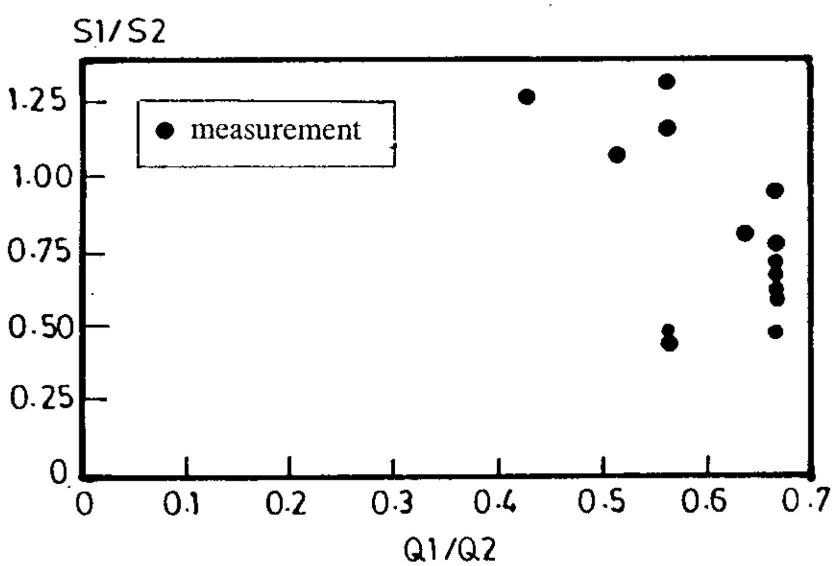

Fig. 3.3 Nodal point relation of bifurcation Westervoort

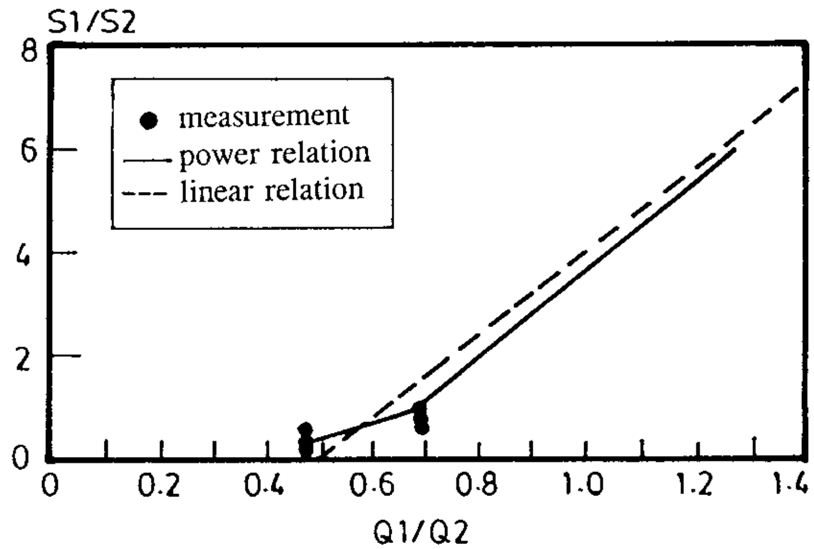

Fig. 3.4 Nodal point relation of Jonglei channel

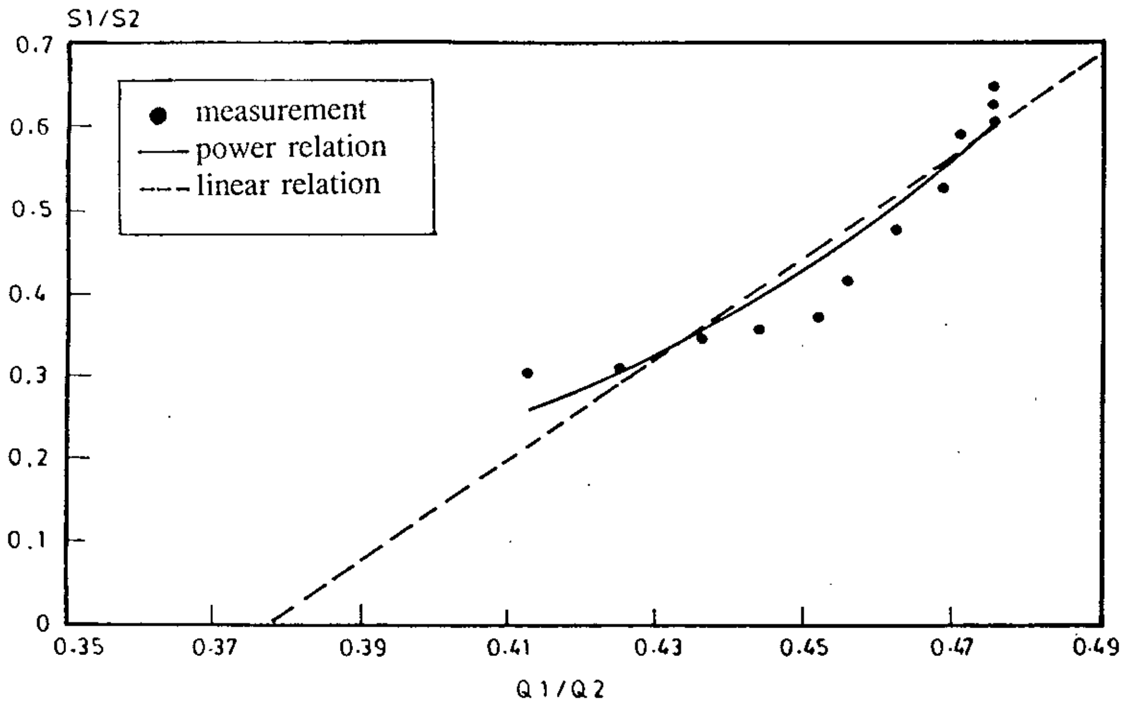

Fig. 3.5 Nodal point relation of Pannerdens using prototype data

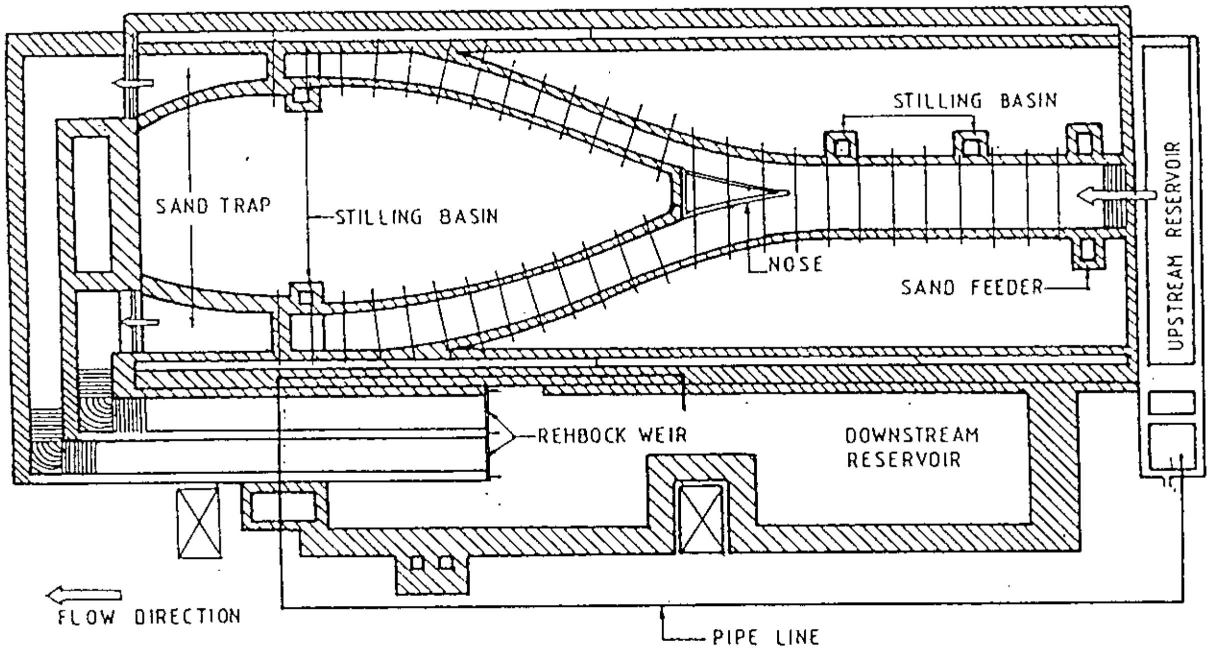

Fig. 4.1 General layout of the set-up

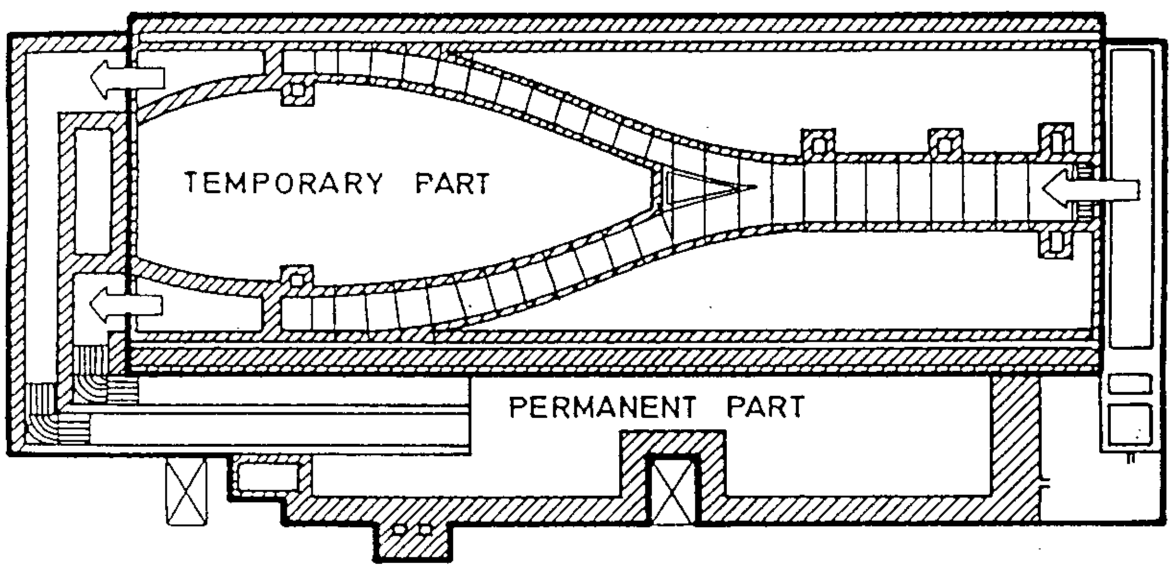

Fig. 4.2 The permanent and temporary part of the model

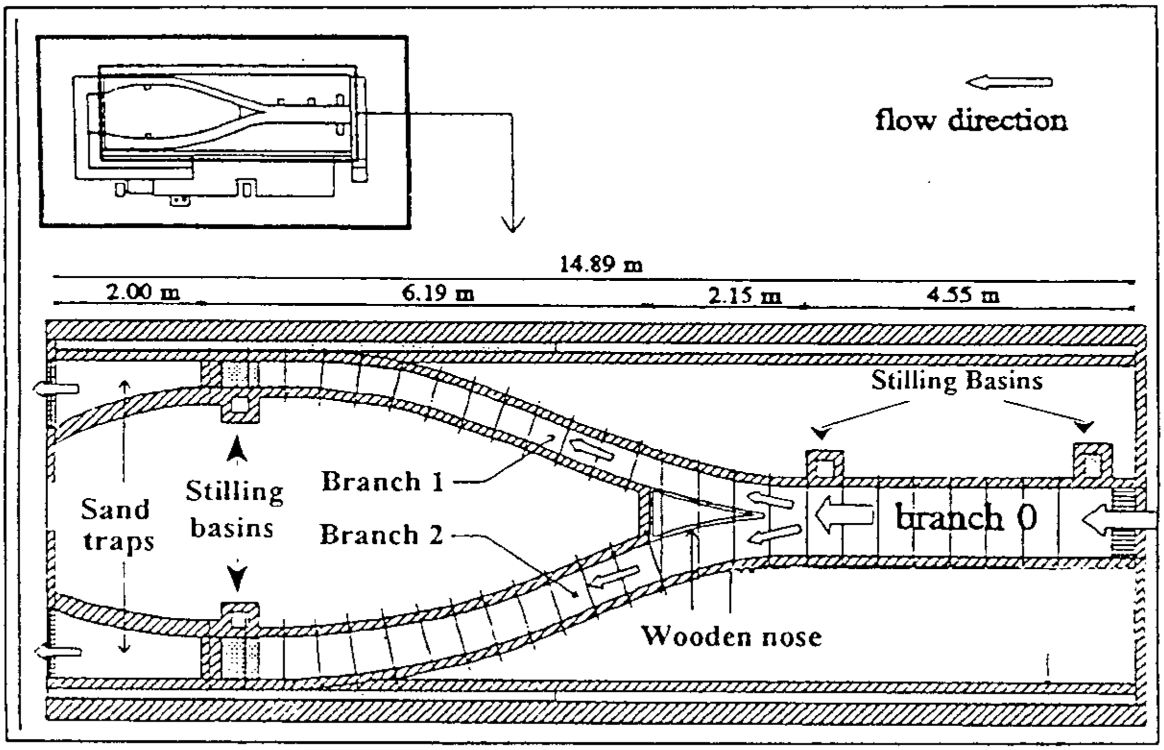

Fig. 4.3 Different elements of temporary parts

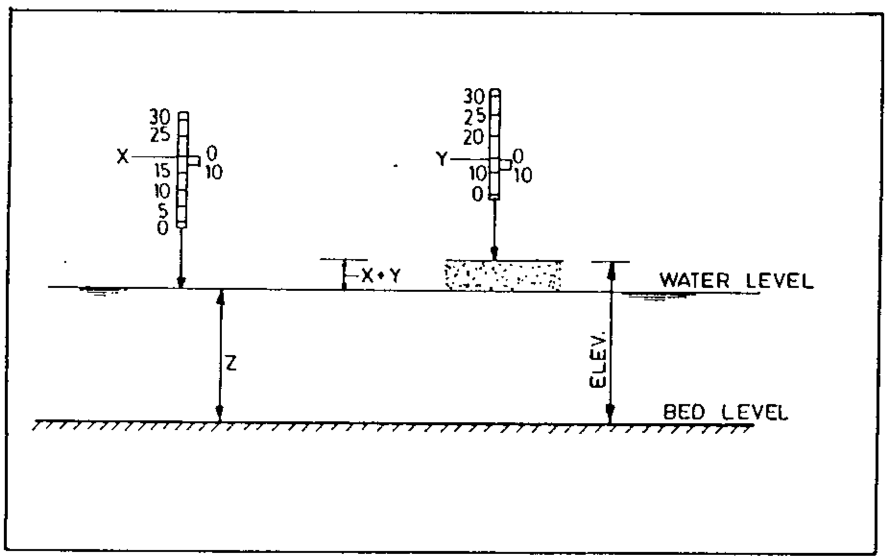

Fig. 4.4 Relating all elements to one reference level

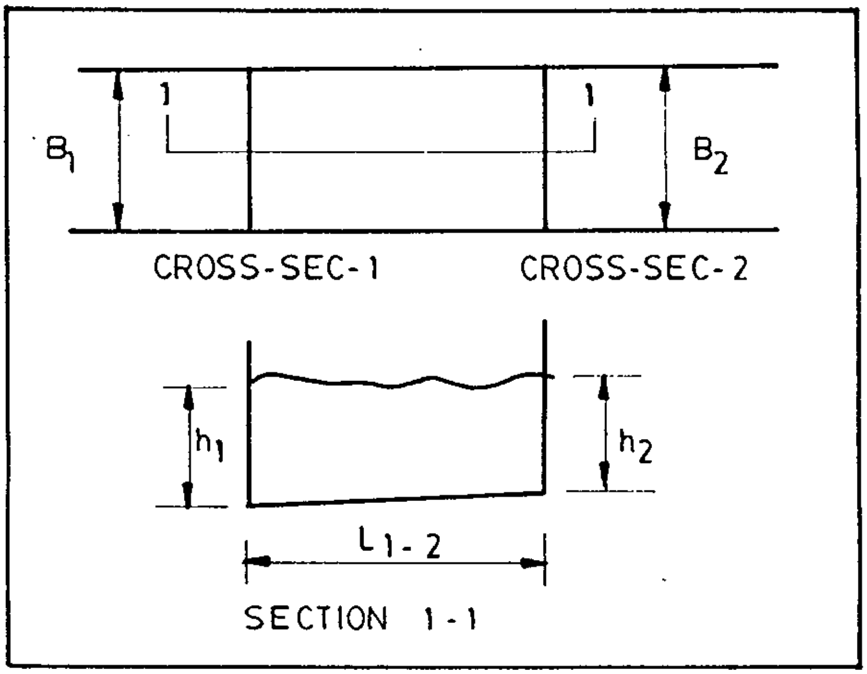

Fig. 4.5 Determination of volume of sand

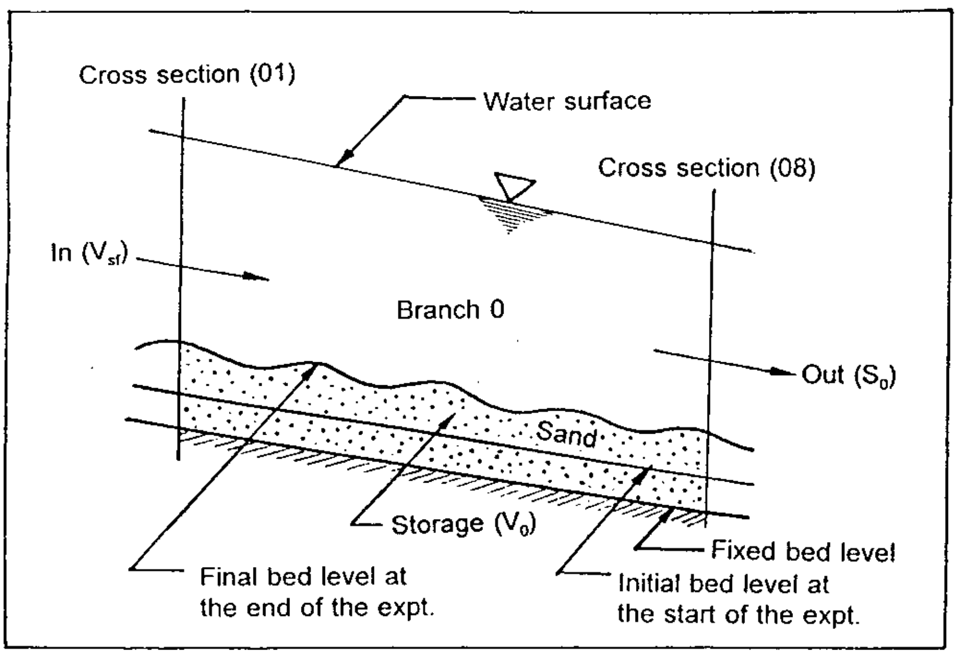

Fig. 4.6 Sediment balance in branch 0

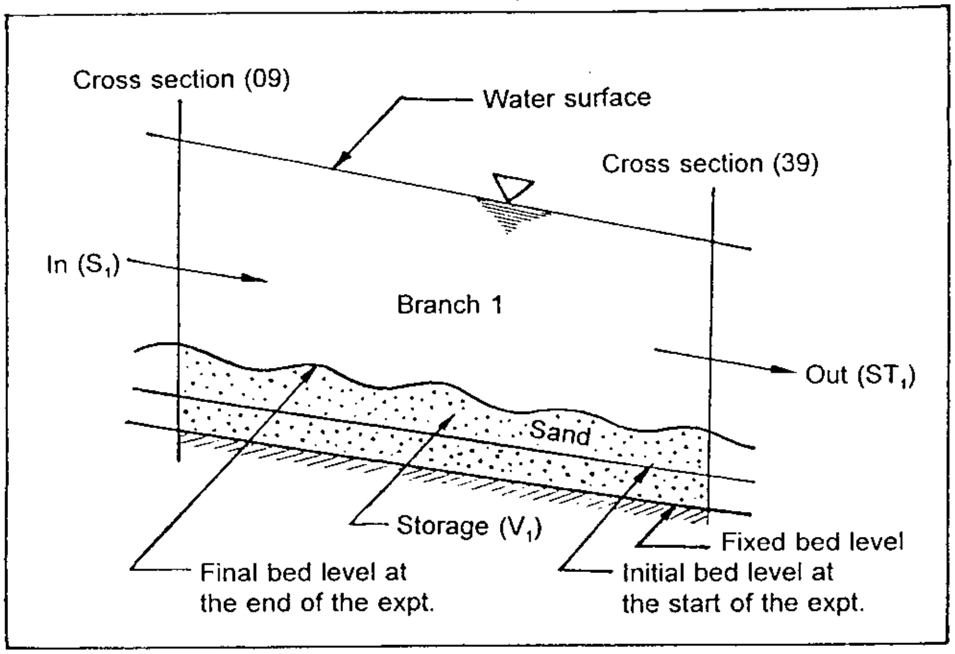

Fig. 4.7 Sediment balance in branch 1

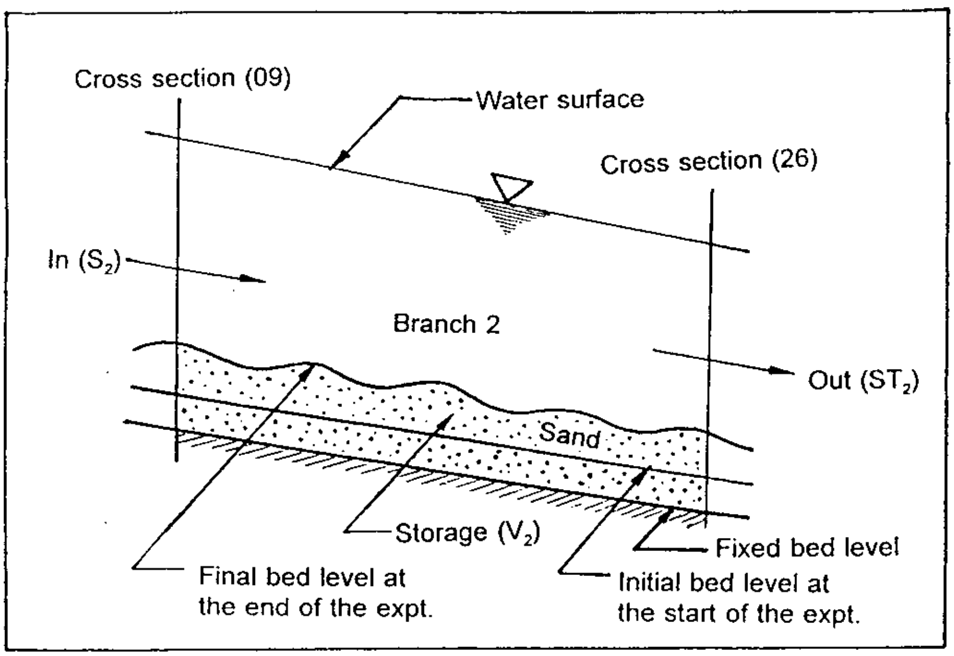

Fig. 4.8 Sediment balance in branch 2

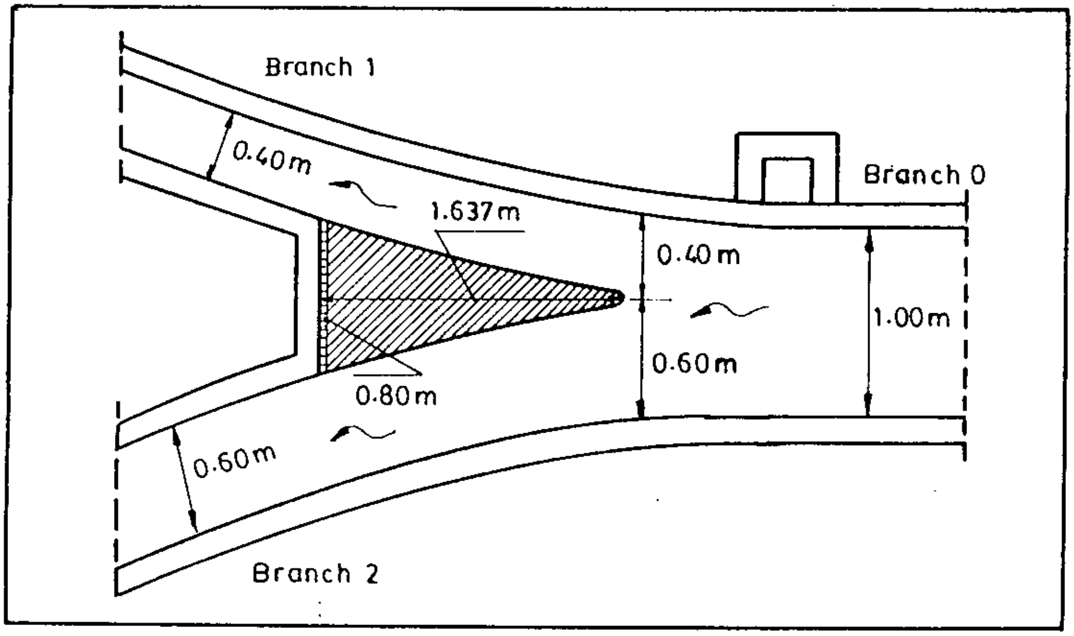

Fig. 4.9 Nose No. 1

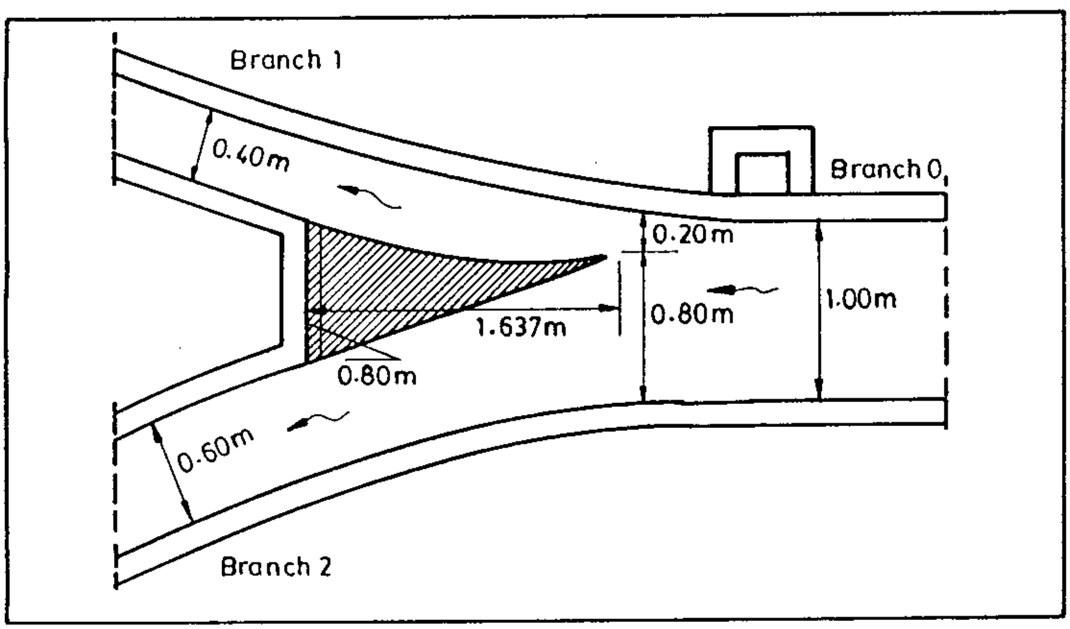

Fig. 4.10 Nose No. 2

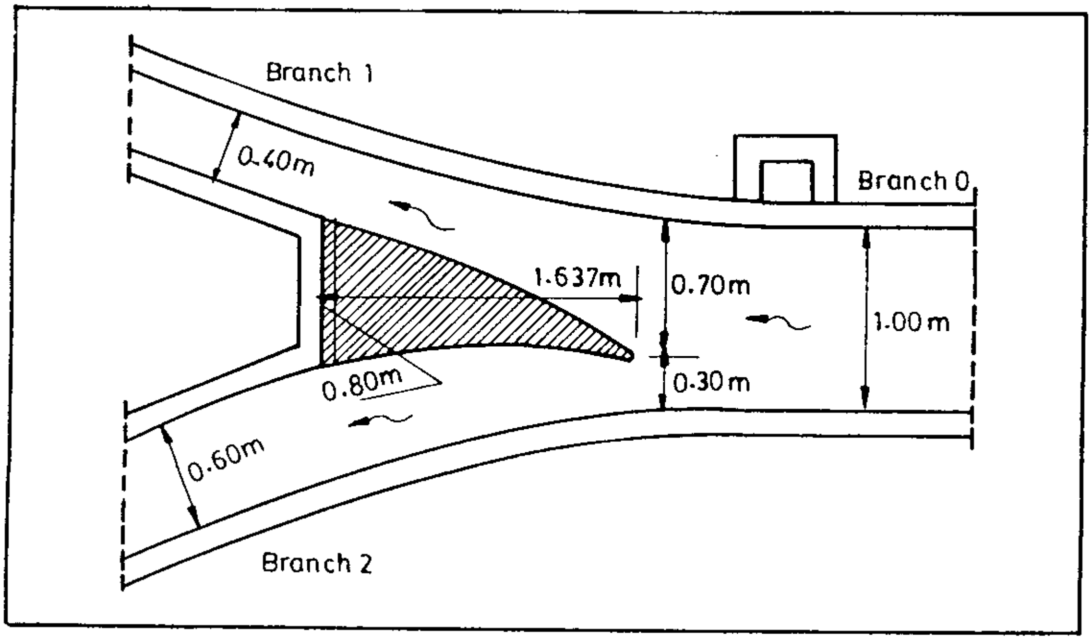

Fig. 4.11 Nose No. 3

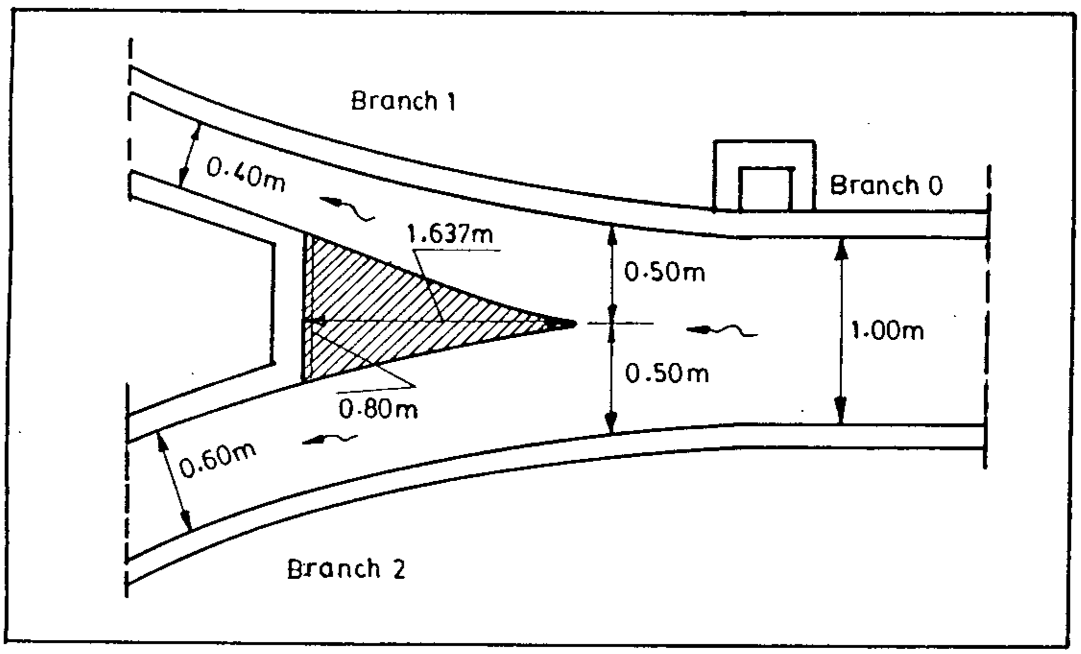

Fig. 4.12 Nose No. 4

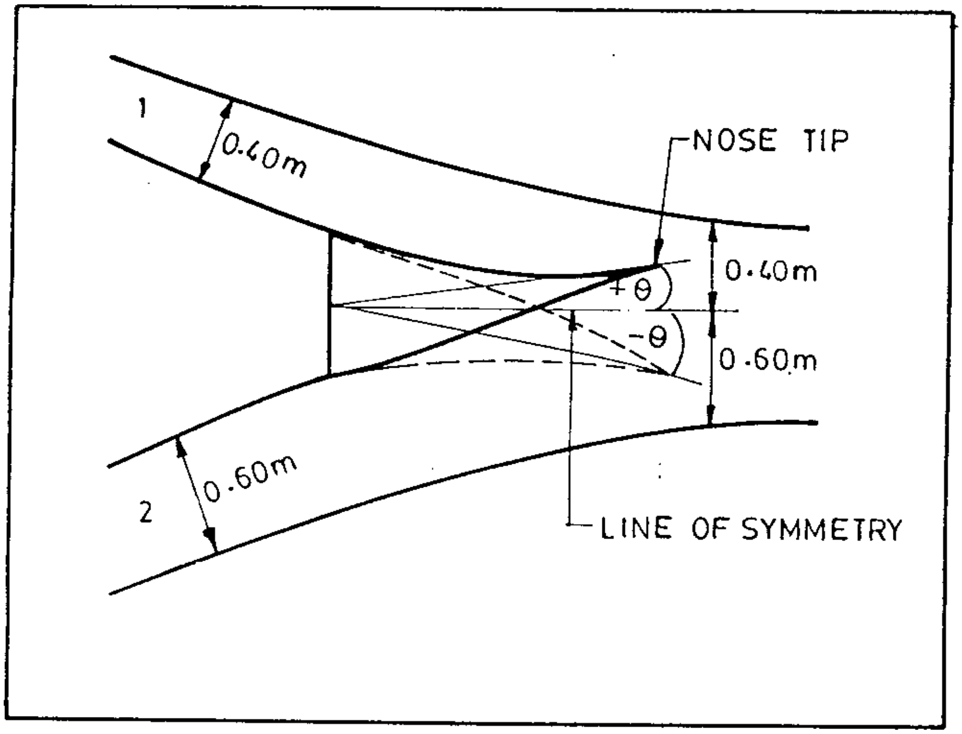

Fig. 4.13 Definition sketch of nose angle

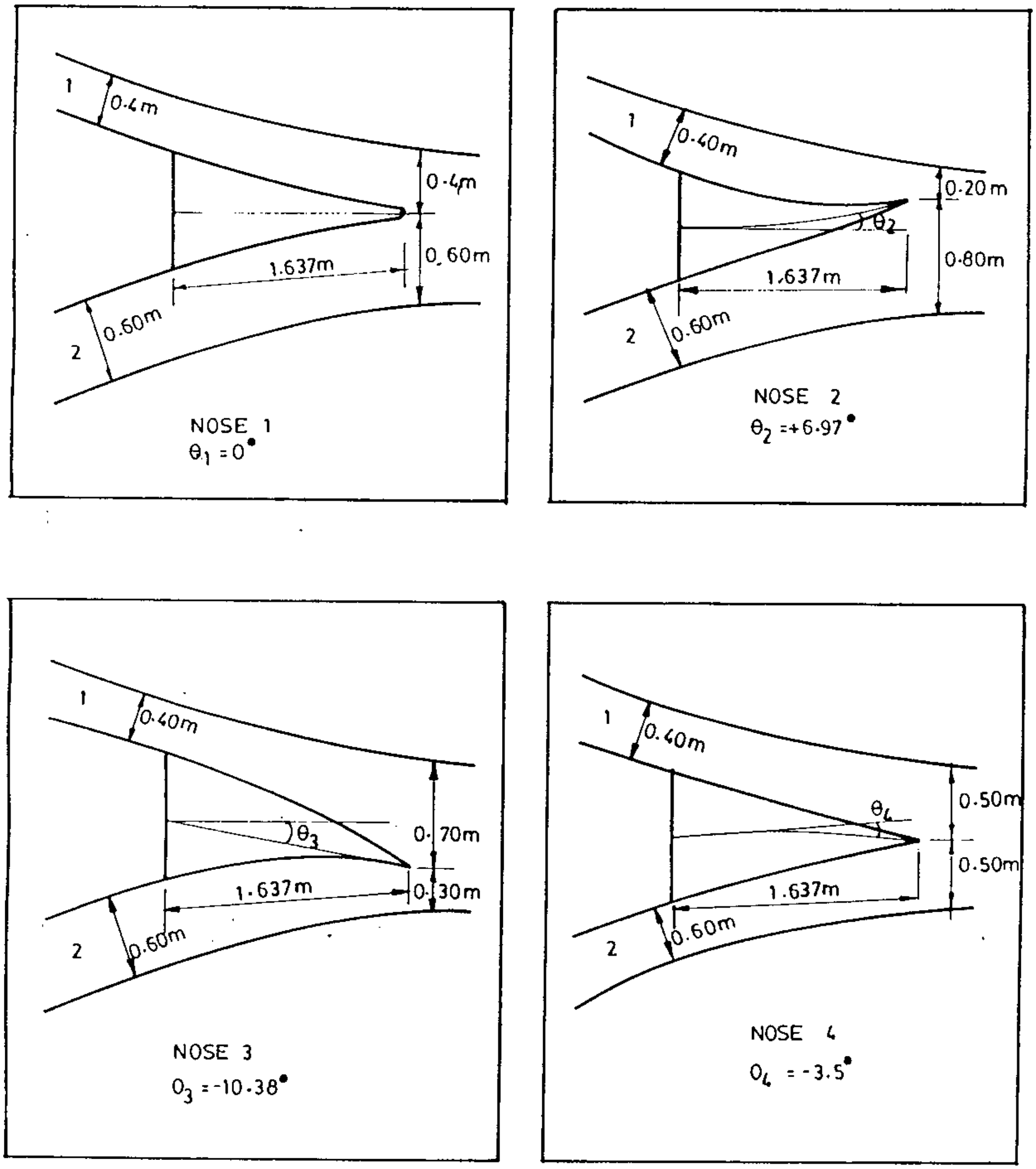

Fig. 4.14 Different nose angles

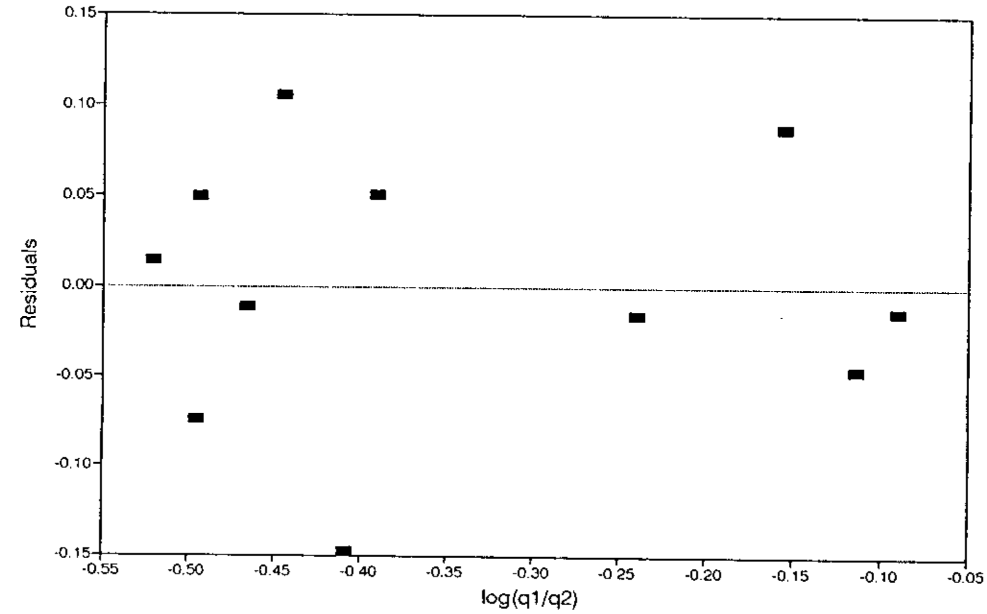

Fig. 5.1 Plot of residuals versus discharge ratio for $\theta = 6.97^0$ and $Q_0 = 20$ l/s

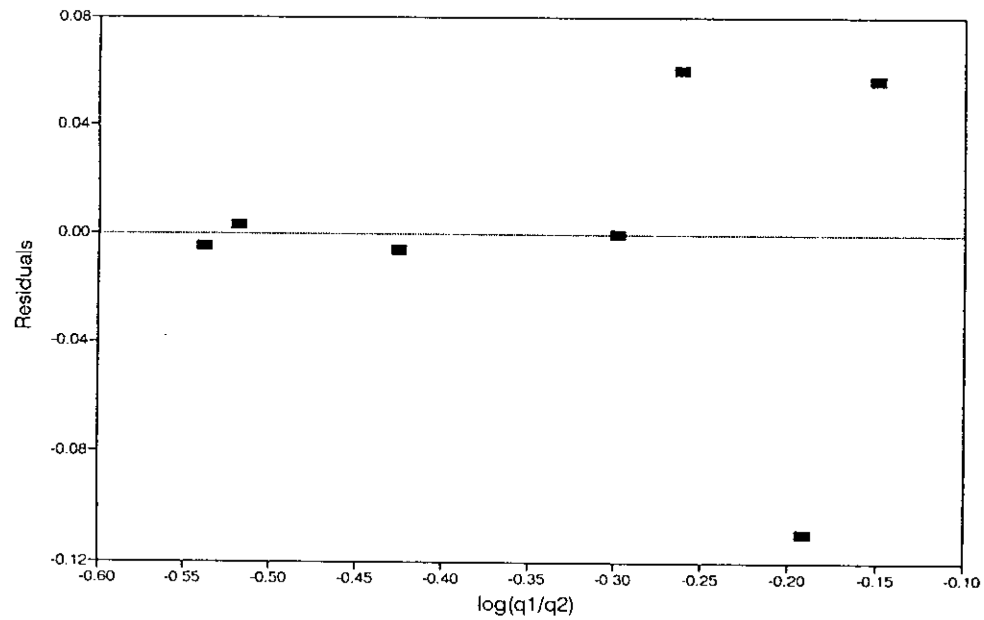

Fig. 5.2 Plot of residuals versus discharge ratio for $\theta = 6.97^0$ and $Q_0 = 30$ l/s

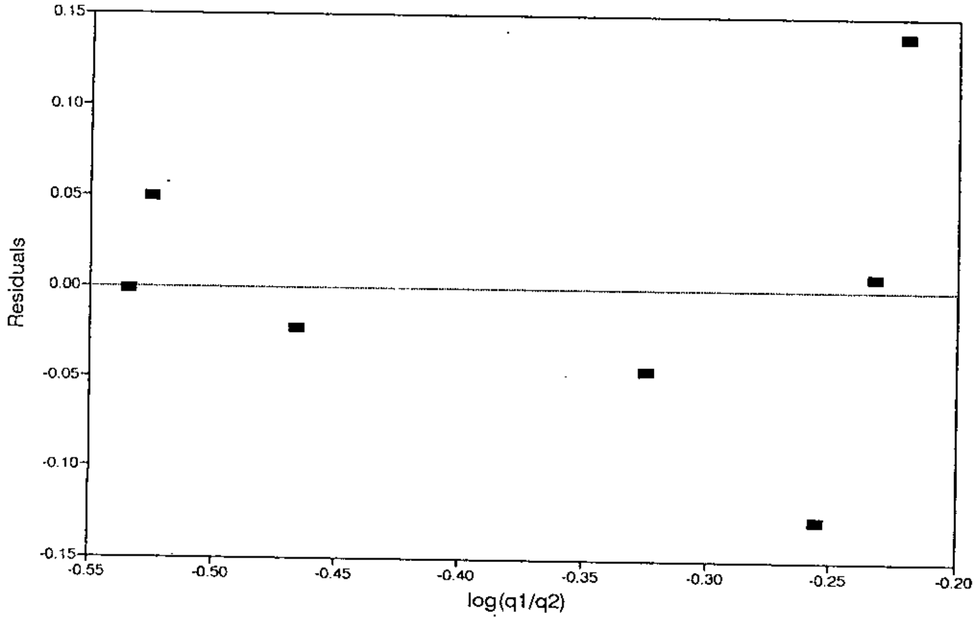

Fig. 5.3 Plot of residuals versus discharge ratio for $\theta = 6.97^0$ and $Q_0 = 40$ l/s

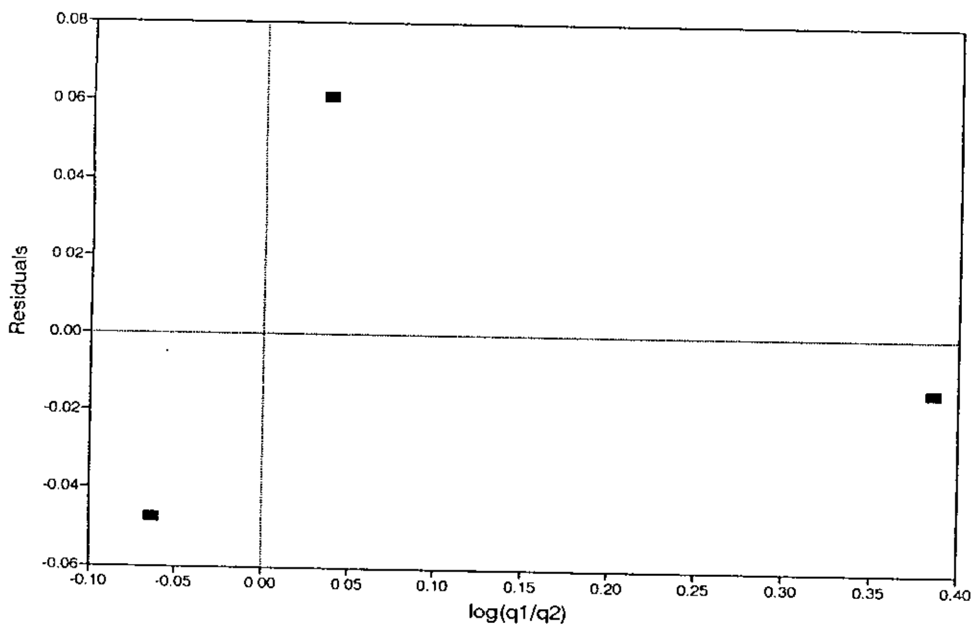

Fig. 5.4 Plot of residuals versus discharge ratio for $\theta = -3.50^0$ and $Q_0 = 20$ l/s

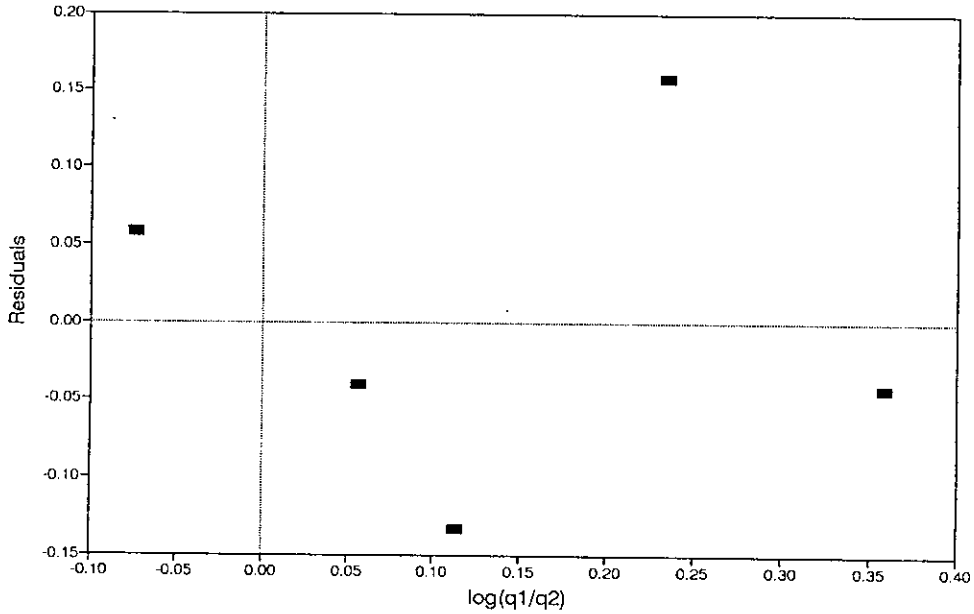

Fig. 5.5 Plot of residuals versus discharge ratio for $\theta = -3.50^0$ and $Q_0 = 30$ l/s

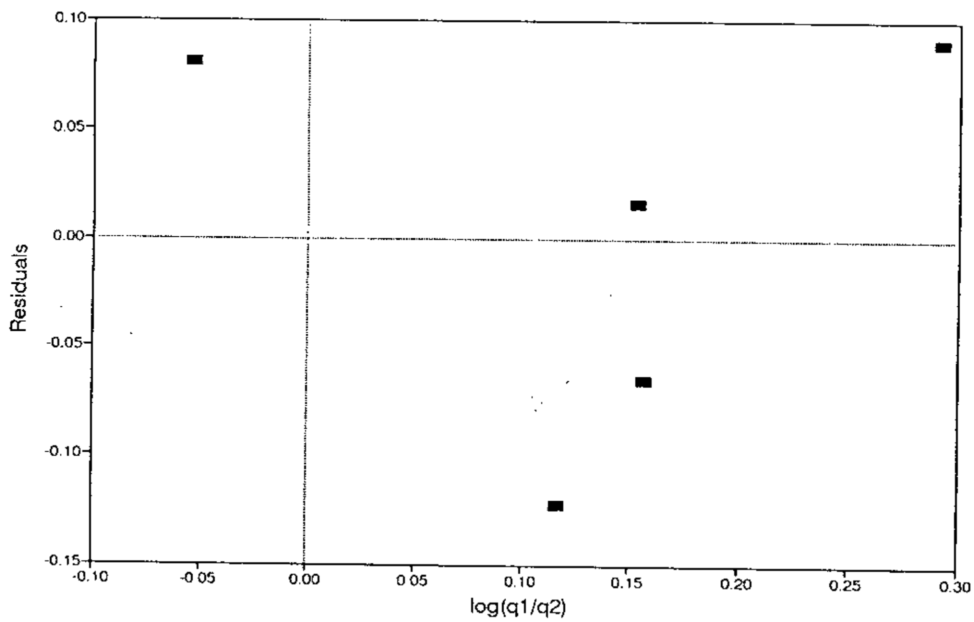

Fig. 5.6 Plot of residuals versus discharge ratio for $\theta = -3.50^0$ and $Q_0 = 40$ l/s

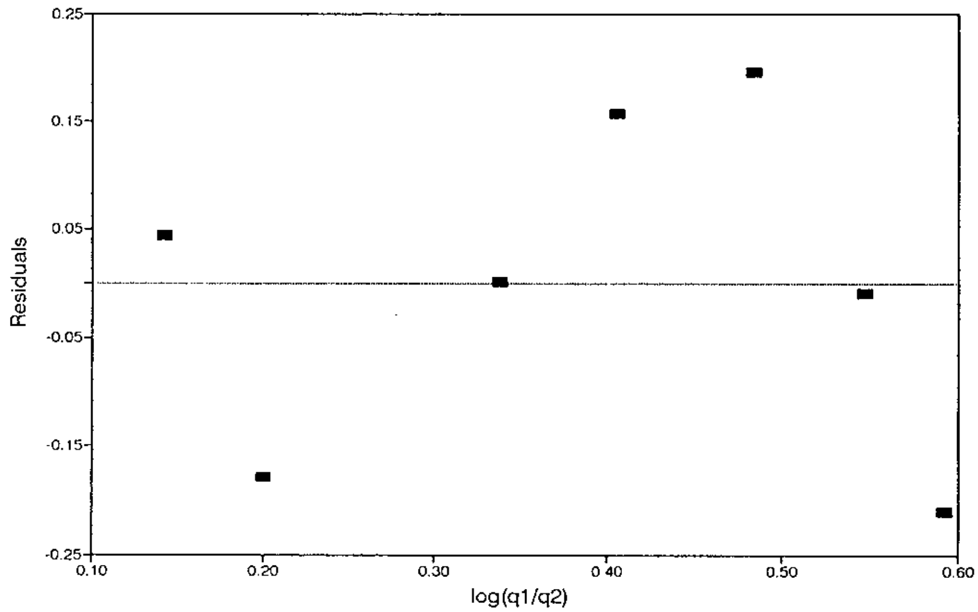

Fig. 5.7 Plot of residuals versus discharge ratio for $\theta = -10.38^0$ and $Q_0 = 20$ l/s

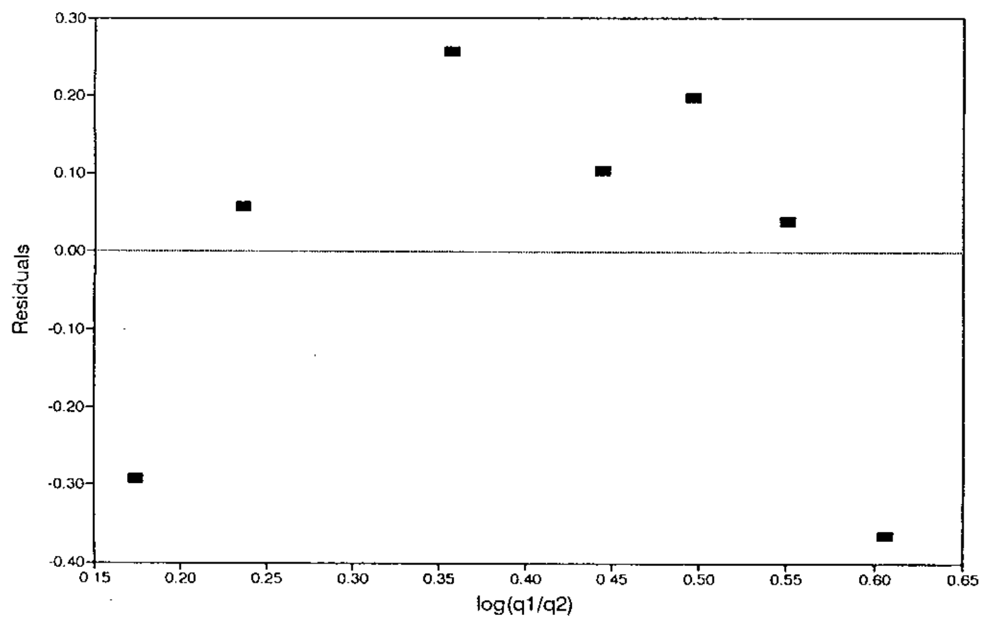

Fig. 5.8 Plot of residuals versus discharge ratio for $\theta = -10.38^0$ and $Q_0 = 30$ l/s

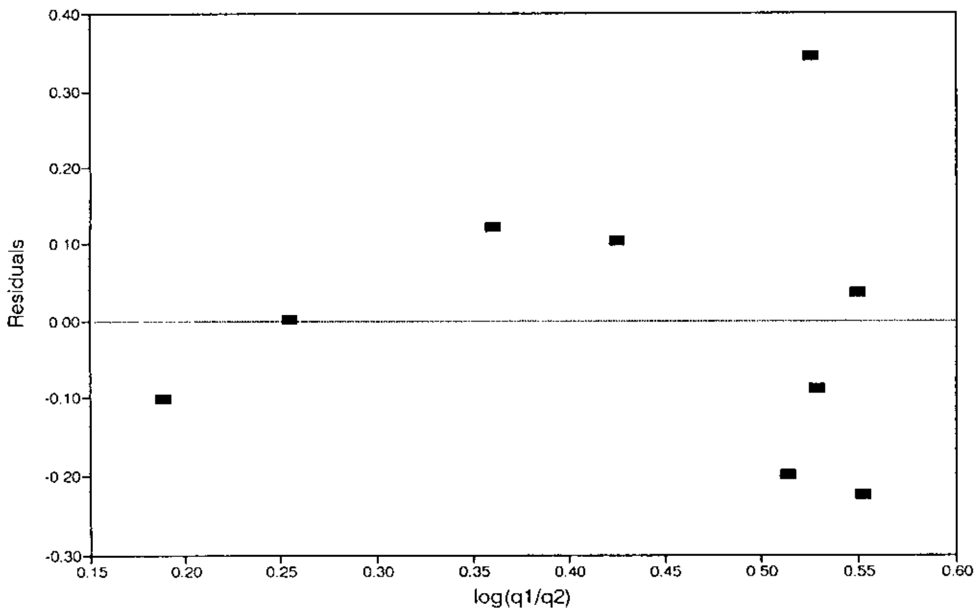

Fig. 5.9 Plot of residuals versus discharge ratio for $\theta = -10.38^0$ and $Q_0 = 40$ l/s

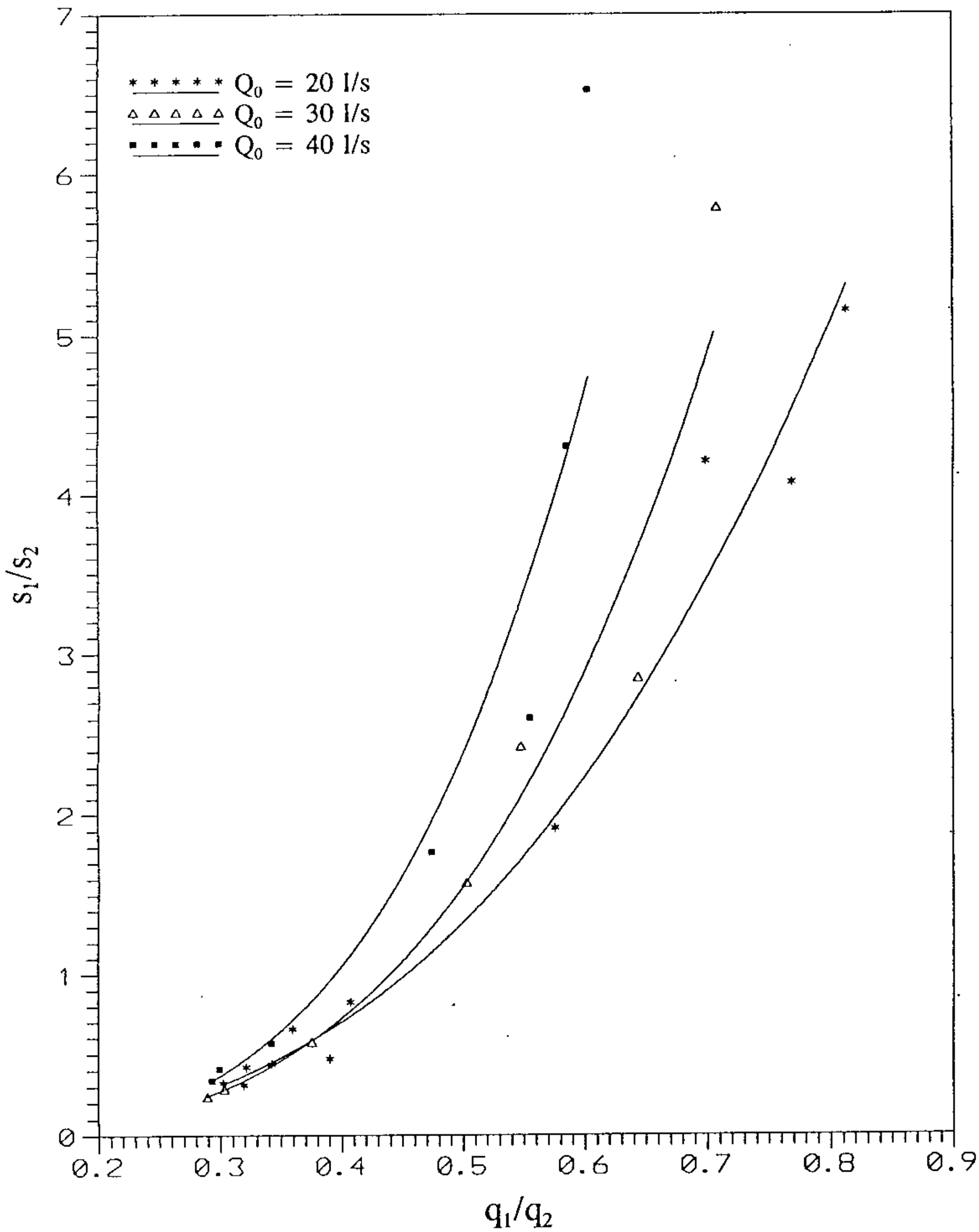

Fig. 5.10 Variation of s_1/s_2 with q_1/q_2 ($\theta = 6.97^0$)

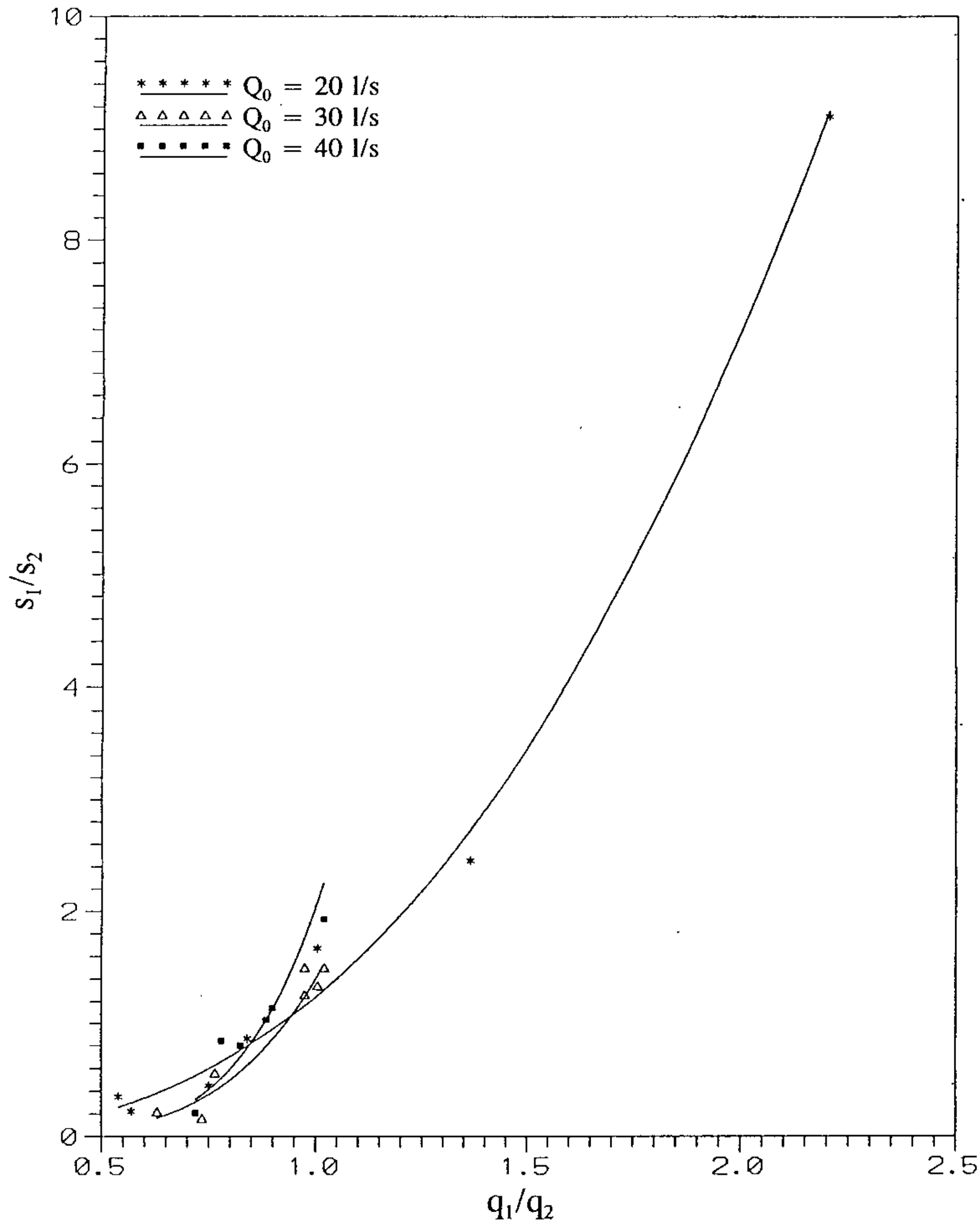

Fig. 5.11 Variation of s_1/s_2 with q_1/q_2 ($\theta = 0^0$)

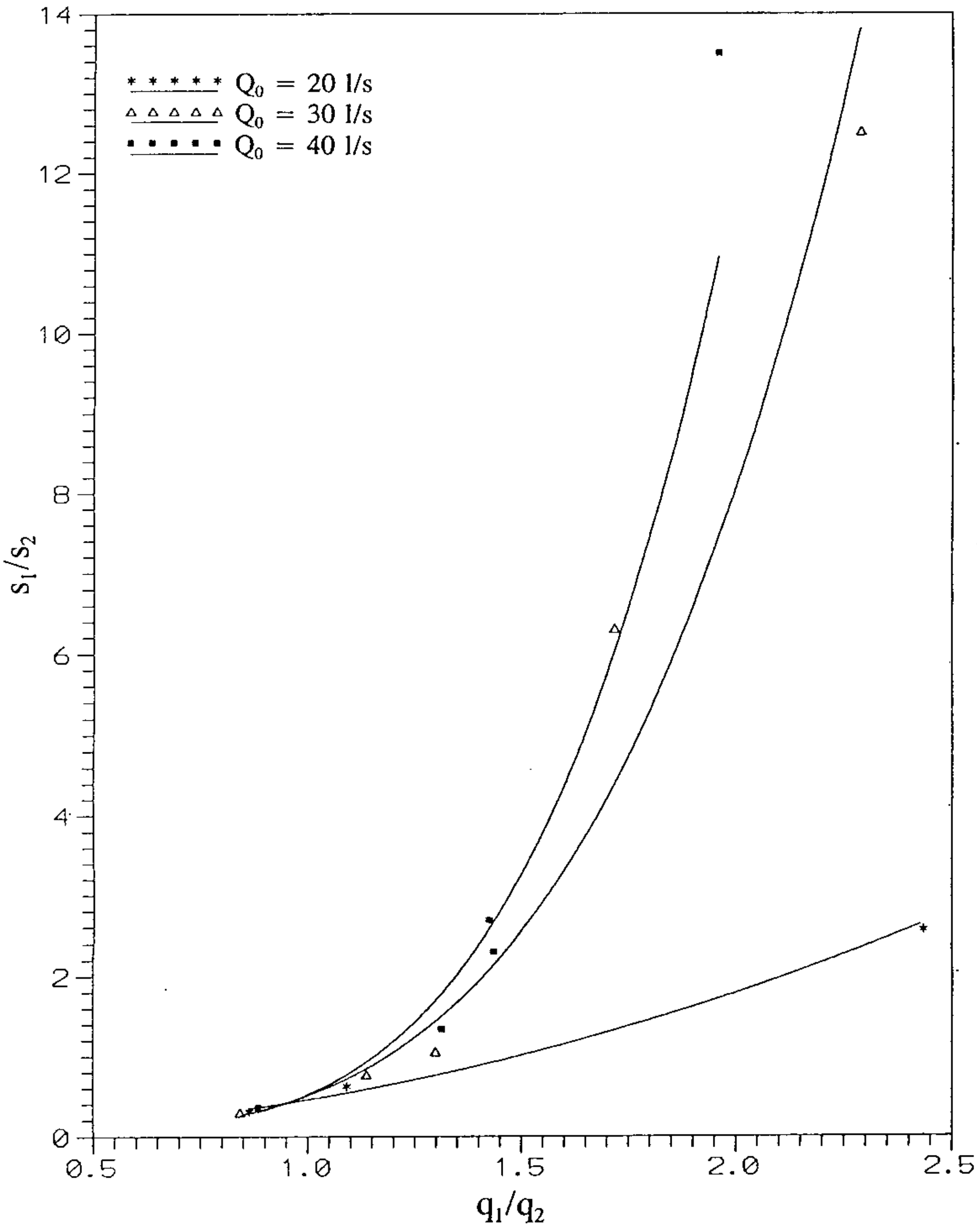

Fig. 5.12 Variation of s_1/s_2 with q_1/q_2 (θ = -3.50^0)

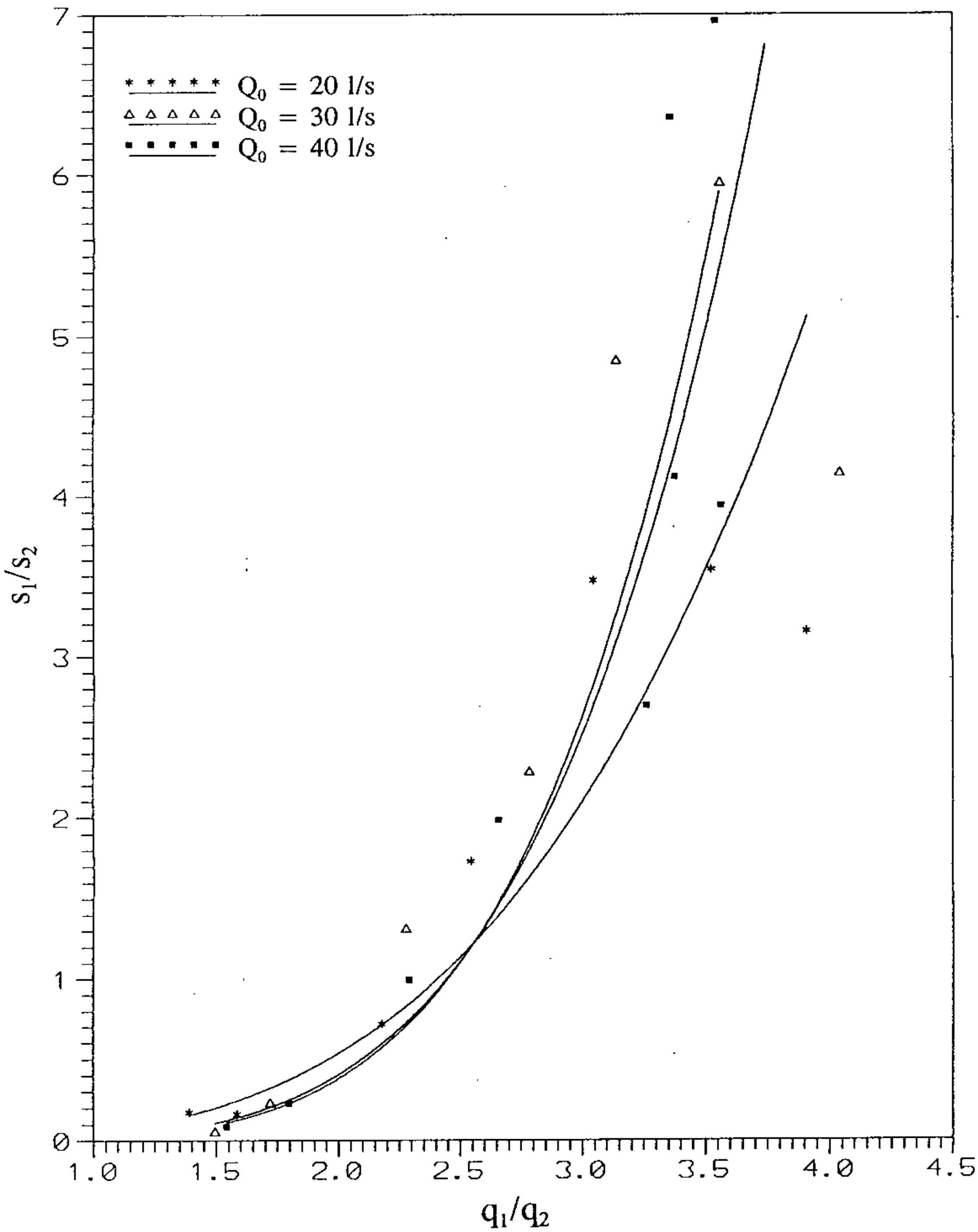

Fig. 5.13 Variation of s_1/s_2 with q_1/q_2 (θ = -10.38^0)

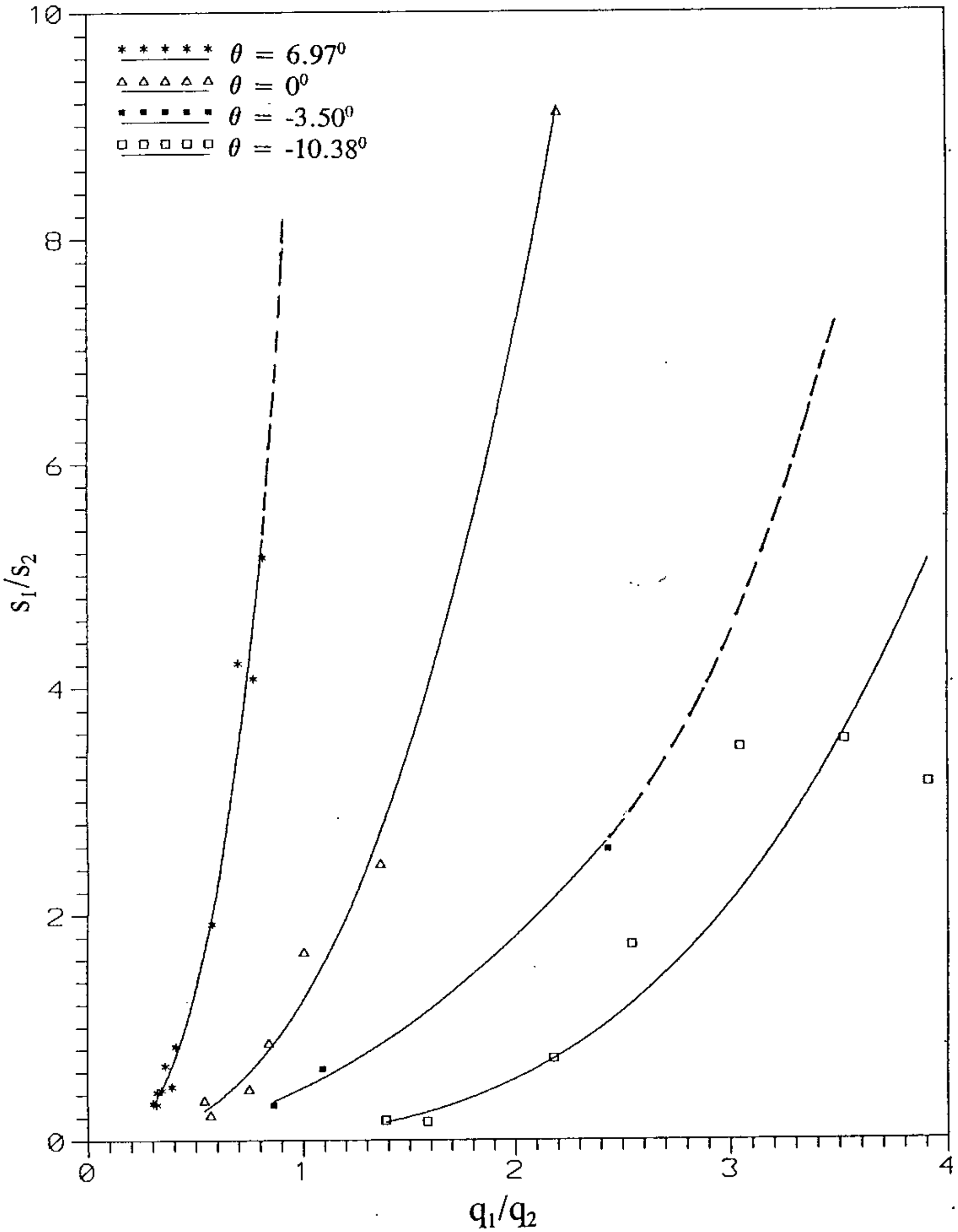

Fig. 5.14 Variation of s_l/s_2 with q_l/q_2 (Q_0 = 20 l/s)

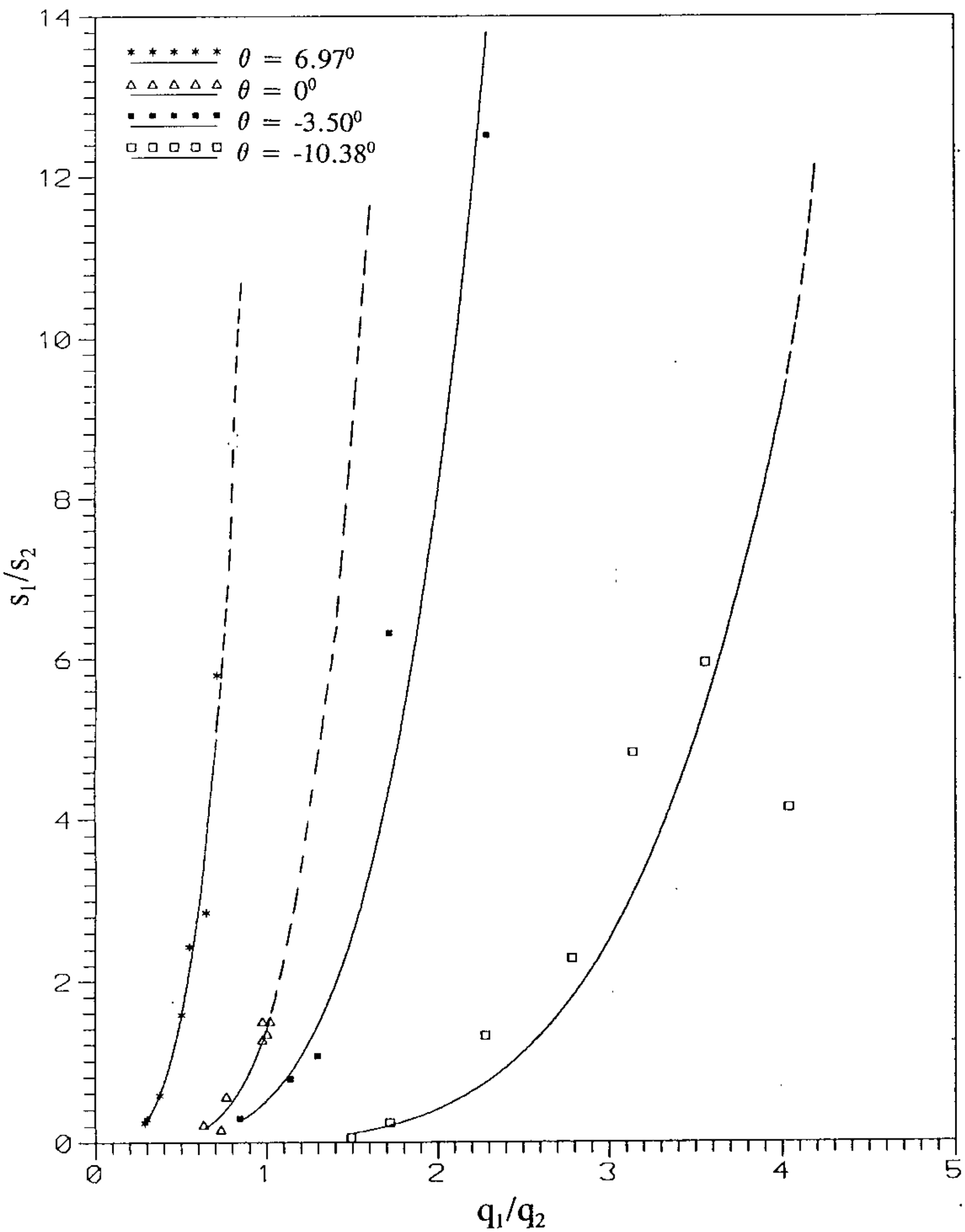

Fig. 5.15 Variation of s_1/s_2 with q_1/q_2 (Q_0 = 30 l/s)

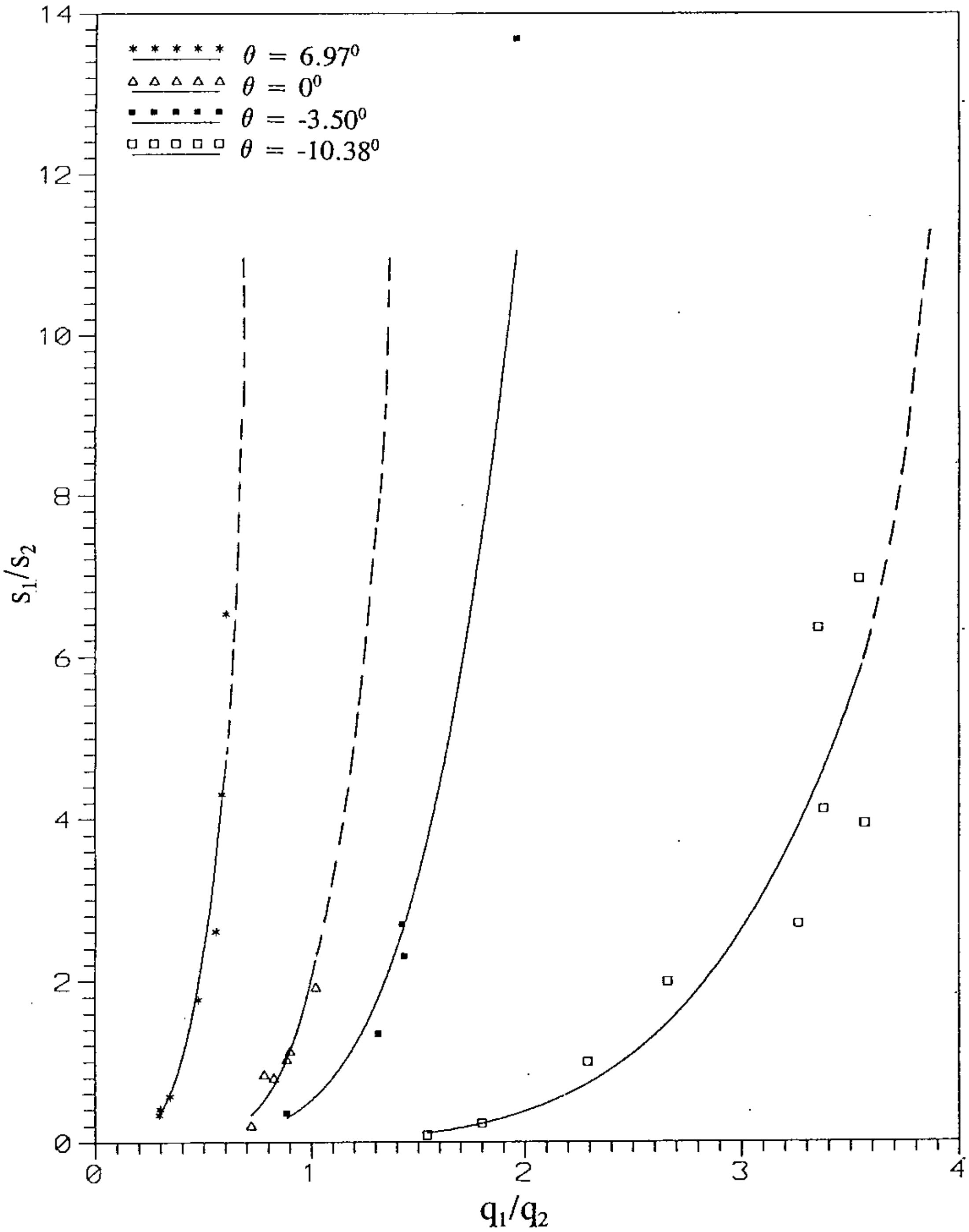

Fig. 5.16 Variation of s_1/s_2 with q_1/q_2 (Q_0 = 40 l/s)

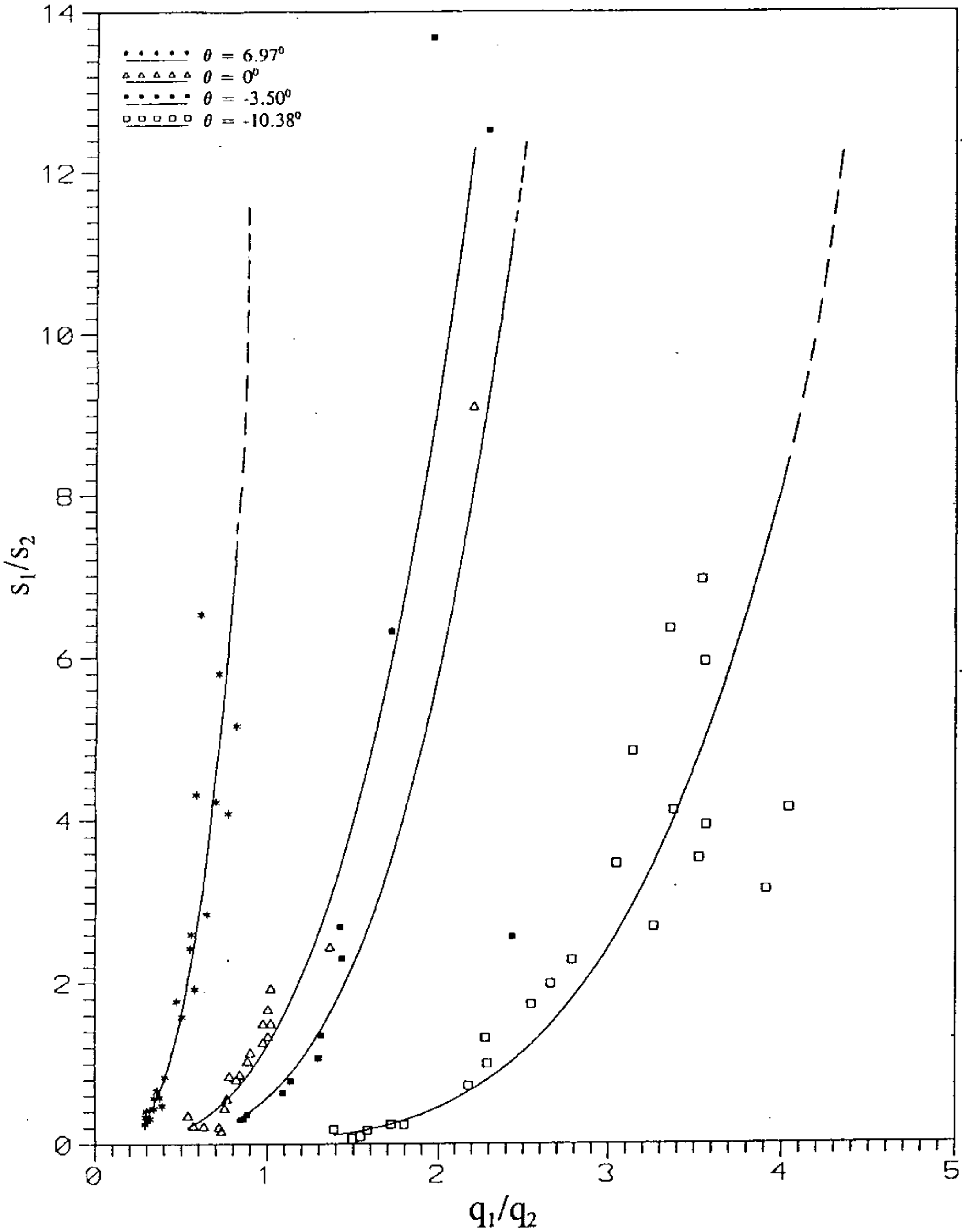

Fig. 5.17 Variation of s_1/s_2 with q_1/q_2 for different nose angles (independent of discharge)

APPENDIX A

FIGURES SHOWING BED LEVEL EVOLUTION FOR VARIOUS RUNS

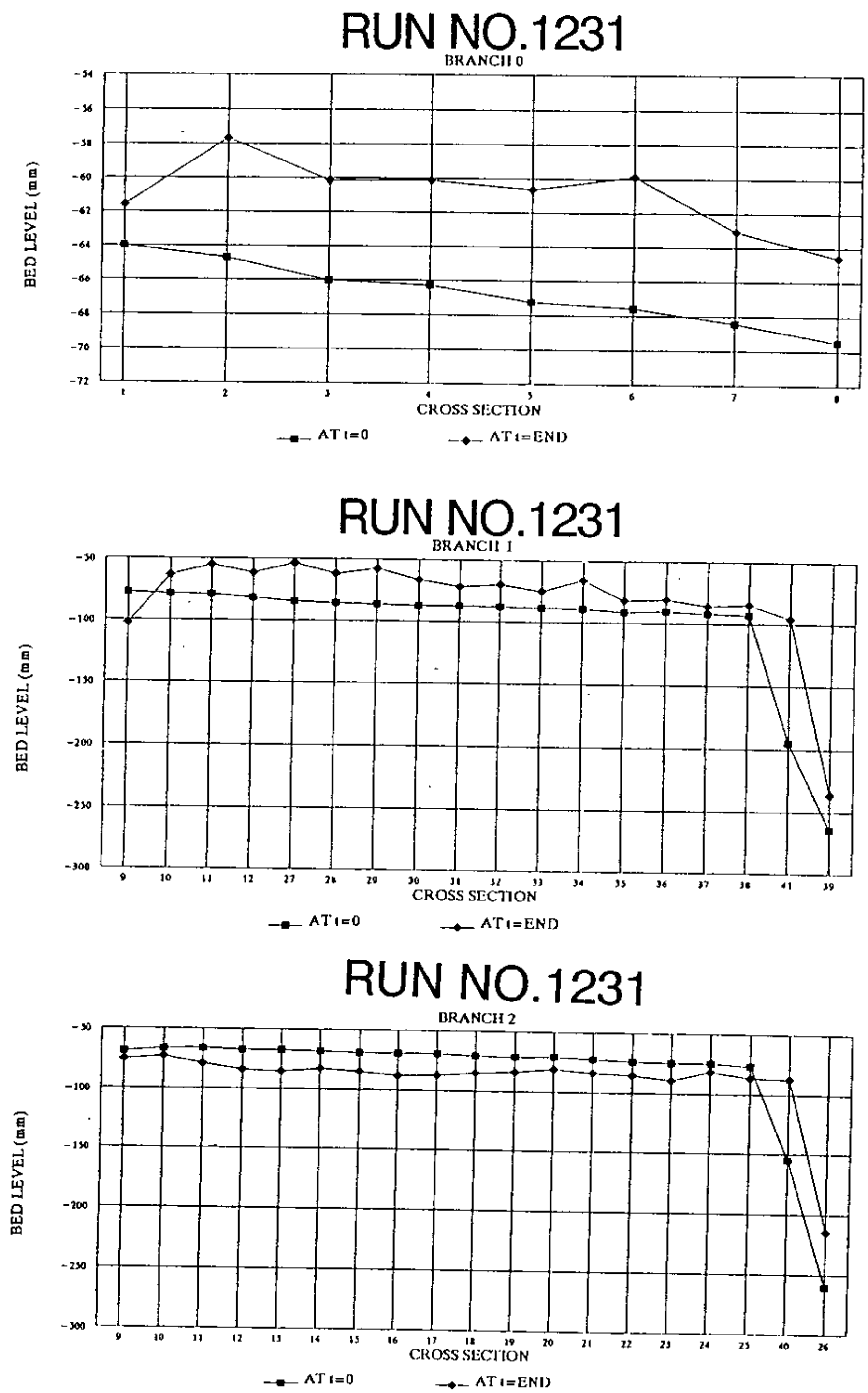

Fig. A.1 Bed level evolution of run no. 1231

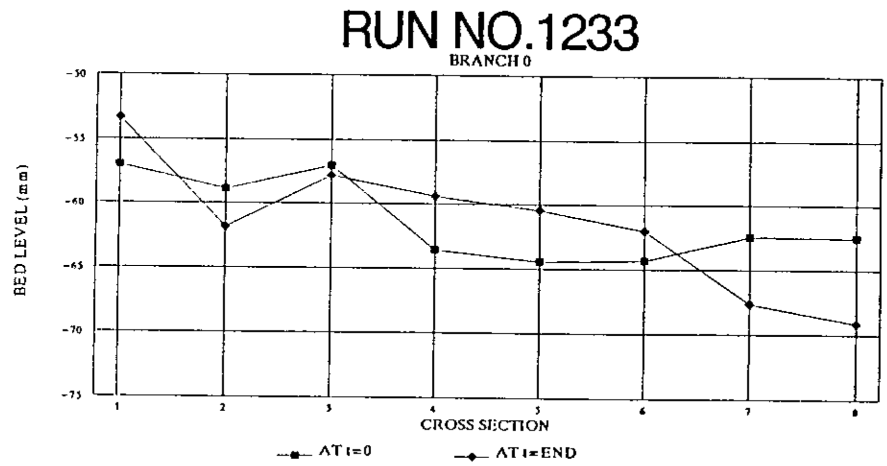

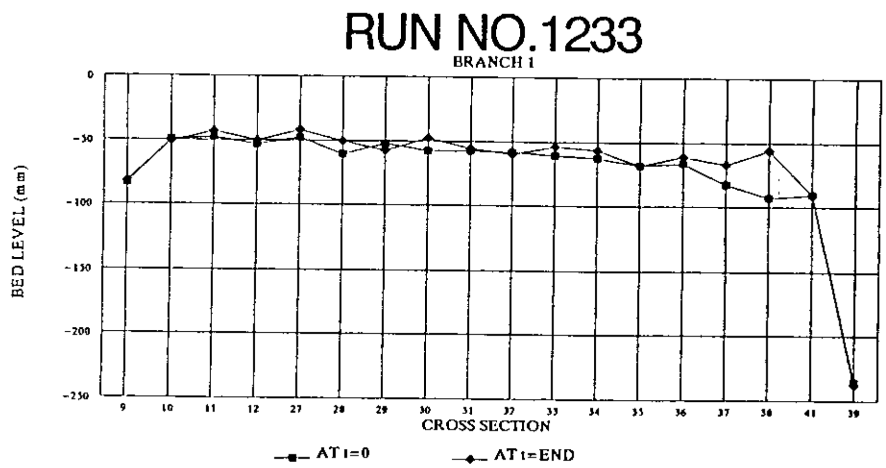

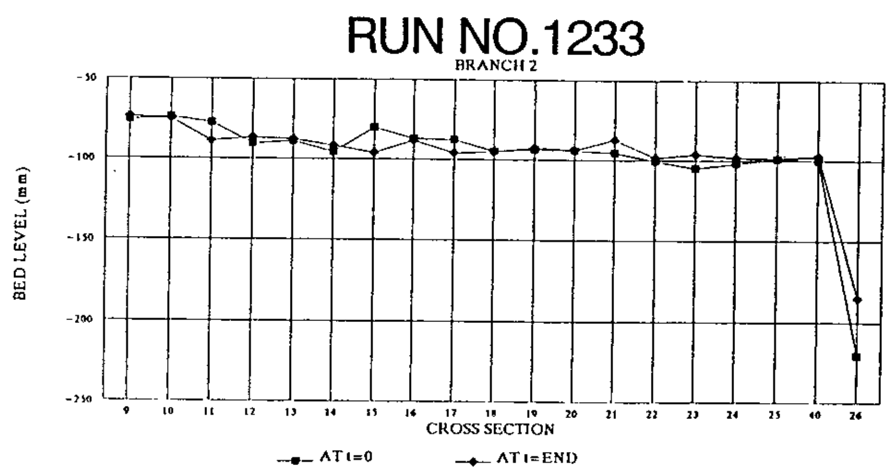

Fig. A.2 Bed level evolution of run no. 1233

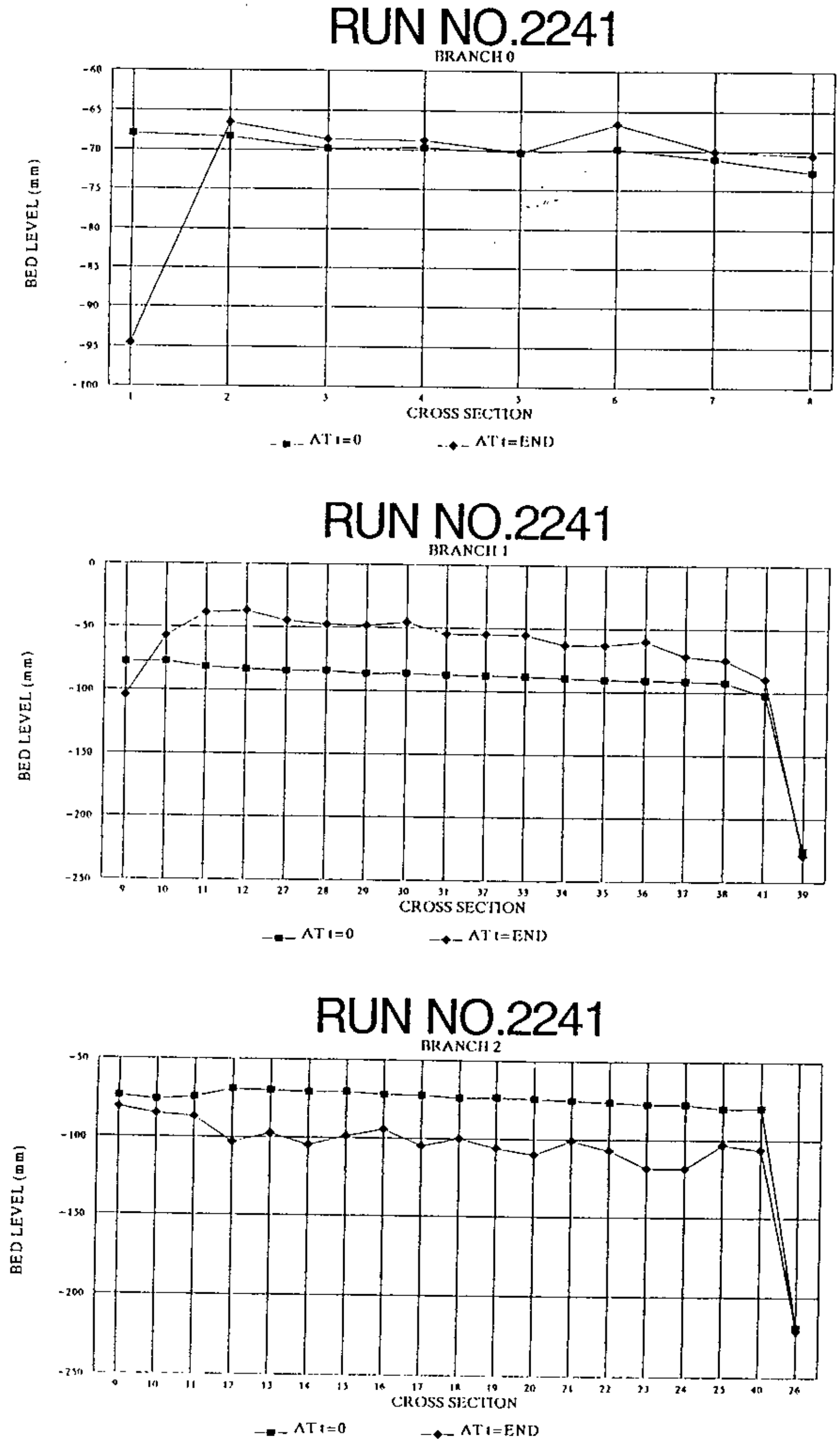

Fig. A.3 Bed level evolution of run no. 2241

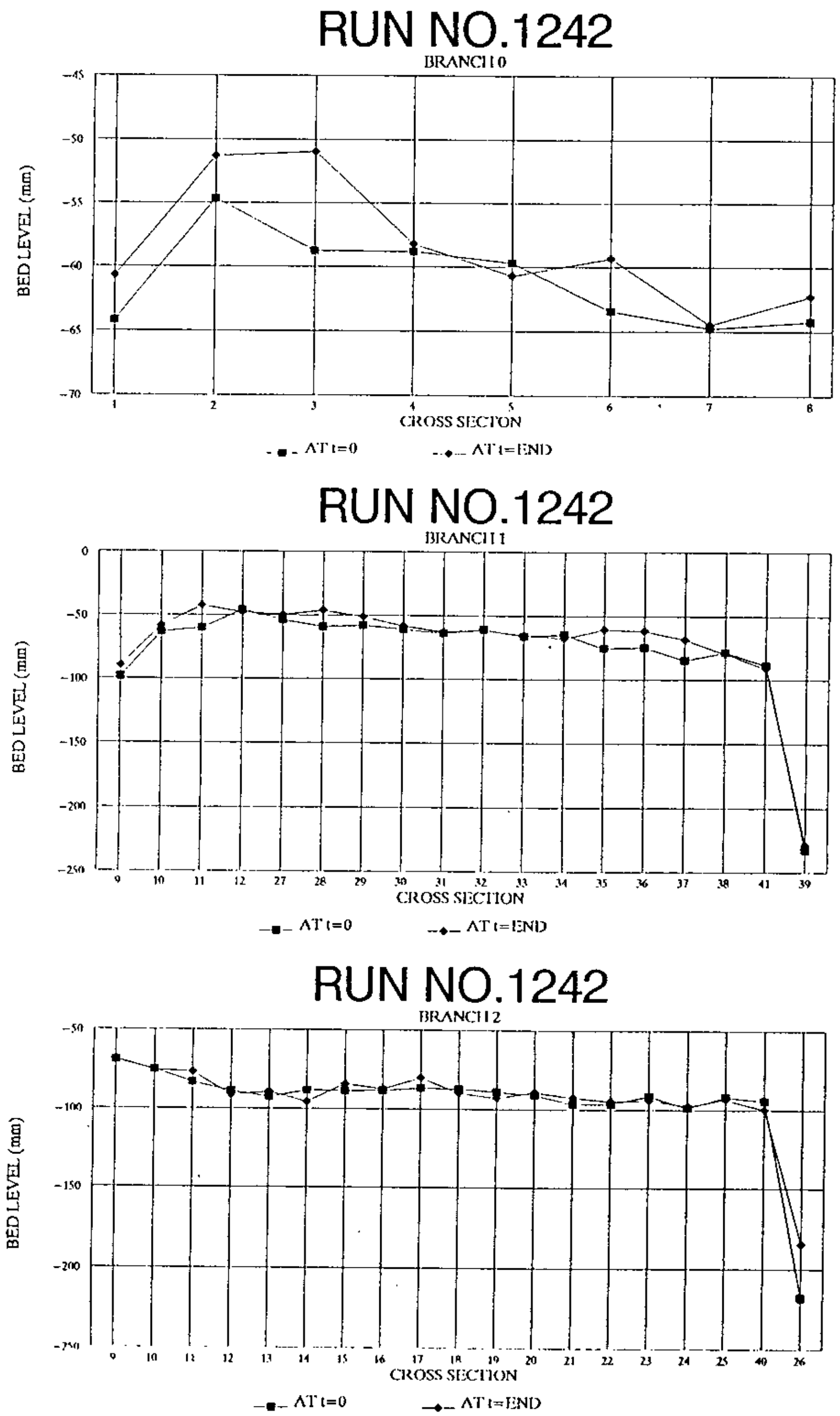

Fig. A.4 Bed level evolution of run no. 2242

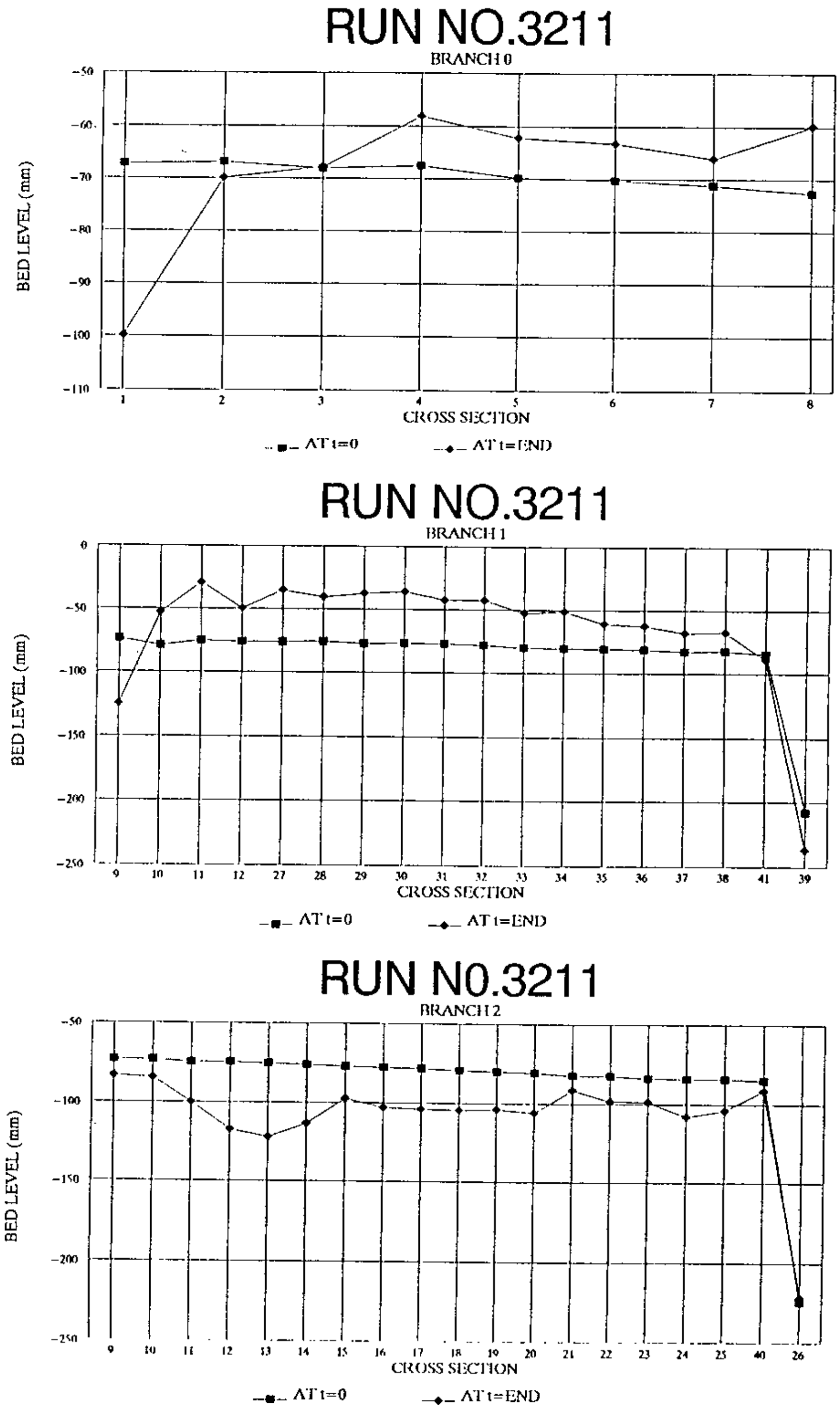

Fig. A.5 Bed level evolution of run no. 3211

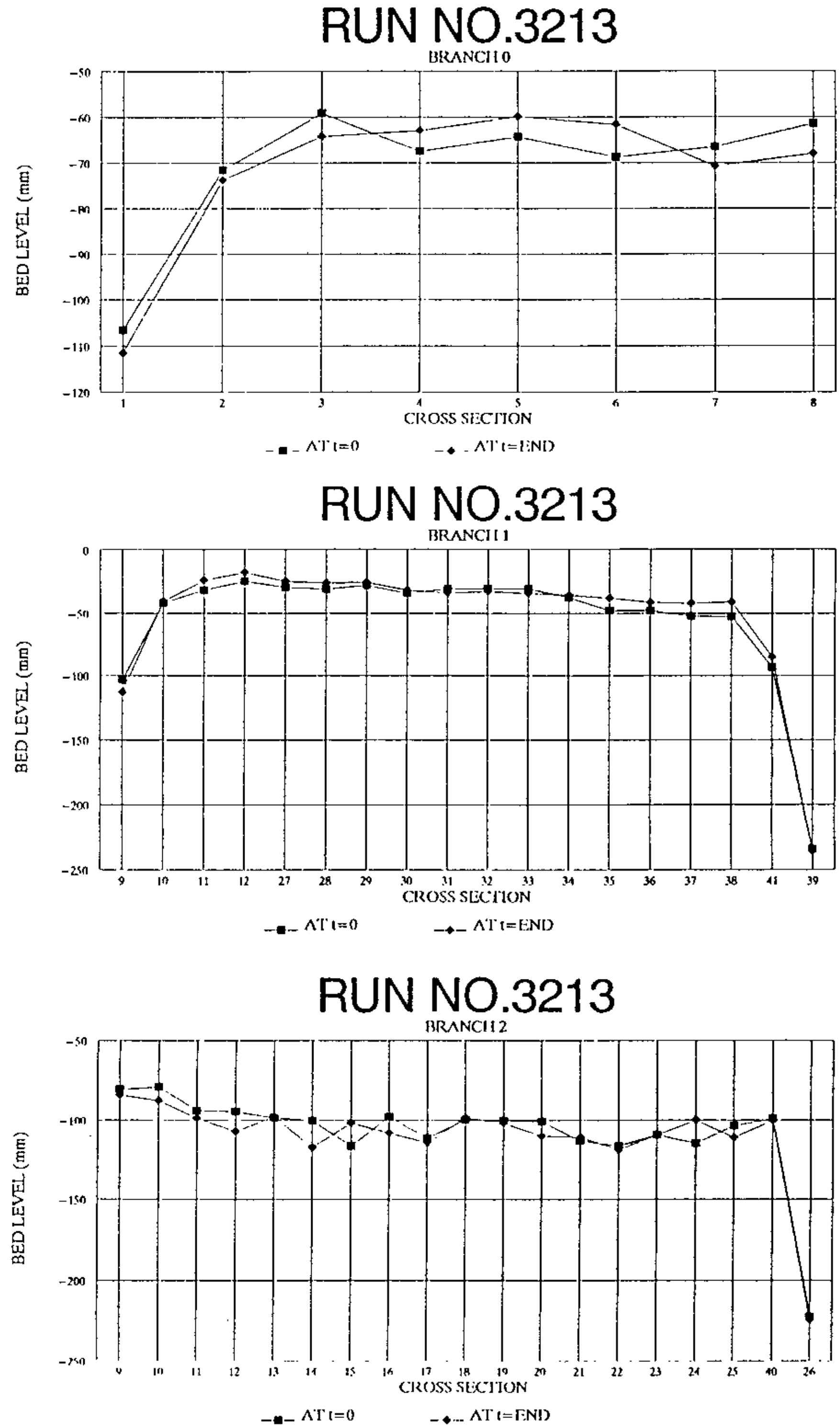

Fig. A.6 Bed level evolution of run no. 3213

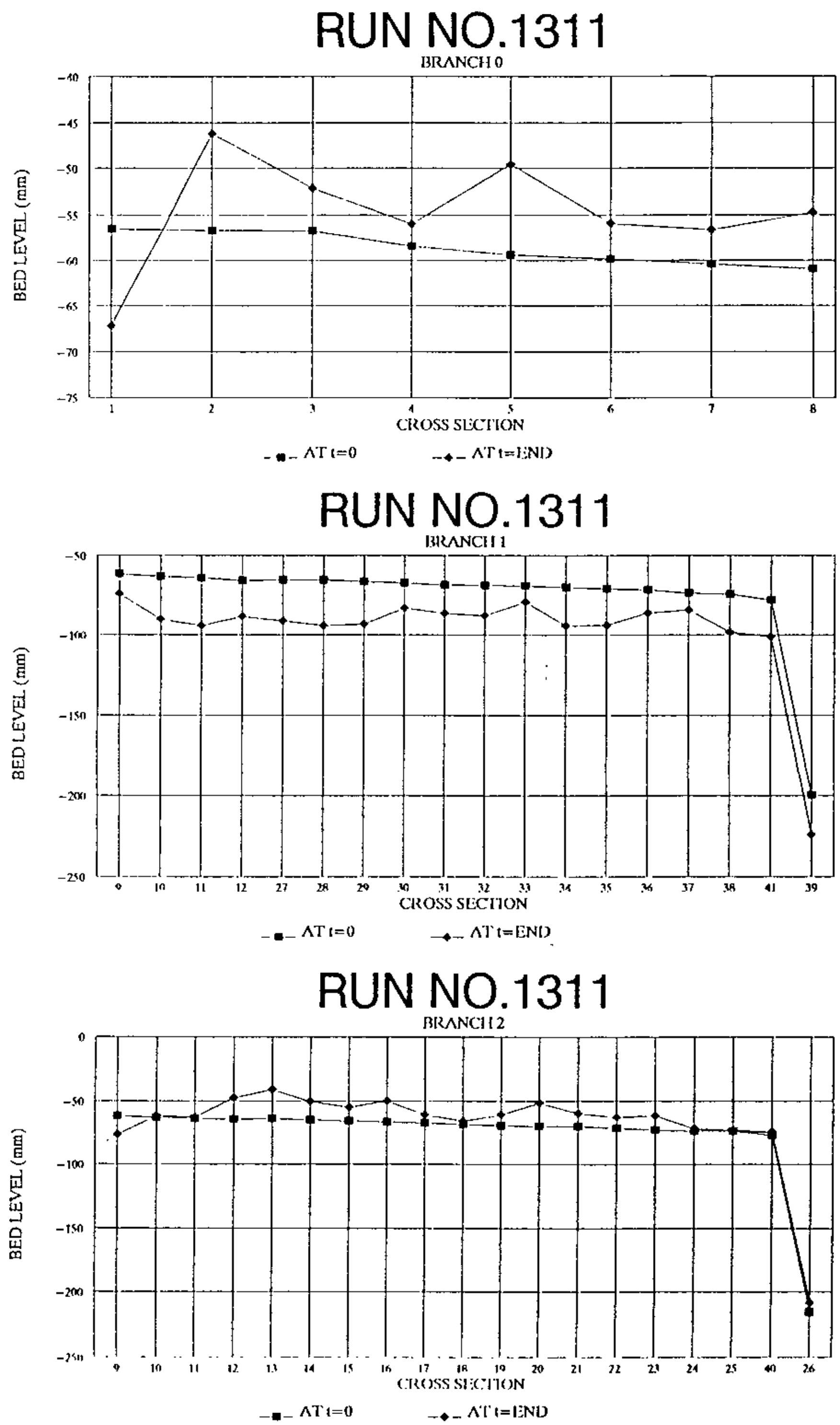

Fig. A.7 Bed level evolution of run no. 1311

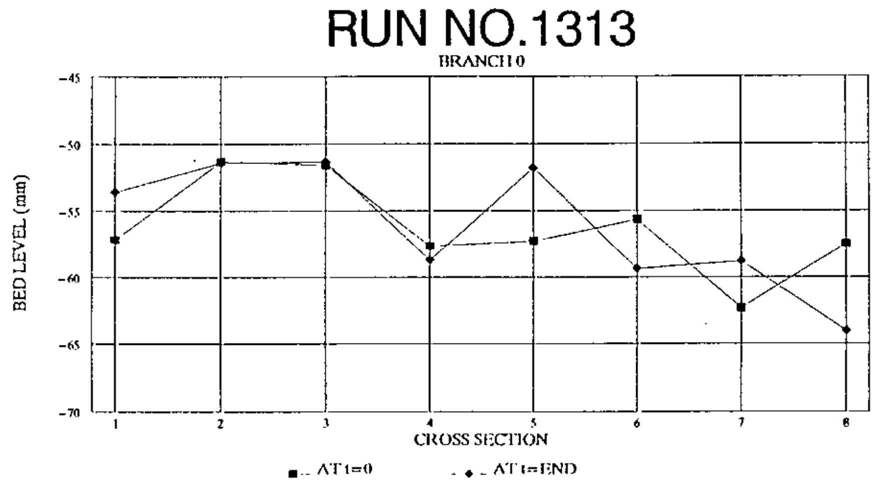

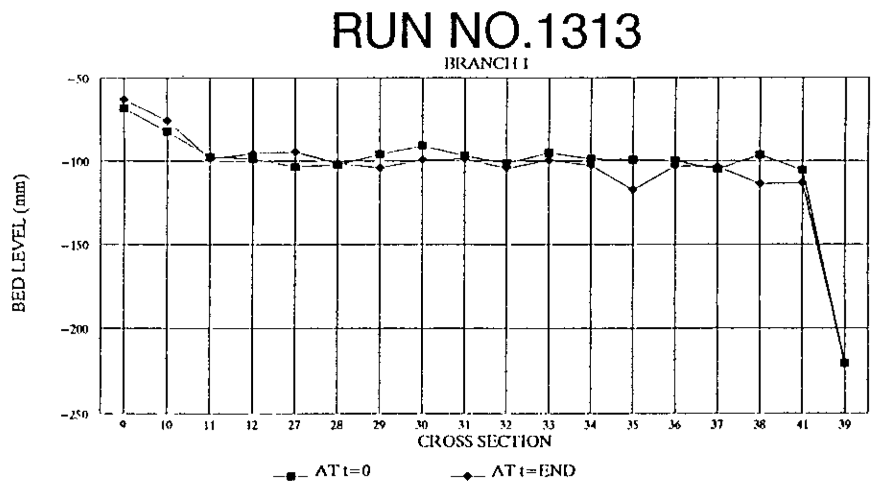

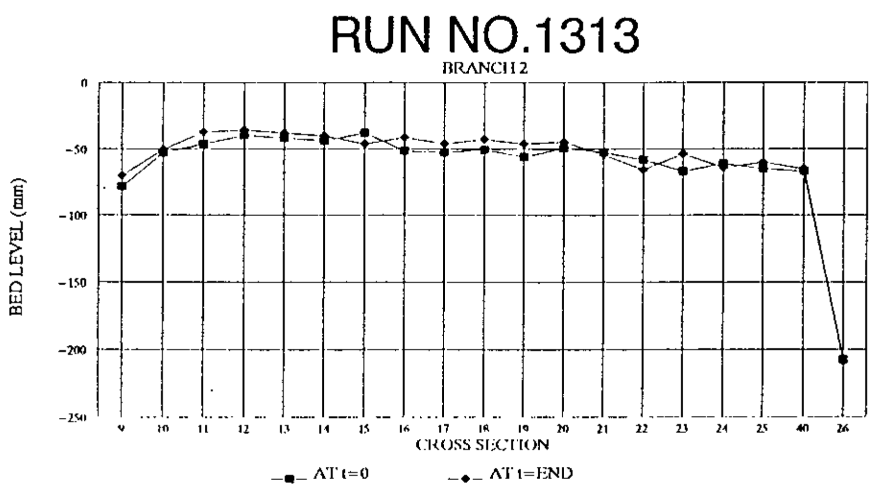

Fig. A.8 Bed level evolution of run no. 1313

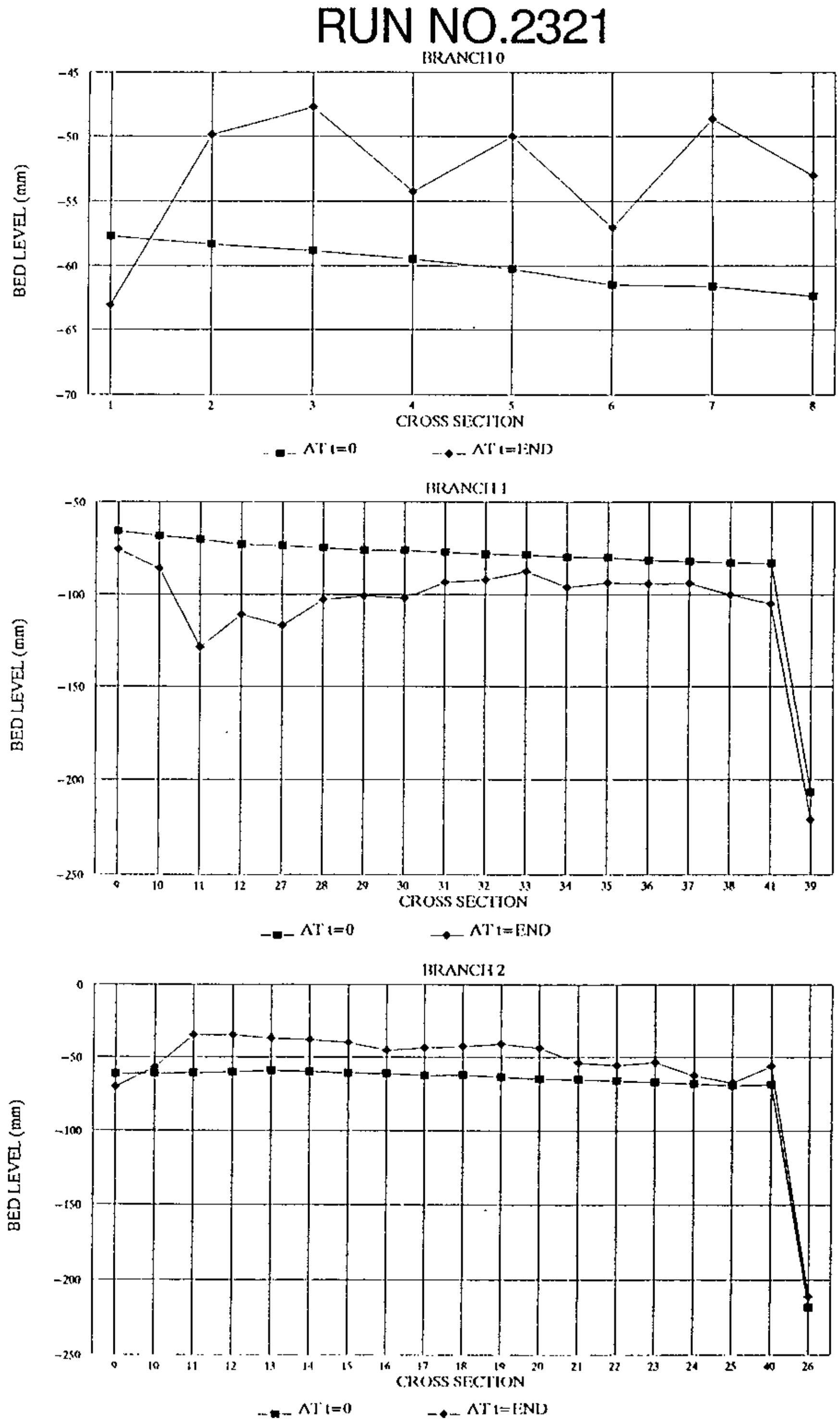

Fig. A.9 Bed level evolution of run no. 2321

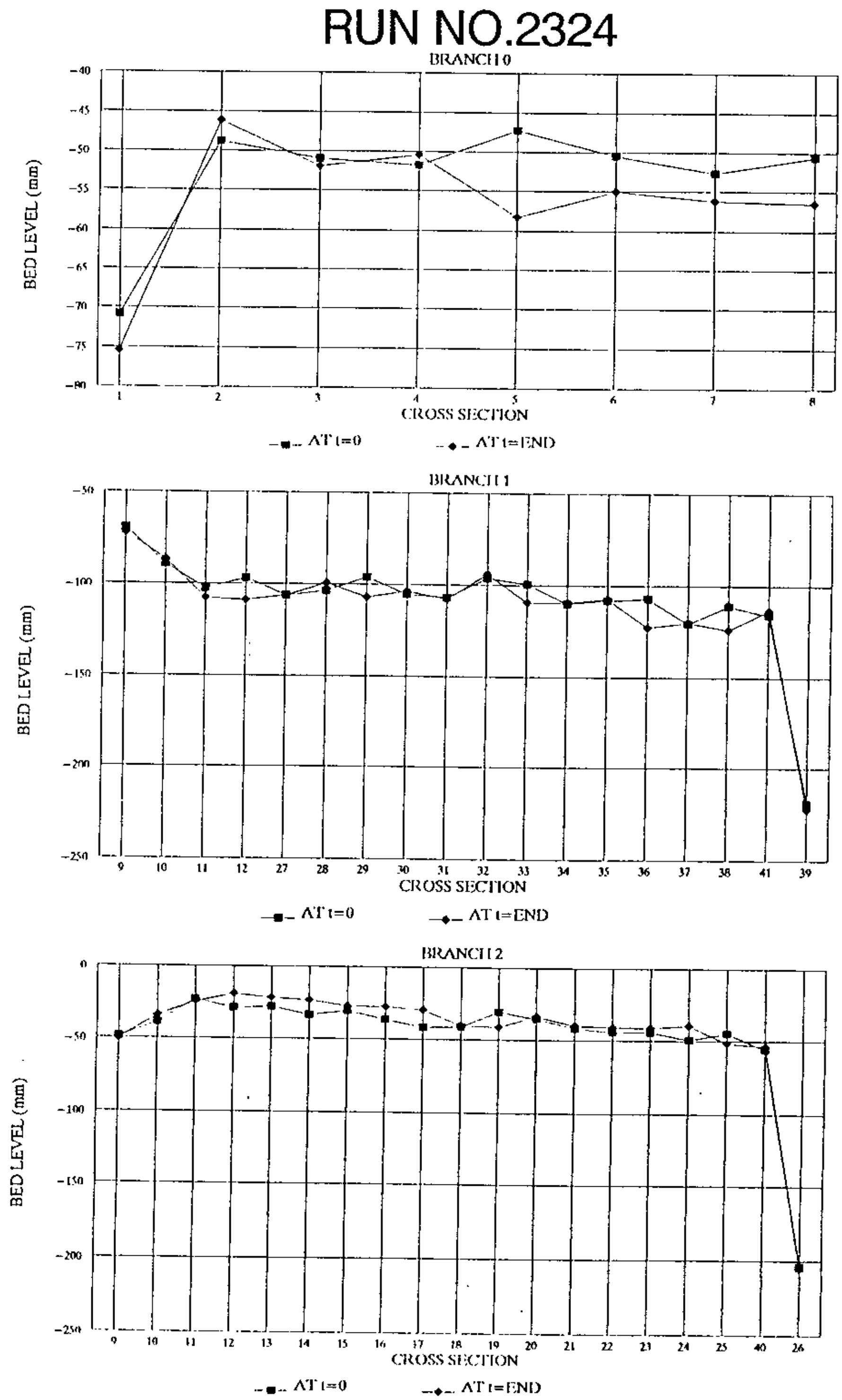

Fig. A.10 Bed level evolution of run no. 2324

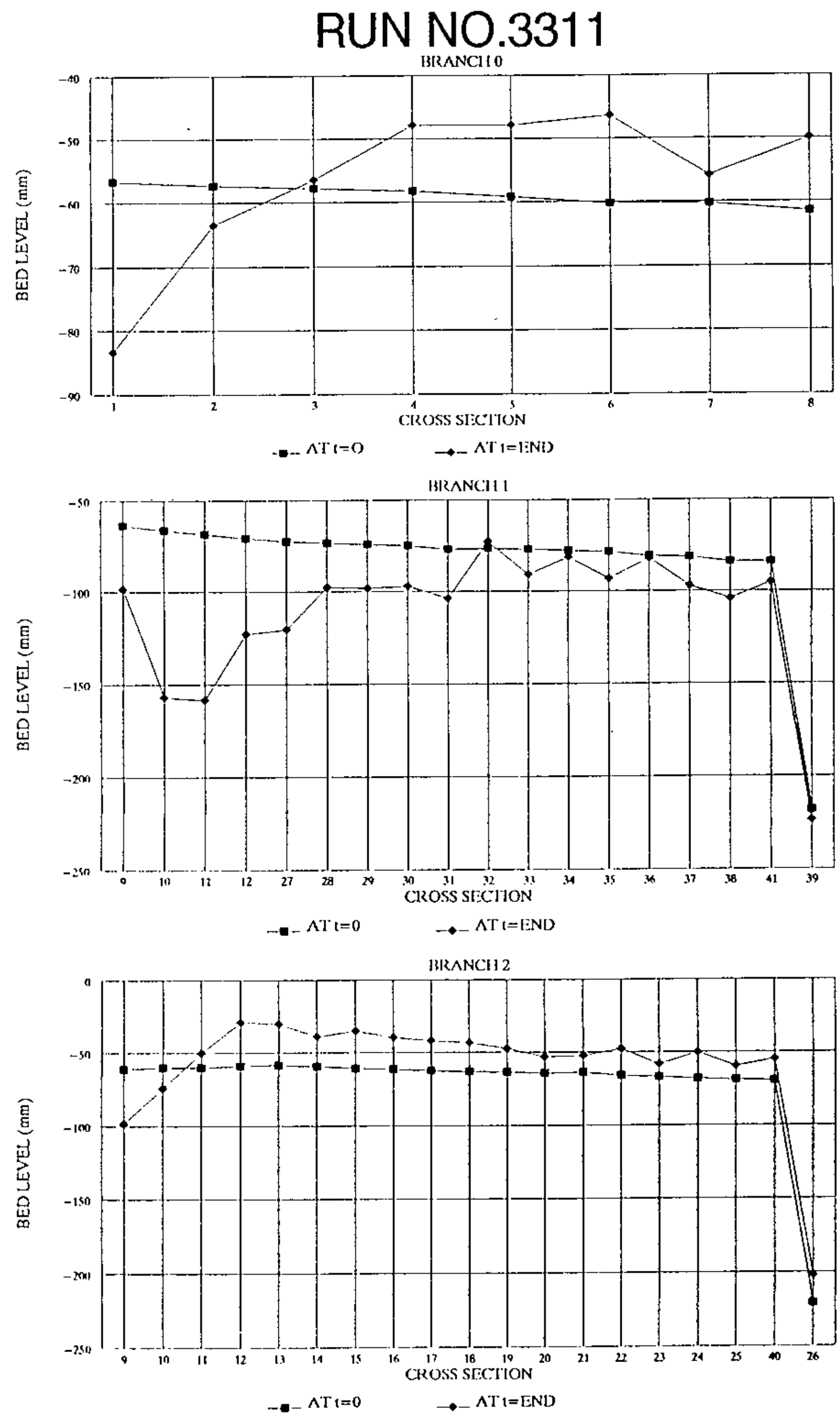

Fig. A.11 Bed level evolution of run no. 3311

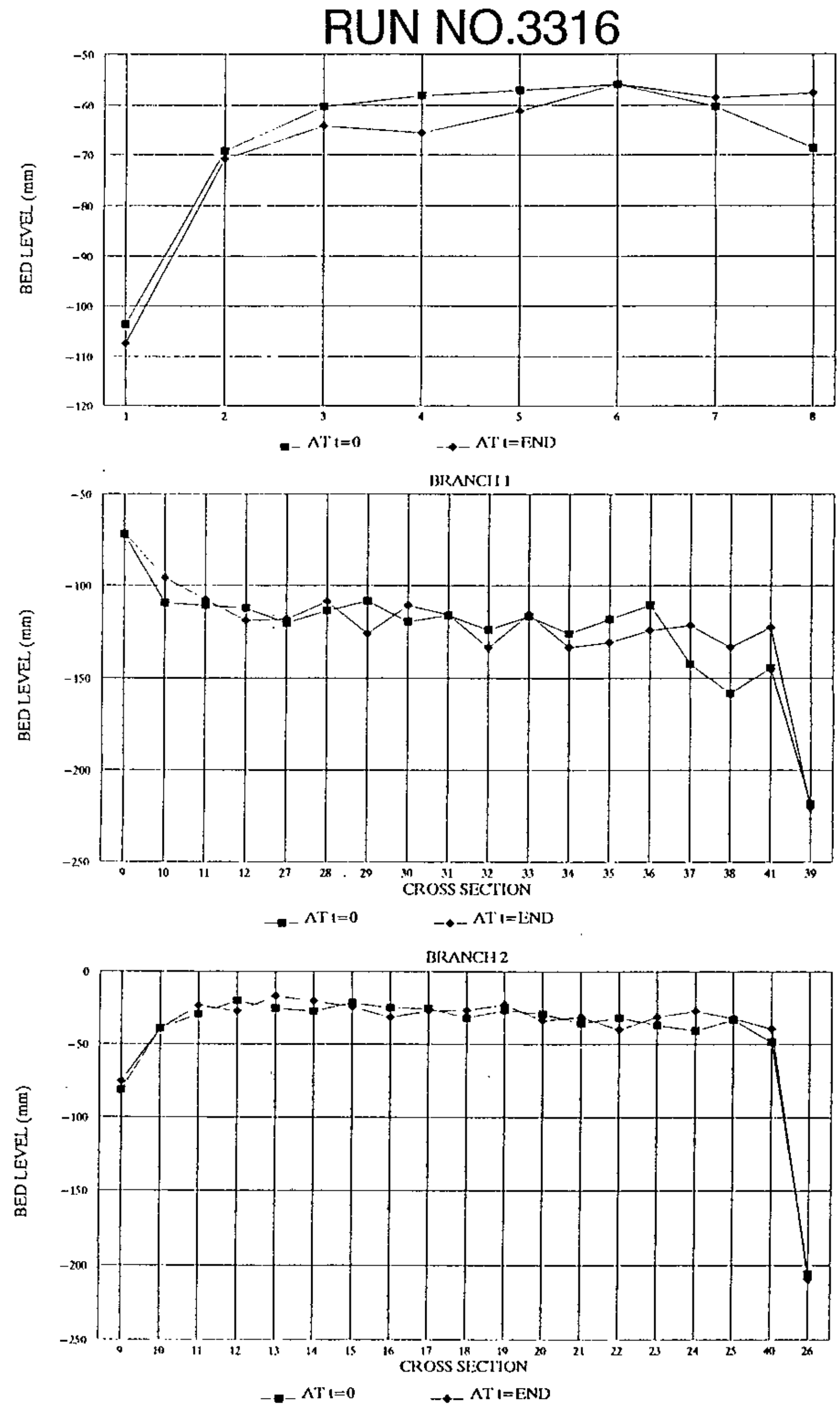

Fig. A.12 Bed level evolution of run no. 3316

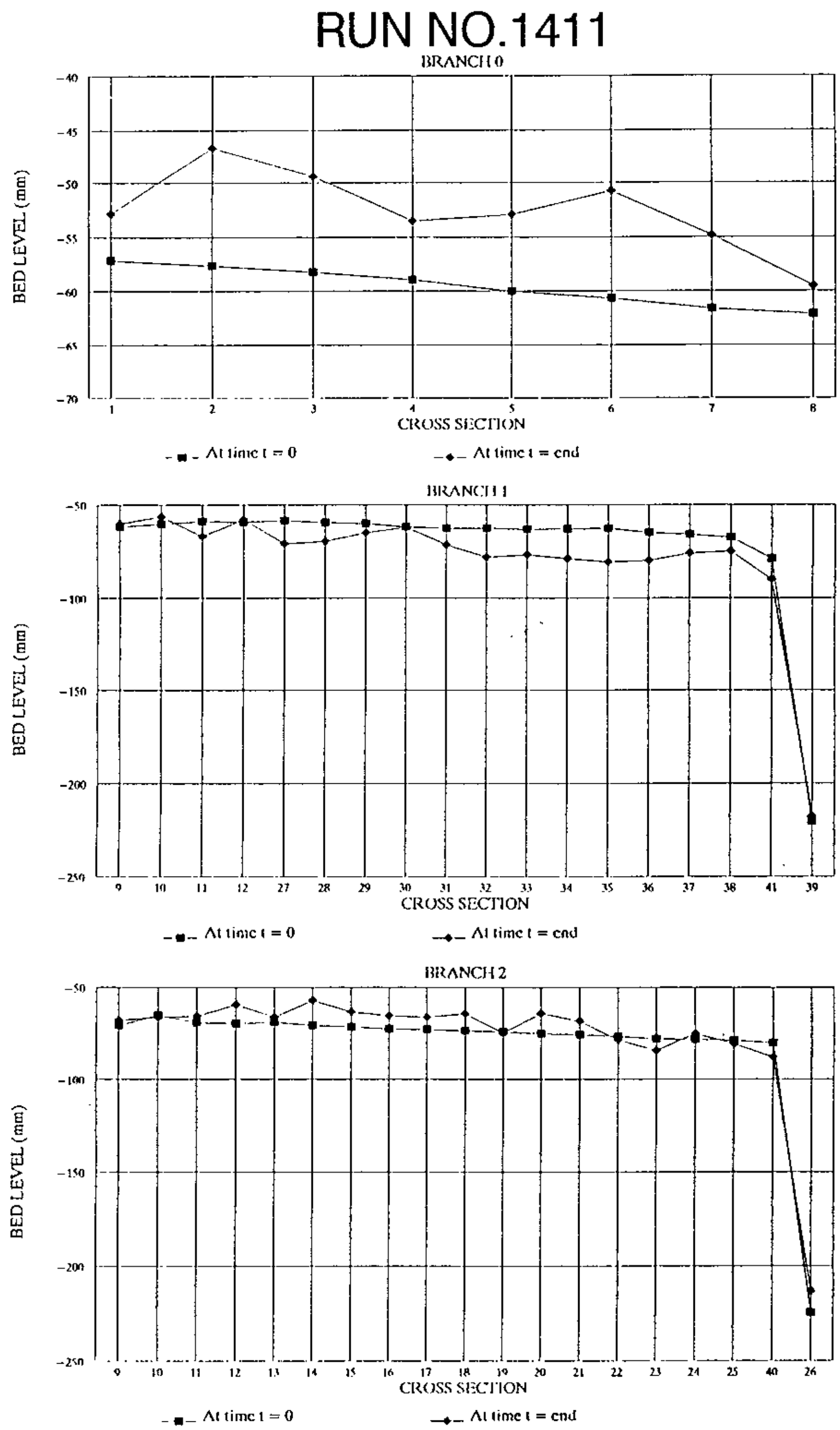

Fig. A.13 Bed level evolution of run no. 1411

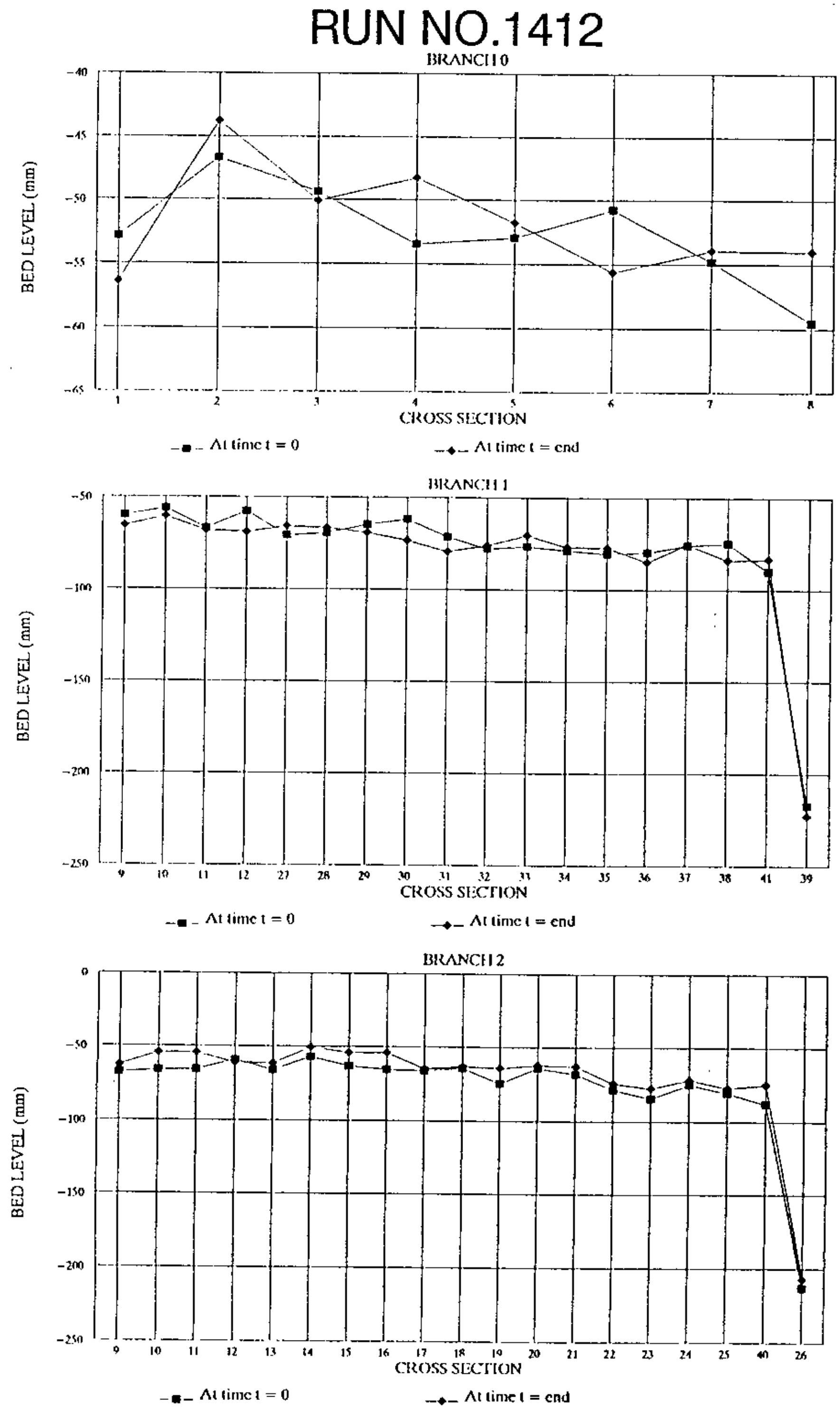

Fig. A.14 Bed level evolution of run no. 1412

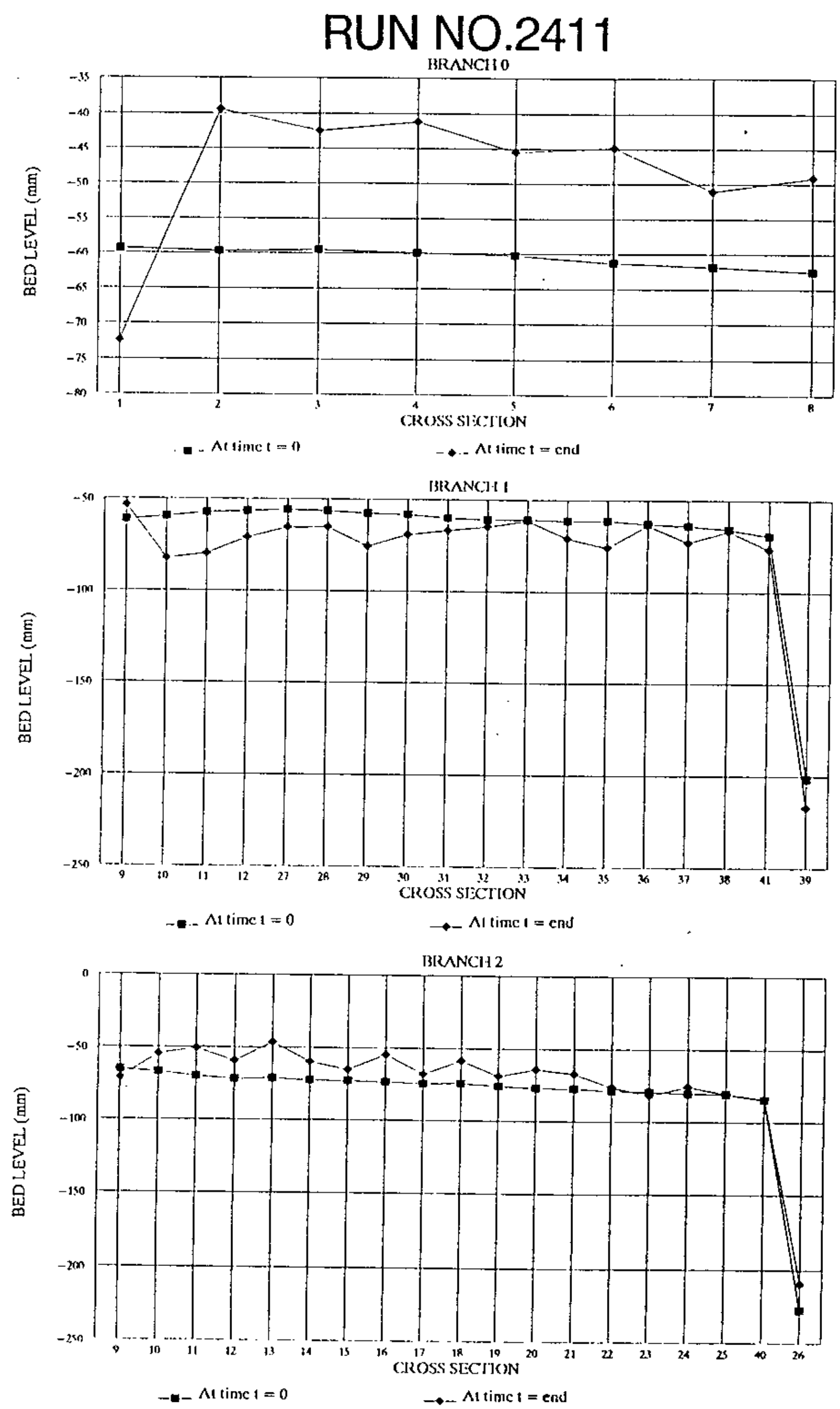

Fig. A.15 Bed level evolution of run no. 2411

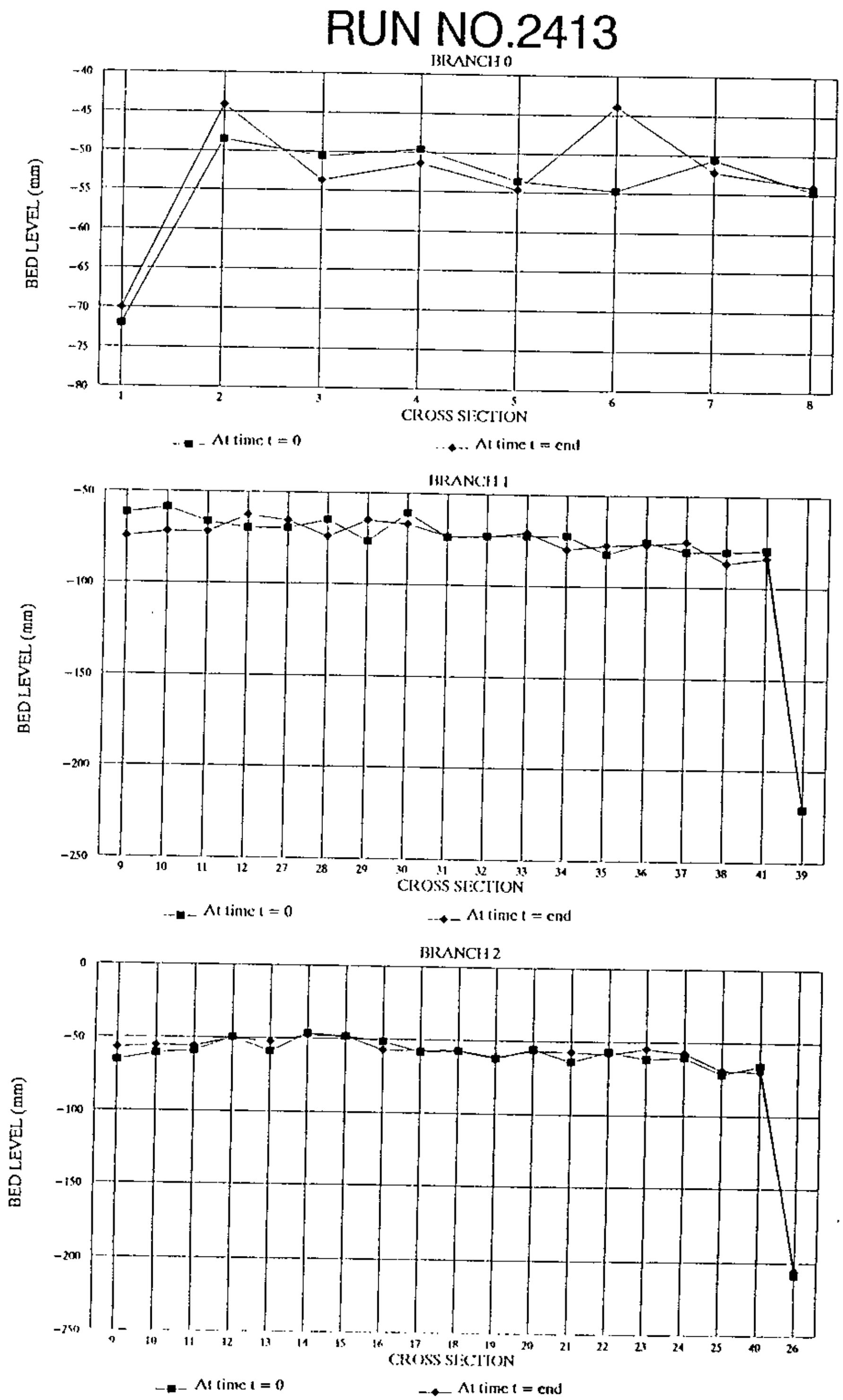

Fig. A.16 Bed level evolution of run no. 2413

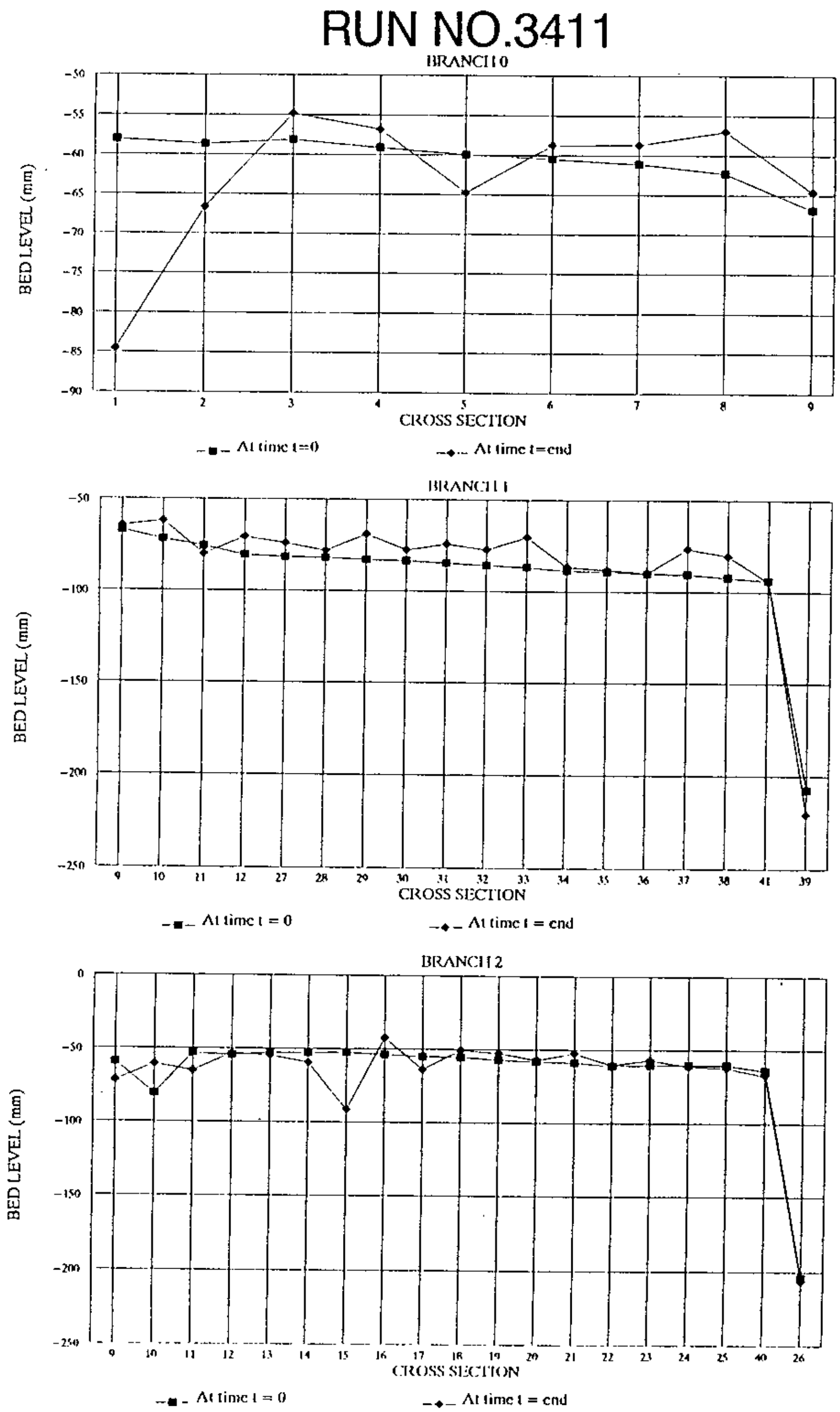

Fig. A.17 Bed level evolution of run no. 3411

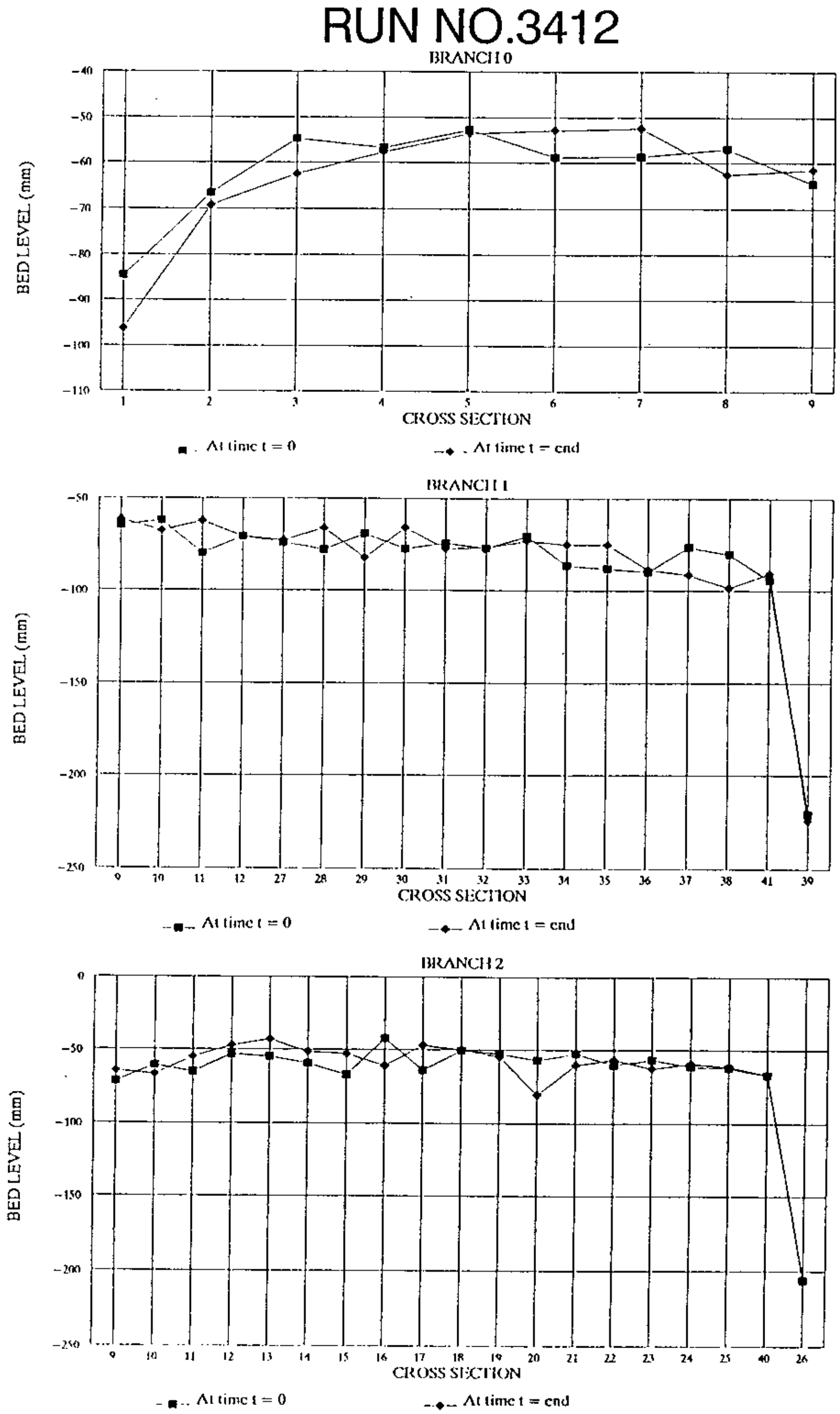

Fig. A.18 Bed level evolution of run no. 3412

APPENDIX B

FIGURES SHOWING VARIATION OF DISCHARGE WITH RUN TIME FOR VARIOUS RUNS

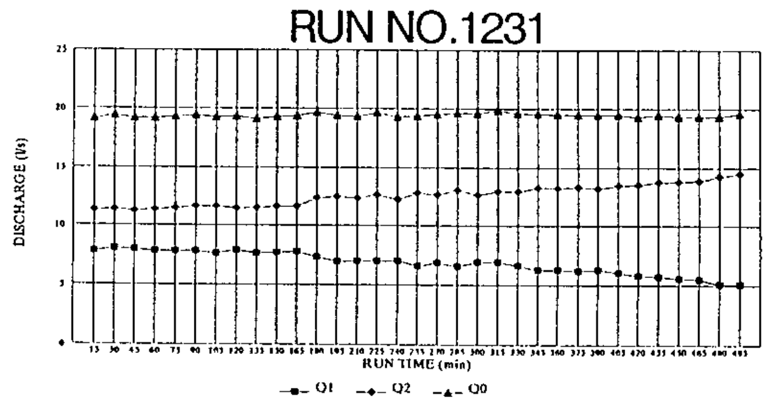

Fig. B.1 Variation of discharge with run time (Run No. 1231)

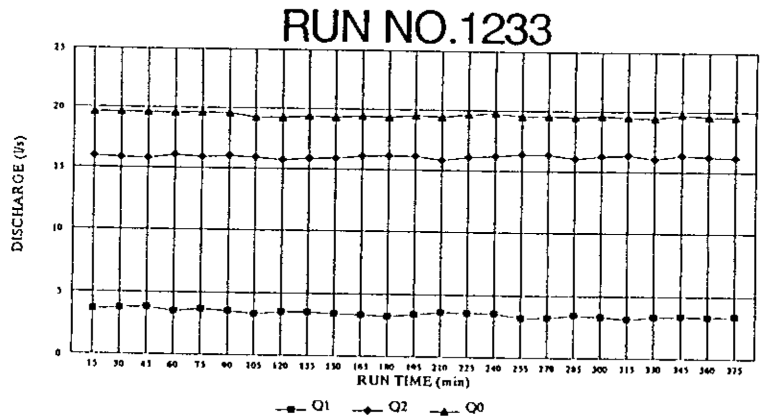

Fig. B.2 Variation of discharge with run time (Run No. 1233)

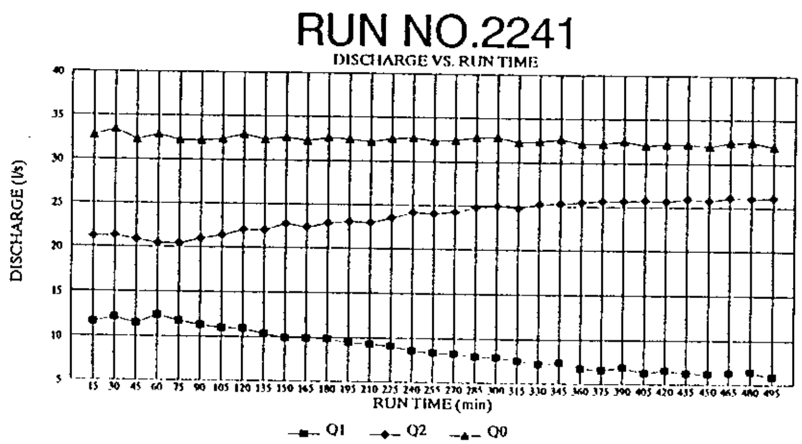

Fig. B.3 Variation of discharge with run time (Run No. 2241)

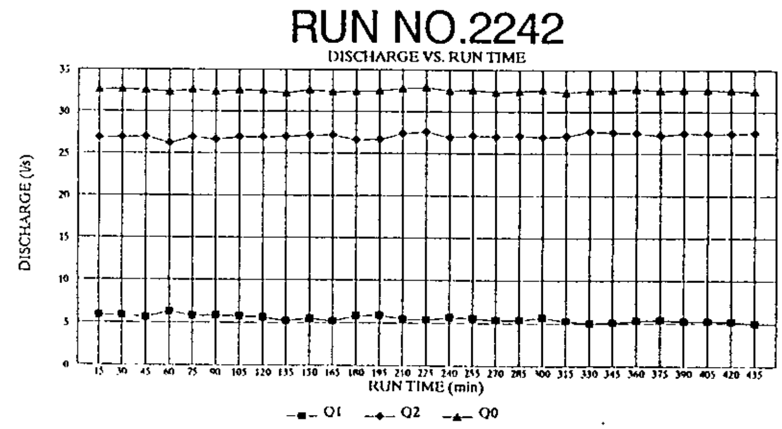

Fig. B.4 Variation of discharge with run time (Run No. 2242)

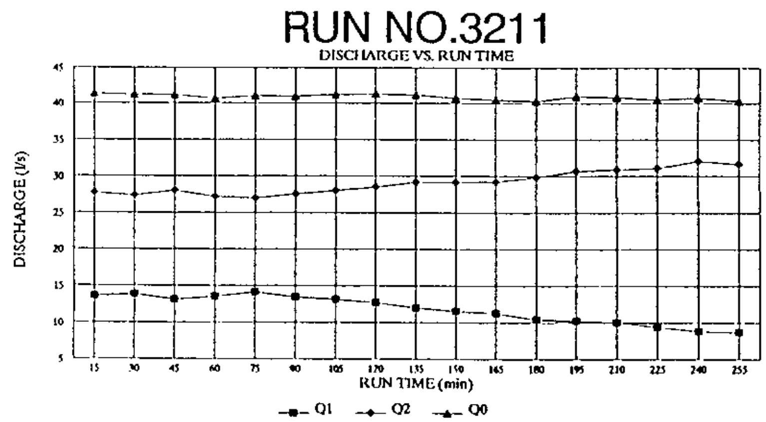

Fig. B.5 Variation of discharge with run time (Run No. 3211)

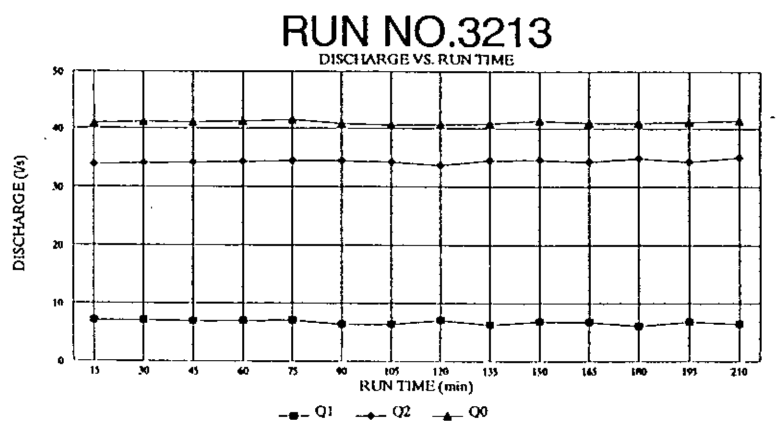

Fig. B.6 Variation of discharge with run time (Run No. 3213)

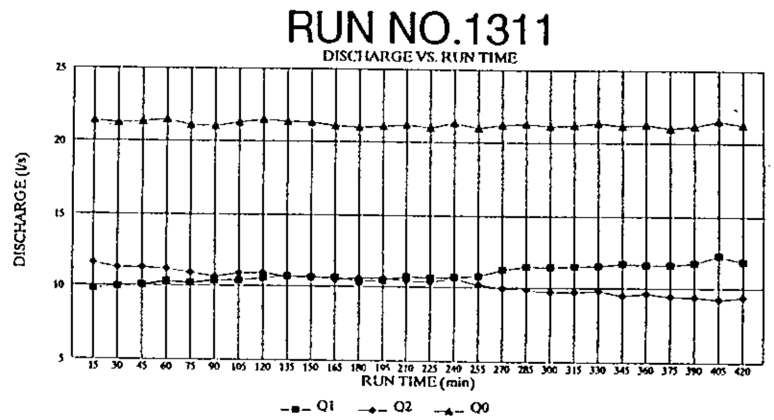

Fig. B.7 Variation of discharge with run time (Run No. 1311)

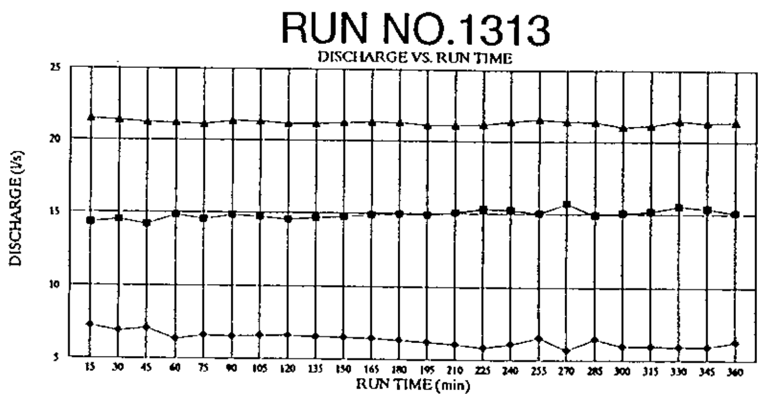

Fig. B.8 Variation of discharge with run time (Run No. 1313)

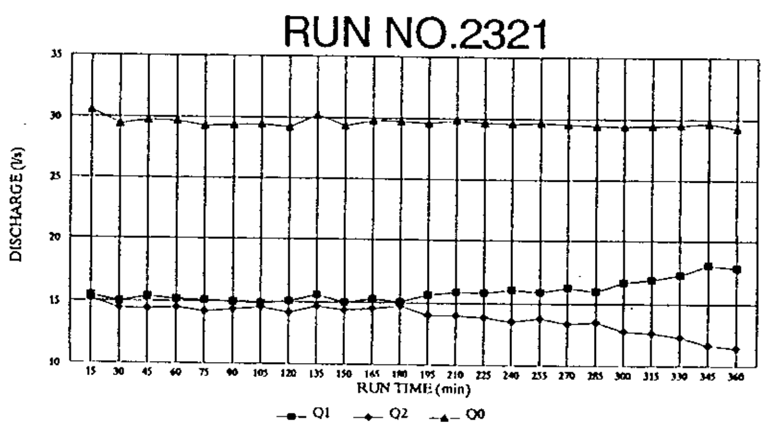

Fig. B.9 Variation of discharge with run time (Run No. 2321)

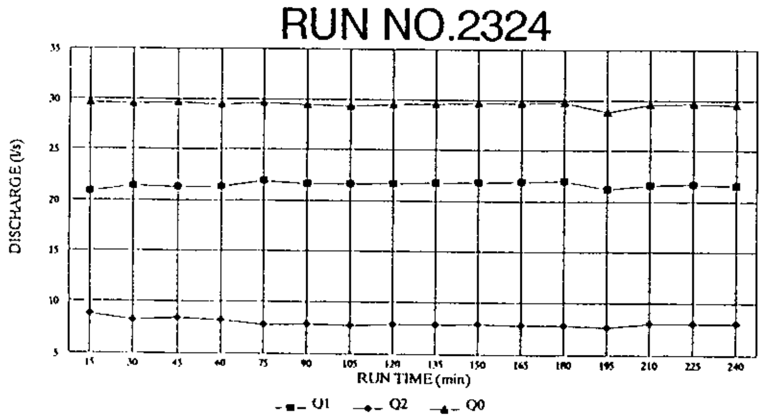

Fig. B.10 Variation of discharge with run time (Run No. 2324)

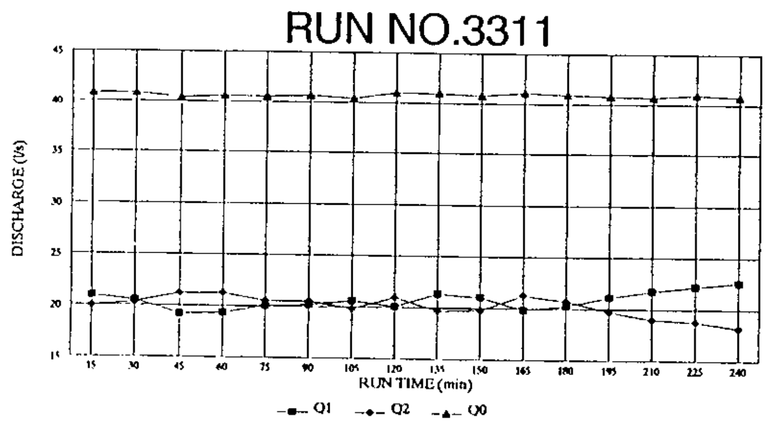

Fig. B.11 Variation of discharge with run time (Run No. 3311)

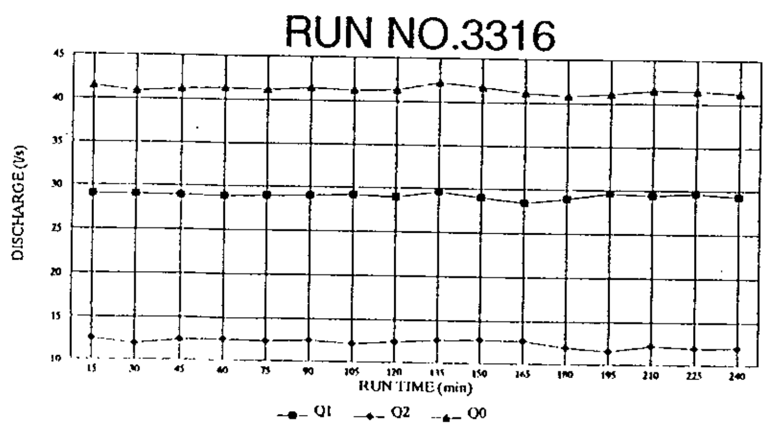

Fig. B.12 Variation of discharge with run time (Run No. 3316)

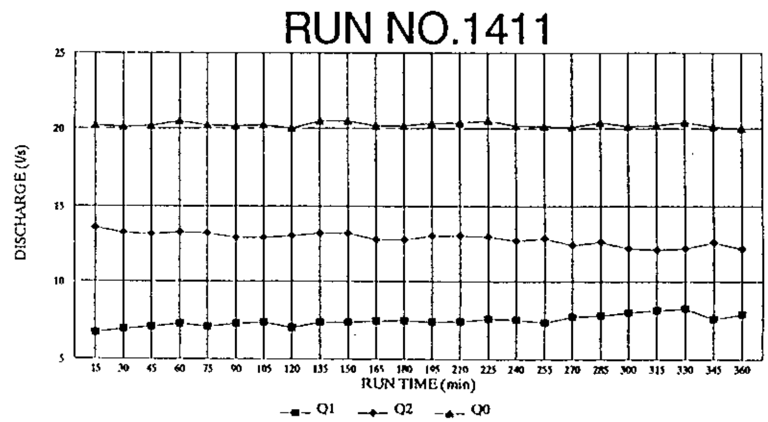

Fig. B.13 Variation of discharge with run time (Run No. 1411)

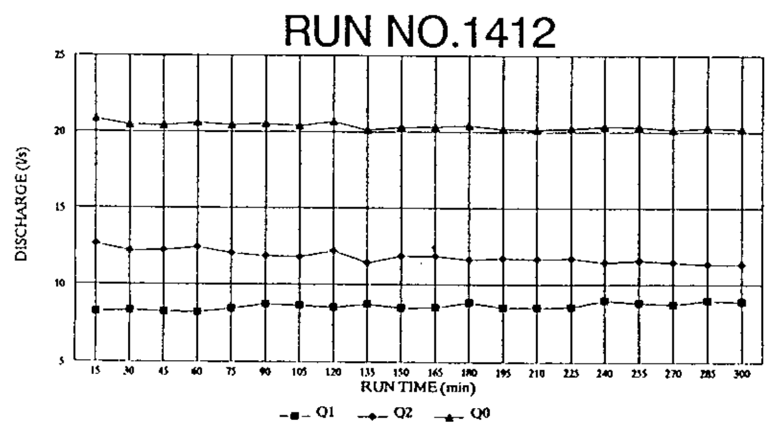

Fig. B.14 Variation of discharge with run time (Run No. 1412)

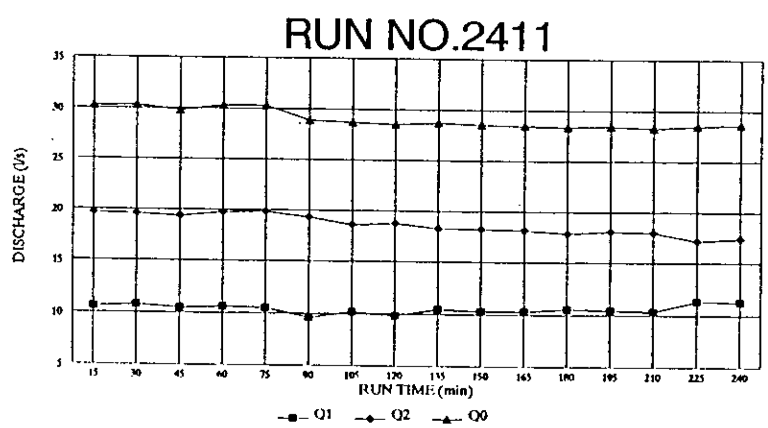

Fig. B.15 Variation of discharge with run time (Run No. 2411)

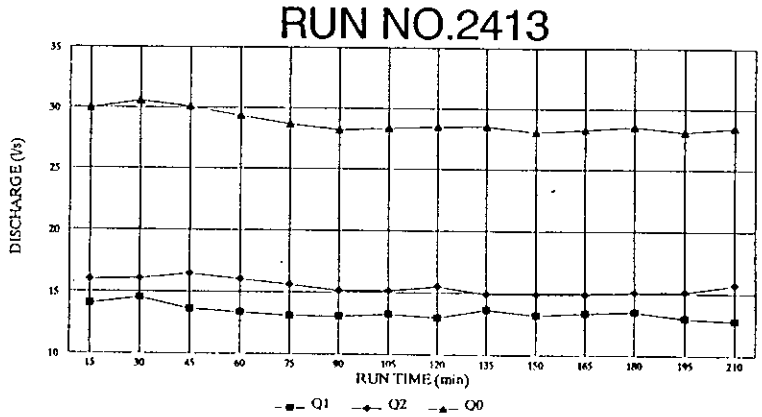

Fig. B.16 Variation of discharge with run time (Run No. 2413)

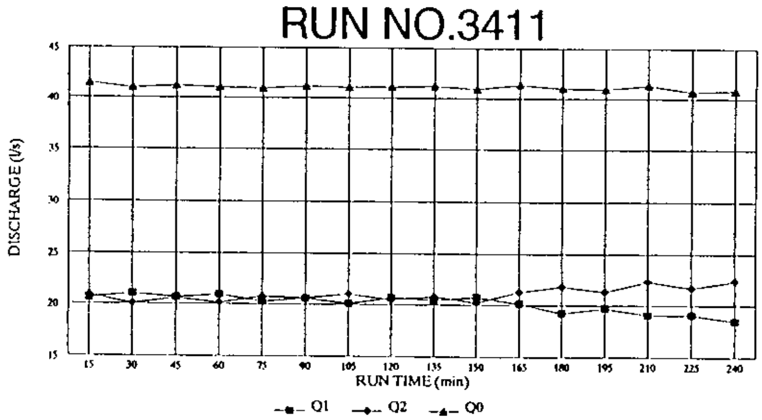

Fig. B.17 Variation of discharge with run time (Run No. 3411)

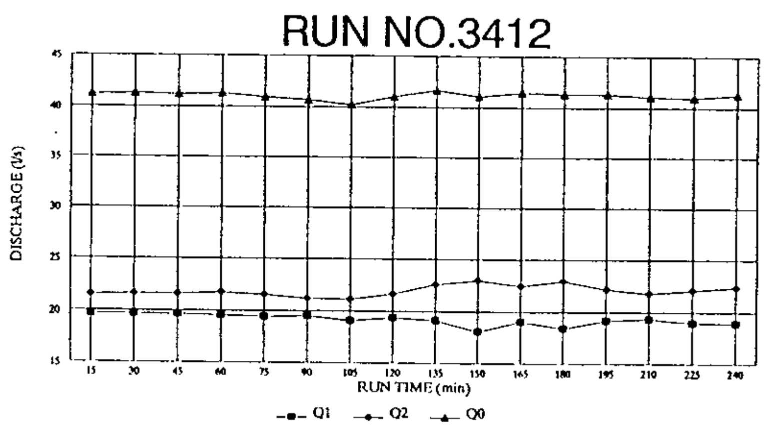

Fig. B.18 Variation of discharge with run time (Run No. 3412)

APPENDIX C

FINAL RESULTS OF VARIOUS RUNS

FINAL RESULTS OF RUN NO. 1211

Total run time, T(min.)	410
Rate of sand supplied by sand feeder, R (kg/hr)	28.1
Volume of sand supplied by sand feeder, V_{sf} (m^3)	0.1207
Discharge in branch 0, Q_0 (l/s)	20.266
Discharge in branch 1, Q_1 (l/s)	3.916
Discharge in branch 2, Q_2 (l/s)	16.349
Volume of sand trapped in sandtrap 1, ST_1 (m^3)	0.0003
Volume of sand trapped in sandtrap 2, ST_2 (m^3)	0.0082
Volume of sand deposited (+) or eroded (-) in branch 0, V_0 (m^3)	0.0782
Volume of sand deposited (+) or eroded (-) in branch 1, V_1 (m^3)	0.0180
Volume of sand deposited (+) or eroded (-) in branch 2, V_2 (m^3)	0.0336
Volume of sand transported through branch 0, S_0 (m^3)	0.0425
Volume of sand transported through branch 1, S_1 (m^3)	0.0183
Volume of sand transported through branch 2, S_2 (m^3)	0.0418
Ratio of Q_1 and Q_2, Q_1/Q_2	0.239
Ratio of S_1 and S_2, S_1/S_2	0.437
Ratio of V_0 and V_{sf}, V_0/V_{sf}	0.647
Error in percentage of sand balance	41.48

FINAL RESULTS OF RUN NO. 1212

Total run time, T(min.)	373
Rate of sand supplied by sand feeder, R (kg/hr)	27
Volume of sand supplied by sand feeder, V_{sf} (m^3)	0.1055
Discharge in branch 0, Q_0 (l/s)	20.455
Discharge in branch 1, Q_1 (l/s)	3.599
Discharge in branch 2, Q_2 (l/s)	16.856
Volume of sand trapped in sandtrap 1, ST_1 (m^3)	0.071×10^{-3}
Volume of sand trapped in sandtrap 2, ST_2 (m^3)	0.0488
Volume of sand deposited (+) or eroded (-) in branch 0, V_0 (m^3)	0.0247
Volume of sand deposited (+) or eroded (-) in branch 1, V_1 (m^3)	0.0175
Volume of sand deposited (+) or eroded (-) in branch 2, V_2 (m^3)	0.0356
Volume of sand transported through branch 0, S_0 (m^3)	0.0808
Volume of sand transported through branch 1, S_1 (m^3)	0.0176
Volume of sand transported through branch 2, S_2 (m^3)	0.0845
Ratio of Q_1 and Q_2, Q_1/Q_2	0.213
Ratio of S_1 and S_2, S_1/S_2	0.208
Ratio of V_0 and V_{sf}, V_0/V_{sf}	0.234
Error in percentage of sand balance	26.43

FINAL RESULTS OF RUN NO. 1213

Total run time, T(min.)	501
Rate of sand supplied by sand feeder, R (kg/hr)	28.3
Volume of sand supplied by sand feeder, V_{sf} (m^3)	0.1486
Discharge in branch 0, Q_0 (l/s)	20.421
Discharge in branch 1, Q_1 (l/s)	3.427
Discharge in branch 2, Q_2 (l/s)	16.994
Volume of sand trapped in sandtrap 1, ST_1 (m^3)	0.036×10^{-3}
Volume of sand trapped in sandtrap 2, ST_2 (m^3)	0.0971
Volume of sand deposited (+) or eroded (-) in branch 0, V_0 (m^3)	0.0045
Volume of sand deposited (+) or eroded (-) in branch 1, V_1 (m^3)	0.0263
Volume of sand deposited (+) or eroded (-) in branch 2, V_2 (m^3)	0.0248
Volume of sand transported through branch 0, S_0 (m^3)	0.1440
Volume of sand transported through branch 1, S_1 (m^3)	0.0264
Volume of sand transported through branch 2, S_2 (m^3)	0.1219
Ratio of Q_1 and Q_2, Q_1/Q_2	0.201
Ratio of S_1 and S_2, S_1/S_2	0.216
Ratio of V_0 and V_{sf}, V_0/V_{sf}	0.030
Error in percentage of sand balance	2.99

FINAL RESULTS OF RUN NO. 1221

Total run time, T(min.)	498
Rate of sand supplied by sand feeder, R (kg/hr)	17.9
Volume of sand supplied by sand feeder, V_{sf} (m^3)	0.0934
Discharge in branch 0, Q_0 (l/s)	20.364
Discharge in branch 1, Q_1 (l/s)	3.782
Discharge in branch 2, Q_2 (l/s)	16.582
Volume of sand trapped in sandtrap 1, ST_1 (m^3)	0.0011
Volume of sand trapped in sandtrap 2, ST_2 (m^3)	0.0674
Volume of sand deposited (+) or eroded (-) in branch 0, V_0 (m^3)	0.0253
Volume of sand deposited (+) or eroded (-) in branch 1, V_1 (m^3)	0.0205
Volume of sand deposited (+) or eroded (-) in branch 2, V_2 (m^3)	0.0068
Volume of sand transported through branch 0, S_0 (m^3)	0.0681
Volume of sand transported through branch 1, S_1 (m^3)	0.0217
Volume of sand transported through branch 2, S_2 (m^3)	0.0743
Ratio of Q_1 and Q_2, Q_1/Q_2	0.228
Ratio of S_1 and S_2, S_1/S_2	0.292
Ratio of V_0 and V_{sf}, V_0/V_{sf}	0.270
Error in percentage of sand balance	40.96

FINAL RESULTS OF RUN NO. 1231

Total run time, T(min.)	501
Rate of sand supplied by sand feeder, R (kg/hr)	17.2
Volume of sand supplied by sand feeder, V_{sf} (m^3)	0.0903
Discharge in branch 0, Q_0 (l/s)	19.416
Discharge in branch 1, Q_1 (l/s)	6.830
Discharge in branch 2, Q_2 (l/s)	12.585
Volume of sand trapped in sandtrap 1, ST_1 (m^3)	0.0025
Volume of sand trapped in sandtrap 2, ST_2 (m^3)	0.0645
Volume of sand deposited (+) or eroded (-) in branch 0, V_0 (m^3)	0.0198
Volume of sand deposited (+) or eroded (-) in branch 1, V_1 (m^3)	0.0594
Volume of sand deposited (+) or eroded (-) in branch 2, V_2 (m^3)	-0.0465
Volume of sand transported through branch 0, S_0 (m^3)	0.0704
Volume of sand transported through branch 1, S_1 (m^3)	0.0619
Volume of sand transported through branch 2, S_2 (m^3)	0.0180
Ratio of Q_1 and Q_2, Q_1/Q_2	0.542
Ratio of S_1 and S_2, S_1/S_2	3.438
Ratio of V_0 and V_{sf}, V_0/V_{sf}	0.219
Error in percentage of sand balance	13.53

FINAL RESULTS OF RUN NO. 1232

Total run time, T(min.)	501
Rate of sand supplied by sand feeder, R (kg/hr)	17.2
Volume of sand supplied by sand feeder, V_{sf} (m^3)	0.0903
Discharge in branch 0, Q_0 (l/s)	19.491
Discharge in branch 1, Q_1 (l/s)	4.162
Discharge in branch 2, Q_2 (l/s)	15.329
Volume of sand trapped in sandtrap 1, ST_1 (m^3)	0.0025
Volume of sand trapped in sandtrap 2, ST_2 (m^3)	0.0824
Volume of sand deposited (+) or eroded (-) in branch 0, V_0 (m^3)	-0.0014
Volume of sand deposited (+) or eroded (-) in branch 1, V_1 (m^3)	0.0220
Volume of sand deposited (+) or eroded (-) in branch 2, V_2 (m^3)	-0.0380
Volume of sand transported through branch 0, S_0 (m^3)	0.0918
Volume of sand transported through branch 1, S_1 (m^3)	0.0245
Volume of sand transported through branch 2, S_2 (m^3)	0.0444
Ratio of Q_1 and Q_2, Q_1/Q_2	0.271
Ratio of S_1 and S_2, S_1/S_2	0.551
Ratio of V_0 and V_{sf}, V_0/V_{sf}	0.016
Error in percentage of sand balance	24.89

FINAL RESULTS OF RUN NO. 1233

Total run time, T(min.)	378
Rate of sand supplied by sand feeder, R (kg/hr)	15.53
Volume of sand supplied by sand feeder, V_{sf} (m^3)	0.0615
Discharge in branch 0, Q_0 (l/s)	19.511
Discharge in branch 1, Q_1 (l/s)	3.449
Discharge in branch 2, Q_2 (l/s)	16.061
Volume of sand trapped in sandtrap 1, ST_1 (m^3)	0.051×10^{-3}
Volume of sand trapped in sandtrap 2, ST_2 (m^3)	0.0607
Volume of sand deposited (+) or eroded (-) in branch 0, V_0 (m^3)	-0.0011
Volume of sand deposited (+) or eroded (-) in branch 1, V_1 (m^3)	0.0172
Volume of sand deposited (+) or eroded (-) in branch 2, V_2 (m^3)	0.0010
Volume of sand transported through branch 0, S_0 (m^3)	0.0626
Volume of sand transported through branch 1, S_1 (m^3)	0.0173
Volume of sand transported through branch 2, S_2 (m^3)	0.0617
Ratio of Q_1 and Q_2, Q_1/Q_2	0.214
Ratio of S_1 and S_2, S_1/S_2	0.280
Ratio of V_0 and V_{sf}, V_0/V_{sf}	0.018
Error in percentage of sand balance	26.11

FINAL RESULTS OF RUN NO. 1241

Total run time, T(min.)	500
Rate of sand supplied by sand feeder, R (kg/hr)	17.1
Volume of sand supplied by sand feeder, V_{sf} (m^3)	0.0896
Discharge in branch 0, Q_0 (l/s)	19.348
Discharge in branch 1, Q_1 (l/s)	5.374
Discharge in branch 2, Q_2 (l/s)	13.973
Volume of sand trapped in sandtrap 1, ST_1 (m^3)	0.0065
Volume of sand trapped in sandtrap 2, ST_2 (m^3)	0.0824
Volume of sand deposited (+) or eroded (-) in branch 0, V_0 (m^3)	0.0254
Volume of sand deposited (+) or eroded (-) in branch 1, V_1 (m^3)	0.0342
Volume of sand deposited (+) or eroded (-) in branch 2, V_2 (m^3)	-0.0505
Volume of sand transported through branch 0, S_0 (m^3)	0.0641
Volume of sand transported through branch 1, S_1 (m^3)	0.0408
Volume of sand transported through branch 2, S_2 (m^3)	0.0318
Ratio of Q_1 and Q_2, Q_1/Q_2	0.384
Ratio of S_1 and S_2, S_1/S_2	1.280
Ratio of V_0 and V_{sf}, V_0/V_{sf}	0.283
Error in percentage of sand balance	13.23

FINAL RESULTS OF RUN NO. 1242

Total run time, T(min.)	378
Rate of sand supplied by sand feeder, R (kg/hr)	16.8
Volume of sand supplied by sand feeder, V_{sf} (m^3)	0.0665
Discharge in branch 0, Q_0 (l/s)	19.498
Discharge in branch 1, Q_1 (l/s)	4.033
Discharge in branch 2, Q_2 (l/s)	15.465
Volume of sand trapped in sandtrap 1, ST_1 (m^3)	0.0006
Volume of sand trapped in sandtrap 2, ST_2 (m^3)	0.0529
Volume of sand deposited (+) or eroded (-) in branch 0, V_0 (m^3)	0.0099
Volume of sand deposited (+) or eroded (-) in branch 1, V_1 (m^3)	0.0172
Volume of sand deposited (+) or eroded (-) in branch 2, V_2 (m^3)	0.0047
Volume of sand transported through branch 0, S_0 (m^3)	0.0566
Volume of sand transported through branch 1, S_1 (m^3)	0.0179
Volume of sand transported through branch 2, S_2 (m^3)	0.0577
Ratio of Q_1 and Q_2, Q_1/Q_2	0.260
Ratio of S_1 and S_2, S_1/S_2	0.310
Ratio of V_0 and V_{sf}, V_0/V_{sf}	0.149
Error in percentage of sand balance	33.65

FINAL RESULTS OF RUN NO. 1251

Total run time, T(min.)	421
Rate of sand supplied by sand feeder, R (kg/hr)	19
Volume of sand supplied by sand feeder, V_{sf} (m^3)	0.0838
Discharge in branch 0, Q_0 (l/s)	20.397
Discharge in branch 1, Q_1 (l/s)	6.922
Discharge in branch 2, Q_2 (l/s)	13.475
Volume of sand trapped in sandtrap 1, ST_1 (m^3)	0.0168
Volume of sand trapped in sandtrap 2, ST_2 (m^3)	0.0754
Volume of sand deposited (+) or eroded (-) in branch 0, V_0 (m^3)	0.0241
Volume of sand deposited (+) or eroded (-) in branch 1, V_1 (m^3)	0.0377
Volume of sand deposited (+) or eroded (-) in branch 2, V_2 (m^3)	-0.0685
Volume of sand transported through branch 0, S_0 (m^3)	0.0596
Volume of sand transported through branch 1, S_1 (m^3)	0.0546
Volume of sand transported through branch 2, S_2 (m^3)	0.0069
Ratio of Q_1 and Q_2, Q_1/Q_2	0.513
Ratio of S_1 and S_2, S_1/S_2	7.898
Ratio of V_0 and V_{sf}, V_0/V_{sf}	0.288
Error in percentage of sand balance	3.12

FINAL RESULTS OF RUN NO. 1261

Total run time, T(min.)	545
Rate of sand supplied by sand feeder, R (kg/hr)	18
Volume of sand supplied by sand feeder, V_{sf} (m^3)	0.1028
Discharge in branch 0, Q_0 (l/s)	20.494
Discharge in branch 1, Q_1 (l/s)	6.559
Discharge in branch 2, Q_2 (l/s)	13.559
Volume of sand trapped in sandtrap 1, ST_1 (m^3)	0.0172
Volume of sand trapped in sandtrap 2, ST_2 (m^3)	0.1081
Volume of sand deposited (+) or eroded (-) in branch 0, V_0 (m^3)	0.0264
Volume of sand deposited (+) or eroded (-) in branch 1, V_1 (m^3)	0.0466
Volume of sand deposited (+) or eroded (-) in branch 2, V_2 (m^3)	-0.0905
Volume of sand transported through branch 0, S_0 (m^3)	0.0763
Volume of sand transported through branch 1, S_1 (m^3)	0.0638
Volume of sand transported through branch 2, S_2 (m^3)	0.0176
Ratio of Q_1 and Q_2, Q_1/Q_2	0.470
Ratio of S_1 and S_2, S_1/S_2	3.623
Ratio of V_0 and V_{sf}, V_0/V_{sf}	0.257
Error in percentage of sand balance	6.69

FINAL RESULTS OF RUN NO. 1271

Total run time, T(min.)	527
Rate of sand supplied by sand feeder, R (kg/hr)	15.7
Volume of sand supplied by sand feeder, V_{sf} (m^3)	0.0867
Discharge in branch 0, Q_0 (l/s)	
Discharge in branch 1, Q_1 (l/s)	
Discharge in branch 2, Q_2 (l/s)	
Volume of sand trapped in sandtrap 1, ST_1 (m^3)	0.0168
Volume of sand trapped in sandtrap 2, ST_2 (m^3)	0.0913
Volume of sand deposited (+) or eroded (-) in branch 0, V_0 (m^3)	0.0173
Volume of sand deposited (+) or eroded (-) in branch 1, V_1 (m^3)	0.0412
Volume of sand deposited (+) or eroded (-) in branch 2, V_2 (m^3)	-0.0700
Volume of sand transported through branch 0, S_0 (m^3)	0.0693
Volume of sand transported through branch 1, S_1 (m^3)	0.0580
Volume of sand transported through branch 2, S_2 (m^3)	0.0212
Ratio of Q_1 and Q_2, Q_1/Q_2	0.513
Ratio of S_1 and S_2, S_1/S_2	2.727
Ratio of V_0 and V_{sf}, V_0/V_{sf}	0.199
Error in percentage of sand balance	14.38

FINAL RESULTS OF RUN NO. 1281

Total run time, T(min.)	527
Rate of sand supplied by sand feeder, R (kg/hr)	15
Volume of sand supplied by sand feeder, V_{sf} (m^3)	0.0828
Discharge in branch 0, Q_0 (l/s)	20.387
Discharge in branch 1, Q_1 (l/s)	6.480
Discharge in branch 2, Q_2 (l/s)	13.905
Volume of sand trapped in sandtrap 1, ST_1 (m^3)	0.0188
Volume of sand trapped in sandtrap 2, ST_2 (m^3)	0.0973
Volume of sand deposited (+) or eroded (-) in branch 0, V_0 (m^3)	0.0202
Volume of sand deposited (+) or eroded (-) in branch 1, V_1 (m^3)	0.0355
Volume of sand deposited (+) or eroded (-) in branch 2, V_2 (m^3)	-0.0780
Volume of sand transported through branch 0, S_0 (m^3)	0.0625
Volume of sand transported through branch 1, S_1 (m^3)	0.0543
Volume of sand transported through branch 2, S_2 (m^3)	0.0192
Ratio of Q_1 and Q_2, Q_1/Q_2	0.466
Ratio of S_1 and S_2, S_1/S_2	2.819
Ratio of V_0 and V_{sf}, V_0/V_{sf}	0.244
Error in percentage of sand balance	17.71

FINAL RESULTS OF RUN NO. 2211

Total run time, T(min.)	502
Rate of sand supplied by sand feeder, R (kg/hr)	32.4
Volume of sand supplied by sand feeder, V_{sf} (m^3)	0.1660
Discharge in branch 0, Q_0 (l/s)	30.651
Discharge in branch 1, Q_1 (l/s)	9.838
Discharge in branch 2, Q_2 (l/s)	20.812
Volume of sand trapped in sandtrap 1, ST_1 (m^3)	0.0250
Volume of sand trapped in sandtrap 2, ST_2 (m^3)	0.1665
Volume of sand deposited (+) or eroded (-) in branch 0, V_0 (m^3)	0.0181
Volume of sand deposited (+) or eroded (-) in branch 1, V_1 (m^3)	0.0985
Volume of sand deposited (+) or eroded (-) in branch 2, V_2 (m^3)	-0.134
Volume of sand transported through branch 0, S_0 (m^3)	0.1478
Volume of sand transported through branch 1, S_1 (m^3)	0.1235
Volume of sand transported through branch 2, S_2 (m^3)	0.0320
Ratio of Q_1 and Q_2, Q_1/Q_2	0.472
Ratio of S_1 and S_2, S_1/S_2	3.860
Ratio of V_0 and V_{sf}, V_0/V_{sf}	0.109
Error in percentage of sand balance	5.17

FINAL RESULTS OF RUN NO. 2221

Total run time, T(min.)	502
Rate of sand supplied by sand feeder, R (kg/hr)	32.4
Volume of sand supplied by sand feeder, V_{sf} (m^3)	0.1704
Discharge in branch 0, Q_0 (l/s)	32.421
Discharge in branch 1, Q_1 (l/s)	8.149
Discharge in branch 2, Q_2 (l/s)	24.271
Volume of sand trapped in sandtrap 1, ST_1 (m^3)	0.0211
Volume of sand trapped in sandtrap 2, ST_2 (m^3)	0.0202
Volume of sand deposited (+) or eroded (-) in branch 0, V_0 (m^3)	0.0072
Volume of sand deposited (+) or eroded (-) in branch 1, V_1 (m^3)	0.0773
Volume of sand deposited (+) or eroded (-) in branch 2, V_2 (m^3)	-0.1089
Volume of sand transported through branch 0, S_0 (m^3)	0.1632
Volume of sand transported through branch 1, S_1 (m^3)	0.0985
Volume of sand transported through branch 2, S_2 (m^3)	0.0935
Ratio of Q_1 and Q_2, Q_1/Q_2	0.335
Ratio of S_1 and S_2, S_1/S_2	1.053
Ratio of V_0 and V_{sf}, V_0/V_{sf}	0.042
Error in percentage of sand balance	17.62

FINAL RESULTS OF RUN NO. 2222

Total run time, T(min.)	384
Rate of sand supplied by sand feeder, R (kg/hr)	33.2
Volume of sand supplied by sand feeder, V_{sf} (m^3)	0.1336
Discharge in branch 0, Q_0 (l/s)	32.092
Discharge in branch 1, Q_1 (l/s)	5.201
Discharge in branch 2, Q_2 (l/s)	26.891
Volume of sand trapped in sandtrap 1, ST_1 (m^3)	0.0048
Volume of sand trapped in sandtrap 2, ST_2 (m^3)	0.1365
Volume of sand deposited (+) or eroded (-) in branch 0, V_0 (m^3)	-0.0096
Volume of sand deposited (+) or eroded (-) in branch 1, V_1 (m^3)	0.0153
Volume of sand deposited (+) or eroded (-) in branch 2, V_2 (m^3)	-0.0102
Volume of sand transported through branch 0, S_0 (m^3)	0.1433
Volume of sand transported through branch 1, S_1 (m^3)	0.0201
Volume of sand transported through branch 2, S_2 (m^3)	0.1263
Ratio of Q_1 and Q_2, Q_1/Q_2	0.193
Ratio of S_1 and S_2, S_1/S_2	0.159
Ratio of V_0 and V_{sf}, V_0/V_{sf}	0.072
Error in percentage of sand balance	2.22

FINAL RESULTS OF RUN NO. 2231

Total run time, T(min.)	501
Rate of sand supplied by sand feeder, R (kg/hr)	32
Volume of sand supplied by sand feeder, V_{sf} (m^3)	0.1680
Discharge in branch 0, Q_0 (l/s)	32.509
Discharge in branch 1, Q_1 (l/s)	12.174
Discharge in branch 2, Q_2 (l/s)	20.334
Volume of sand trapped in sandtrap 1, ST_1 (m^3)	0.0419
Volume of sand trapped in sandtrap 2, ST_2 (m^3)	0.2282
Volume of sand deposited (+) or eroded (-) in branch 0, V_0 (m^3)	0.0023
Volume of sand deposited (+) or eroded (-) in branch 1, V_1 (m^3)	0.1321
Volume of sand deposited (+) or eroded (-) in branch 2, V_2 (m^3)	-0.2322
Volume of sand transported through branch 0, S_0 (m^3)	0.1657
Volume of sand transported through branch 1, S_1 (m^3)	0.1740
Volume of sand transported through branch 2, S_2 (m^3)	-0.0039
Ratio of Q_1 and Q_2, Q_1/Q_2	0.598
Ratio of S_1 and S_2, S_1/S_2	-43.601
Ratio of V_0 and V_{sf}, V_0/V_{sf}	0.013
Error in percentage of sand balance	2.62

FINAL RESULTS OF RUN NO. 2232

Total run time, T(min.)	441
Rate of sand supplied by sand feeder, R (kg/hr)	32.4
Volume of sand supplied by sand feeder, V_{sf} (m^3)	0.1497
Discharge in branch 0, Q_0 (l/s)	32.666
Discharge in branch 1, Q_1 (l/s)	6.540
Discharge in branch 2, Q_2 (l/s)	26.126
Volume of sand trapped in sandtrap 1, ST_1 (m^3)	0.0035
Volume of sand trapped in sandtrap 2, ST_2 (m^3)	0.1195
Volume of sand deposited (+) or eroded (-) in branch 0, V_0 (m^3)	-0.0159
Volume of sand deposited (+) or eroded (-) in branch 1, V_1 (m^3)	0.0372
Volume of sand deposited (+) or eroded (-) in branch 2, V_2 (m^3)	-0.0132
Volume of sand transported through branch 0, S_0 (m^3)	0.1657
Volume of sand transported through branch 1, S_1 (m^3)	0.0408
Volume of sand transported through branch 2, S_2 (m^3)	0.1063
Ratio of Q_1 and Q_2, Q_1/Q_2	0.250
Ratio of S_1 and S_2, S_1/S_2	0.383
Ratio of V_0 and V_{sf}, V_0/V_{sf}	0.106
Error in percentage of sand balance	11.21

FINAL RESULTS OF RUN NO. 2241

Total run time, T(min.)	501
Rate of sand supplied by sand feeder, R (kg/hr)	31.4
Volume of sand supplied by sand feeder, V_{sf} (m^3)	0.1648
Discharge in branch 0, Q_0 (l/s)	32.403
Discharge in branch 1, Q_1 (l/s)	8.681
Discharge in branch 2, Q_2 (l/s)	23.721
Volume of sand trapped in sandtrap 1, ST_1 (m^3)	0.0187
Volume of sand trapped in sandtrap 2, ST_2 (m^3)	0.1999
Volume of sand deposited (+) or eroded (-) in branch 0, V_0 (m^3)	-0.0042
Volume of sand deposited (+) or eroded (-) in branch 1, V_1 (m^3)	0.0898
Volume of sand deposited (+) or eroded (-) in branch 2, V_2 (m^3)	-0.1329
Volume of sand transported through branch 0, S_0 (m^3)	0.1691
Volume of sand transported through branch 1, S_1 (m^3)	0.1086
Volume of sand transported through branch 2, S_2 (m^3)	0.0669
Ratio of Q_1 and Q_2, Q_1/Q_2	0.365
Ratio of S_1 and S_2, S_1/S_2	1.621
Ratio of V_0 and V_{sf}, V_0/V_{sf}	0.025
Error in percentage of sand balance	3.82

FINAL RESULTS OF RUN NO. 2242

Total run time, T(min.)	439
Rate of sand supplied by sand feeder, R (kg/hr)	32.4
Volume of sand supplied by sand feeder, V_{sf} (m^3)	0.1490
Discharge in branch 0, Q_0 (l/s)	32.546
Discharge in branch 1, Q_1 (l/s)	5.479
Discharge in branch 2, Q_2 (l/s)	27.066
Volume of sand trapped in sandtrap 1, ST_1 (m^3)	0.0034
Volume of sand trapped in sandtrap 2, ST_2 (m^3)	0.1454
Volume of sand deposited (+) or eroded (-) in branch 0, V_0 (m^3)	0.0059
Volume of sand deposited (+) or eroded (-) in branch 1, V_1 (m^3)	0.0206
Volume of sand deposited (+) or eroded (-) in branch 2, V_2 (m^3)	-0.0183
Volume of sand transported through branch 0, S_0 (m^3)	0.1431
Volume of sand transported through branch 1, S_1 (m^3)	0.0240
Volume of sand transported through branch 2, S_2 (m^3)	0.1271
Ratio of Q_1 and Q_2, Q_1/Q_2	0.202
Ratio of S_1 and S_2, S_1/S_2	0.189
Ratio of V_0 and V_{sf}, V_0/V_{sf}	0.039
Error in percentage of sand balance	5.62

FINAL RESULTS OF RUN NO. 2251

Total run time, T(min.)	511
Rate of sand supplied by sand feeder, R (kg/hr)	34.5
Volume of sand supplied by sand feeder, V_{sf} (m^3)	0.1847
Discharge in branch 0, Q_0 (l/s)	30.202
Discharge in branch 1, Q_1 (l/s)	9.074
Discharge in branch 2, Q_2 (l/s)	21.127
Volume of sand trapped in sandtrap 1, ST_1 (m^3)	0.0249
Volume of sand trapped in sandtrap 2, ST_2 (m^3)	0.1727
Volume of sand deposited (+) or eroded (-) in branch 0, V_0 (m^3)	0.0273
Volume of sand deposited (+) or eroded (-) in branch 1, V_1 (m^3)	0.0905
Volume of sand deposited (+) or eroded (-) in branch 2, V_2 (m^3)	-0.1120
Volume of sand transported through branch 0, S_0 (m^3)	0.1574
Volume of sand transported through branch 1, S_1 (m^3)	0.1154
Volume of sand transported through branch 2, S_2 (m^3)	0.0606
Ratio of Q_1 and Q_2, Q_1/Q_2	0.429
Ratio of S_1 and S_2, S_1/S_2	1.902
Ratio of V_0 and V_{sf}, V_0/V_{sf}	0.147
Error in percentage of sand balance	11.87

FINAL RESULTS OF RUN NO. 3211

Total run time, T(min.)	260
Rate of sand supplied by sand feeder, R (kg/hr)	46.9
Volume of sand supplied by sand feeder, V_{sf} (m^3)	0.1278
Discharge in branch 0, Q_0 (l/s)	40.855
Discharge in branch 1, Q_1 (l/s)	11.733
Discharge in branch 2, Q_2 (l/s)	29.121
Volume of sand trapped in sandtrap 1, ST_1 (m^3)	0.0175
Volume of sand trapped in sandtrap 2, ST_2 (m^3)	0.1312
Volume of sand deposited (+) or eroded (-) in branch 0, V_0 (m^3)	0.0068
Volume of sand deposited (+) or eroded (-) in branch 1, V_1 (m^3)	0.0788
Volume of sand deposited (+) or eroded (-) in branch 2, V_2 (m^3)	-0.1091
Volume of sand transported through branch 0, S_0 (m^3)	0.1209
Volume of sand transported through branch 1, S_1 (m^3)	0.0963
Volume of sand transported through branch 2, S_2 (m^3)	0.0221
Ratio of Q_1 and Q_2, Q_1/Q_2	0.402
Ratio of S_1 and S_2, S_1/S_2	4.351
Ratio of V_0 and V_{sf}, V_0/V_{sf}	0.053
Error in percentage of sand balance	2.09

FINAL RESULTS OF RUN NO. 3212

Total run time, T(min.)	275
Rate of sand supplied by sand feeder, R (kg/hr)	45.5
Volume of sand supplied by sand feeder, V_{sf} (m^3)	0.1311
Discharge in branch 0, Q_0 (l/s)	41.028
Discharge in branch 1, Q_1 (l/s)	7.624
Discharge in branch 2, Q_2 (l/s)	33.404
Volume of sand trapped in sandtrap 1, ST_1 (m^3)	0.0084
Volume of sand trapped in sandtrap 2, ST_2 (m^3)	0.1168
Volume of sand deposited (+) or eroded (-) in branch 0, V_0 (m^3)	-0.0056
Volume of sand deposited (+) or eroded (-) in branch 1, V_1 (m^3)	0.0338
Volume of sand deposited (+) or eroded (-) in branch 2, V_2 (m^3)	-0.0048
Volume of sand transported through branch 0, S_0 (m^3)	0.1367
Volume of sand transported through branch 1, S_1 (m^3)	0.0422
Volume of sand transported through branch 2, S_2 (m^3)	0.1119
Ratio of Q_1 and Q_2, Q_1/Q_2	0.228
Ratio of S_1 and S_2, S_1/S_2	0.377
Ratio of V_0 and V_{sf}, V_0/V_{sf}	0.043
Error in percentage of sand balance	12.78

FINAL RESULTS OF RUN NO. 3213

Total run time, T(min.)	214
Rate of sand supplied by sand feeder, R (kg/hr)	45.4
Volume of sand supplied by sand feeder, V_{sf} (m^3)	0.1018
Discharge in branch 0, Q_0 (l/s)	41.079
Discharge in branch 1, Q_1 (l/s)	6.727
Discharge in branch 2, Q_2 (l/s)	34.351
Volume of sand trapped in sandtrap 1, ST_1 (m^3)	0.0074
Volume of sand trapped in sandtrap 2, ST_2 (m^3)	0.0947
Volume of sand deposited (+) or eroded (-) in branch 0, V_0 (m^3)	-0.0033
Volume of sand deposited (+) or eroded (-) in branch 1, V_1 (m^3)	0.0110
Volume of sand deposited (+) or eroded (-) in branch 2, V_2 (m^3)	-0.0122
Volume of sand transported through branch 0, S_0 (m^3)	0.1052
Volume of sand transported through branch 1, S_1 (m^3)	0.0184
Volume of sand transported through branch 2, S_2 (m^3)	0.0825
Ratio of Q_1 and Q_2, Q_1/Q_2	0.195
Ratio of S_1 and S_2, S_1/S_2	0.224
Ratio of V_0 and V_{sf}, V_0/V_{sf}	0.033
Error in percentage of sand balance	4.01

FINAL RESULTS OF RUN NO. 3221

Total run time, T(min.)	185
Rate of sand supplied by sand feeder, R (kg/hr)	45.7
Volume of sand supplied by sand feeder, V_{sf} (m^3)	0.0886
Discharge in branch 0, Q_0 (l/s)	40.938
Discharge in branch 1, Q_1 (l/s)	14.818
Discharge in branch 2, Q_2 (l/s)	26.119
Volume of sand trapped in sandtrap 1, ST_1 (m^3)	0.0216
Volume of sand trapped in sandtrap 2, ST_2 (m^3)	0.1081
Volume of sand deposited (+) or eroded (-) in branch 0, V_0 (m^3)	0.0081
Volume of sand deposited (+) or eroded (-) in branch 1, V_1 (m^3)	0.0671
Volume of sand deposited (+) or eroded (-) in branch 2, V_2 (m^3)	-0.1263
Volume of sand transported through branch 0, S_0 (m^3)	0.0805
Volume of sand transported through branch 1, S_1 (m^3)	0.0887
Volume of sand transported through branch 2, S_2 (m^3)	-0.0182
Ratio of Q_1 and Q_2, Q_1/Q_2	0.567
Ratio of S_1 and S_2, S_1/S_2	-4.867
Ratio of V_0 and V_{sf}, V_0/V_{sf}	0.091
Error in percentage of sand balance	12.44

FINAL RESULTS OF RUN NO. 3222

Total run time, T(min.)	246
Rate of sand supplied by sand feeder, R (kg/hr)	45.8
Volume of sand supplied by sand feeder, V_{sf} (m^3)	0.1181
Discharge in branch 0, Q_0 (l/s)	40.650
Discharge in branch 1, Q_1 (l/s)	9.773
Discharge in branch 2, Q_2 (l/s)	30.877
Volume of sand trapped in sandtrap 1, ST_1 (m^3)	0.0101
Volume of sand trapped in sandtrap 2, ST_2 (m^3)	0.1205
Volume of sand deposited (+) or eroded (-) in branch 0, V_0 (m^3)	-0.0028
Volume of sand deposited (+) or eroded (-) in branch 1, V_1 (m^3)	0.0695
Volume of sand deposited (+) or eroded (-) in branch 2, V_2 (m^3)	-0.053
Volume of sand transported through branch 0, S_0 (m^3)	0.1209
Volume of sand transported through branch 1, S_1 (m^3)	0.0796
Volume of sand transported through branch 2, S_2 (m^3)	0.0674
Ratio of Q_1 and Q_2, Q_1/Q_2	0.316
Ratio of S_1 and S_2, S_1/S_2	1.180
Ratio of V_0 and V_{sf}, V_0/V_{sf}	0.024
Error in percentage of sand balance	21.67

FINAL RESULTS OF RUN NO. 3223

Total run time, T(min.)	244
Rate of sand supplied by sand feeder, R (kg/hr)	45.2
Volume of sand supplied by sand feeder, V_{sf} (m^3)	0.1156
Discharge in branch 0, Q_0 (l/s)	40.716
Discharge in branch 1, Q_1 (l/s)	6.774
Discharge in branch 2, Q_2 (l/s)	33.942
Volume of sand trapped in sandtrap 1, ST_1 (m^3)	0.0044
Volume of sand trapped in sandtrap 2, ST_2 (m^3)	0.1042
Volume of sand deposited (+) or eroded (-) in branch 0, V_0 (m^3)	-0.0062
Volume of sand deposited (+) or eroded (-) in branch 1, V_1 (m^3)	0.0220
Volume of sand deposited (+) or eroded (-) in branch 2, V_2 (m^3)	-0.0069
Volume of sand transported through branch 0, S_0 (m^3)	0.1218
Volume of sand transported through branch 1, S_1 (m^3)	0.0264
Volume of sand transported through branch 2, S_2 (m^3)	0.0972
Ratio of Q_1 and Q_2, Q_1/Q_2	0.199
Ratio of S_1 and S_2, S_1/S_2	0.271
Ratio of V_0 and V_{sf}, V_0/V_{sf}	0.054
Error in percentage of sand balance	1.48

FINAL RESULTS OF RUN NO. 3231

Total run time, T(min.)	244
Rate of sand supplied by sand feeder, R (kg/hr)	46.9
Volume of sand supplied by sand feeder, V_{sf} (m^3)	0.1199
Discharge in branch 0, Q_0 (l/s)	41.331
Discharge in branch 1, Q_1 (l/s)	11.164
Discharge in branch 2, Q_2 (l/s)	30.167
Volume of sand trapped in sandtrap 1, ST_1 (m^3)	0.0145
Volume of sand trapped in sandtrap 2, ST_2 (m^3)	0.1289
Volume of sand deposited (+) or eroded (-) in branch 0, V_0 (m^3)	-0.0030
Volume of sand deposited (+) or eroded (-) in branch 1, V_1 (m^3)	0.0668
Volume of sand deposited (+) or eroded (-) in branch 2, V_2 (m^3)	-0.0821
Volume of sand transported through branch 0, S_0 (m^3)	0.1230
Volume of sand transported through branch 1, S_1 (m^3)	0.0813
Volume of sand transported through branch 2, S_2 (m^3)	0.0467
Ratio of Q_1 and Q_2, Q_1/Q_2	0.370
Ratio of S_1 and S_2, S_1/S_2	1.737
Ratio of V_0 and V_{sf}, V_0/V_{sf}	0.025
Error in percentage of sand balance	4.11

FINAL RESULTS OF RUN NO. 3241

Total run time, T(min.)	286
Rate of sand supplied by sand feeder, R (kg/hr)	43.5
Volume of sand supplied by sand feeder, V_{sf} (m^3)	0.1304
Discharge in branch 0, Q_0 (l/s)	39.980
Discharge in branch 1, Q_1 (l/s)	11.218
Discharge in branch 2, Q_2 (l/s)	28.762
Volume of sand trapped in sandtrap 1, ST_1 (m^3)	0.0176
Volume of sand trapped in sandtrap 2, ST_2 (m^3)	0.1285
Volume of sand deposited (+) or eroded (-) in branch 0, V_0 (m^3)	0.0138
Volume of sand deposited (+) or eroded (-) in branch 1, V_1 (m^3)	0.0809
Volume of sand deposited (+) or eroded (-) in branch 2, V_2 (m^3)	-0.0941
Volume of sand transported through branch 0, S_0 (m^3)	0.1165
Volume of sand transported through branch 1, S_1 (m^3)	0.0986
Volume of sand transported through branch 2, S_2 (m^3)	0.0343
Ratio of Q_1 and Q_2, Q_1/Q_2	0.390
Ratio of S_1 and S_2, S_1/S_2	2.871
Ratio of V_0 and V_{sf}, V_0/V_{sf}	0.106
Error in percentage of sand balance	14.14

FINAL RESULTS OF RUN NO. 1311

Total run time, T(min.)	424
Rate of sand supplied by sand feeder, R (kg/hr)	18
Volume of sand supplied by sand feeder, V_{sf} (m^3)	0.0800
Discharge in branch 0, Q_0 (l/s)	21.206
Discharge in branch 1, Q_1 (l/s)	10.896
Discharge in branch 2, Q_2 (l/s)	10.310
Volume of sand trapped in sandtrap 1, ST_1 (m^3)	0.0762
Volume of sand trapped in sandtrap 2, ST_2 (m^3)	0.0247
Volume of sand deposited (+) or eroded (-) in branch 0, V_0 (m^3)	0.0146
Volume of sand deposited (+) or eroded (-) in branch 1, V_1 (m^3)	-0.0692
Volume of sand deposited (+) or eroded (-) in branch 2, V_2 (m^3)	0.0400
Volume of sand transported through branch 0, S_0 (m^3)	0.0653
Volume of sand transported through branch 1, S_1 (m^3)	0.0070
Volume of sand transported through branch 2, S_2 (m^3)	0.0648
Ratio of Q_1 and Q_2, Q_1/Q_2	1.056
Ratio of S_1 and S_2, S_1/S_2	0.108
Ratio of V_0 and V_{sf}, V_0/V_{sf}	0.182
Error in percentage of sand balance	9.84

FINAL RESULTS OF RUN NO. 1312

Total run time, T(min.)	425
Rate of sand supplied by sand feeder, R (kg/hr)	17.85
Volume of sand supplied by sand feeder, V_{sf} (m^3)	0.0795
Discharge in branch 0, Q_0 (l/s)	21.305
Discharge in branch 1, Q_1 (l/s)	13.404
Discharge in branch 2, Q_2 (l/s)	7.901
Volume of sand trapped in sandtrap 1, ST_1 (m^3)	0.0696
Volume of sand trapped in sandtrap 2, ST_2 (m^3)	0.0106
Volume of sand deposited (+) or eroded (-) in branch 0, V_0 (m^3)	-0.0078
Volume of sand deposited (+) or eroded (-) in branch 1, V_1 (m^3)	-0.0218
Volume of sand deposited (+) or eroded (-) in branch 2, V_2 (m^3)	0.0307
Volume of sand transported through branch 0, S_0 (m^3)	0.0874
Volume of sand transported through branch 1, S_1 (m^3)	0.0478
Volume of sand transported through branch 2, S_2 (m^3)	0.0414
Ratio of Q_1 and Q_2, Q_1/Q_2	1.696
Ratio of S_1 and S_2, S_1/S_2	1.155
Ratio of V_0 and V_{sf}, V_0/V_{sf}	0.099
Error in percentage of sand balance	2.07

FINAL RESULTS OF RUN NO. 1313

Total run time, T(min.)	365
Rate of sand supplied by sand feeder, R (kg/hr)	19.25
Volume of sand supplied by sand feeder, V_{sf} (m^3)	0.0736
Discharge in branch 0, Q_0 (l/s)	21.273
Discharge in branch 1, Q_1 (l/s)	14.922
Discharge in branch 2, Q_2 (l/s)	6.350
Volume of sand trapped in sandtrap 1, ST_1 (m^3)	0.0653
Volume of sand trapped in sandtrap 2, ST_2 (m^3)	0.0063
Volume of sand deposited (+) or eroded (-) in branch 0, V_0 (m^3)	0.0013
Volume of sand deposited (+) or eroded (-) in branch 1, V_1 (m^3)	-0.0087
Volum of sand deposited (+) or eroded (-) in branch 2, V_2 (m^3)	0.0176
Volume of sand transported through branch 0, S_0 (m^3)	0.0723
Volume of sand transported through branch 1, S_1 (m^3)	0.0565
Volume of sand transported through branch 2, S_2 (m^3)	0.0239
Ratio of Q_1 and Q_2, Q_1/Q_2	2.349
Ratio of S_1 and S_2, S_1/S_2	2.361
Ratio of V_0 and V_{sf}, V_0/V_{sf}	0.018
Error in percentage of sand balance	11.39

FINAL RESULTS OF RUN NO. 1321

Total run time, T(min.)	485
Rate of sand supplied by sand feeder, R (kg/hr)	17.9
Volume of sand supplied by sand feeder, V_{sf} (m^3)	0.0910
Discharge in branch 0, Q_0 (l/s)	21.323
Discharge in branch 1, Q_1 (l/s)	8.1831
Discharge in branch 2, Q_2 (l/s)	13.1402
Volume of sand trapped in sandtrap 1, ST_1 (m^3)	0.0735
Volume of sand trapped in sandtrap 2, ST_2 (m^3)	0.0556
Volume of sand deposited (+) or eroded (-) in branch 0, V_0 (m^3)	0.0101
Volume of sand deposited (+) or eroded (-) in branch 1, V_1 (m^3)	-0.0918
Volume of sand deposited (+) or eroded (-) in branch 2, V_2 (m^3)	0.0459
Volume of sand transported through branch 0, S_0 (m^3)	0.0808
Volume of sand transported through branch 1, S_1 (m^3)	-0.0182
Volume of sand transported through branch 2, S_2 (m^3)	0.1016
Ratio of Q_1 and Q_2, Q_1/Q_2	0.622
Ratio of S_1 and S_2, S_1/S_2	-0.179
Ratio of V_0 and V_{sf}, V_0/V_{sf}	0.111
Error in percentage of sand balance	3.07

FINAL RESULTS OF RUN NO. 1322

Total run time, T(min.)	244
Rate of sand supplied by sand feeder, R (kg/hr)	17.6
Volume of sand supplied by sand feeder, V_{sf} (m^3)	0.0450
Discharge in branch 0, Q_0 (l/s)	21.450
Discharge in branch 1, Q_1 (l/s)	10.316
Discharge in branch 2, Q_2 (l/s)	11.134
Volume of sand trapped in sandtrap 1, ST_1 (m^3)	0.0249
Volume of sand trapped in sandtrap 2, ST_2 (m^3)	0.0153
Volume of sand deposited (+) or eroded (-) in branch 0, V_0 (m^3)	0.0043
Volume of sand deposited (+) or eroded (-) in branch 1, V_1 (m^3)	-0.0201
Volume of sand deposited (+) or eroded (-) in branch 2, V_2 (m^3)	0.0258
Volume of sand transported through branch 0, S_0 (m^3)	0.0406
Volume of sand transported through branch 1, S_1 (m^3)	0.0047
Volume of sand transported through branch 2, S_2 (m^3)	0.0411
Ratio of Q_1 and Q_2, Q_1/Q_2	0.926
Ratio of S_1 and S_2, S_1/S_2	0.116
Ratio of V_0 and V_{sf}, V_0/V_{sf}	0.096
Error in percentage of sand balance	12.94

FINAL RESULTS OF RUN NO. 1323

Total run time, T(min.)	245
Rate of sand supplied by sand feeder, R (kg/hr)	18.2
Volume of sand supplied by sand feeder, V_{sf} (m^3)	0.0467
Discharge in branch 0, Q_0 (l/s)	21.500
Discharge in branch 1, Q_1 (l/s)	12.732
Discharge in branch 2, Q_2 (l/s)	8.7680
Volume of sand trapped in sandtrap 1, ST_1 (m^3)	0.0449
Volume of sand trapped in sandtrap 2, ST_2 (m^3)	0.0051
Volume of sand deposited (+) or eroded (-) in branch 0, V_0 (m^3)	-0.0066
Volume of sand deposited (+) or eroded (-) in branch 1, V_1 (m^3)	-0.0258
Volume of sand deposited (+) or eroded (-) in branch 2, V_2 (m^3)	0.0347
Volume of sand transported through branch 0, S_0 (m^3)	0.0534
Volume of sand transported through branch 1, S_1 (m^3)	0.0190
Volume of sand transported through branch 2, S_2 (m^3)	0.0398
Ratio of Q_1 and Q_2, Q_1/Q_2	1.452
Ratio of S_1 and S_2, S_1/S_2	0.479
Ratio of V_0 and V_{sf}, V_0/V_{sf}	0.142
Error in percentage of sand balance	10.32

FINAL RESULTS OF RUN NO. 1324

Total run time, T(min.)	362
Rate of sand supplied by sand feeder, R (kg/hr)	18.8
Volume of sand supplied by sand feeder, V_{sf} (m^3)	0.0713
Discharge in branch 0, Q_0 (l/s)	21.475
Discharge in branch 1, Q_1 (l/s)	14.388
Discharge in branch 2, Q_2 (l/s)	7.086
Volume of sand trapped in sandtrap 1, ST_1 (m^3)	0.0561
Volume of sand trapped in sandtrap 2, ST_2 (m^3)	0.0034
Volume of sand deposited (+) or eroded (-) in branch 0, V_0 (m^3)	0.0097
Volume of sand deposited (+) or eroded (-) in branch 1, V_1 (m^3)	-0.0114
Volume of sand deposited (+) or eroded (-) in branch 2, V_2 (m^3)	0.0158
Volume of sand transported through branch 0, S_0 (m^3)	0.0615
Volume of sand transported through branch 1, S_1 (m^3)	0.0446
Volume of sand transported through branch 2, S_2 (m^3)	0.0192
Ratio of Q_1 and Q_2, Q_1/Q_2	2.030
Ratio of S_1 and S_2, S_1/S_2	2.316
Ratio of V_0 and V_{sf}, V_0/V_{sf}	0.136
Error in percentage of sand balance	3.90

FINAL RESULTS OF RUN NO. 1325

Total run time, T(min.)	364
Rate of sand supplied by sand feeder, R (kg/hr)	19.4
Volume of sand supplied by sand feeder, V_{sf} (m^3)	0.0740
Discharge in branch 0, Q_0 (l/s)	21.509
Discharge in branch 1, Q_1 (l/s)	15.545
Discharge in branch 2, Q_2 (l/s)	5.964
Volume of sand trapped in sandtrap 1, ST_1 (m^3)	0.0650
Volume of sand trapped in sandtrap 2, ST_2 (m^3)	0.0037
Volume of sand deposited (+) or eroded (-) in branch 0, V_0 (m^3)	0.0012
Volume of sand deposited (+) or eroded (-) in branch 1, V_1 (m^3)	-0.0152
Volume of sand deposited (+) or eroded (-) in branch 2, V_2 (m^3)	0.0199
Volume of sand transported through branch 0, S_0 (m^3)	0.0727
Volume of sand transported through branch 1, S_1 (m^3)	0.0498
Volume of sand transported through branch 2, S_2 (m^3)	0.0236
Ratio of Q_1 and Q_2, Q_1/Q_2	2.606
Ratio of S_1 and S_2, S_1/S_2	2.106
Ratio of V_0 and V_{sf}, V_0/V_{sf}	0.017
Error in percentage of sand balance	0.99

FINAL RESULTS OF RUN NO. 2311

Total run time, T(min.)	277
Rate of sand supplied by sand feeder, R (kg/hr)	31.25
Volume of sand supplied by sand feeder, V_{sf} (m^3)	0.0907
Discharge in branch 0, Q_0 (l/s)	29.679
Discharge in branch 1, Q_1 (l/s)	14.813
Dischage in branch 2, Q_2 (l/s)	14.866
Volume of sand trapped in sandtrap 1, ST_1 (m^3)	0.0670
Volume of sand trapped in sandtrap 2, ST_2 (m^3)	0.0276
Volume of sand deposited (+) or eroded (-) in branch 0, V_0 (m^3)	0.0220
Volume of sand deposited (+) or eroded (-) in branch 1, V_1 (m^3)	-0.0638
Volume of sand deposited (+) or eroded (-) in branch 2, V_2 (m^3)	0.0596
Volume of sand transported through branch 0, S_0 (m^3)	0.0686
Volume of sand transported through branch 1, S_1 (m^3)	0.0032
Volume of sand transported through branch 2, S_2 (m^3)	0.0872
Ratio of Q_1 and Q_2, Q_1/Q_2	0.996
Ratio of S_1 and S_2, S_1/S_2	0.037
Ratio of V_0 and V_{sf}, V_0/V_{sf}	0.243
Error in percentage of sand balance	31.77

FINAL RESULTS OF RUN NO. 2312

Total run time, T(min.)	246
Rate of sand supplied by sand feeder, R (kg/hr)	31.2
Volume of sand supplied by sand feeder, V_{sf} (m^3)	0.0804
Discharge in branch 0, Q_0 (l/s)	29.553
Discharge in branch 1, Q_1 (l/s)	17.820
Discharge in branch 2, Q_2 (l/s)	11.733
Volume of sand trapped in sandtrap 1, ST_1 (m^3)	0.0665
Volume of sand trapped in sandtrap 2, ST_2 (m^3)	0.0142
Volume of sand deposited (+) or eroded (-) in branch 0, V_0 (m^3)	0.0004
Volume of sand deposited (+) or eroded (-) in branch 1, V_1 (m^3)	-0.0249
Volume of sand deposited (+) or eroded (-) in branch 2, V_2 (m^3)	0.0331
Volume of sand transported through branch 0, S_0 (m^3)	0.0800
Volume of sand transported through branch 1, S_1 (m^3)	0.0416
Volume of sand transported through branch 2, S_2 (m^3)	0.0473
Ratio of Q_1 and Q_2, Q_1/Q_2	1.518
Ratio of S_1 and S_2, S_1/S_2	0.878
Ratio of V_0 and V_{sf}, V_0/V_{sf}	0.005
Error in percentage of sand balance	11.15

FINAL RESULTS OF RUN NO. 2313

Total run time, T(min.)	243
Rate of sand supplied by sand feeder, R (kg/hr)	31.2
Volume of sand supplied by sand feeder, V_{sf} (m^3)	0.0794
Discharge in branch 0, Q_0 (l/s)	29.565
Discharge in branch 1, Q_1 (l/s)	20.002
Discharge in branch 2, Q_2 (l/s)	9.562
Volume of sand trapped in sandtrap 1, ST_1 (m^3)	0.0571
Volume of sand trapped in sandtrap 2, ST_2 (m^3)	0.0092
Volume of sand deposited (+) or eroded (-) in branch 0, V_0 (m^3)	-0.0037
Volume of sand deposited (+) or eroded (-) in branch 1, V_1 (m^3)	-0.0061
Volume of sand deposited (+) or eroded (-) in branch 2, V_2 (m^3)	0.0065
Volume of sand transported through branch 0, S_0 (m^3)	0.0832
Volume of sand transported through branch 1, S_1 (m^3)	0.0510
Volume of sand transported through branch 2, S_2 (m^3)	0.0157
Ratio of Q_1 and Q_2, Q_1/Q_2	2.091
Ratio of S_1 and S_2, S_1/S_2	3.231
Ratio of V_0 and V_{sf}, V_0/V_{sf}	0.047
Error in percentage of sand balance	19.75

FINAL RESULTS OF RUN NO. 2321

Total run time, T(min.)	365
Rate of sand supplied by sand feeder, R (kg/hr)	31.2
Volume of sand supplied by sand feeder, V_{sf} (m^3)	0.1193
Discharge in branch 0, Q_0 (l/s)	29.627
Discharge in branch 1, Q_1 (l/s)	15.833
Discharge in branch 2, Q_2 (l/s)	13.793
Volume of sand trapped in sandtrap 1, ST_1 (m^3)	0.0880
Volume of sand trapped in sandtrap 2, ST_2 (m^3)	0.0314
Volume of sand deposited (+) or eroded (-) in branch 0, V_0 (m^3)	0.0273
Volume of sand deposited (+) or eroded (-) in branch 1, V_1 (m^3)	-0.0719
Volume of sand deposited (+) or eroded (-) in branch 2, V_2 (m^3)	0.0708
Volume of sand transported through branch 0, S_0 (m^3)	0.0920
Volume of sand transported through branch 1, S_1 (m^3)	0.0161
Volume of sand transported through branch 2, S_2 (m^3)	0.0022
Ratio of Q_1 and Q_2, Q_1/Q_2	1.147
Ratio of S_1 and S_2, S_1/S_2	0.157
Ratio of V_0 and V_{sf}, V_0/Vsf	0.228
Error in percentage of sand balance	28.61

FINAL RESULTS OF RUN NO. 2322

Total run time, T(min.)	335
Rate of sand supplied by sand feeder, R (kg/hr)	30.2
Volume of sand supplied by sand feeder, V_{sf} (m^3)	0.1060
Discharge in branch 0, Q_0 (l/s)	29.561
Discharge in branch 1, Q_1 (l/s)	19.212
Discharge in branch 2, Q_2 (l/s)	10.348
Volume of sand trapped in sandtrap 1, ST_1 (m^3)	0.0840
Volume of sand trapped in sandtrap 2, ST_2 (m^3)	0.0111
Volume of sand deposited (+) or eroded (-) in branch 0, V_0 (m^3)	-0.0106
Volume of sand deposited (+) or eroded (-) in branch 1, V_1 (m^3)	-0.0101
Volume of sand deposited (+) or eroded (-) in branch 2, V_2 (m^3)	0.0371
Volume of sand transported through branch 0, S_0 (m^3)	0.1166
Volume of sand transported through branch 1, S_1 (m^3)	0.0738
Volume of sand transported through branch 2, S_2 (m^3)	0.0483
Ratio of Q_1 and Q_2, Q_1/Q_2	1.856
Ratio of S_1 and S_2, S_1/S_2	1.527
Ratio of V_0 and V_{sf}, V_0/V_{sf}	0.100
Error in percentage of sand balance	4.67

FINAL RESULTS OF RUN NO. 2323

Total run time, T(min.)	245
Rate of sand supplied by sand feeder, R (kg/hr)	30
Volume of sand supplied by sand feeder, V_{sf} (m^3)	0.0770
Discharge in branch 0, Q_0 (l/s)	29.629
Discharge in branch 1, Q_1 (l/s)	20.841
Discharge in branch 2, Q_2 (l/s)	8.788
Volume of sand trapped in sandtrap 1, ST_1 (m^3)	0.0624
Volume of sand trapped in sandtrap 2, ST_2 (m^3)	0.0083
Volume of sand deposited (+) or eroded (-) in branch 0, V_0 (m^3)	0.0150
Volume of sand deposited (+) or eroded (-) in branch 1, V_1 (m^3)	-0.0024
Volume of sand deposited (+) or eroded (-) in branch 2, V_2 (m^3)	0.0067
Volume of sand transported through branch 0, S_0 (m^3)	0.0619
Volume of sand transported through branch 1, S_1 (m^3)	0.0600
Volume of sand transported through branch 2, S_2 (m^3)	0.0151
Ratio of Q_1 and Q_2, Q_1/Q_2	2.371
Ratio of S_1 and S_2, S_1/S_2	3.968
Ratio of V_0 and V_{sf}, V_0/V_{sf}	0.195
Error in percentage of sand balance	21.28

FINAL RESULTS OF RUN NO. 2324

Total run time, T(min.)	244
Rate of sand supplied by sand feeder, R (kg/hr)	31.25
Volume of sand supplied by sand feeder, V_{sf} (m^3)	0.0799
Discharge in branch 0, Q_0 (l/s)	29.562
Discharge in branch 1, Q_1 (l/s)	21.562
Discharge in branch 2, Q_2 (l/s)	8.007
Volume of sand trapped in sandtrap 1, ST_1 (m^3)	0.0713
Volume of sand trapped in sandtrap 2, ST_2 (m^3)	0.0069
Volume of sand deposited (+) or eroded (-) in branch 0, V_0 (m^3)	-0.0125
Volume of sand deposited (+) or eroded (-) in branch 1, V_1 (m^3)	-0.0097
Volume of sand deposited (+) or eroded (-) in branch 2, V_2 (m^3)	0.0152
Volume of sand transported through branch 0, S_0 (m^3)	0.0924
Volume of sand transported through branch 1, S_1 (m^3)	0.0616
Volume of sand transported through branch 2, S_2 (m^3)	0.0222
Ratio of Q_1 and Q_2, Q_1/Q_2	2.692
Ratio of S_1 and S_2, S_1/S_2	2.768
Ratio of V_0 and V_{sf}, V_0/V_{sf}	0.157
Error in percentage of sand balance	9.31

FINAL RESULTS OF RUN NO. 3311

Total run time, T(min.)	243
Rate of sand supplied by sand feeder, R (kg/hr)	44.6
Volume of sand supplied by sand feeder, V_{sf} (m^3)	0.1136
Discharge in branch 0, Q_0 (l/s)	40.785
Discharge in branch 1, Q_1 (l/s)	20.678
Discharge in branch 2, Q_2 (l/s)	20.106
Volume of sand trapped in sandtrap 1, ST_1 (m^3)	0.1062
Volume of sand trapped in sandtrap 2, ST_2 (m^3)	0.0552
Volume of sand deposited (+) or eroded (-) in branch 0, V_0 (m^3)	0.0079
Volume of sand deposited (+) or eroded (-) in branch 1, V_1 (m^3)	-0.0990
Volume of sand deposited (+) or eroded (-) in branch 2, V_2 (m^3)	0.0687
Volume of sand transported through branch 0, S_0 (m^3)	0.1056
Volume of sand transported through branch 1, S_1 (m^3)	0.0071
Volume of sand transported through branch 2, S_2 (m^3)	0.1239
Ratio of Q_1 and Q_2, Q_1/Q_2	1.028
Ratio of S_1 and S_2, S_1/S_2	0.057
Ratio of V_0 and V_{sf}, V_0/V_{sf}	0.069
Error in percentage of sand balance	24.08

FINAL RESULTS OF RUN NO. 3312

Total run time, T(min.)	245
Rate of sand supplied by sand feeder, R (kg/hr)	44.6
Volume of sand supplied by sand feeder, V_{sf} (m^3)	0.1145
Discharge in branch 0, Q_0 (l/s)	40.918
Discharge in branch 1, Q_1 (l/s)	24.719
Discharge in branch 2, Q_2 (l/s)	16.198
Volume of sand trapped in sandtrap 1, ST_1 (m^3)	0.1103
Volume of sand trapped in sandtrap 2, ST_2 (m^3)	0.0339
Volume of sand deposited (+) or eroded (-) in branch 0, V_0 (m^3)	-0.0094
Volume of sand deposited (+) or eroded (-) in branch 1, V_1 (m^3)	-0.0559
Volume of sand deposited (+) or eroded (-) in branch 2, V_2 (m^3)	0.0479
Volume of sand transported through branch 0, S_0 (m^3)	0.1240
Volume of sand transported through branch 1, S_1 (m^3)	0.0544
Volume of sand transported through branch 2, S_2 (m^3)	0.0819
Ratio of Q_1 and Q_2, Q_1/Q_2	1.526
Ratio of S_1 and S_2, S_1/S_2	0.663
Ratio of V_0 and V_{sf}, V_0/V_{sf}	0.082
Error in percentage of sand balance	9.96

FINAL RESULTS OF RUN NO. 3313

Total run time, T(min.)	244
Rate of sand supplied by sand feeder, R (kg/hr)	45.3
Volume of sand supplied by sand feeder, V_{sf} (m^3)	0.1158
Discharge in branch 0, Q_0 (l/s)	40.999
Discharge in branch 1, Q_1 (l/s)	28.084
Discharge in branch 2, Q_2 (l/s)	12.914
Volume of sand trapped in sandtrap 1, ST_1 (m^3)	0.0657
Volume of sand trapped in sandtrap 2, ST_2 (m^3)	0.0202
Volume of sand deposited (+) or eroded (-) in branch 0, V_0 (m^3)	-0.0088
Volume of sand deposited (+) or eroded (-) in branch 1, V_1 (m^3)	0.0122
Volume of sand deposited (+) or eroded (-) in branch 2, V_2 (m^3)	0.0231
Volume of sand transported through branch 0, S_0 (m^3)	0.0124
Volume of sand transported through branch 1, S_1 (m^3)	0.0780
Volume of sand transported through branch 2, S_2 (m^3)	0.0433
Ratio of Q_1 and Q_2, Q_1/Q_2	2.174
Ratio of S_1 and S_2, S_1/S_2	1.799
Ratio of V_0 and V_{sf}, V_0/V_{sf}	0.076
Error in percentage of sand balance	2.64

FINAL RESULTS OF RUN NO. 3314

Total run time, T(min.)	214
Rate of sand supplied by sand feeder, R (kg/hr)	45.2
Volume of sand supplied by sand feeder, V_{sf} (m^3)	0.1013
Discharge in branch 0, Q_0 (l/s)	40.952
Discharge in branch 1, Q_1 (l/s)	28.353
Discharge in branch 2, Q_2 (l/s)	12.598
Volume of sand trapped in sandtrap 1, ST_1 (m^3)	0.0841
Volume of sand trapped in sandtrap 2, ST_2 (m^3)	0.0194
Volume of sand deposited (+) or eroded (-) in branch 0, V_0 (m^3)	0.0025
Volume of sand deposited (+) or eroded (-) in branch 1, V_1 (m^3)	0.0167
Volume of sand deposited (+) or eroded (-) in branch 2, V_2 (m^3)	0.0171
Volume of sand transported through branch 0, S_0 (m^3)	0.0988
Volume of sand transported through branch 1, S_1 (m^3)	0.1009
Volume of sand transported through branch 2, S_2 (m^3)	0.0366
Ratio of Q_1 and Q_2, Q_1/Q_2	2.250
Ratio of S_1 and S_2, S_1/S_2	2.750
Ratio of V_0 and V_{sf}, V_0/V_{sf}	0.024
Error in percentage of sand balance	39.13

FINAL RESULTS OF RUN NO. 3315

Total run time, T(min.)	244
Rate of sand supplied by sand feeder, R (kg/hr)	43.7
Volume of sand supplied by sand feeder, V_{sf} (m^3)	0.1117
Discharge in branch 0, Q_0 (l/s)	41.155
Discharge in branch 1, Q_1 (l/s)	28.910
Discharge in branch 2, Q_2 (l/s)	12.245
Volume of sand trapped in sandtrap 1, ST_1 (m^3)	0.1024
Volume of sand trapped in sandtrap 2, ST_2 (m^3)	0.0264
Volume of sand deposited (+) or eroded (-) in branch 0, V_0 (m^3)	-0.0142
Volume of sand deposited (+) or eroded (-) in branch 1, V_1 (m^3)	-0.0110
Volume of sand deposited (+) or eroded (-) in branch 2, V_2 (m^3)	-0.0067
Volume of sand transported through branch 0, S_0 (m^3)	0.1260
Volume of sand transported through branch 1, S_1 (m^3)	0.0913
Volume of sand transported through branch 2, S_2 (m^3)	0.0197
Ratio of Q_1 and Q_2, Q_1/Q_2	2.361
Ratio of S_1 and S_2, S_1/S_2	4.638
Ratio of V_0 and V_{sf}, V_0/V_{sf}	0.127
Error in percentage of sand balance	11.88

FINAL RESULTS OF RUN NO. 3316

Total run time, T(min.)	244
Rate of sand supplied by sand feeder, R (kg/h)	44.4
Volume of sand supplied by sand feeder, V_{sf} (m^3)	0.1135
Discharge in branch 0, Q_0 (l/s)	41.342
Discharge in branch 1, Q_1 (l/s)	29.098
Discharge in branch 2, Q_2 (l/s)	12.244
Volume of sand trapped in sandtrap 1, ST_1 (m^3)	0.0852
Volume of sand trapped in sandtrap 2, ST_2 (m^3)	0.0260
Volume of sand deposited (+) or eroded (-) in branch 0, V_0 (m^3)	-0.0024
Volume of sand deposited (+) or eroded (-) in branch 1, V_1 (m^3)	0.0048
Volume of sand deposited (+) or eroded (-) in branch 2, V_2 (m^3)	0.0082
Volume of sand transported through branch 0, S_0 (m^3)	0.1160
Volume of sand transported through branch 1, S_1 (m^3)	0.0901
Volume of sand transported through branch 2, S_2 (m^3)	0.0342
Ratio of Q_1 and Q_2, Q_1/Q2	2.376
Ratio of S_1 and S_2, S_1/S_2	2.630
Ratio of V_0 and V_{sf}, V_0/V_{sf}	0.021
Error in percentage of sand balance	7.17

FINAL RESULTS OF RUN NO. 3321

Total run time, T(min.)	243
Rate of sand supplied by sand feeder, R (kg/hr)	45.7
Volume of sand supplied by sand feeder, V_{sf} (m^3)	0.1164
Discharge in branch 0, Q_0 (l/s)	40.941
Discharge in branch 1, Q_1 (l/s)	22.316
Discharge in branch 2, Q_2 (l/s)	18.625
Volume of sand trapped in sandtrap 1, ST_1 (m^3)	0.1010
Volume of sand trapped in sandtrap 2, ST_2 (m^3)	0.0422
Volume of sand deposited (+) or eroded (-) in branch 0, V_0 (m^3)	0.0055
Volume of sand deposited (+) or eroded (-) in branch 1, V_1 (m^3)	-0.0828
Volume of sand deposited (+) or eroded (-) in branch 2, V_2 (m^3)	0.0769
Volume of sand transported through branch 0, S_0 (m^3)	0.1108
Volume of sand transported through branch 1, S_1 (m^3)	0.0182
Volume of sand transported through branch 2, S_2 (m^3)	0.1191
Ratio of Q_1 and Q_2, Q_1/Q_2	1.198
Ratio of S_1 and S_2, S_1/S_2	0.153
Ratio of V_0 and V_{sf}, V_0/V_{sf}	0.047
Error in percentage of sand balance	23.91

FINAL RESULTS OF RUN NO. 3322

Total run time, T(min.)	274
Rate of sand supplied by sand feeder, R (kg/hr)	45.6
Volume of sand supplied by sand feeder, V_{sf} (m^3)	0.1309
Discharge in branch 0, Q_0 (l/s)	40.960
Discharge in branch 1, Q_1 (l/s)	26.185
Discharge in branch 2, Q_2 (l/s)	14.774
Volume of sand trapped in sandtrap 1, ST_1 (m^3)	0.1253
Volume of sand trapped in sandtrap 2, ST_2 (m^3)	0.0347
Volume of sand deposited (+) or eroded (-) in branch 0, V_0 (m^3)	-0.0212
Volume of sand deposited (+) or eroded (-) in branch 1, V_1 (m^3)	-0.0359
Volume of sand deposited (+) or eroded (-) in branch 2, V_2 (m^3)	0.0327
Volume of sand transported through branch 0, S_0 (m^3)	0.1521
Volume of sand transported through branch 1, S_1 (m^3)	0.0893
Volume of sand transported through branch 2, S_2 (m^3)	0.0674
Ratio of Q_1 and Q_2, Q_1/Q_2	1.772
Ratio of S_1 and S_2, S_1/S_2	1.325
Ratio of V_0 and V_{sf}, V_0/V_{sf}	0.162
Error in percentage of sand balance	3.06

FINAL RESULTS OF RUN NO. 3323

Total run time, T(min.)	244
Rate of sand supplied by sand feeder, R (kg/hr)	46
Volume of sand supplied by sand feeder, V_{sf} (m^3)	0.1176
Discharge in branch 0, Q_0 (l/s)	40.914
Discharge in branch 1, Q_1 (l/s)	28.274
Discharge in branch 2, Q_2 (l/s)	12.639
Volume of sand trapped in sandtrap 1, ST_1 (m^3)	0.0828
Volume of sand trapped in sandtrap 2, ST_2 (m^3)	0.0228
Volume of sand deposited (+) or eroded (-) in branch 0, V_0 (m^3)	0.0095
Volume of sand deposited (+) or eroded (-) in branch 1, V_1 (m^3)	0.0157
Volume of sand deposited (+) or eroded (-) in branch 2, V_2 (m^3)	0.0003
Volume of sand transported through branch 0, S_0 (m^3)	0.1081
Volume of sand transported through branch 1, S_1 (m^3)	0.0986
Volume of sand transported through branch 2, S_2 (m^3)	0.0232
Ratio of Q_1 and Q_2, Q_1/Q_2	2.236
Ratio of S_1 and S_2, S_1/S_2	4.238
Ratio of V_0 and V_{sf}, V_0/V_{sf}	0.080
Error in percentage of sand balance	12.69

FINAL RESULTS OF RUN NO. 1411

Total run time, T(min.)	361
Rate of sand supplied by sand feeder, R (kg/hr)	22.3
Volume of sand supplied by sand feeder, V_{sf} (m^3)	0.0843
Discharge in branch 0, Q_0 (l/s)	20.223
Discharge in branch 1, Q_1 (l/s)	7.398
Discharge in branch 2, Q_2 (l/s)	12.824
Volume of sand trapped in sandtrap 1, ST_1 (m^3)	0.0388
Volume of sand trapped in sandtrap 2, ST_2 (m^3)	0.0397
Volume of sand deposited (+) or eroded (-) in branch 0, V_0 (m^3)	0.0275
Volume of sand deposited (+) or eroded (-) in branch 1, V_1 (m^3)	-0.0288
Volume of sand deposited (+) or eroded (-) in branch 2, V_2 (m^3)	0.0195
Volume of sand transported through branch 0, S_0 (m^3)	0.0568
Volume of sand transported through branch 1, S_1 (m^3)	0.0122
Volume of sand transported through branch 2, S_2 (m^3)	0.0593
Ratio of Q_1 and Q_2, Q_1/Q_2	0.576
Ratio of S_1 and S_2, S_1/S_2	0.205
Ratio of V_0 and V_{sf}, V_0/V_{sf}	0.326
Error in percentage of sand balance	25.75

FINAL RESULTS OF RUN NO. 1412

Total run time, T(min.)	302
Rate of sand supplied by sand feeder, R (kg/hr)	22.7
Volume of sand supplied by sand feeder, V_{sf} (m^3)	0.0718
Discharge in branch 0, Q_0 (l/s)	20.355
Discharge in branch 1, Q_1 (l/s)	8.574
Discharge in branch 2, Q_2 (l/s)	11.781
Volume of sand trapped in sandtrap 1, ST_1 (m^3)	0.0304
Volume of sand trapped in sandtrap 2, ST_2 (m^3)	0.0290
Volume of sand deposited (+) or eroded (-) in branch 0, V_0 (m^3)	0.0040
Volume of sand deposited (+) or eroded (-) in branch 1, V_1 (m^3)	-0.0064
Volume of sand deposited (+) or eroded (-) in branch 2, V_2 (m^3)	0.0283
Volume of sand transported through branch 0, S_0 (m^3)	0.0677
Volume of sand transported through branch 1, S_1 (m^3)	0.0239
Volume of sand transported through branch 2, S_2 (m^3)	0.0574
Ratio of Q_1 and Q_2, Q_1/Q_2	0.727
Ratio of S_1 and S_2, S_1/S_2	0.417
Ratio of V_0 and V_{sf}, V_0/V_{sf}	0.094
Error in percentage of sand balance	20.16

FINAL RESULTS OF RUN NO. 1421

Total run time, T(min.)	363
Rate of sand supplied by sand feeder, R (kg/hr)	22.2
Volume of sand supplied by sand feeder, V_{sf} (m^3)	0.0844
Discharge in branch 0, Q_0 (l/s)	20.429
Discharge in branch 1, Q_1 (l/s)	12.639
Discharge in branch 2, Q_2 (l/s)	7.789
Volume of sand trapped in sandtrap 1, ST_1 (m^3)	0.0353
Volume of sand trapped in sandtrap 2, ST_2 (m^3)	0.0454
Volume of sand deposited (+) or eroded (-) in branch 0, V_0 (m^3)	0.0330
Volume of sand deposited (+) or eroded (-) in branch 1, V_1 (m^3)	0.0008
Volume of sand deposited (+) or eroded (-) in branch 2, V_2 (m^3)	-0.0244
Volume of sand transported through branch 0, S_0 (m^3)	0.0514
Volume of sand transported through branch 1, S_1 (m^3)	0.0361
Volume of sand transported through branch 2, S_2 (m^3)	0.0210
Ratio of Q_1 and Q_2, Q_1/Q_2	1.622
Ratio of S_1 and S_2, S_1/S_2	1.718
Ratio of V_0 and V_{sf}, V_0/V_{sf}	0.390
Error in percentage of sand balance	11.19

FINAL RESULTS OF RUN NO. 2411

Total run time, T(min.)	244
Rate of sand supplied by sand feeder, R (kg/hr)	48.9
Volume of sand supplied by sand feeder, V_{sf} (m^3)	0.1250
Discharge in branch 0, Q_0 (l/s)	29.067
Discharge in branch 1, Q_1 (l/s)	10.468
Discharge in branch 2, Q_2 (l/s)	18.599
Volume of sand trapped in sandtrap 1, ST_1 (m^3)	0.0312
Volume of sand trapped in sandtrap 2, ST_2 (m^3)	0.0311
Volume of sand deposited (+) or eroded (-) in branch 0, V_0 (m^3)	0.0525
Volume of sand deposited (+) or eroded (-) in branch 1, V_1 (m^3)	-0.0305
Volume of sand deposited (+) or eroded (-) in branch 2, V_2 (m^3)	0.0441
Volume of sand transported through branch 0, S_0 (m^3)	0.0724
Volume of sand transported through branch 1, S_1 (m^3)	0.0006
Volume of sand transported through branch 2, S_2 (m^3)	0.0753
Ratio of Q_1 and Q_2, Q_1/Q_2	0.562
Ratio of S_1 and S_2, S_1/S_2	0.009
Ratio of V_0 and V_{sf}, V_0/V_{sf}	0.420
Error in percentage of sand balance	4.85

FINAL RESULTS OF RUN NO. 2412

Total run time, T(min.)	213
Rate of sand supplied by sand feeder, R (kg/hr)	34
Volume of sand supplied by sand feeder, V_{sf} (m^3)	0.0759
Discharge in branch 0, Q_0 (l/s)	29.873
Discharge in branch 1, Q_1 (l/s)	12.888
Discharge in branch 2, Q_2 (l/s)	16.984
Volume of sand trapped in sandtrap 1, ST_1 (m^3)	0.0424
Volume of sand trapped in sandtrap 2, ST_2 (m^3)	0.0350
Volume of sand deposited (+) or eroded (-) in branch 0, V_0 (m^3)	-0.0246
Volume of sand deposited (+) or eroded (-) in branch 1, V_1 (m^3)	-0.0059
Volume of sand deposited (+) or eroded (-) in branch 2, V_2 (m^3)	0.0355
Volume of sand transported through branch 0, S_0 (m^3)	0.1005
Volume of sand transported through branch 1, S_1 (m^3)	0.0365
Volume of sand transported through branch 2, S_2 (m^3)	0.0705
Ratio of Q_1 and Q_2, Q_1/Q_2	0.758
Ratio of S_1 and S_2, S_1/S_2	0.517
Ratio of V_0 and V_{sf}, V_0/V_{sf}	0.324
Error in percentage of sand balance	6.56

FINAL RESULTS OF RUN NO. 2413

Total run time, T(min.)	215
Rate of sand supplied by sand feeder, R (kg/hr)	33.7
Volume of sand supplied by sand feeder, V_{sf} (m^3)	0.0759
Discharge in branch 0, Q_0 (l/s)	28.821
Discharge in branch 1, Q_1 (l/s)	13.374
Discharge in branch 2, Q_2 (l/s)	15.446
Volume of sand trapped in sandtrap 1, ST_1 (m^3)	0.0379
Volume of sand trapped in sandtrap 2, ST_2 (m^3)	0.0389
Volume of sand deposited (+) or eroded (-) in branch 0, V_0 (m^3)	0.0041
Volume of sand deposited (+) or eroded (-) in branch 1, V_1 (m^3)	-0.0052
Volume of sand deposited (+) or eroded (-) in branch 2, V_2 (m^3)	0.0117
Volume of sand transported through branch 0, S_0 (m^3)	0.0717
Volume of sand transported through branch 1, S_1 (m^3)	0.0326
Volume of sand transported through branch 2, S_2 (m^3)	0.0460
Ratio of Q_1 and Q_2, Q_1/Q_2	0.865
Ratio of S_1 and S_2, S_1/S_2	0.708
Ratio of V_0 and V_{sf}, V_0/V_{sf}	0.055
Error in percentage of sand balance	9.86

FINAL RESULTS OF RUN NO. 2421

Total run time, T(min.)	214
Rate of sand supplied by sand feeder, R (kg/hr)	36.4
Volume of sand supplied by sand feeder, V_{sf} (m^3)	0.0816
Discharge in branch 0, Q_0 (l/s)	30.051
Discharge in branch 1, Q_1 (l/s)	18.145
Discharge in branch 2, Q_2 (l/s)	11.906
Volume of sand trapped in sandtrap 1, ST_1 (m^3)	0.0407
Volume of sand trapped in sandtrap 2, ST_2 (m^3)	0.0395
Volume of sand deposited (+) or eroded (-) in branch 0, V_0 (m^3)	0.0380
Volume of sand deposited (+) or eroded (-) in branch 1, V_1 (m^3)	0.0387
Volume of sand deposited (+) or eroded (-) in branch 2, V_2 (m^3)	-0.0532
Volume of sand transported through branch 0, S_0 (m^3)	0.0588
Volume of sand transported through branch 1, S_1 (m^3)	0.0639
Volume of sand transported through branch 2, S_2 (m^3)	0.0076
Ratio of Q_1 and Q_2, Q_1/Q_2	1.524
Ratio of S_1 and S_2, S_1/S_2	8.345
Ratio of V_0 and V_{sf}, V_0/V_{sf}	0.466
Error in percentage of sand balance	21.75

FINAL RESULTS OF RUN NO. 2422

Total run time, T(min.)	217
Rate of sand supplied by sand feeder, R (kg/hr)	34
Volume of sand supplied by sand feeder, V_{sf} (m^3)	0.0773
Discharge in branch 0, Q_0 (l/s)	29.195
Discharge in branch 1, Q_1 (l/s)	15.578
Discharge in branch 2, Q_2 (l/s)	13.616
Volume of sand trapped in sandtrap 1, ST_1 (m^3)	0.0326
Volume of sand trapped in sandtrap 2, ST_2 (m^3)	0.0369
Volume of sand deposited (+) or eroded (-) in branch 0, V_0 (m^3)	0.0078
Volume of sand deposited (+) or eroded (-) in branch 1, V_1 (m^3)	0.0327
Volume of sand deposited (+) or eroded (-) in branch 2, V_2 (m^3)	-0.0213
Volume of sand transported through branch 0, S_0 (m^3)	0.0694
Volume of sand transported through branch 1, S_1 (m^3)	0.0654
Volume of sand transported through branch 2, S_2 (m^3)	0.0155
Ratio of Q_1 and Q_2, Q_1/Q_2	1.144
Ratio of S_1 and S_2, S_1/S_2	4.213
Ratio of V_0 and V_{sf}, V_0/V_{sf}	0.102
Error in percentage of sand balance	16.67

FINAL RESULTS OF RUN NO. 3411

Total run time, T(min.)	242
Rate of sand supplied by sand feeder, R (kg/hr)	45
Volume of sand supplied by sand feeder, V_{sf} (m^3)	0.1141
Discharge in branch 0, Q_0 (l/s)	41.076
Discharge in branch 1, Q_1 (l/s)	20.080
Discharge in branch 2, Q_2 (l/s)	20.995
Volume of sand trapped in sandtrap 1, ST_1 (m^3)	0.0599
Volume of sand trapped in sandtrap 2, ST_2 (m^3)	0.0601
Volume of sand deposited (+) or eroded (-) in branch 0, V_0 (m^3)	-0.0067
Volume of sand deposited (+) or eroded (-) in branch 1, V_1 (m^3)	0.0206
Volume of sand deposited (+) or eroded (-) in branch 2, V_2 (m^3)	-0.0077
Volume of sand transported through branch 0, S_0 (m^3)	0.1208
Volume of sand transported through branch 1, S_1 (m^3)	0.0806
Volume of sand transported through branch 2, S_2 (m^3)	0.0523
Ratio of Q_1 and Q_2, Q_1/Q_2	0.956
Ratio of S_1 and S_2, S_1/S_2	1.539
Ratio of V_0 and V_{sf}, V_0/V_{sf}	0.058
Error in percentage of sand balance	10.04

FINAL RESULTS OF RUN NO. 3412

Total run time, T(min.)	245
Rate of sand supplied by sand feeder, R (kg/hr)	44.2
Volume of sand supplied by sand feeder, V_{sf} (m^3)	0.1135
Discharge in branch 0, Q_0 (l/s)	41.127
Discharge in branch 1, Q_1 (l/s)	19.195
Discharge in branch 2, Q_2 (l/s)	21.932
Volume of sand trapped in sandtrap 1, ST_1 (m^3)	0.0631
Volume of sand trapped in sandtrap 2, ST_2 (m^3)	0.0726
Volume of sand deposited (+) or eroded (-) in branch 0, V_0 (m^3)	-0.0074
Volume of sand deposited (+) or eroded (-) in branch 1, V_1 (m^3)	0.0057
Volume of sand deposited (+) or eroded (-) in branch 2, V_2 (m^3)	0.0024
Volume of sand transported through branch 0, S_0 (m^3)	0.1179
Volume of sand transported through branch 1, S_1 (m^3)	0.0666
Volume of sand transported through branch 2, S_2 (m^3)	0.0740
Ratio of Q_1 and Q_2, Q_1/Q_2	0.875
Ratio of S_1 and S_2, S_1/S_2	0.899
Ratio of V_0 and V_{sf}, V_0/V_{sf}	0.065
Error in percentage of sand balance	19.27

FINAL RESULTS OF RUN NO. 3421

Total run time, T(min.)	249
Rate of sand supplied by sand feeder, R (kg/hr)	46.2
Volume of sand supplied by sand feeder, V_{sf} (m^3)	0.1205
Discharge in branch 0, Q_0 (l/s)	41.065
Discharge in branch 1, Q_1 (l/s)	12.269
Discharge in branch 2, Q_2 (l/s)	28.796
Volume of sand trapped in sandtrap 1, ST_1 (m^3)	0.0367
Volume of sand trapped in sandtrap 2, ST_2 (m^3)	0.0998
Volume of sand deposited (+) or eroded (-) in branch 0, V_0 (m^3)	-0.0016
Volume of sand deposited (+) or eroded (-) in branch 1, V_1 (m^3)	-0.0668
Volume of sand deposited (+) or eroded (-) in branch 2, V_2 (m^3)	0.0526
Volume of sand transported through branch 0, S_0 (m^3)	0.1222
Volume of sand transported through branch 1, S_1 (m^3)	-0.0301
Volume of sand transported through branch 2, S_2 (m^3)	0.1524
Ratio of Q_1 and Q_2, Q_1/Q_2	0.426
Ratio of S_1 and S_2, S_1/S_2	-0.197
Ratio of V_0 and V_{sf}, V_0/V_{sf}	0.013
Error in percentage of sand balance	0.10

FINAL RESULTS OF RUN NO. 3422

Total run time, T(min.)	243
Rate of sand supplied by sand feeder, R (kg/hr)	48.2
Volume of sand supplied by sand feeder, V_{sf} (m^3)	0.1227
Discharge in branch 0, Q_0 (l/s)	41.312
Discharge in branch 1, Q_1 (l/s)	15.320
Discharge in branch 2, Q_2 (l/s)	25.992
Volume of sand trapped in sandtrap 1, ST_1 (m^3)	0.0781
Volume of sand trapped in sandtrap 2, ST_2 (m^3)	0.0833
Volume of sand deposited (+) or eroded (-) in branch 0, V_0 (m^3)	-0.0012
Volume of sand deposited (+) or eroded (-) in branch 1, V_1 (m^3)	0.0412
Volume of sand deposited (+) or eroded (-) in branch 2, V_2 (m^3)	0.0274
Volume of sand transported through branch 0, S_0 (m^3)	0.1239
Volume of sand transported through branch 1, S_1 (m^3)	0.0369
Volume of sand transported through branch 2, S_2 (m^3)	0.1108
Ratio of Q_1 and Q_2, Q_1/Q_2	0.589
Ratio of S_1 and S_2, S_1/S_2	0.333
Ratio of V_0 and V_{sf}, V_0/V_{sf}	0.009
Error in percentage of sand balance	19.18

FINAL RESULTS OF RUN NO. 3431

Total run time, T(min.)	212
Rate of sand supplied by sand feeder, R (kg/hr)	45.8
Volume of sand supplied by sand feeder, V_{sf} (m^3)	0.1017
Discharge in branch 0, Q_0 (l/s)	41.246
Discharge in branch 1, Q_1 (l/s)	23.359
Discharge in branch 2, Q_2 (l/s)	17.886
Volume of sand trapped in sandtrap 1, ST_1 (m^3)	0.0535
Volume of sand trapped in sandtrap 2, ST_2 (m^3)	0.0659
Volume of sand deposited (+) or eroded (-) in branch 0, V_0 (m^3)	-0.0008
Volume of sand deposited (+) or eroded (-) in branch 1, V_1 (m^3)	0.0450
Volume of sand deposited (+) or eroded (-) in branch 2, V_2 (m^3)	-0.0652
Volume of sand transported through branch 0, S_0 (m^3)	0.1025
Volume of sand transported through branch 1, S_1 (m^3)	0.0985
Volume of sand transported through branch 2, S_2 (m^3)	0.0006
Ratio of Q_1 and Q_2, Q_1/Q_2	1.305
Ratio of S_1 and S_2, S_1/S_2	140.997
Ratio of V_0 and V_{sf}, V_0/V_{sf}	0.008
Error in percentage of sand balance	3.28

FINAL RESULTS OF RUN NO. 3432

Total run time, T(min.)	215
Rate of sand supplied by sand feeder, R (kg/hr)	46.5
Volume of sand supplied by sand feeder, V_{sf} (m^3)	0.1047
Discharge in branch 0, Q_0 (l/s)	40.917
Discharge in branch 1, Q_1 (l/s)	19.931
Discharge in branch 2, Q_2 (l/s)	20.985
Volume of sand trapped in sandtrap 1, ST_1 (m^3)	0.0470
Volume of sand trapped in sandtrap 2, ST_2 (m^3)	0.0655
Volume of sand deposited (+) or eroded (-) in branch 0, V_0 (m^3)	-0.0067
Volume of sand deposited (+) or eroded (-) in branch 1, V_1 (m^3)	0.0275
Volume of sand deposited (+) or eroded (-) in branch 2, V_2 (m^3)	-0.0240
Volume of sand transported through branch 0, S_0 (m^3)	0.1115
Volume of sand transported through branch 1, S_1 (m^3)	0.0746
Volume of sand transported through branch 2, S_2 (m^3)	0.0415
Ratio of Q_1 and Q_2, Q_1/Q_2	0.949
Ratio of S_1 and S_2, S_1/S_2	1.795
Ratio of V_0 and V_{sf}, V_0/V_{sf}	0.064
Error in percentage of sand balance	4.14